UNIVERSITA` DEGLI STUDI DI PADOVA

SCUOLA DI INGEGNERIA

Dipartimento ICEA
Corso di Laurea Magistrale in Ingegneria Civile

TESI DI LAUREA

SOIL-STRUCTURE INTERACTION:

REVIEW OF THE FUNDAMENTAL THEORIES

Relatore: Prof. Roberto Scotta
Correlatore: Prof. Marek Lefik
Correlatore: Prof. Giampaolo Cortellazzo

Laureando: Andrea Pomarè Montin

Matricola: 1019850

ANNO ACCADEMICO 2013/2014

Contents

Preface

The purpose of this project is to analyze the interaction between horizontal and vertical civil structures and the soil. First, it is important to define the "interaction between soil and structure": there is interaction when the response, under load, of the soil is influenced by the response of the structure, according to the stiffness and the geometrical characteristics of the latter.

Horizontal structures are analyzed in the first part of this report: the theoretical introduction of Winkler's solution has been exposed and Winkler's constant was calculated by studying the trend of stresses within the ground; the adopted method allows the estimation of the stress distribution within the ground under an embankment: this issue adequately represents the plain strain model that will be used in the FEM solution; subsequently a calculation for a beam foundation has been produced (the 2D plain strain is used: the beam is a section of an infinitely extended element in the orthogonal direction to the plane of the section) using the previously found Winkler's constant applied to the differential equations for an elastic soil (implementation of solutions on a spreadsheet). Then, a comparison between analytical solutions of the beam on elastic foundation, and FEM models has been made. With FEM, elastic and elastic-plastic solutions have been compared; particular focus has been placed on the dependence between the solution and the choice of parameters, the constitutive model of the soil and of the stresses within the ground: the purpose is to understand whether the elastic model adopted in previous analysis adequately describes the issue. Alternative analytical solution of Pasternak has been illustrated and compared with the previous solutions of Winkler and FEM, then applications of this theory has been shown, both in 2D and 3D models.

In the second part the focus shifts on the vertical structures: theoretical description of the methods used in the study of the behavior of sheet piles under horizontal load of the soil after excavation has been made. Simplified limit equilibrium method, numerical solution based on the theory of Winkler's elastic-plastic springs (dependent pressure) and FEM methods are used. Comparison of the solutions obtained by the different approaches has been made, distinguishing the case of an excavation in a clay soil from that in a sandy soil. For both cases the behavior of the structure has been observed, either when the embedment length widely ensures the equilibrium, also in situations close to instability: in particular the contribution that the "interface" element provides to the solution has been studied.

The effect of the water table on the soil-structure interaction was not taken into account in this report.

Aims and workflow can be summarized as follows:

- Analytical methods: theoretical description, implementation, results
- Numerical methods: description of the model, modeling, calculation

- Comparison: systematic observation of the different results from different solutions, verify the compatibility of the approaches
- Approximation: determination of which approach better simulates the real behavior of the soil-structure model
- Analytical versus numerical analyses: acceptability, limits of both of them

1 Horizontal structures

1.1 Winkler's solution

1.1.1 Theoretical introduction

In order to transfer the upper load of a building or another layer into the soil, a structure is required and the purpose of this structure is to support the super-structure, avoiding the failure and having settlements inside certain acceptable limits (Figure 1). The half-space of the soil could be nonhomogeneous, anisotropic in its material, and the constitutive relations will be complex and unknown or even undeterminable, so simplifications must be taken.

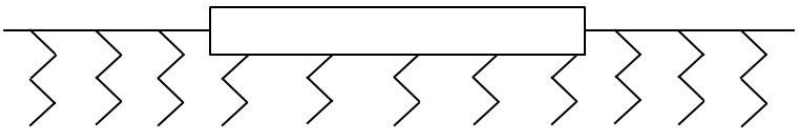

Figure 1: Winkler's springs

The behavior of the soil is taken as linearly elastic or rigid plastic when mathematical analyses are used (Figure 2). The Boussinesq problem is when a linearly elastic material is used, that's to say where all layers have the same elastic properties.

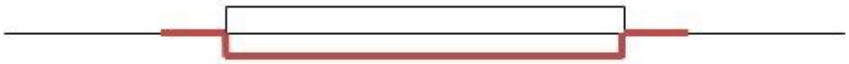

Figure 2: Winkler's model

A used calculation technique refers to Winkler model, and concentrates on the behavior of the upper stiff layer, "the structure", a "beam" usually; according to this theory the soil has only a supporting role. The continuum representation of half space can't be used for this model. The foundation material which Winkler adopted is now called Winkler foundation, and is a model substitution. In this model the pressure, p, acting at a point is equal to the deflection of the ground at that point, w, multiplied by a proportionality constant, k_0, so that

$$p = k_0 w \quad (1)$$

The constant, k_0, is the foundation stiffness, but other used names are "coefficient of subgrade reaction" or "subgrade modulus". Its dimensions are FL^{-3}.

The first analysis deals with the behavior of the rigid beam,: the complete problem is one of plane strain, in fact the focus could be on either a real beam of finite width b or may a strip of unit width, that's to say a typical element of a slab impressed with line loads, moments, or displacements. The situation in either of these cases is two-dimensional, so the basic subgrade modulus k_0, to give an appropriate value for use in analysis, must be multiplied by the beam (b) or strip (1) width:

$$k = k_0 b \tag{2}$$

or

$$k = k_0 * 1 \tag{3}$$

and has dimensions FL^{-3} [1].

Anyway, the focus will be on the flexible beams on Winkler foundation.

1.1.2 Flexible beams on Winkler foundation

For a general description has been considered a beam of constant cross section and with its axis in the x-direction; q is the load on the beam (a force per unit length), w is the vertical displacement (in z-direction)(Figure 3).

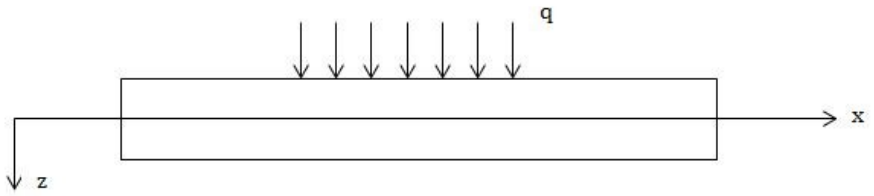

Figure 3: Beam with uniform load

The formulae describing the behavior of a beam are listed below. In order to respect the condition of equilibrium in z-direction (the direction perpendicular to the axis of the beam) the following condition must be satisfied (Figure 4):

$$\frac{dT(x)}{dx} = -q(x) \tag{4}$$

where T is the shear force. It's been assumed that, when the force on a surface with its normal in the positive *x*-direction is acting in the positive *z*-direction, then it is conventionally positive.

The second condition to be satisfied is the equation of equilibrium of moments

$$\frac{dM(x)}{dx} = T(x) \tag{5}$$

where M is the bending moment. In this case a positive stress (tension) on the positive side of the axis of the beam it's equivalent of a positive bending moment.

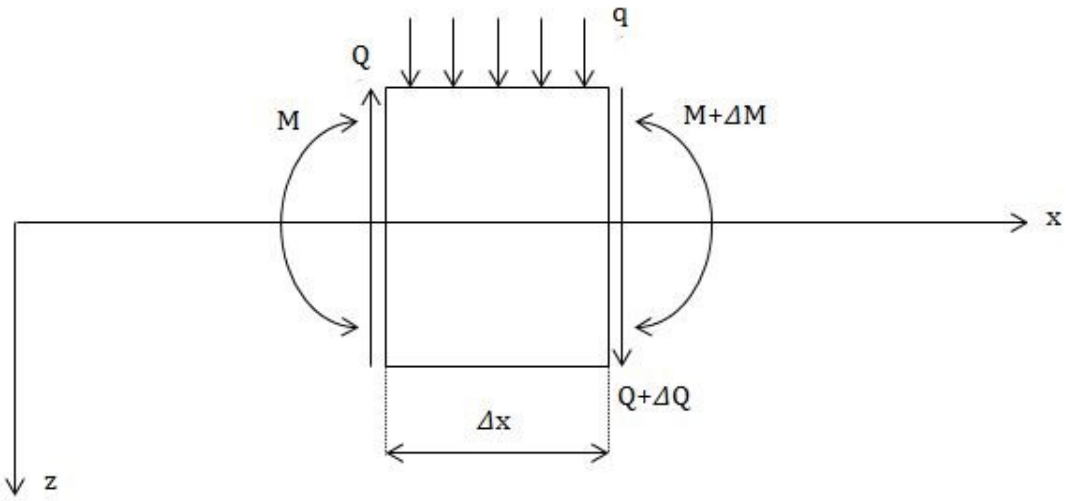

Figure 4: Equilibrium of a part of a beam

The combination of these two equations gives the first basic equation of the theory of bending of moments

$$\frac{d^2M(x)}{dx^2} = -q(x) \tag{6}$$

It's been applied the Bernoulli's hypothesis for the plane cross sections of the beam (it remains plane after deformation) and it's been assumed that the rotation dw/dx is small compared to one. In this way it's possible to obtain the second basic equation of the theory of bending of moments which concerns the deformation of the beam

$$EI\frac{d^2w(x)}{dx^2} = -M(x) \tag{7}$$

where EI is the flexural rigidity of the beam.

The combination of these two equations gives the basic equation of the classical theory of bending of beams, a fourth order differential equation for the lateral displacement

$$EI\frac{d^4w(x)}{dx^4} = q(x) \tag{8}$$

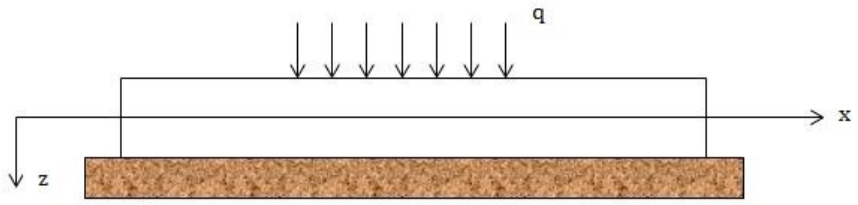

Figure 5: Beam on elastic soil

The external load and the soil reaction are considered the lateral load in case of a beam resting on an elastic foundation (Figure 5). As a first approximation it's possible to assume that the soil reaction is equal to the lateral displacement multiplied by the subgrade modulus k, and in this case the differential equation is

$$EI\frac{d^4w(x)}{dx^4} = q(x) - kw(x) \Rightarrow \tag{9}$$

$$\frac{d^4w(x)}{dx^4} = \frac{q(x)}{EI} - \frac{kw(x)}{EI} \tag{10}$$

with typical substitution

$$\lambda = \sqrt[4]{\frac{k}{4EI}} \tag{11}$$

leads to the Winkler's formula

$$\frac{d^4w(x)}{dx^4} + 4\lambda^4 w(x) = \frac{q(x)}{EI} \tag{12}$$

The form of the solution of the homogeneous equation (when q = 0) is

$$w(x) = e^{\lambda x}(C_1 \sin(\lambda x) + C_2 \cos(\lambda x)) + e^{((-\lambda)x)}(C_3 \sin(\lambda x) + C_4 \cos(\lambda x)) \tag{13}$$

[2] [3].

1.1.3 Winkler's constant

The first target to be achieved is the Winkler's constant "k". On a spreadsheet a general situation of double layer of soil has been created, the first one is composed of sand (coarse soil), and the second one of clay (fine soil). The characteristics of the materials have been chosen so as to be absolutely generic. These are the values:

Table 1: Soil's parameters

SAND - COARSE					CLAY - FINE				
T1	E1	c'1	ϕ'1	ν1	T2	E2	c'2	ϕ'2	ν2
[m]	[kPa]	[kPa]	[°]	[-]	[m]	[kPa]	[kPa]	[°]	[-]
5	37000	0	37	0.3	5	8000	0	25	0.3

The layers have a depth of 5 meters each, and above the first layer there is a concrete beam foundation with general characteristics. Two concentrated forces act on the beam (Figure 6), but for this topic they are considered as distributed force on the surface: it is a strong approximation, because the two models are different. In the next chapters the solution with two forces on the beam has been considered more adequate for the analysis, hence this first schematization has been considered acceptable, considering the stiffness of the beam that allows to estimate the foundation as a "rigid" element. The dimension of the beam and the magnitude of the force have been varied so as to have an interpretation of the behavior of the Winkler's "k".

Figure 6: Loaded beam

According to find the "k" for a particular combination of forces and dimensions, the layers have been divided in substrates and in each one the stress has been calculated using the formula adopted to estimate the trend of stress under an embankment: this issue, as said in the preface, properly describes the "plain strain" model which is implemented in the FEM programs that will be adopted in the following chapters

(the beam is a section of an infinitely extended foundation in the orthogonal direction to the plane of the section).
The formula (14) could be substituted by Navfac's abacus (1982) [4], and it is usually used for the calculation of stresses under embankments (Figure 7).

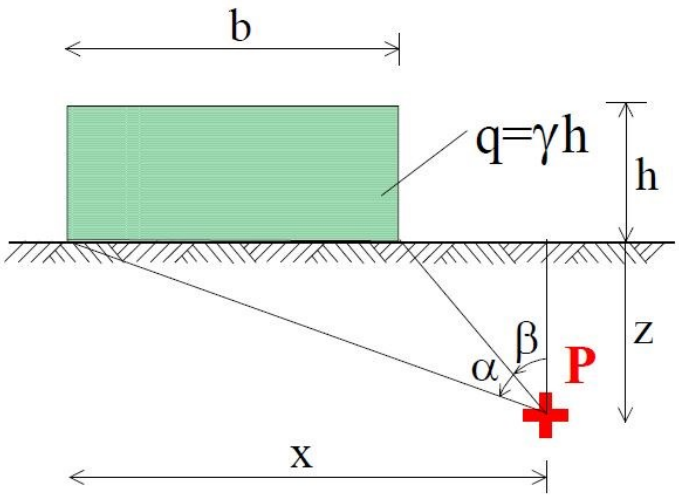

Figure 7: Stress under an embankment [4]

$$\Delta\sigma_v = \frac{q}{\pi}[\alpha + \sin\alpha\cos(\alpha + 2\beta)] \quad \textbf{(14)}$$

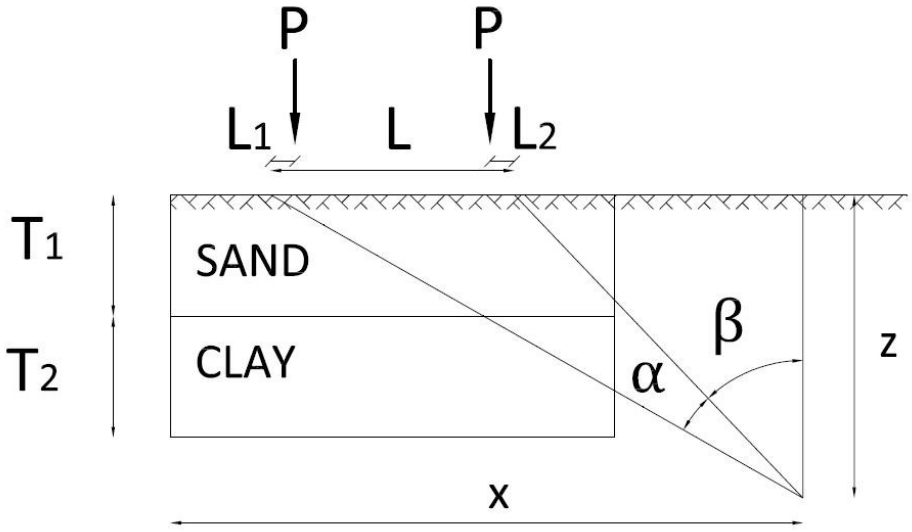

Figure 8: The analyzed model

From the stress, the displacement for each substrate has been estimated and, accordingly, the total displacement has been calculated. Finally the "k" has been obtained from the ratio between the pressure on the beam and the displacement.
Below the parameters (Table 2) adopted in the spreadsheet, the ground settlement "w" and "k" are listed: the latter is the value which will be used in the further calculations.

Table 2: Parameters for the calculation of "k"

w	k	H	B	L	L/B	A	P1	P2	q
[m]	[kN/m^3]	[m]	[m]	[m]	[-]	[m^2]	[kN]	[kN]	[kN/m]
0.010965	1824.064	1	1	10	10	10	100	100	20

As illustrated in the table, the settlements that will be considered in the following calculations are the ones obtained with L/B = 10 m, P1 = P2 = 100 kN and q = (P1 + P2) /L = 20 kN/m.
A graphic (Figure 9) has been created to illustrate the variation of the stress under the foundation varying the depth and the load on the beam.

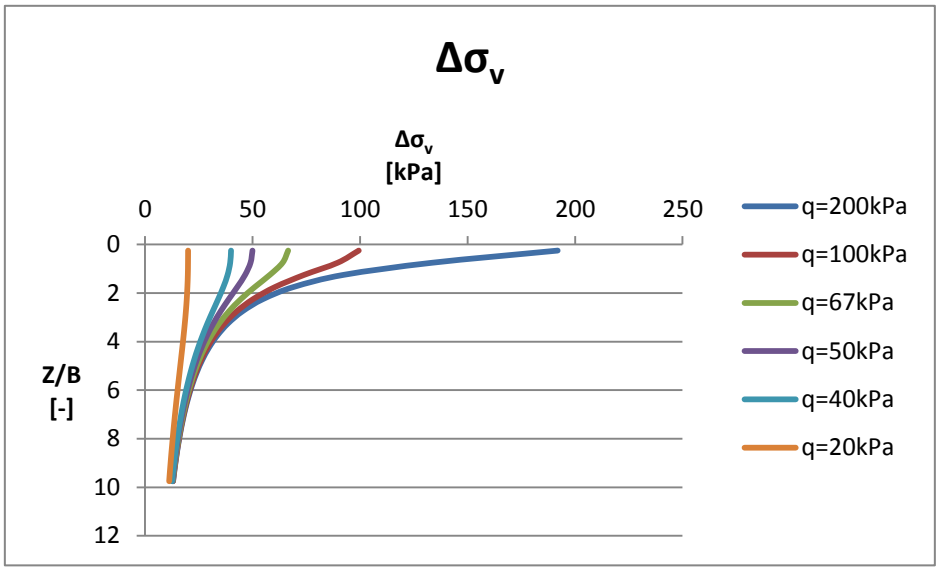

Figure 9: Stress distribution varying the pressure on the ground

1.1.4 Theoretical solution - Winkler

On a new spreadsheet, according to simulate the behavior of the beam on Winkler's springs , have been used the values taken from the previous spreadsheet obtained with a 10 meters beam with two forces of 100 kN each acting 1 m inside the two edges.
According to simplify the structure the beam has been divided into two parts of 5 meters each, with boundary conditions that respect the former situation of forces and constraints. The new beam rests on the Winkler's springs obtained from the previous spreadsheet and has been divided into fifty parts, and for each part has been calculated the settlement obtained with the formula from Winkler's theory of the beam on elastic soil, and for the same part has been calculated from the first to the fourth derivative of the previous formula. In this way is easy to calculate the settlement, the shear force, bending moment and rotation in each part of the beam.
As said before, it's been considered only half-beam, the left one: to find the solution one need to adopte k, in this case it's been used the k obtained by the former spreadsheet adopted for the stress calculation.

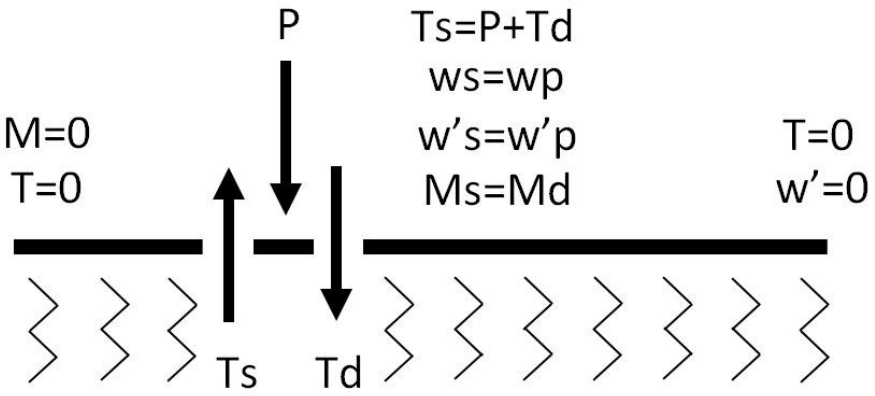

Figure 10: Border conditions for Winkler's solution

Solution of the beam on the left-hand side of point of application of the force:

$$w_1(x) = e^{\lambda x}\left(C_{1\_1}\sin(\lambda x) + C_{2\_1}\cos(\lambda x)\right) + e^{((-\lambda)x)}\left(C_{3\_1}\sin(\lambda x) + C_{4\_1}\cos(\lambda x)\right) \quad \textbf{(15)}$$

Solution of the beam on the right-hand side of point of application of the force:

$$w_2(x) = e^{\lambda x}\left(C_{1\_2}\sin(\lambda x) + C_{2\_2}\cos(\lambda x)\right) + e^{((-\lambda)x)}\left(C_{3\_2}\sin(\lambda x) + C_{4\_2}\cos(\lambda x)\right) \quad \textbf{(16)}$$

Conditions for the eight constants.

On the right end of the beam (telescope):

$$T\left(w_2(x), x = \frac{L}{2}\right) = 0 \quad \textbf{(17)}$$

$$\frac{dw_2(x)}{dx}\left(x = \frac{L}{2}\right) = 0 \quad \textbf{(18)}$$

At the section of action of the force:

$$T\left(w_1(x), x = \frac{L}{10}\right) = T\left(w_2(x), x = \frac{L}{10}\right) + P1 \quad \textbf{(19)}$$

$$M\left(w_1(x), x = \frac{L}{10}\right) = M\left(w_2(x), x = \frac{L}{10}\right) \quad \textbf{(20)}$$

$$w_1(x)\left(x = \frac{L}{10}\right) = w_2(x)\left(x = \frac{L}{10}\right) \quad \textbf{(21)}$$

$$\frac{dw_1(x)}{dx}\left(x=\frac{L}{10}\right)=\frac{dw_2(x)}{dx}\left(x=\frac{L}{10}\right) \quad (22)$$

On the left end of the beam:

$$M(w_1(x), x=0)=0 \quad (23)$$

$$T(w_1(x), x=0)=0 \quad (24)$$

Have been created graphics to show the trend of these variables (bending moment, shear force, displacement) along the beam, and the tables illustrate the main values of the beam.

Table 3: Parameters of the beam

C1_1	C2_1	C3_1	C4_1	C1_2	C2_2	C3_2	C4_2
-0.00032	0.005325	-0.00032	0.005975	0.002163	0.002179	0.003644	0.009114

H	B	L	L1	L2	E	J
[m]	[m]	[m]	[m]	[m]	[kPa]	[m^4]
1	1	5	1	4	30000000	0.083333

EJ	λ	λ*L	k	P1	P2	Δx
[kNm^2]	[m^{-1}]	[-]	[kN/m^3]	[kN]	[kN]	[m]
2500000	0.116214	0.581072	1824.064	100	100	0.1

Tmax	Tmin	Mmax	Mmin	Wmax	Wmin
[kN]	[kN]	[kNm]	[kNm]	[w]	[w]
20.4727	-79.5273	10.25935	-147.808	0.011299	0.010759

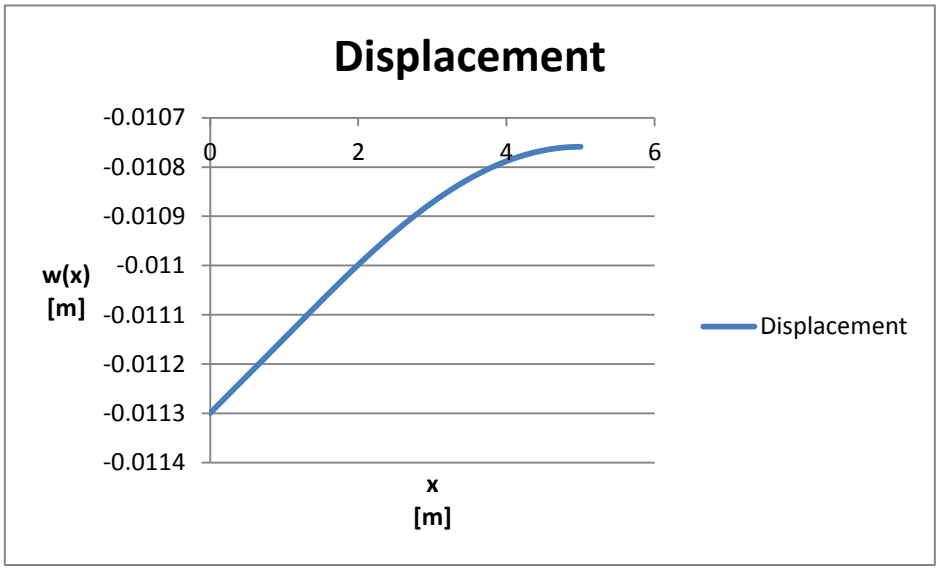

Figure 11: Displacement (analytical)

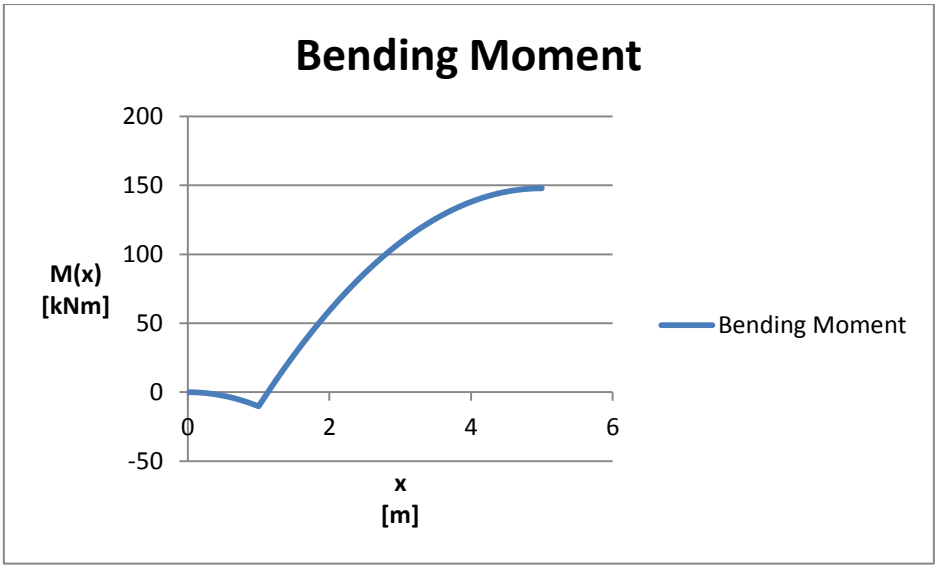

Figure 12: Bending moment (analytical)

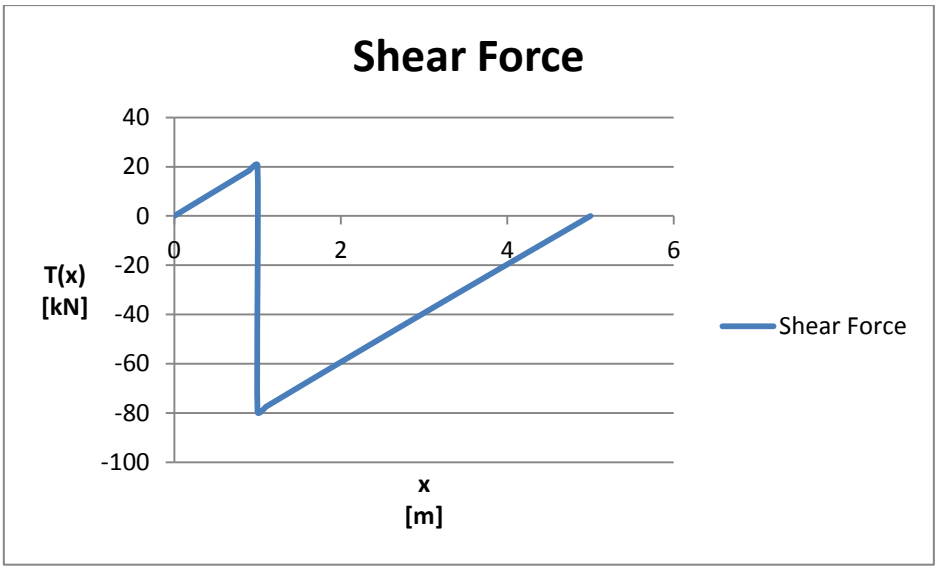

Figure 13: Shear force (analytical)

1.1.5 Beam on 2D model

The results obtained with the analytical model, that's to say from mathematical solution, are compared with the ones from 2D models done by GeoStudio FEM program. The soil has been assumed as linear elastic material (chapter 1.3.1): the parameters are the Young's modulus E, the self-weight γ and the Poisson's ration ν. Also the cohesion and friction angle are taken into account as data in this model: they aren't used in the solution but the Contour program uses them as well as Mohr-Coulomb failure criterion to better illustrate yield regions; in fact in this way the lack of a yield value, that cannot be defined in a linear elastic model and could cause unrealistic strains in the calculation, is filled, and the theoretical yield stresses may be compared visually with shear stresses obtained by the calculation [5].

Table 4: Parameters of the soils and of the beam

SAND				CLAY			
H	γ	ν	Es	H	γ	ν	Es
[m]	[kN/m^3]	[-]	[kPa]	[m]	[kN/m^3]	[-]	[kPa]
5	0	0.3	37x10^3	5	0	0.3	8x10^3

BEAM						
Eb	L	A	J	P1	P2	q
[kPa]	[m]	[m^2]	[m^4]	[kN]	[kN]	[kN/m]
30x10^6	10	1	0.083333	100	100	20

In the following chapters different models of the same problem will be analyzed and a comparison between them will be made.

1.1.5.1 First model – Beam 1

The first model is based on a beam of 10 meters resting on two layers of soil, 5 meters of depth each, with the same characteristics of the analytical model. The length of the two layers is 30 meters (for a good approximation it's necessary to have at least the same meters of the length of the beam on the right and on the left). The boundary conditions are applied to the borders of the whole macro region, and they fixed the x and y displacements on the base, and fixed the x displacement on the sides. In the following graphics it's possible to check the differences between this model and the analytical one.
A different approach to the discretization has been also considered: in fact first has been made a model ("rough version") in which the discretization is not accurate, so the results are not acceptable. Then a "refined" model has been made: it uses a good discretization, and gives acceptable results. The other two models ("1st and 2nd discretization) show that the previous discretization doesn't need other improvements (that could cause an increase of the computational effort), and is sufficient to describe the situation. The mesh is different according to the level of discretization used, and for the same reason also the size of the elements has been modified in the points where the accuracy of the solution could be increased. In the following examples each level of discretization will be more widely explained.

1.1.5.1.1 Rough version

The mesh has 341 nodes and 300 elements and is composed by 4-noded quadrilaterals and 3-noded triangles, thus the integration points (and the integration orders) are four and three respectively; the approximate global element size is 1 m. There is no increase of discretization at strategic points or along the beam. This mesh has been automatically generated by the program. In this case it's

easy to see how a too simple model gives unacceptable results: the aim is to have an accurate distribution of displacement, bending moment and shear force on the beam: the 4-noded quadrilaterals and 3-noded triangles (default element) can't give adequate information regarding the behavior of the beam element.

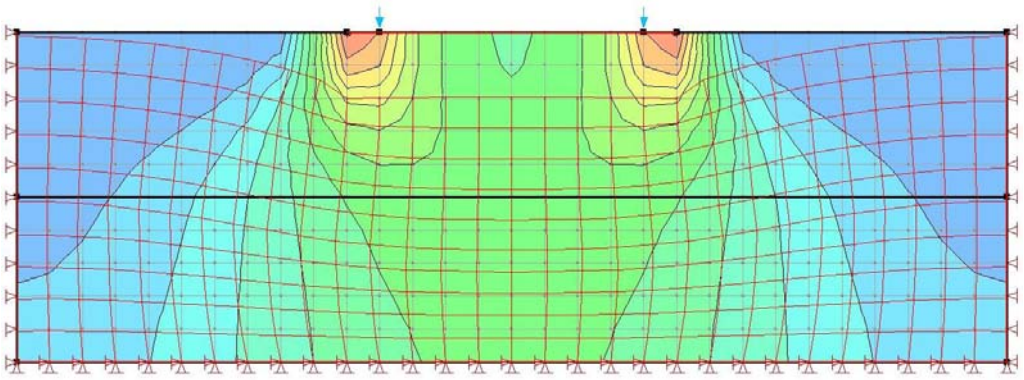

Figure 14: Mesh beam 1 "Rough version"-A

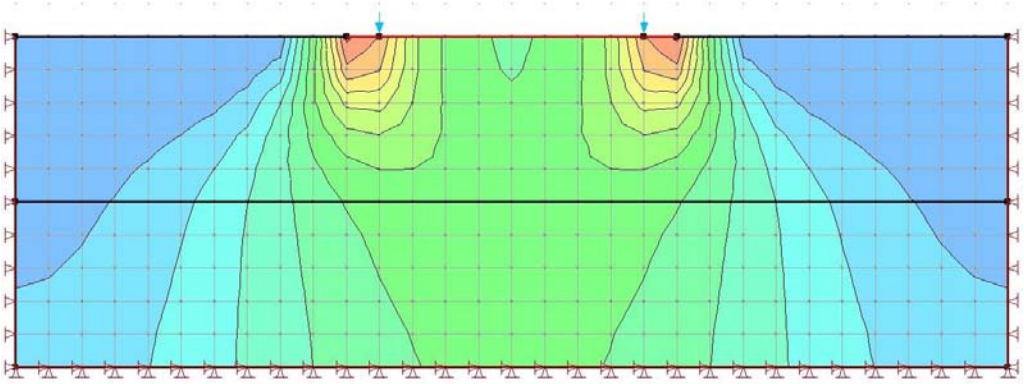

Figure 15: Mesh beam 1 "Rough version"-B

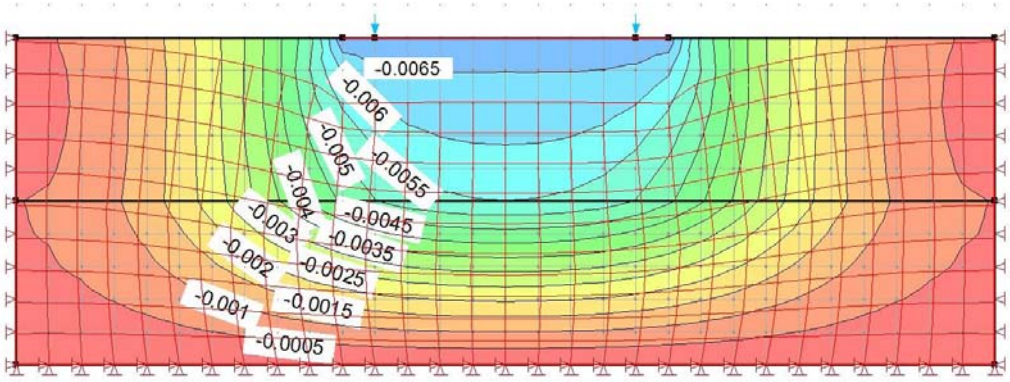

Figure 16: Displacement beam 1 "Rough Version"

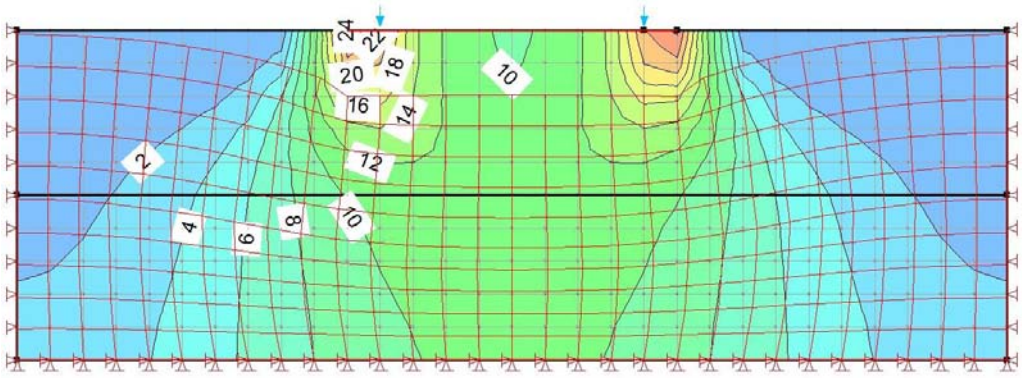

Figure 17: Total stress YY beam 1 "Rough version"

The mesh is too large, too "simple", and because of this the graphics of bending moment, shear force and displacement aren't precise.

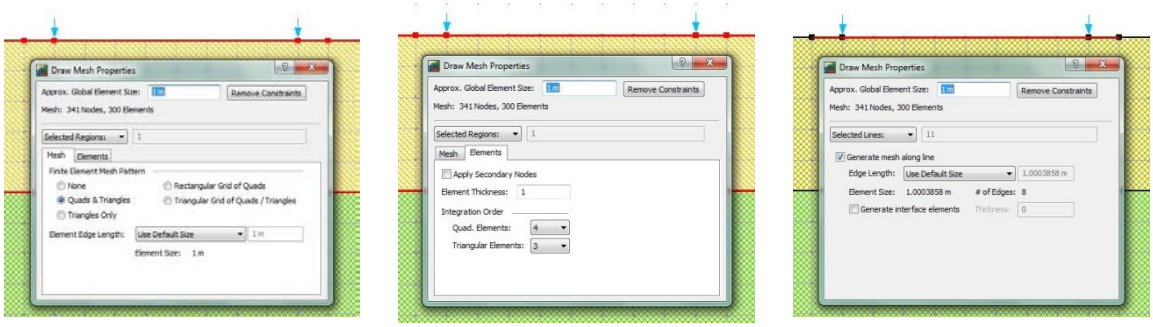

Figure 18: Discretization beam 1 "Rough version"

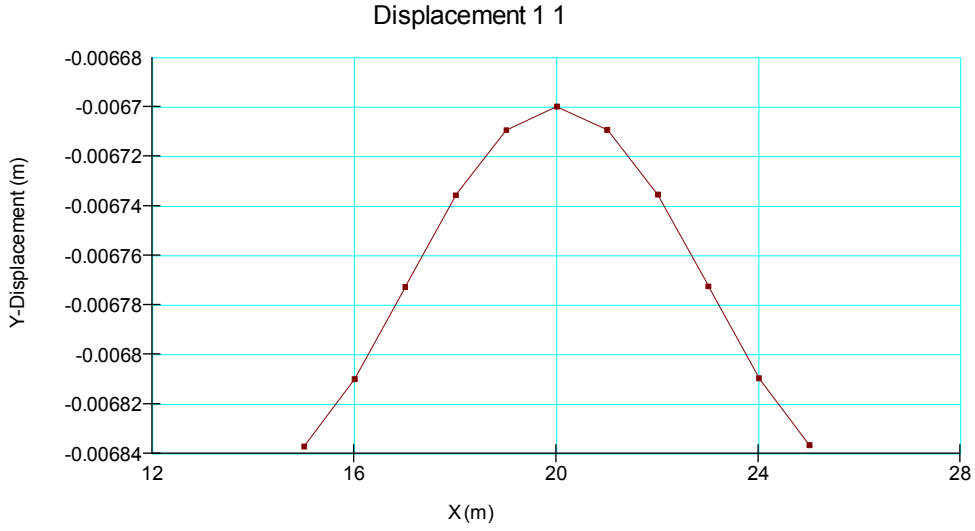

Figure 19: Displacement beam 1 "Rough version"

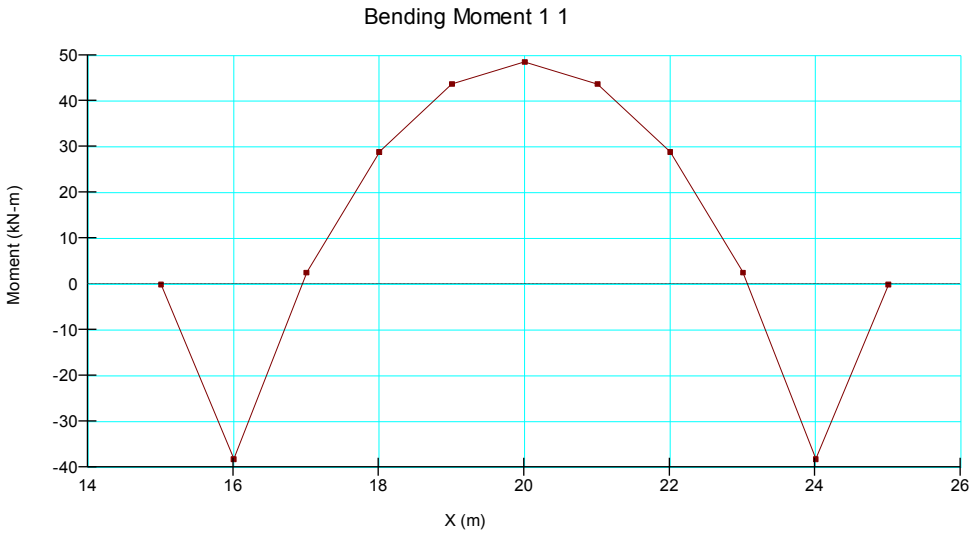

Figure 20: Bending moment beam 1 "Rough version"

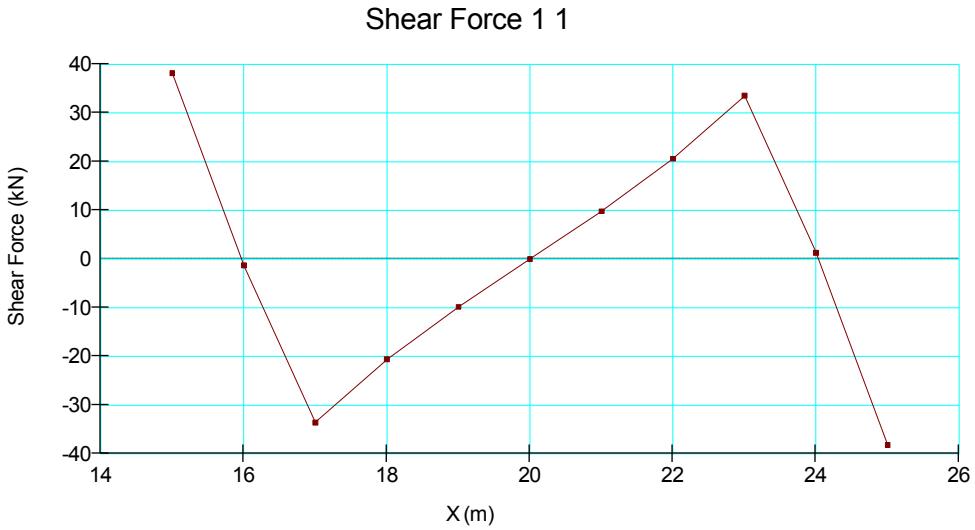

Figure 21: Shear force beam 1 "Rough version"

The problems are more evident for the shear force because it is the third derivative of the displacement, so the error is bigger.

1.1.5.1.2 Refined version

In this model, secondary nodes have been applied to the mesh elements, and their integration order has been increased; the mesh has been generated along the line of the beam, decreasing the size of the mesh elements under the beam and near the most important points of the latter: the edges and the forces' application points. This level of discretization will also be used in the next models. The mesh contains 1434 nodes and 453 elements, and is composed of 8-noded quadrilaterals and 6-noded triangles, thus the integration points (and the integration orders) are four (with nine Gauss points the element would be too rigid) and three respectively; the approximate global element size is 1 m.

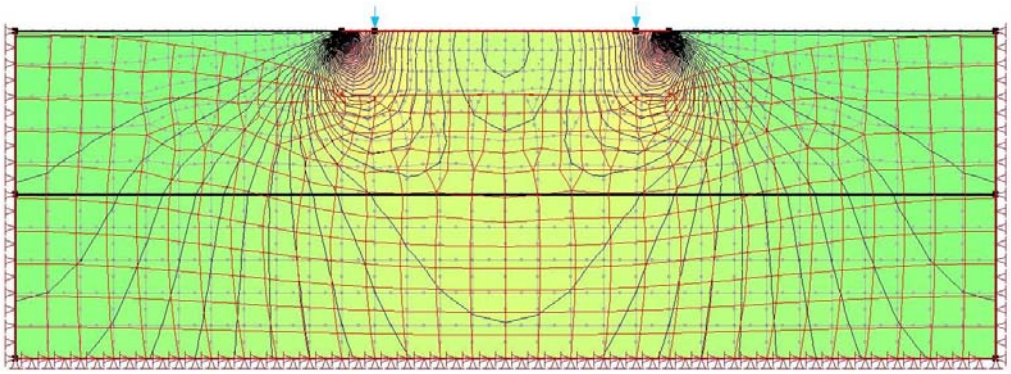

Figure 22: Mesh beam "Refined version"-A

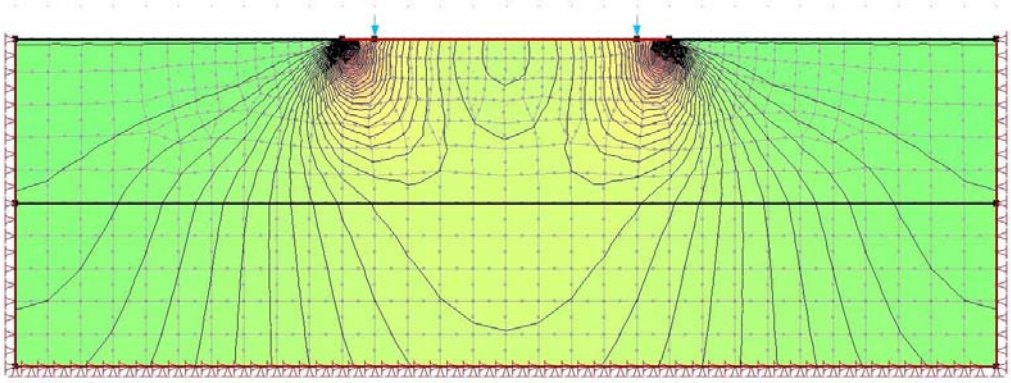

Figure 23: Mesh beam "Refined version"-B

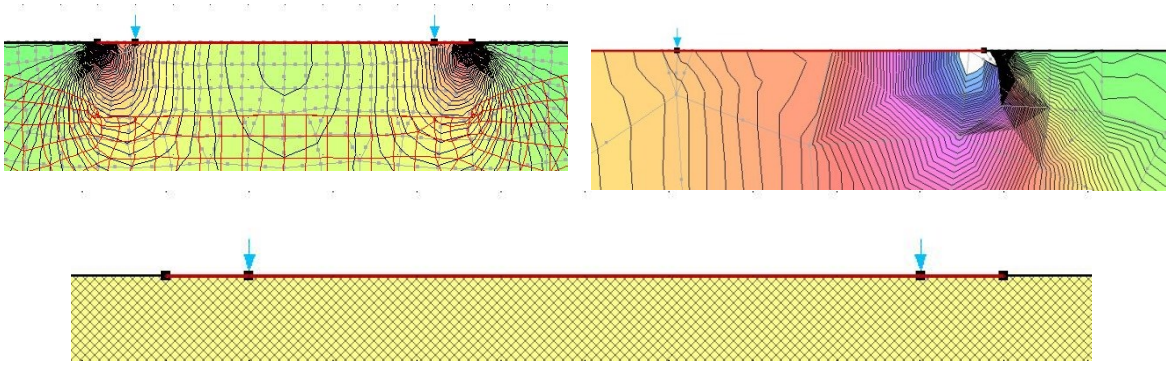

Figure 24: Mesh particular A-B, Beam Model

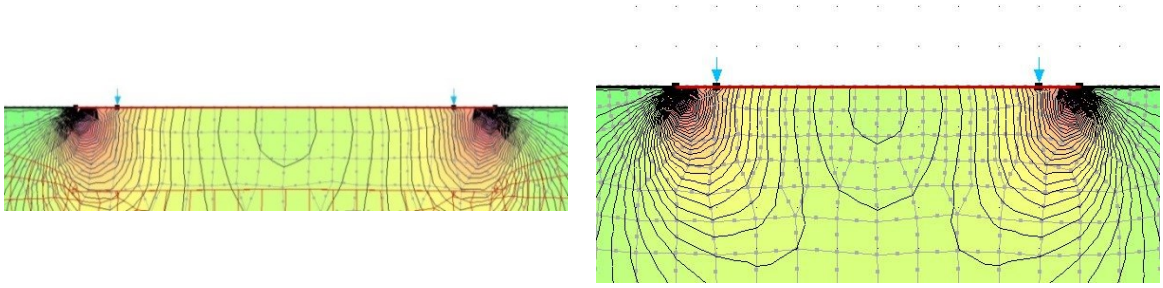

Figure 25: Discretization of mesh A-B

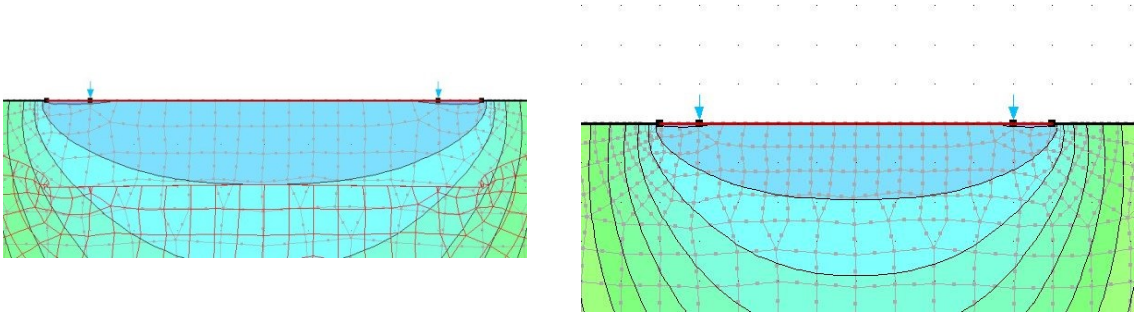

Figure 26: Discretization of mesh C-D

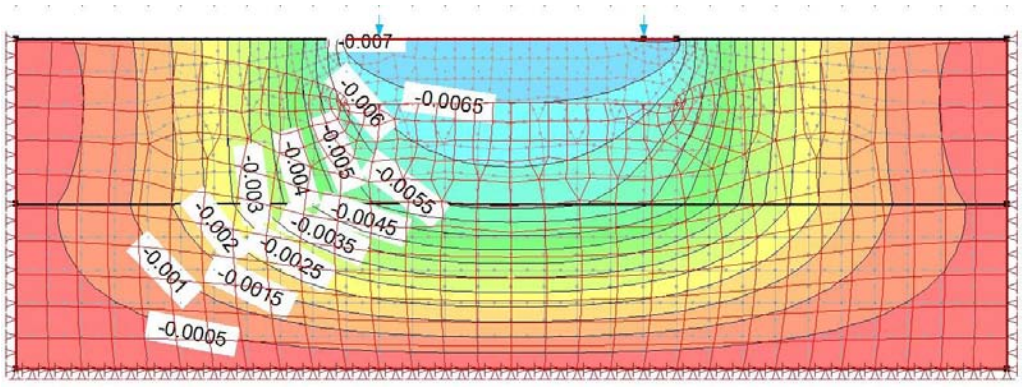

Figure 27: Displacement Beam 1 "Refined version"

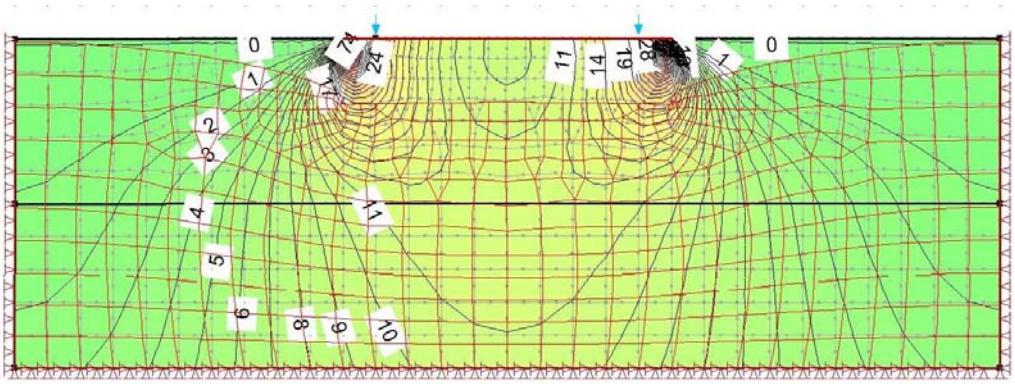

Figure 28: Total Stress YY Beam 1 "Refined version"

This better discretization gives better results; in fact the graphics are much more precise.

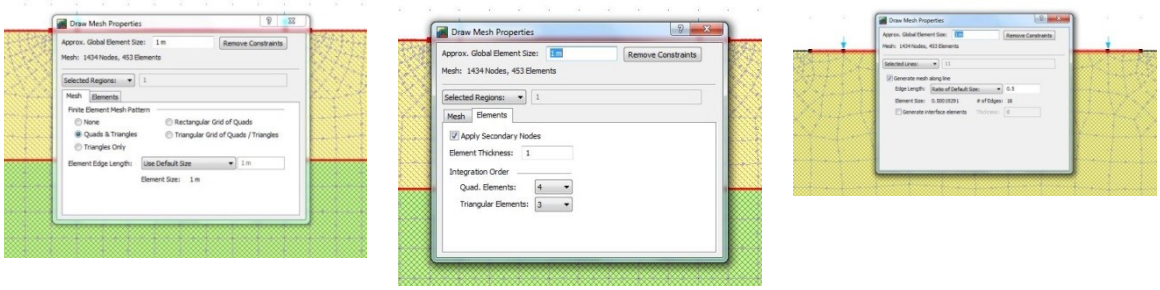

Figure 29: Discretization Beam 1 "Refined version"

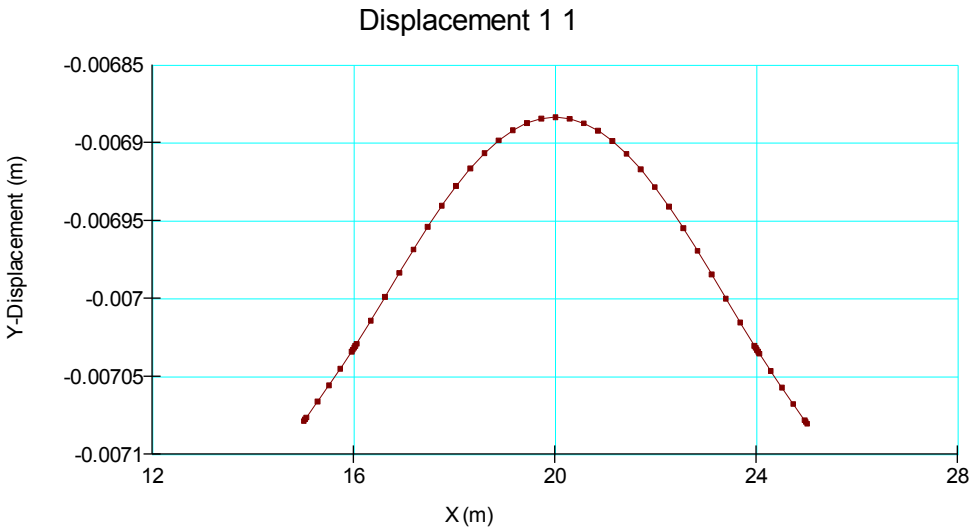

Figure 30: Displacement beam 1 "Refined version"

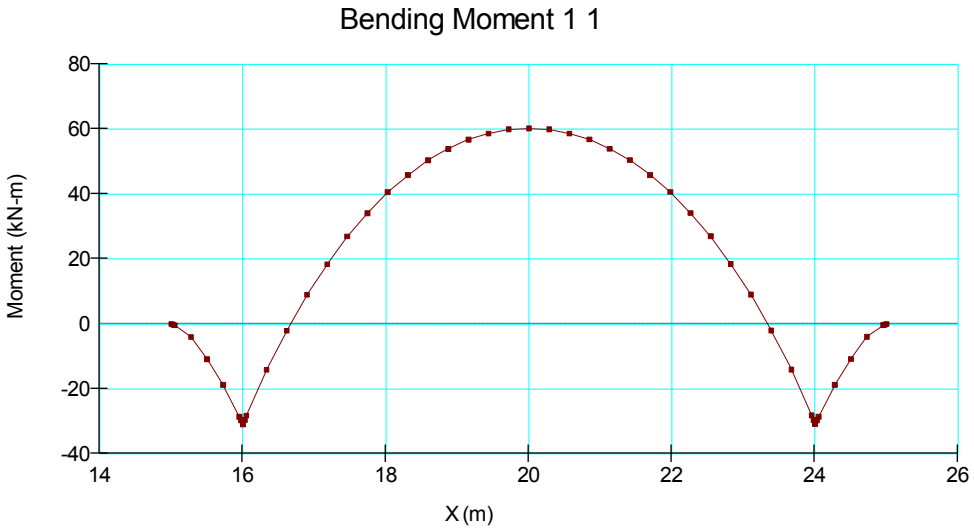

Figure 31: Bending moment beam 1 "Refined version"

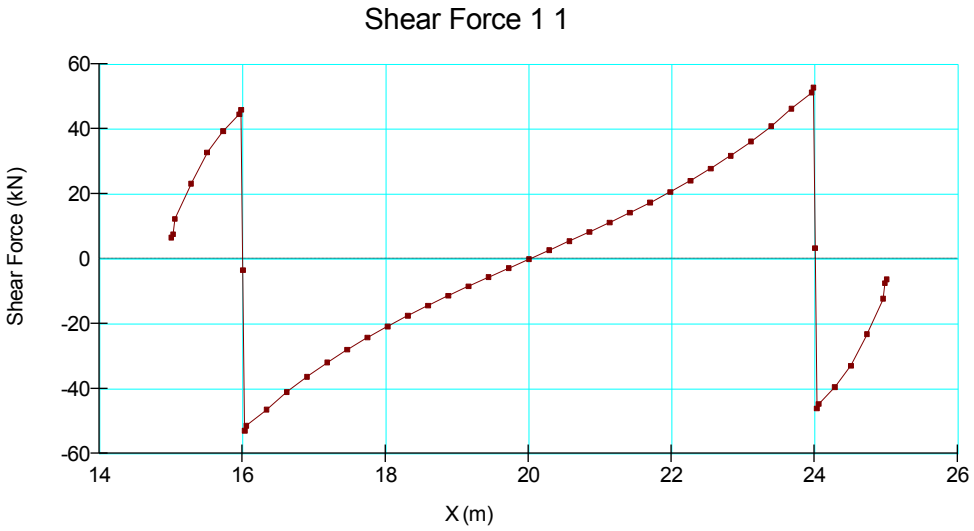

Figure 32: Shear force beam 1 "Refined version"

1.1.5.1.3 1st discretization

It is quite evident that this discretization does not significantly affect the results of the previous model; this means that the former model was rather accurate: such an accurate discretization is excessively high. The mesh has 5479 nodes and 1778 elements and is composed by 8-noded quadrilaterals and 6-noded triangles, thus the integration points (and the integration orders) are four and three respectively; the approximate global element size is 0.5 m. The computational effort is high and unnecessary.

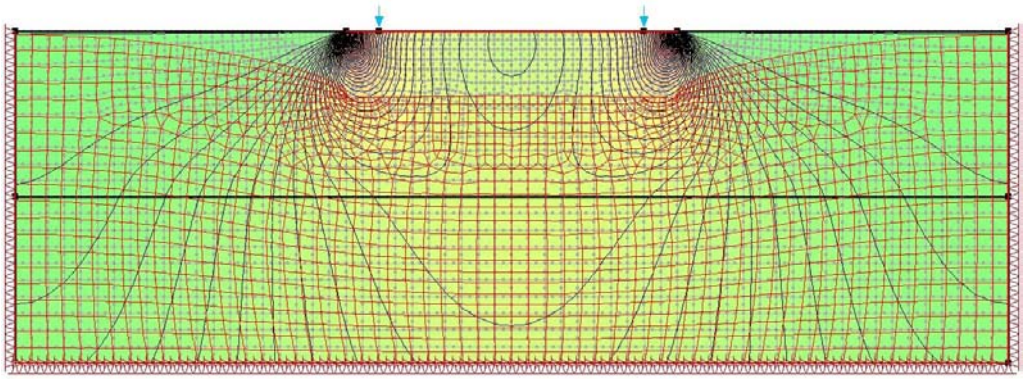

Figure 33: Mesh 1st discretization A

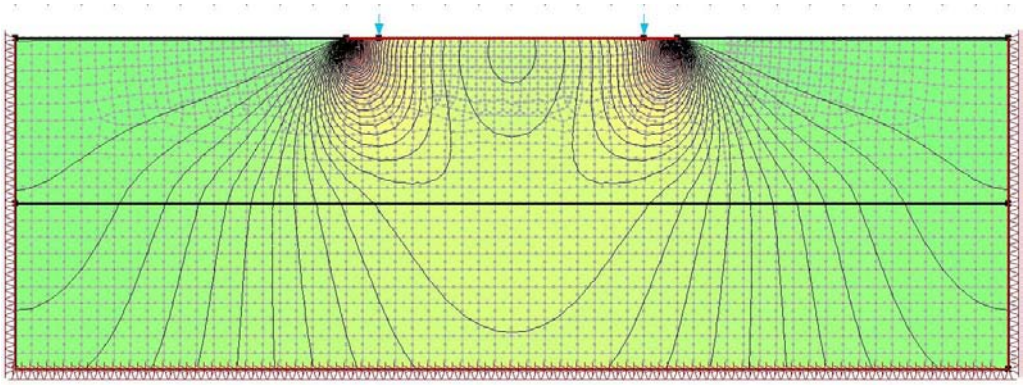

Figure 34: Mesh 1st discretization B

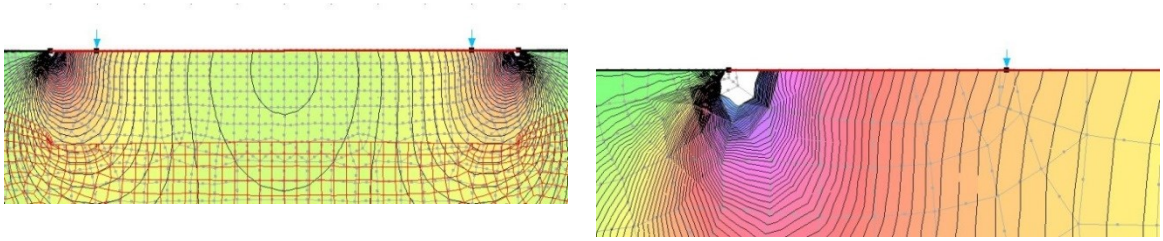

Figure 35: 1st discretization particular A-B

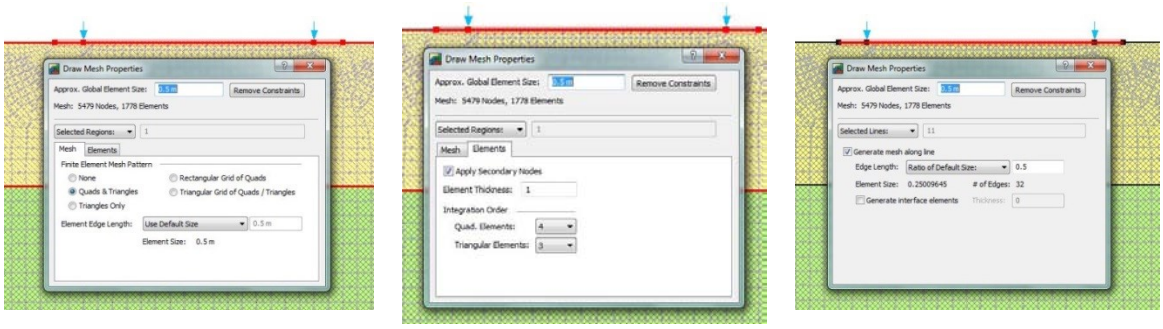

Figure 36: Discretization Beam 1, 1st discretization

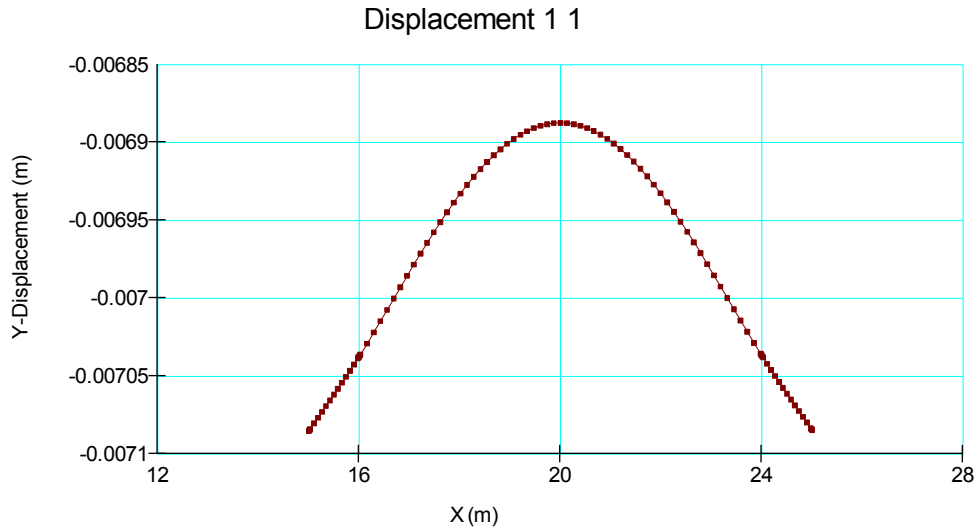

Figure 37: Displacement beam 1 "1st discretization"

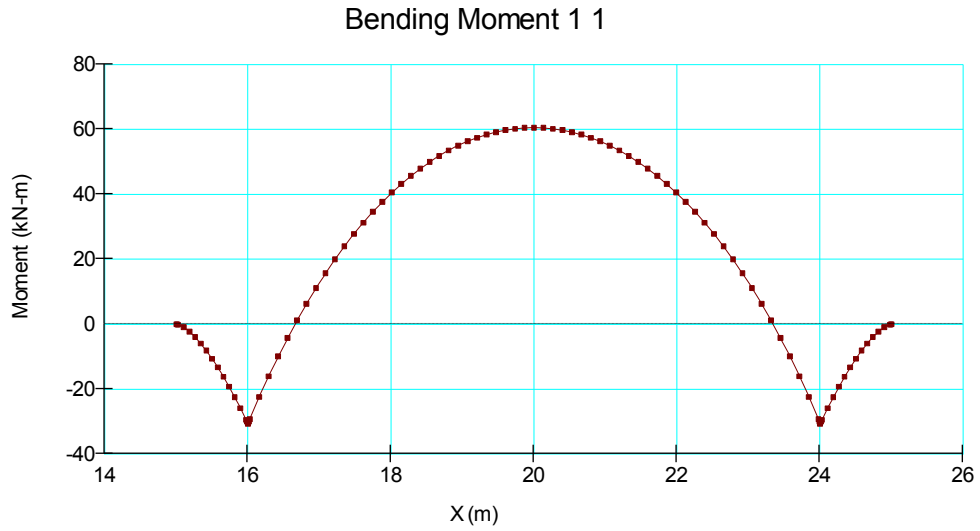

Figure 38: Bending moment beam 1 "1st discretization"

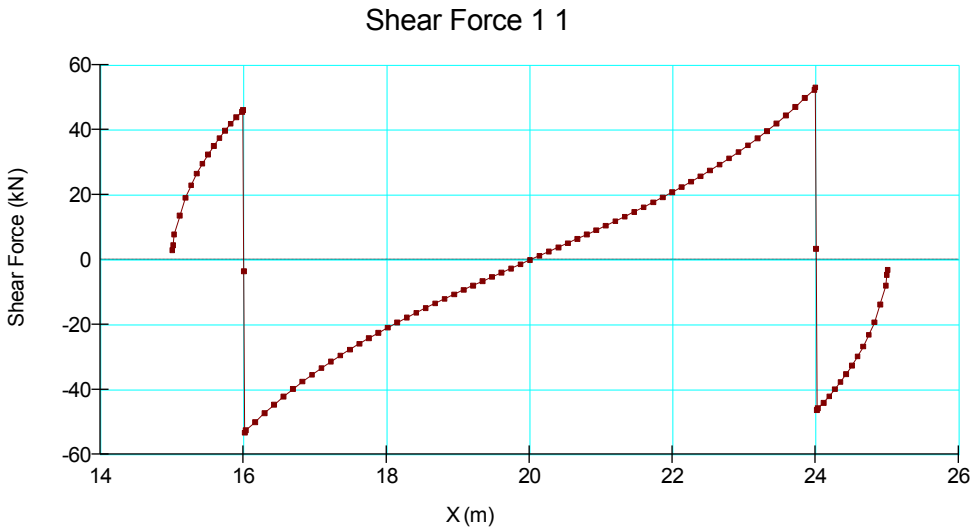

Figure 39: Shear force beam 1 "1st discretization"

1.1.5.1.4 2nd discretization

This discretization is a little less precise than the "refined" one, but nevertheless not so different to have completely incompatible results. The mesh has 459 nodes and 149 elements and it is composed by 8-noded quadrilaterals and 6-noded triangles, thus the integration points (and the integration orders) are four and three respectively; the global element size is 2 m.

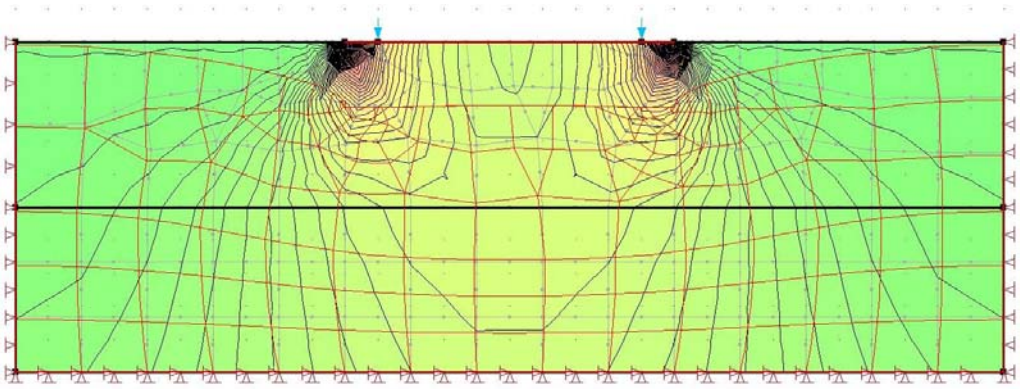

Figure 40: Mesh 2nd discretization A

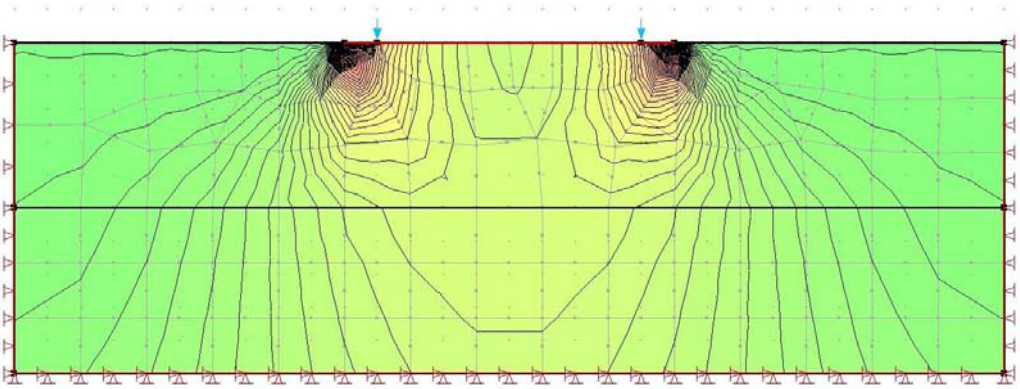

Figure 41: Mesh 2nd discretization A

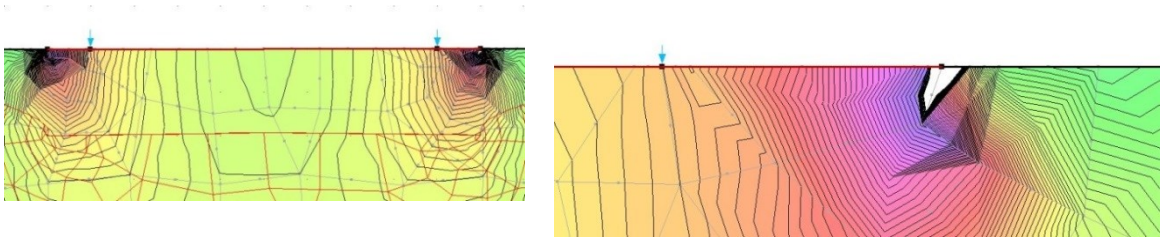

Figure 42: 2nd discretization particular A-B

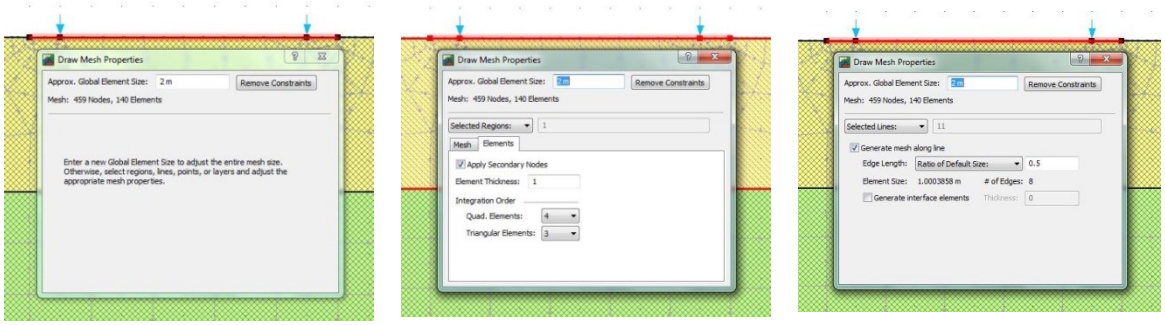

Figure 43: Discretization Beam 1, 2nd discretization

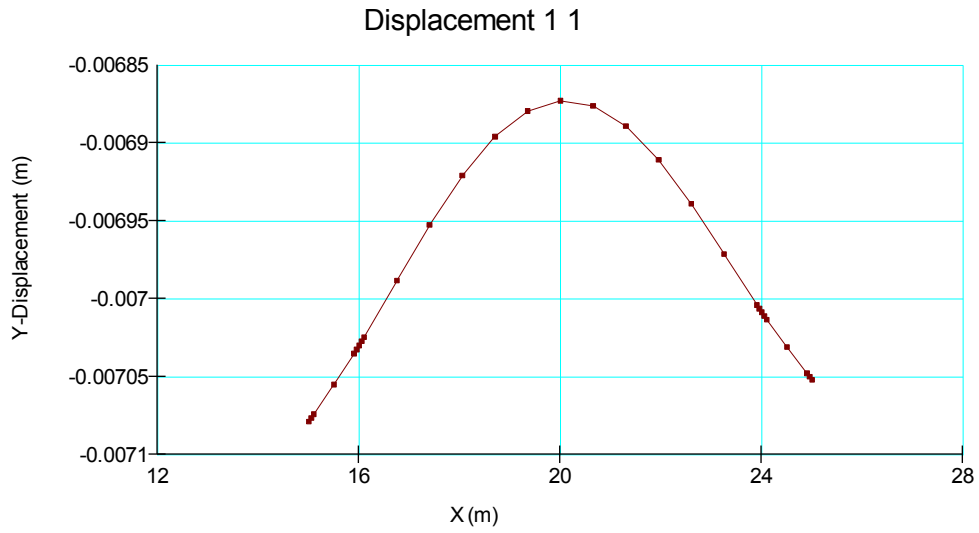

Figure 44: Displacement beam 1 "2nd discretization"

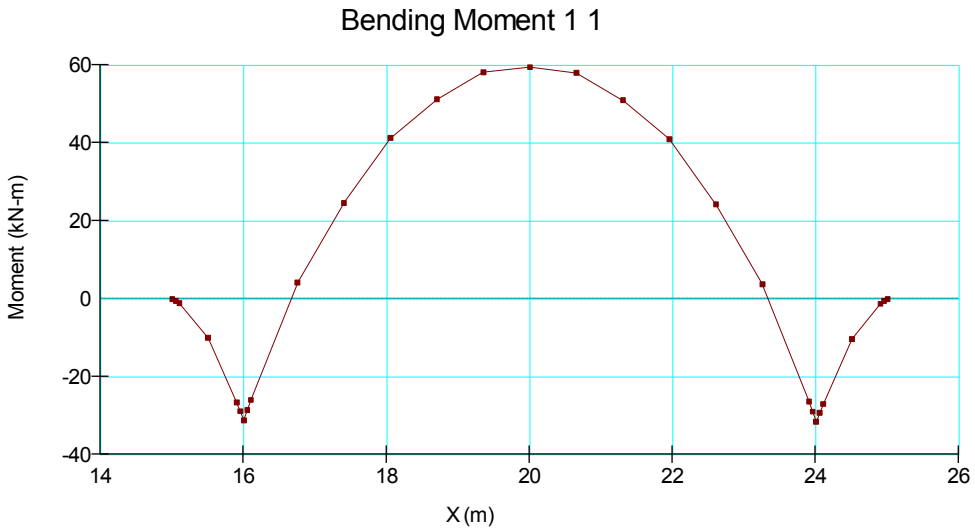

Figure 45: Bending moment beam 1 "2nd discretization"

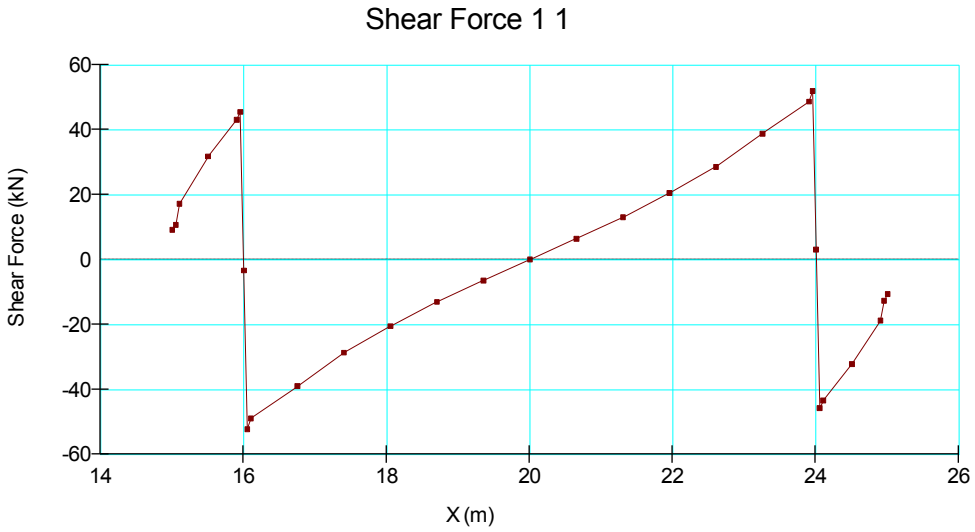

Figure 46: Shear force beam 1 "2nd discretization"

1.1.5.1.5 Comparison of results from various discretizations

In these graphics it's possible to check how the difference between the last three models is not significant: on the contrary the first "rough" model is too simple. After this comparison the "refined version" has been chosen as the most suitable to describe the problem, and it is also cost effective for the computational calculation.

Regarding the displacement in the right hand side of the beam, it's interesting to notice the difference between "1st discretization", "refined" and "2nd discretization", probably due to a numerical error.

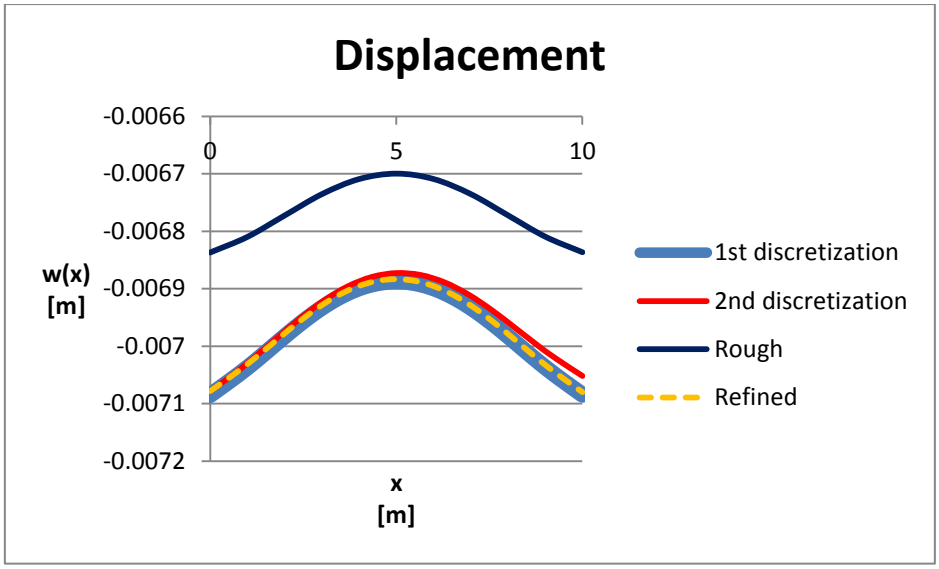

Figure 47: Displacement, different discretization

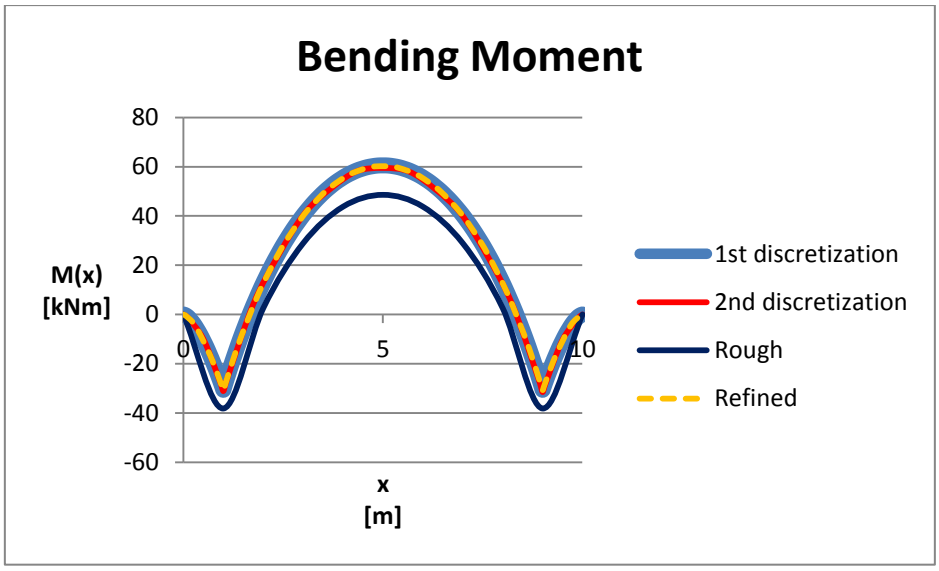

Figure 48: Bending foment, different discretization

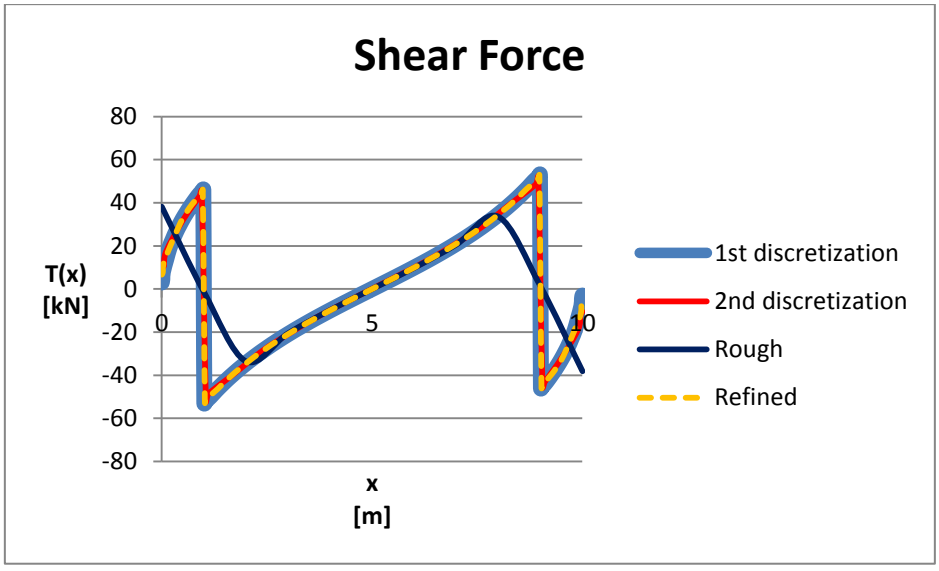

Figure 49: Shear force, different discretization

1.1.5.1.6 Comparison with analytical result

Considering the "refined version" as the correct solution for the 1st model a comparison between the analytical solution and that obtained with GeoStudio has been made.

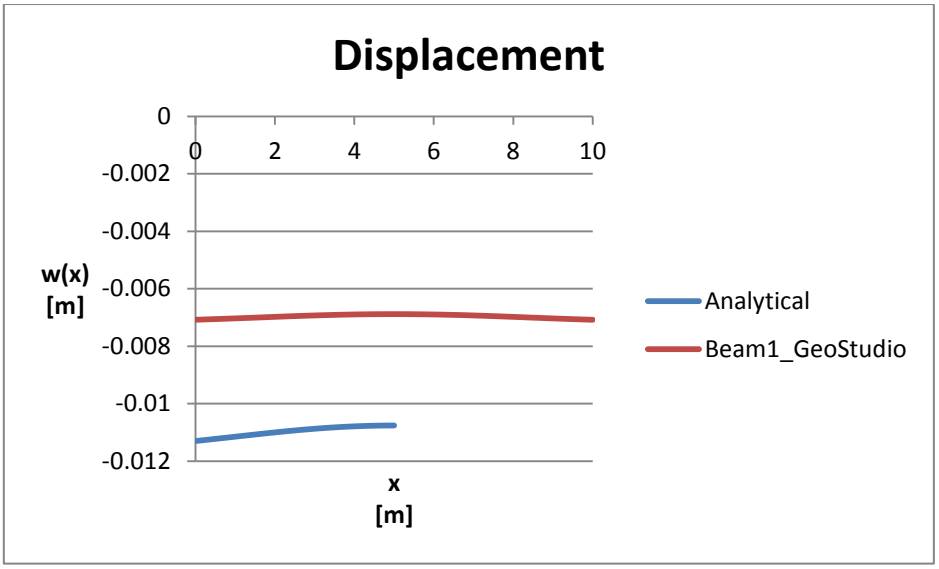

Figure 50: Displacement, Analytical-beam 1 GeoStudio

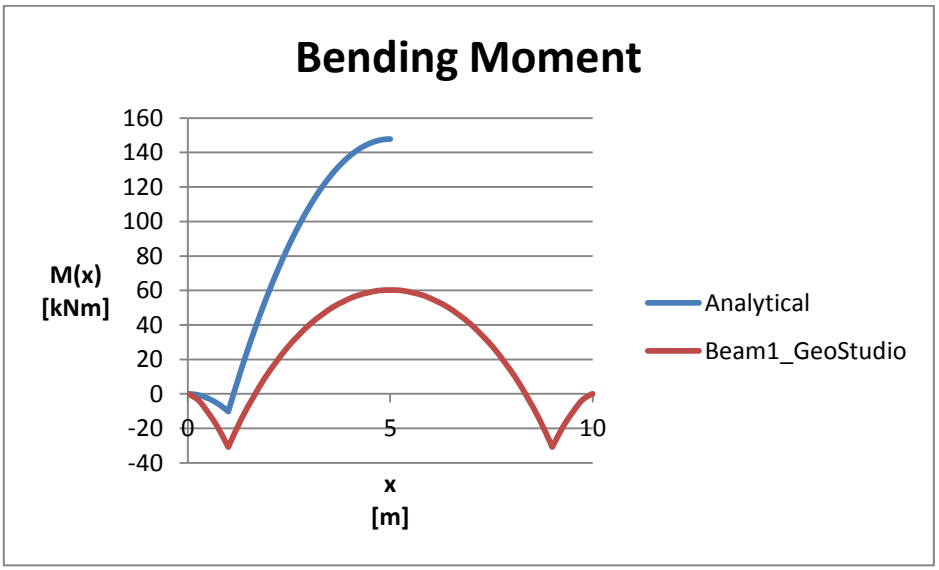

Figure 51: Bending Moment, Analytical -beam 1 GeoStudio

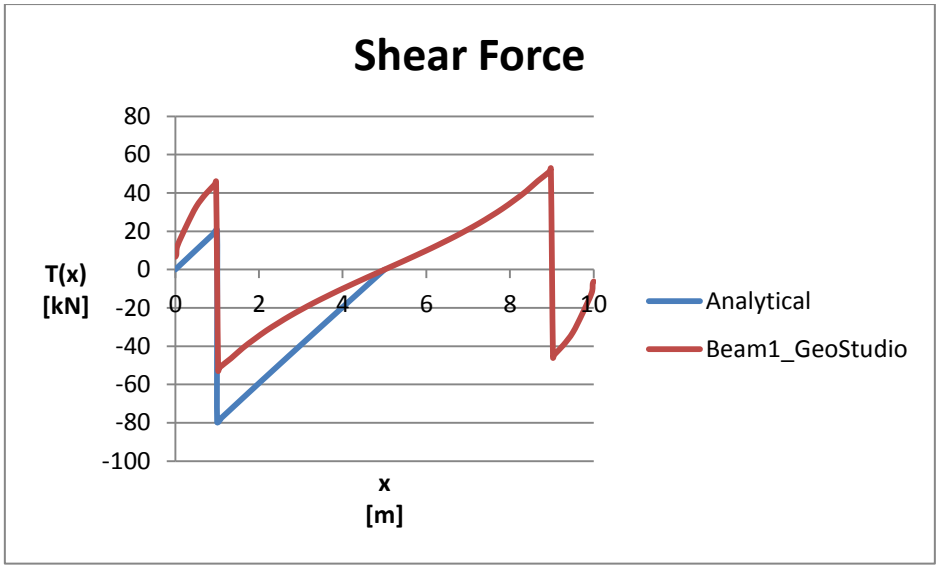

Figure 52: Shear force, Analytical -beam 1 GeoStudio

1.1.5.2 Second model – Beam 2

The second model represent half beam, that's to say 5 meters only , and as boundary condition on the section of division it's been created a proper beam, a "link", with a stiffness of an order of magnitude more than that of the previous beam, in this way the conditions of the complete beam are fulfilled. The soil below the beam is divided into two layers of 5 meters each, the characteristics are the same of the previous examples. The solution completely matches the previous one, thus it hasn't been represented.

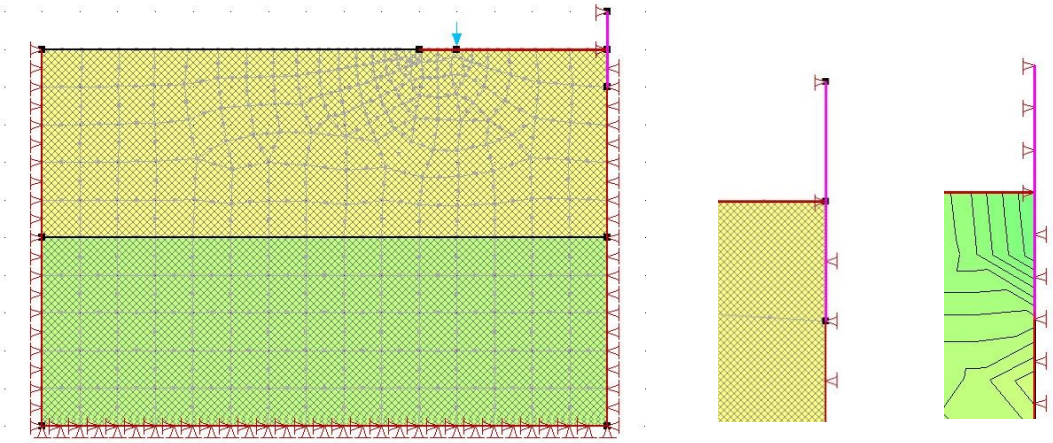

Figure 53: Mesh beam 2, rigid link 1, rigid link 2

1.1.5.3 Third model – Beam 3N

The third model (where "N" is for "normal") is completely different from the former ones, because in this case hasn't been used the soil below the 10 m beam, but the beam is free. In order to have the same conditions of the soil this beam has as boundary conditions, in addition to the forces, Winkler's springs acting on each node of the beam. The constant of the springs is the one obtained from the analytical model: the influence length of the concentrated spring is 1 m.
In this model and in all the models with "springs", the bending moment has opposite values compared to those of the solution with no springs due to the sign convention: consequently, in the comparison with the other solutions the diagram of the aforementioned stress parameter has been inverted. These are the results.

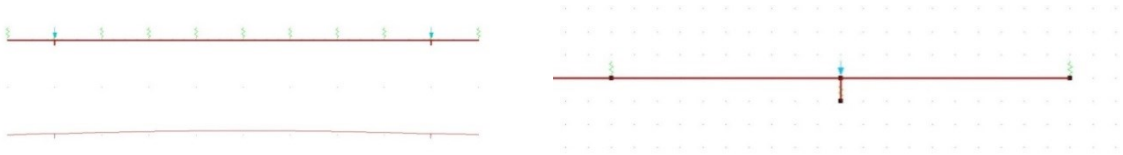

Figure 54: Mesh beam 3N, trick

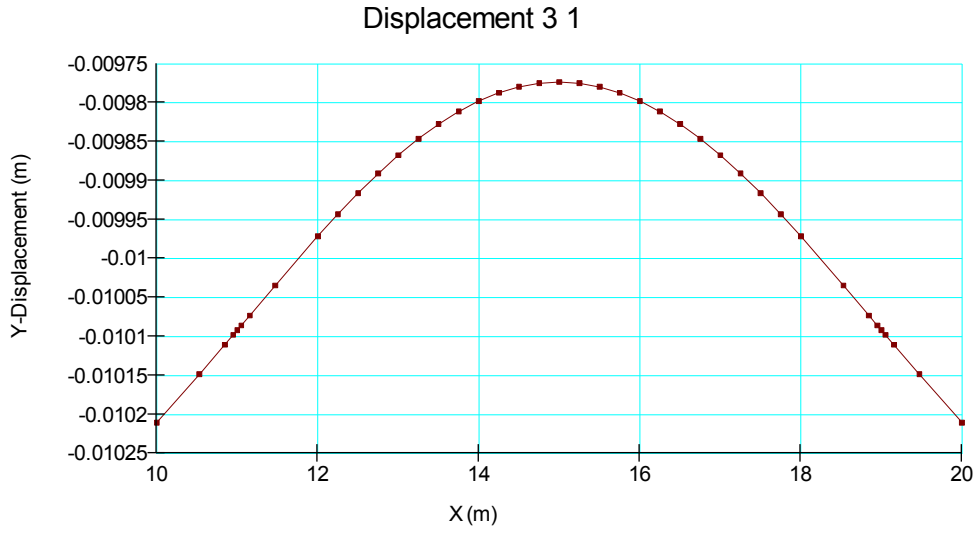

Figure 55: Displacement beam 3N

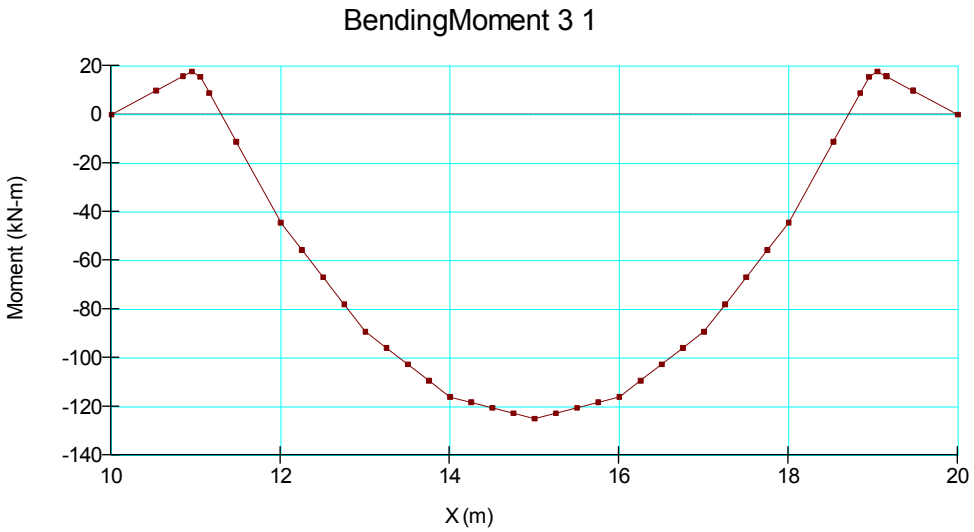

Figure 56: Bending moment beam 3N

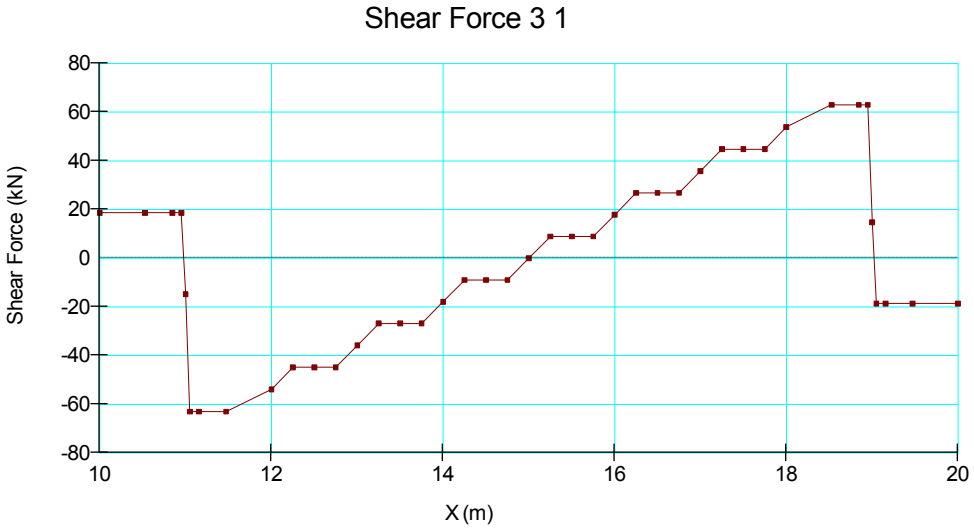

Figure 57: Shear force beam 3N

1.1.5.3.1 Comparison with analytical result

As for the previous chapter the following graphics compare the analytical solution and Geostudio; in order to have a suitable comparison between the two solutions the bending moment's diagram obtained with GeoStudio will be inverted.

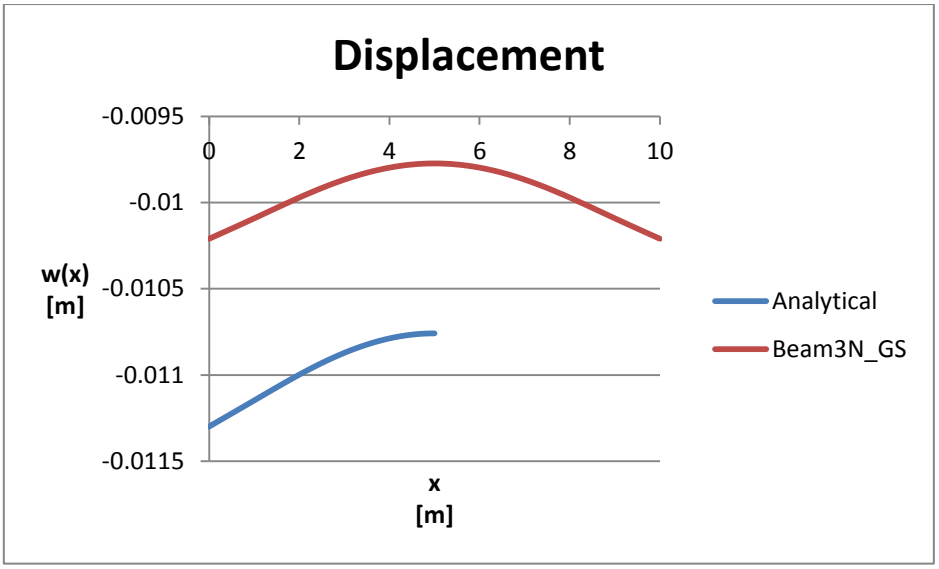

Figure 58: Displacement, Analytical-beam 3N GeoStudio

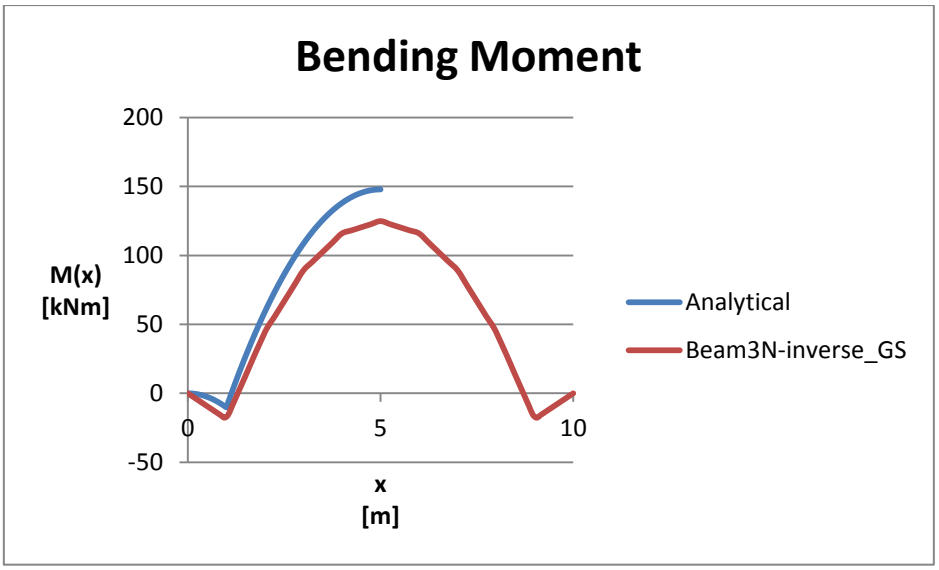

Figure 59: Bending moment, Analytical-beam 3N GeoStudio

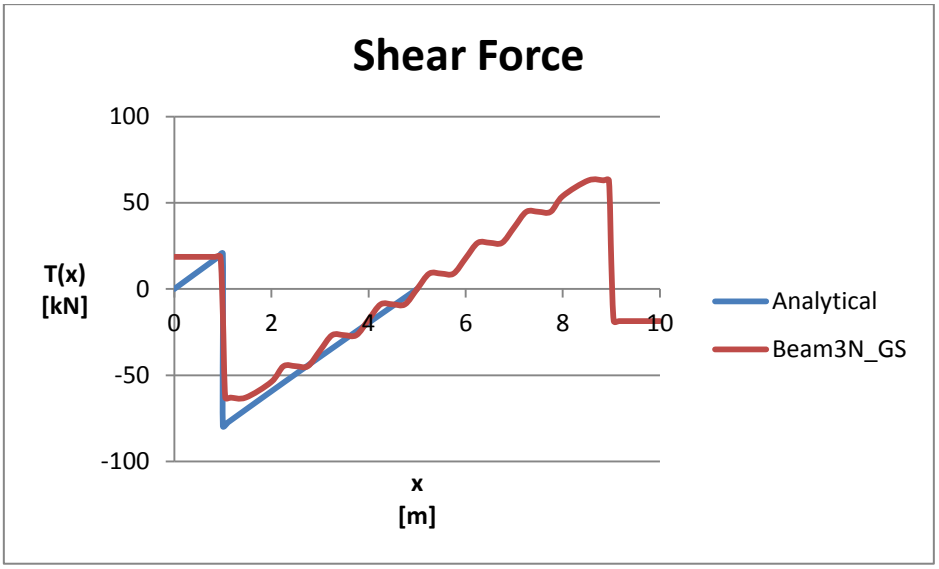

Figure 60: Shear force, Analytical-beam 3N GeoStudio

1.1.5.4 Fourth model – Beam 3BD

The fourth model (where "BD" is for "better discretization") is the same of the previous one, but with a better discretization: in fact each spring is applied on an area of 0.1 cm multiplied by 1 m, so the value of the k of each spring is equal to the value of the former k divided by ten.
The solution is shown below.

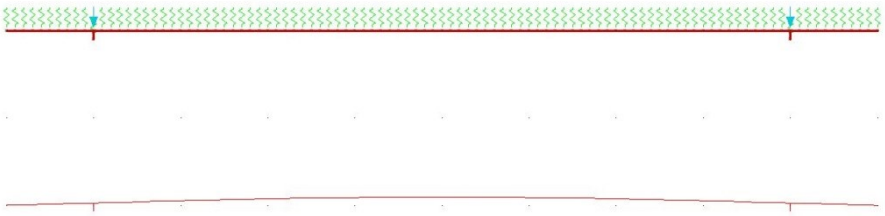

Figure 61: Mesh beam 3BD

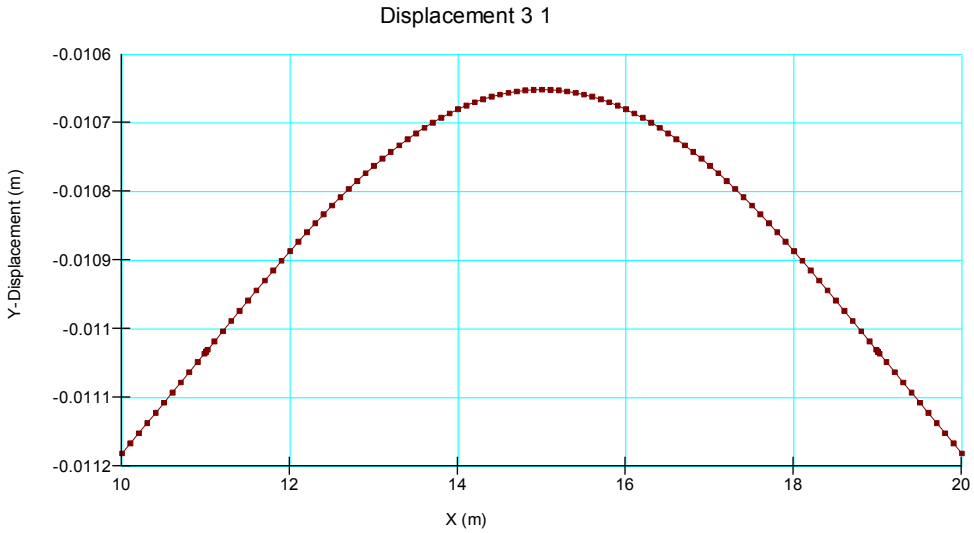

Figure 62: Displacement beam 3BD

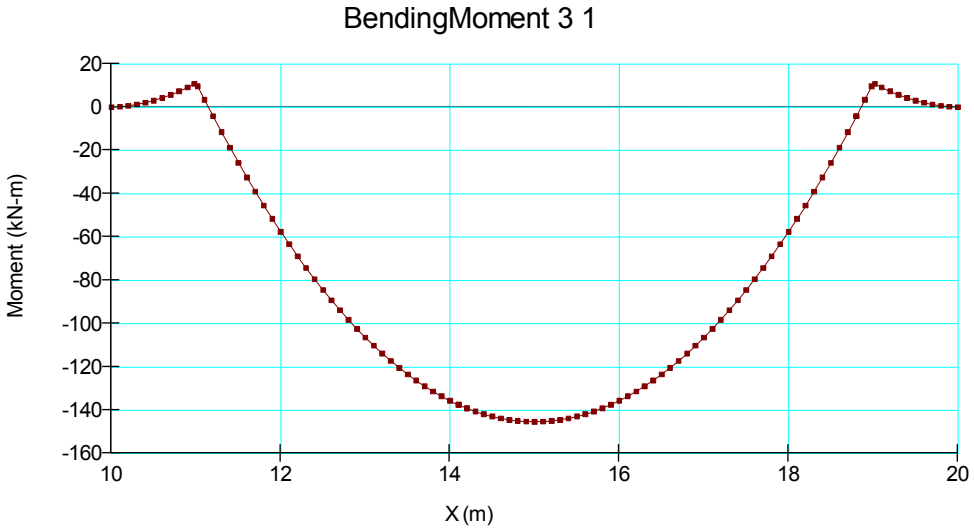

Figure 63: Bending moment beam 3BD

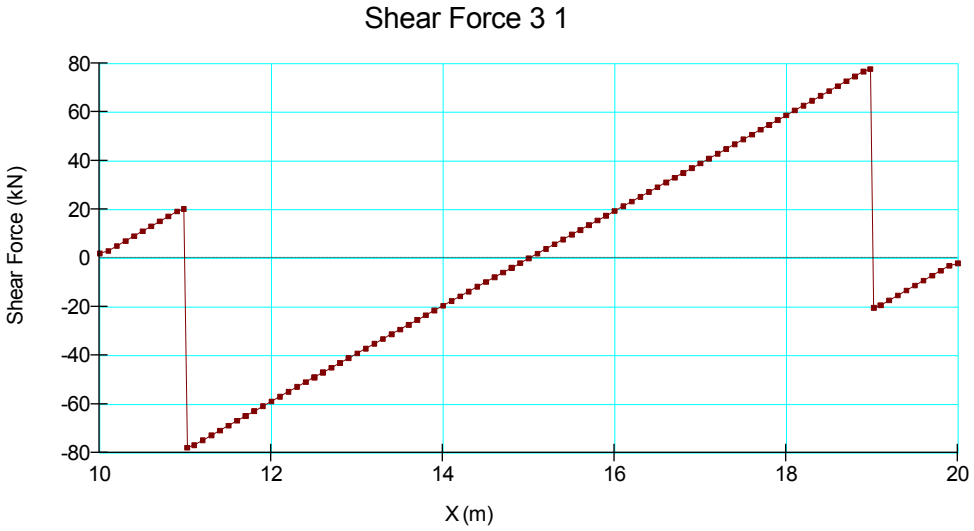

Figure 64: Shear force beam 3BD

1.1.5.4.1 Comparison with analytical result

Graphics with a comparison between the results obtained with the analytical solution and with GeoStudio will be proposed. As for the former chapter the bending moment's diagram obtained with GeoStudio will be inverted. These solutions match almost perfectly because both of them adopt the same "k", and because the distribution of the springs along the beam is thicker.

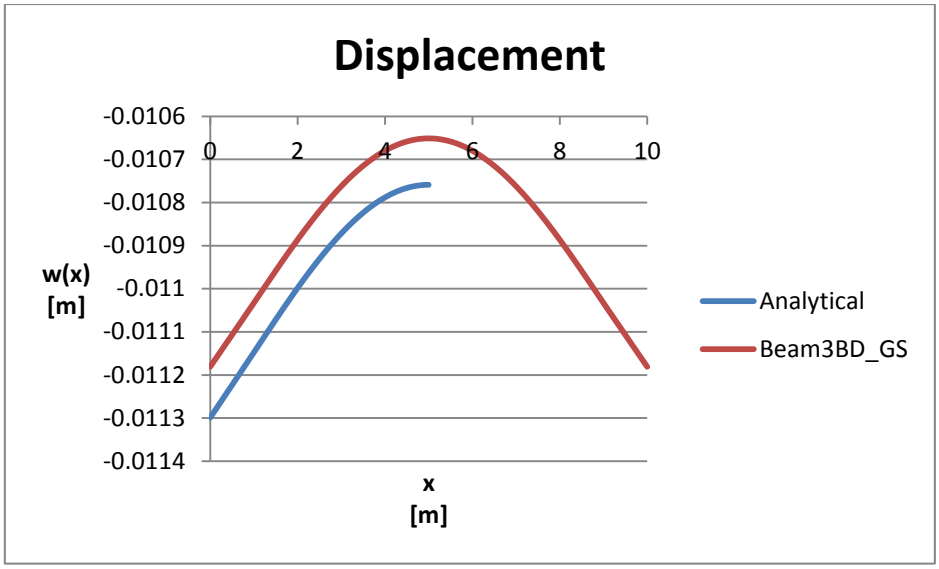

Figure 65: Displacement, Analytical-beam 3BD GeoStudio

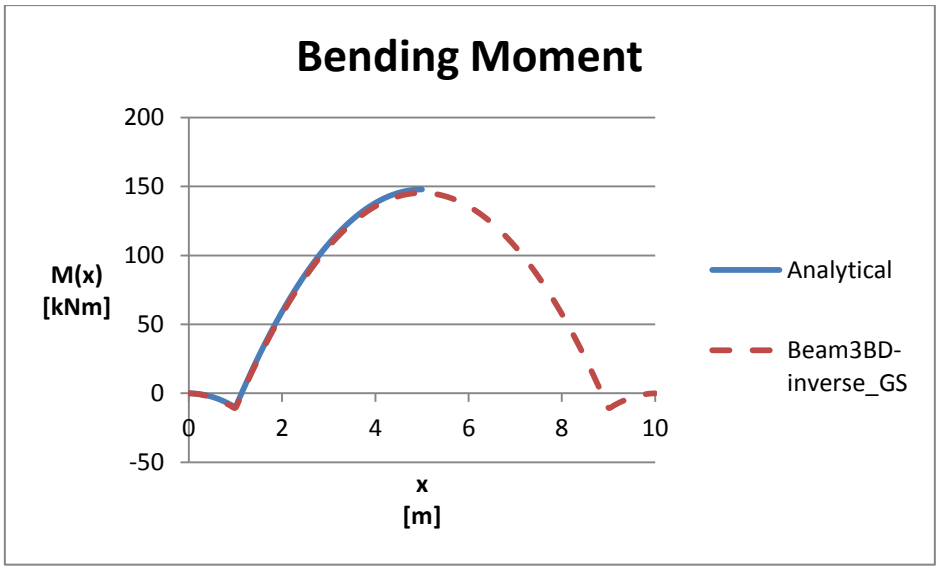

Figure 66: Bending moment, Analytical-beam 3BD GeoStudio

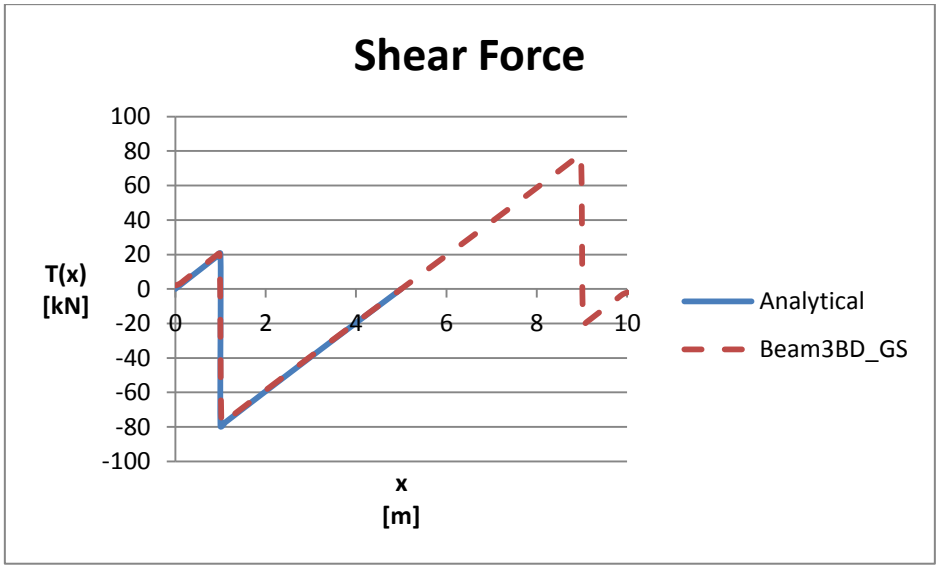

Figure 67: Shear force, Analytical-beam 3BD GeoStudio

1.1.5.5 Fifth model – Beam 4N

The fifth model (where "N" is for "normal") represents the same situation of the third, but only half beam with a link as boundary condition (as the second model) has been created, the springs replace the soil.
The results are the following.

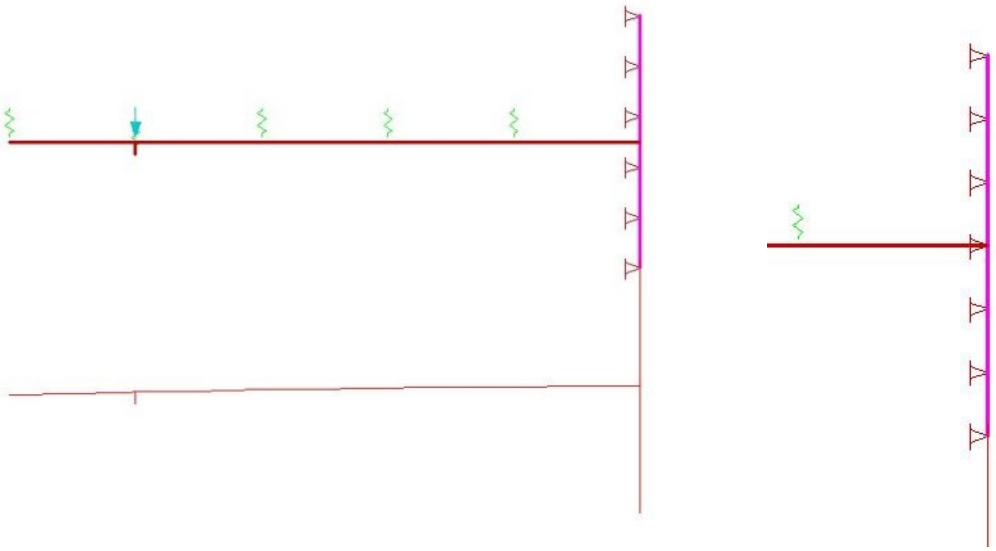

Figure 68: Mesh beam 4N, rigid link 3

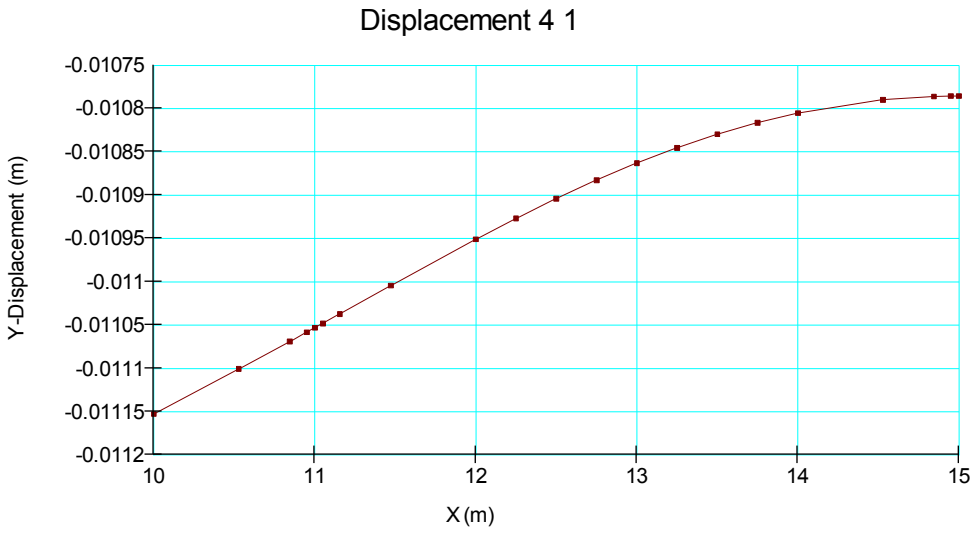

Figure 69: Displacement beam 4N

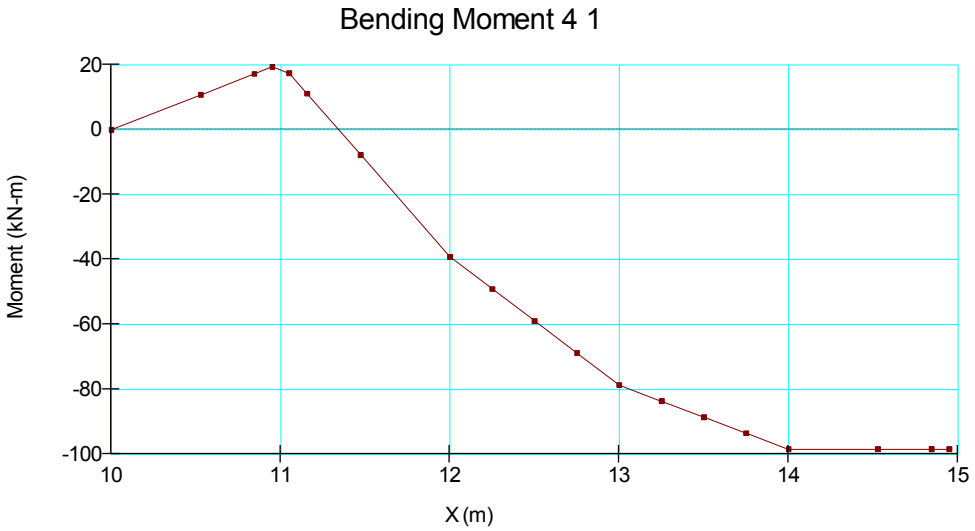

Figure 70: Bending moment beam 4N

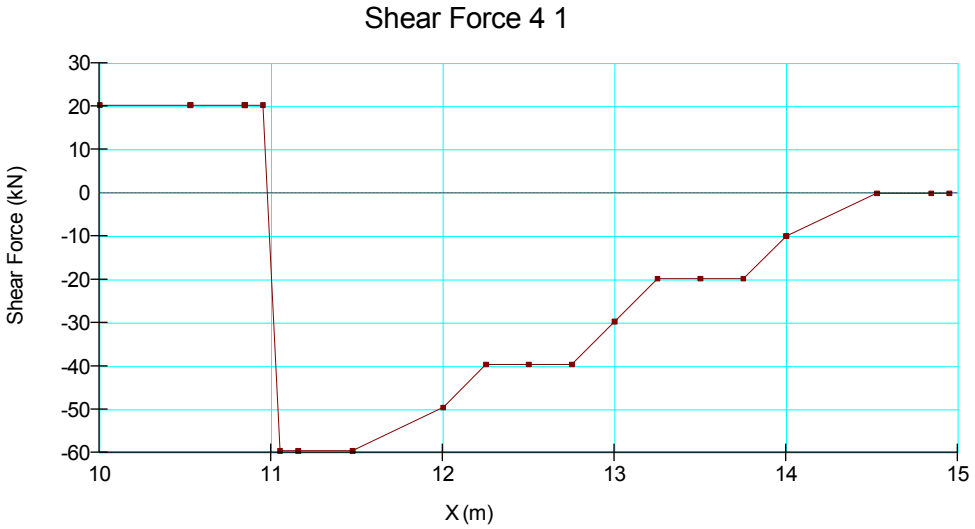

Figure 71: Shear force beam 4N

1.1.5.5.1 Comparison with analytical result

As for the former chapters, a comparison between the solution obtained with analytical solution and the one obtained with GeoStudio will be proposed. As in the previous graphics the GeoStudio's bending moment's diagram will be inverted.

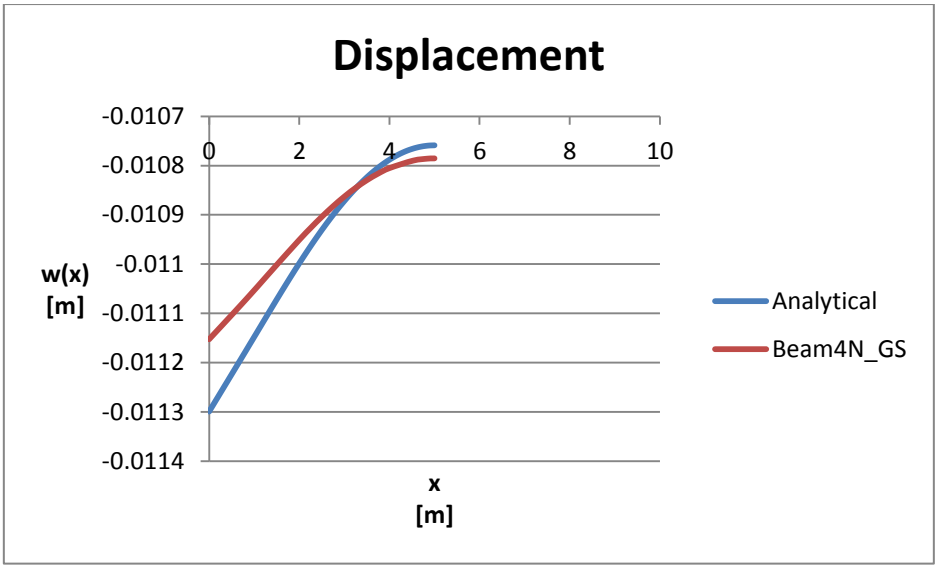

Figure 72: Displacement, Analytical-beam 4N GeoStudio

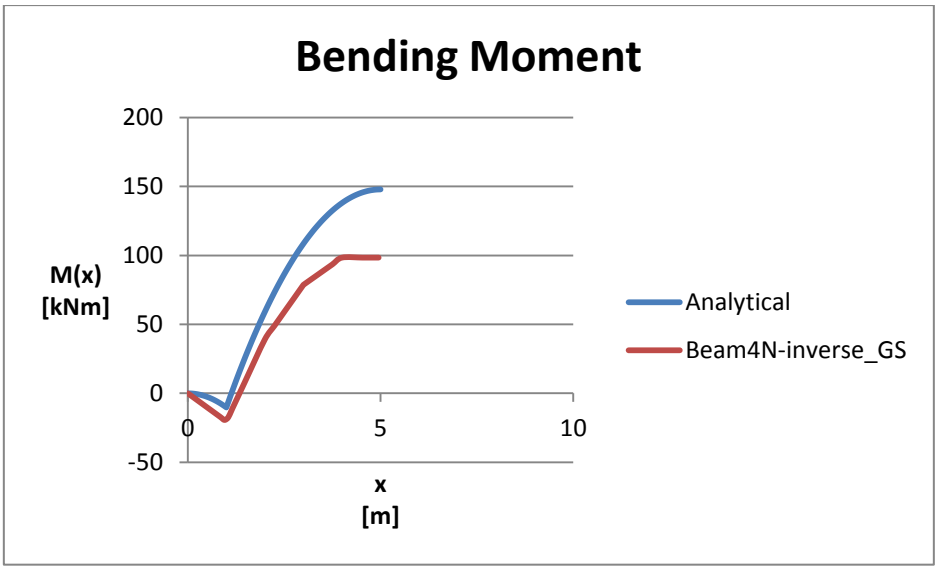

Figure 73: Bending moment, Analytical-beam 4N GeoStudio

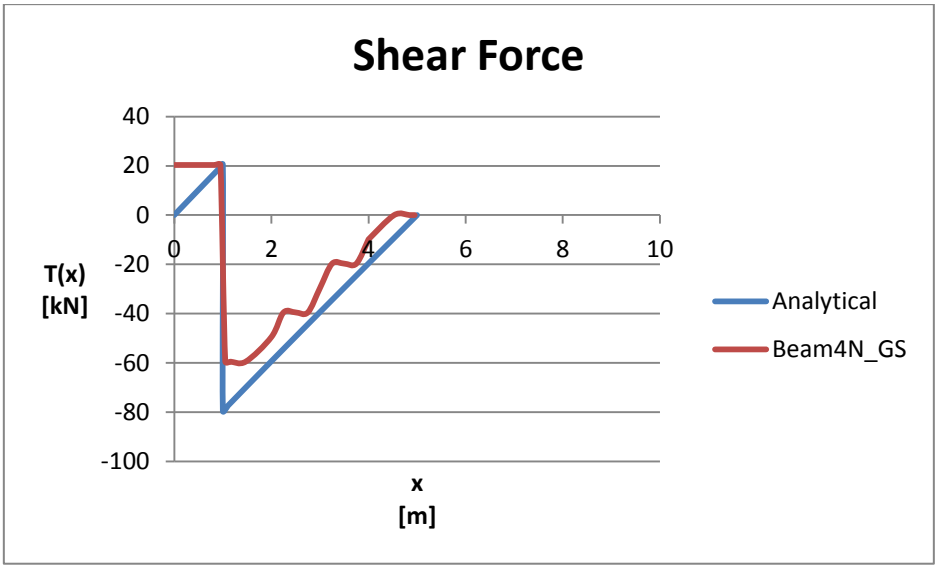

Figure 74: Shear force, Analytical-beam 4N GeoStudio

1.1.5.6 Sixth model – Beam 4BD

The sixth model has the same characteristics of the fifth one (half beam on springs), but the discretization is the same as the one adopted to the third model (springs every 0.1 m).

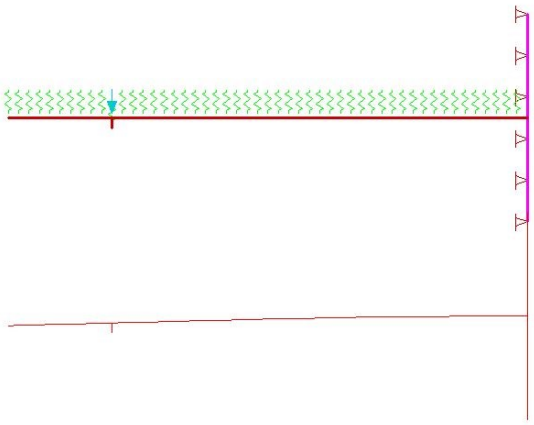

Figure 75: Mesh beam 4BD

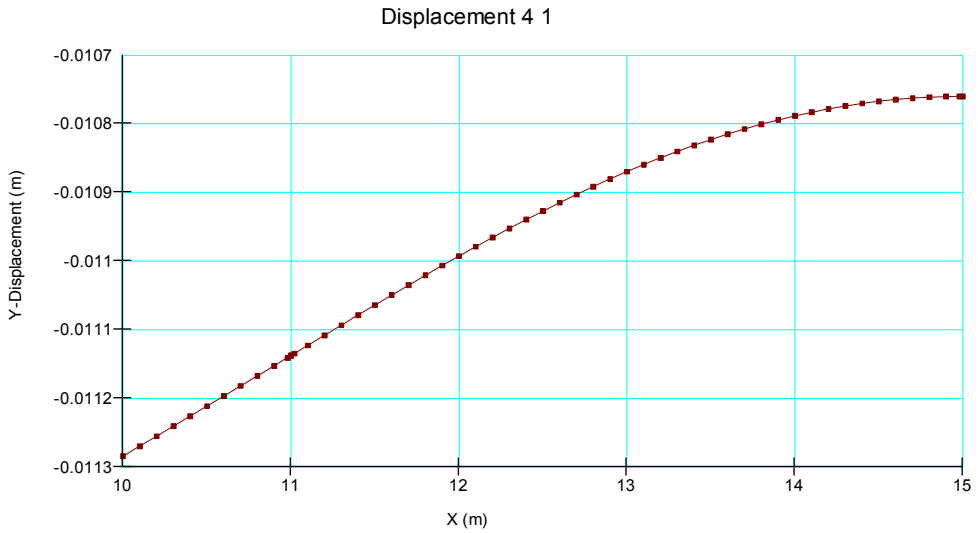

Figure 76: Displacement beam 4BD

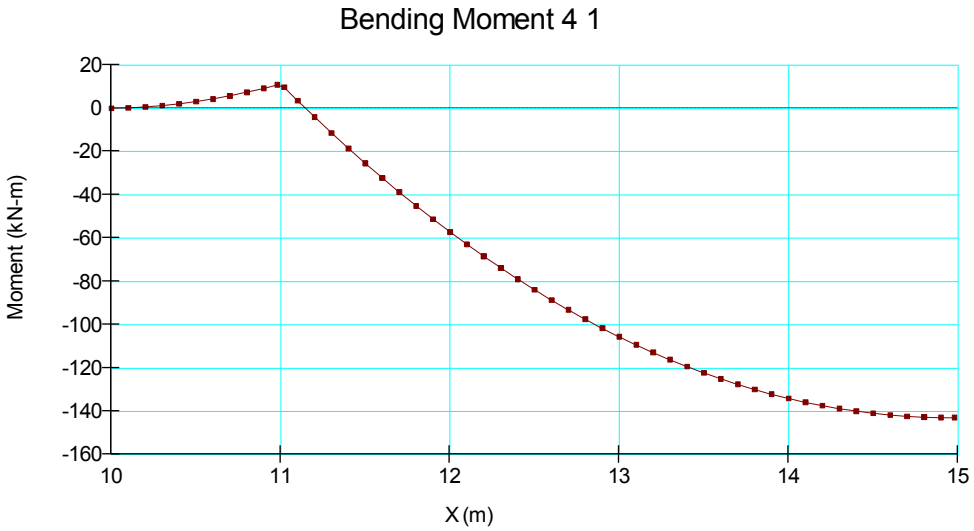

Figure 77: Moment 4BD

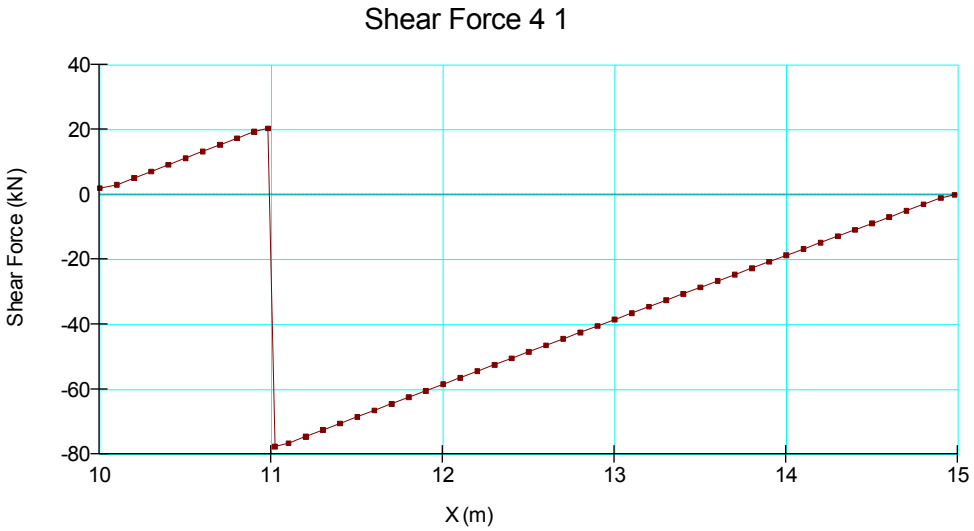

Figure 78: Shear force beam 4BD

1.1.5.6.1 Comparison with analytical result

In this section a comparison between the solution obtained with GeoStudio and the one obtained with the analytical solution will proposed. As in the previous graphics the GeoStudio's bending moment's diagram will be inverted.

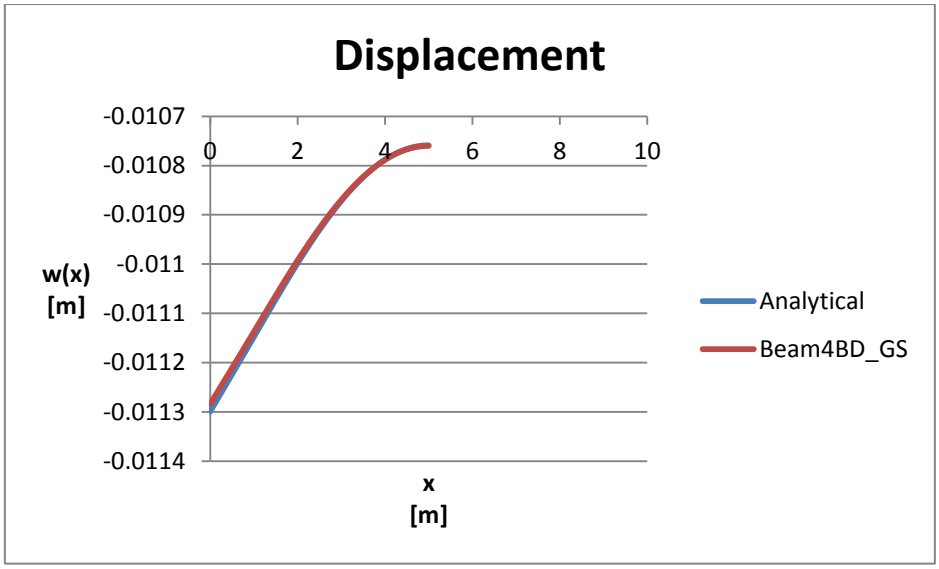

Figure 79: Displacement, Analytical-beam 4BD GeoStudio

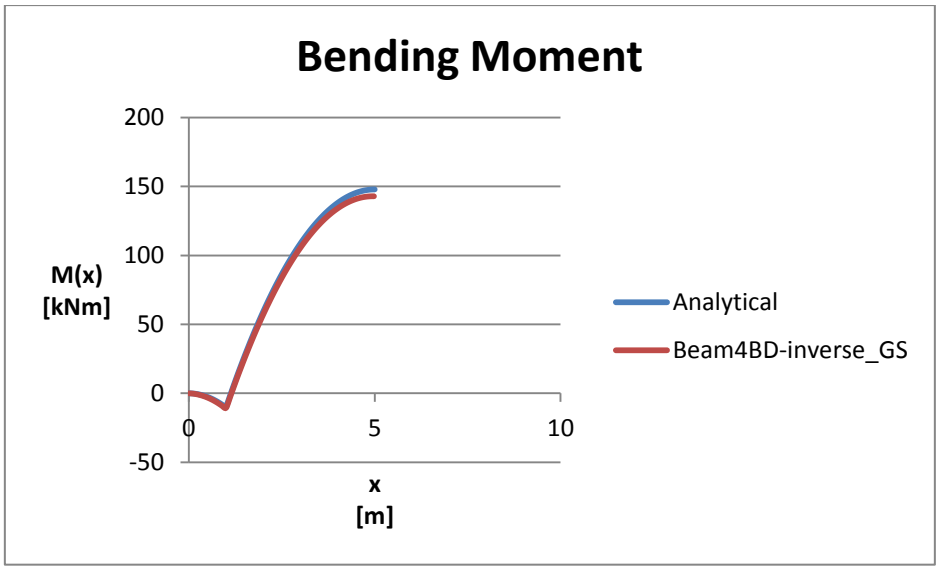

Figure 80: Bending moment, Analytical-beam 4BD GeoStudio

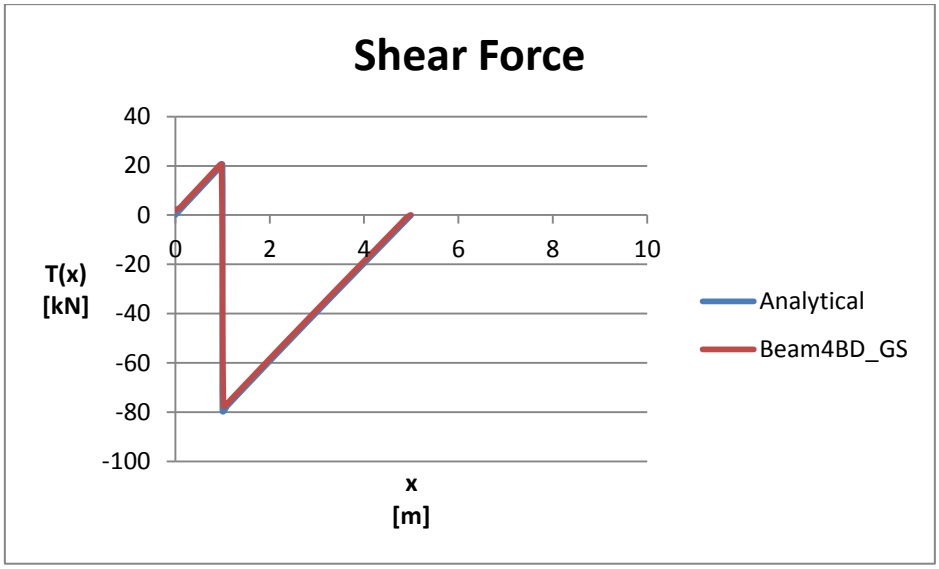

Figure 81: Shear force, Analytical-beam 4BD GeoStudio

1.1.5.7 Comparison

In the following graphics it's possible to compare all the models with the one obtained with the analytical solution. The results of the models that take into account the "springs" match the analytical one because in these for the springs have been used the same value of k used for the analytical solution, on the contrary the models with "real" layers of soil use the parameters required for the linear-elastic analysis and not "k".

The only case which differs is "Beam 3N" regarding the displacement, probably because of the low discretization; fact that is replied regarding the shear force with "Beam 3N" and "Beam 4N".

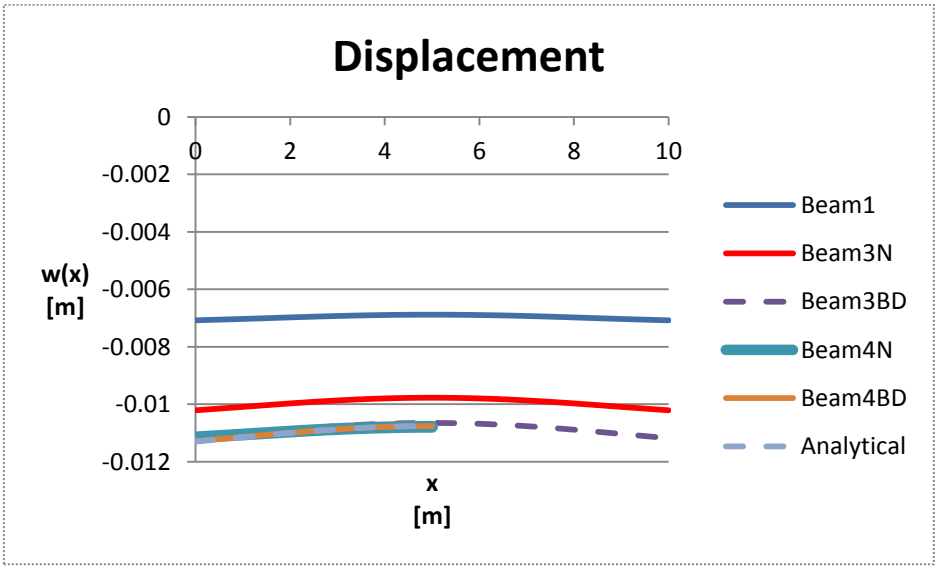

Figure 82: Displacement, different models

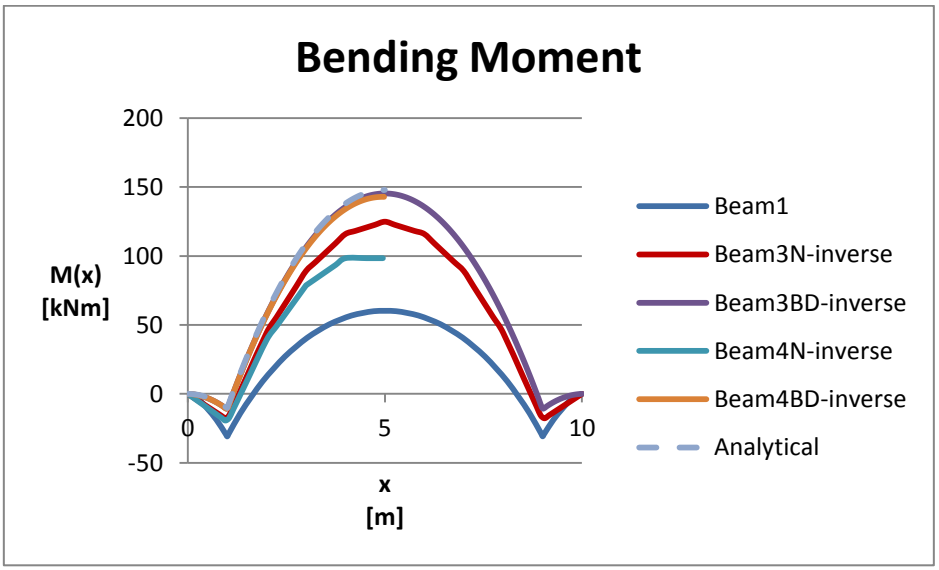

Figure 83: Bending moment, different models

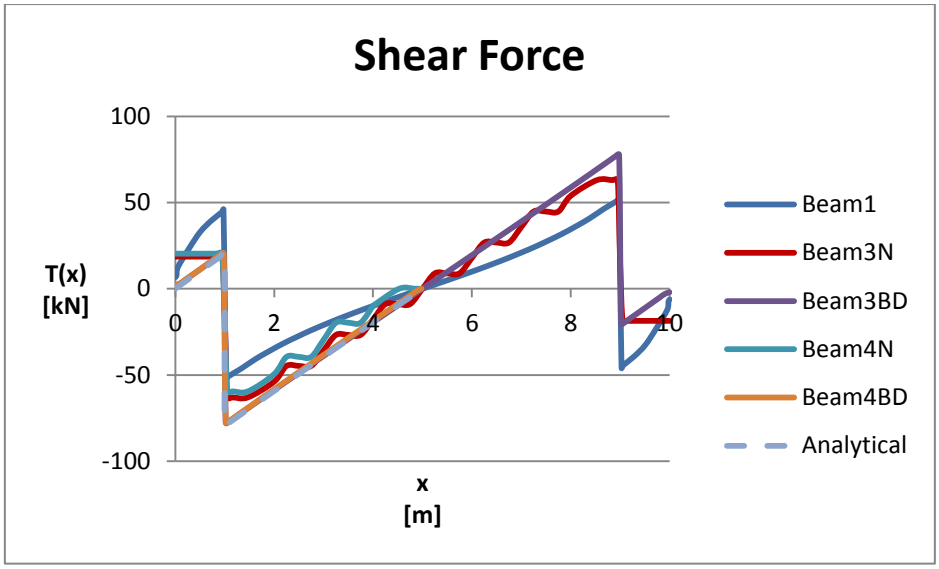

Figure 84: Shear force, different models

1.2 Pasternak's solution

1.2.1 Theoretical introduction

Pasternak created a model a little more complex than the Winkler's one. As for the Winkler's model, it's important to understand how the soil deformation influences the behavior of the beam. One can notice that the stress at the interface and the soil-beam interaction depend on the geometrical characteristics of the beam and on the mechanical properties (elastic) of the soil.

The Pasternak solution takes into account both the soil below the beam and the soil next to it (Figure 85): this is an obvious difference from Winkler's model, in which only the loaded region under the beam settles, while the adjacent surface remains unchanged. The soil nearby the beam forms a "wave" due to the deformation and because the material is a connected continuum. Pasternak created a model to get sag which qualitatively describes this behavior.

Figure 85: Pasternak's behavior of the soil

It is assumed that the reaction at each point of the ground under the beam is in proportion to the displacement of the ground at that point (Winkler setting), but this component of the reaction depends on the curvature of the beam at that point. The constant of proportionality is the modulus of soil stiffness, the Winkler's k.

The curvature coefficient is used for the reaction coefficient (S) introduced by Pasternak, and it's interpreted as a traction force under the beam (slab) provided by a fictitious membrane placed between the beam (slab) and the soil.

Pasternak model has two parameters (not only λ, but also α and β).

Other assumptions are chosen without changing the scheme of the Winkler beam: movement of the beam and displacement of the ground are the same only when the soil is compressed and, only in special cases, when it is in traction. In the formulation of the problem is not taken into account the possibility of a difference between the displacement of the beam and the movement of the soil.

The description can be as follows: a membrane layer between the ground and the beam (thick gray line in the Figure 86). This layer is a "diaphragm" which is placed in traction by a constant force S that acts in the tangential direction to the membrane surface. The vertical resultant force acts on the bottom of the beam (or plate). It's possible to analyze the linear section of the diaphragm (black section in the Figure 86):

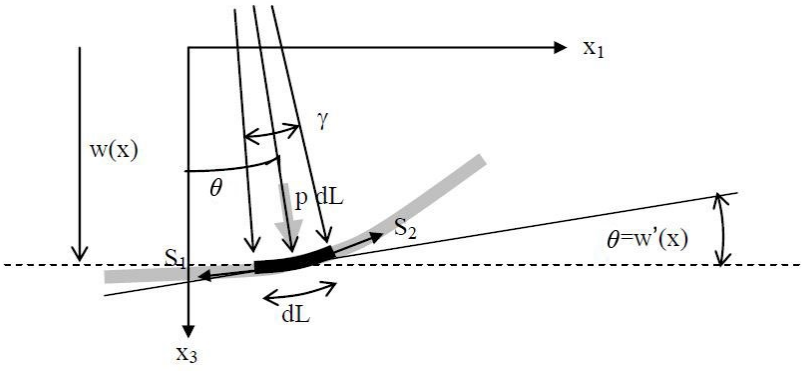

Figure 86: Membrane behavior

The sum of projections on the tangential axis to the membrane results in:

$$2S\sin\frac{\gamma}{2} = pdL \;\Rightarrow\; \frac{2S\sin\frac{\gamma}{2}}{dL} \cong \frac{2S\frac{\gamma}{2}}{dL} \tag{25}$$

because dL = Rγ where R is the local radius of curvature, one can write:

$$p = \frac{S\gamma}{dL} = \frac{S}{R} = S\frac{1}{R} = -S\frac{d^2w}{dx^2} \tag{26}$$

The inverse of the curvature radius is approximately equal to the second derivative of the deflection line.

The relationship between the pressure force resulting from the curvature of the beam and the force of the "membrane" is shown as follows:

$$p_p = -S\frac{d^2w}{dx^2} \tag{27}$$

This extra load is a supplement to the Winkler's model and leads to the following equations.

Starting from the equilibrium equations of the beam:

$$\frac{d^2M(x)}{dx^2} + p(x) = 0 \tag{28}$$

where M is the bending moment, p is the load perpendicular to the axis of the beam: the axis the of the beam is oriented to the x-direction.

We take into account the Winkler assumption, total load on the ground is p, distributed load is q and soil reaction is r = -kw(x).

$$p(x) = q(x) - kw(x) + S\frac{d^2w(x)}{dx^2} \tag{29}$$

$$M(x) + q(x) - kw(x) + S\frac{d^2w(x)}{dx^2} = 0 \tag{30}$$

If EI (flexural stiffness of the beam, E Young's modulus of the beam's material, I moment of inertia about the axis of the center) is independent of x, we can obtain a simple equation:

$$EI\frac{d^4w(x)}{dx^4} - S\frac{d^2w(x)}{dx^2} + kw(x) = q(x) \Rightarrow \tag{31}$$

$$\frac{d^4w(x)}{dx^4} - \frac{S}{EI}\frac{d^2w(x)}{dx^2} + \frac{kw(x)}{EI} = \frac{q(x)}{EI} \quad (32)$$

with the typical substitution:

$$\lambda = \sqrt[4]{\frac{k}{4EI}} \quad (33)$$

leads to the Pasternak's formula:

$$\frac{d^4w(x)}{dx^4} - \frac{S}{EI}\frac{d^2w(x)}{dx^2} + 4\lambda^4 w(x) = \frac{q(x)}{EI} \quad (34)$$

particular solution of the equation (with zero on the right) (which is easy to check by substitution) is of the form:

$$w(x) = e^{\beta x}(C_1 \sin(\alpha x) + C_2 \cos(\alpha x)) + e^{((-\beta)x)}(C_3 \sin(\alpha x) + C_4 \cos(\alpha x)) \quad (35)$$

$$\alpha = \frac{\sqrt{4\lambda^2 - \frac{S}{EI}}}{2} \quad (36)$$

$$\beta = \frac{\sqrt{4\lambda^2 + \frac{S}{EI}}}{2} \quad (37)$$

S is a concentrated force ([kN]) that already takes into account the membrane thickness and the width of the interval (for example, the width of the beam B).

If one want to check, for S = 0 is obtained the solution of the Winkler equation.

Complete solution is obtained by adding any specific solution.

If q(x) is (as usual) solid (or solid pieces), it is a particular solution and is, as before, in Winkler, the following:

$$w = \frac{q}{k} \tag{38}$$

Note further that, in accordance with the intuitive interpretation, one may assume that the solution of the "membrane" refers to the surface of the ground "outside" the beam.

This is important because in the case of ground covered by an actual membrane (geosynthetics) the equation outside the beam is as follows:

$$0 = q(x) - kw(x) + S\frac{d^2w(x)}{dx^2} \tag{39}$$

The solution of this equation is the special form:

$$w(x) = C_1 e^{\sqrt{\frac{k}{S}}x} + C_2 e^{-\sqrt{\frac{k}{S}}x} \tag{40}$$

Coefficient k is the coefficient of Winkler, calculated as it was shown before.

The “S” coefficient has a simple interpretation of the "strength of the membrane." Unfortunately, this membrane is fictitious. Therefore, S is a highly speculative factor.

Even if the membrane was real (geostucture), unfortunately, the “S” factor is still difficult to determine, because it can be interpreted as the strength of the membrane and therefore it would be part of the solution task and not the output value.

The problem gets "non-linear", and a method of trial and correction is required.

Starting from the theory of elastic half-space, the resultant of the horizontal stress that occur within the soil when the area under the beam (plate) is compressed can be calculated.

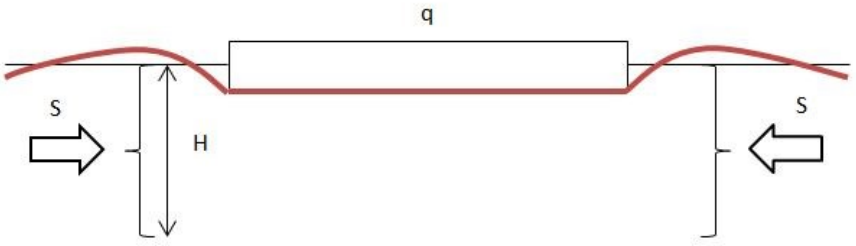

Figure 87: Pasternak’s model

S is the resultant of the layer with a certain thickness H.

The Figure 87 above shows the intuitive cooperation of the land beyond the line of the foundation.

According to the method of Vlasov and Leontiev, the following formula it has been obtained (commonly, also different formulae are used, giving similar results):

$$S = \frac{E_0 B}{2 + 2\nu_0} \int_0^{\infty} g(z)^2 \, dz \tag{41}$$

g is a function describing the change in the vertical displacement with the depth. One can take g from the formula:

$$g(z) = e^{-\mu z} \tag{42}$$

where μ can be reasonably taken as a constant.

E is Young's modulus, ν is Poisson's ratio.

In practice, the condition to be fulfilled is:

$$\frac{1}{B} < \mu < \frac{2}{B} \tag{43}$$

Assuming the lower limit for μ one obtains:

$$S = \frac{E}{4 + 4\nu} \tag{44}$$

Using geosynthetics (membrane, geogrid) under the foundation, the classical solutions is not correct (geosynthetics have 10, max 20 years). Pasternak model could be useful in that application but in this case S is a part of the solution: nevertheless the value of S per unit of width ("B") can be is easily found [6].

1.2.2 Theoretical solution – Pasternak

In the example the same beam used on the Winkler's soil has been considered, but on the left-hand side there is a new element, the fictitious geosynthetic. For this part the formulae shown in the previous pages have been used. The boundary conditions are different from the Winkler's ones.

Under consideration, the left half-beam and the soil with the fictitious geosynthetic: in order to find the solution one need to calculate k, to adopt S and then calculate α and β.

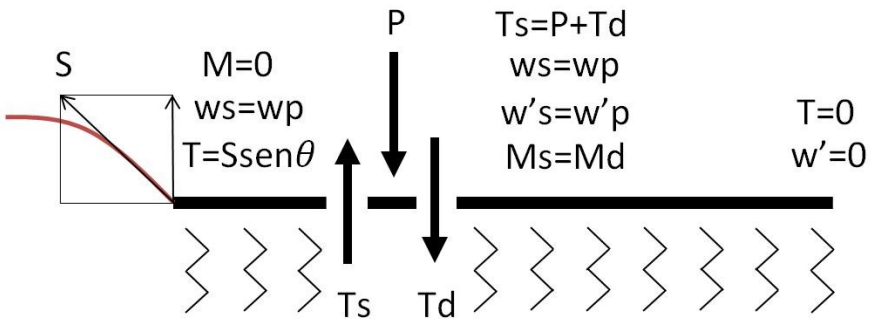

Figure 88: Border conditions of Pasternak's solution

Solution of the beam on the left-hand side of point of application of the force:

$$w_1(x) = e^{\beta x}\left(C_{1\_1}\sin(\alpha x) + C_{2\_1}\cos(\alpha x)\right) + e^{((-\beta)x)}\left(C_{3\_1}\sin(\alpha x) + C_{4\_1}\cos(\alpha x)\right) \quad (45)$$

Solution of the beam on the right-hand side of point of application of the force:

$$w_2(x) = e^{\beta x}\left(C_{1\_2}\sin(\alpha x) + C_{2\_2}\cos(\alpha x)\right) + e^{((-\beta)x)}\left(C_{3\_2}\sin(\alpha x) + C_{4\_2}\cos(\alpha x)\right) \quad (46)$$

Solution on the left, for the "membrane":

$$w_M(x) = C_{1\_M}e^{\sqrt{\frac{k}{S}}x} + C_{2\_M}e^{-\sqrt{\frac{k}{S}}x} \quad (47)$$

Conditions for the ten constants:

on the right end of the beam (telescope):

$$T\left(w_2(x), x = \frac{L}{2}\right) = 0 \quad (48)$$

$$\frac{dw_2(x)}{dx}\left(x = \frac{L}{2}\right) = 0 \quad (49)$$

At the section of action of the force:

$$T\left(w_1(x), x = \frac{L}{10}\right) = T\left(w_2(x), x = \frac{L}{10}\right) + P1 \quad (50)$$

$$M\left(w_1(x), x = \frac{L}{10}\right) = M\left(w_2(x), x = \frac{L}{10}\right) \quad (51)$$

$$w_1(x)\left(x = \frac{L}{10}\right) = w_2(x)\left(x = \frac{L}{10}\right) \quad (52)$$

$$\frac{dw_1(x)}{dx}\left(x = \frac{L}{10}\right) = \frac{dw_2(x)}{dx}\left(x = \frac{L}{10}\right) \quad (53)$$

On the left end of the beam:

$$w_M(x)(x = 0) = w_1(x)(x = 0) \quad (54)$$

$$S\frac{dw_1(x)}{dx}(x = 0) = T(w_1(x), x = 0) \quad (55)$$

$$M(w_1(x), x = 0) = 0 \quad (56)$$

The last condition is satisfied placing:

$$C_{1\_M} = 0 \quad (57)$$

in this way, the curve tends to infinity on the left side.

In the following graphics it is possible to notice the comparison between the solution obtained with Winkler and with Pasternak; three different outputs of the Pasternak's solution changing the value of S have been illustrated: the first is obtained with the previous formula, the second is obtained placing S = 1 kN , the third obtained placing S = 1 kN.

The results that obtained with GeoStudio are more similar to the ones obtained with the Pasternak's model (analytical) than the ones obtained with Winkler (analytical) (Figure 89): in particular the Pasternak's model simulates with good accuracy the behavior of the soil nearby the beam, the bending moment and the shear force. With S= 1 kN Pasternak's model (analytical) matches the solution of Winkler (analytical), that's to say that the "membrane" doesn't work (Figure 92).

Table 5: Parameters for the calculation with Pasternak (analytical); the implemented values is for the case "S calc"

C1_M	C2_M	C1_1	C2_1	C3_1	C4_1	C1_2	C2_2	C3_2	C4_2
0	0.00804	-0.0013	0.00474	-0.0009	0.00310	0.00136	0.00166	0.00305	0.0064

H	B	L	L1	L2	E	J	EJ	λ	λ*L
[m]	[m]	[m]	[m]	[m]	[kPa]	[m^4]	[kNm^2]	[m^{-1}]	[-]
1	1	5	1	4	30000000	0.083333	2500000	0.116214	0.581072

α	β	E1	ν	S	S*SENθ	k	P1	P2	Δx
[m^{-1}]	[m^{-1}]	[kPa]	[-]	[kN]	[kN]	[kN/m^3]	[kN]	[kN]	[m]
0.113112	0.119236	37000	0.3	7115.385	28.95427	1824.064	100	100	0.1

Tmax	Tmin	Mmax	Mmin	Wmax	Wmin
[kN]	[kN]	[kNm]	[kNm]	[m]	[m]
43.59109	-56.4089	33.11338	-57.6556	0.008037	0.007729

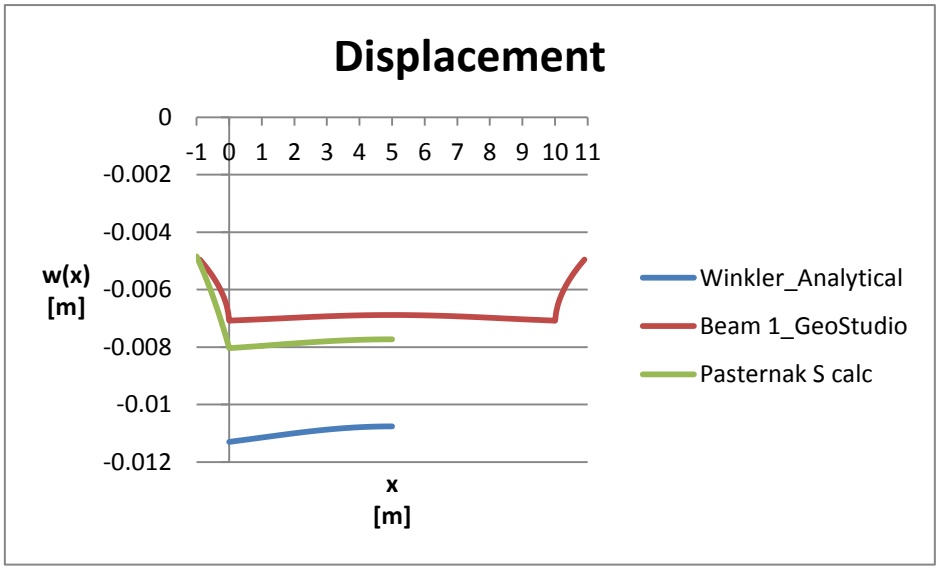

Figure 89: Displacement obtained with Winkler (analytical), GeoStudio (FEM), Pasternak (analytical)

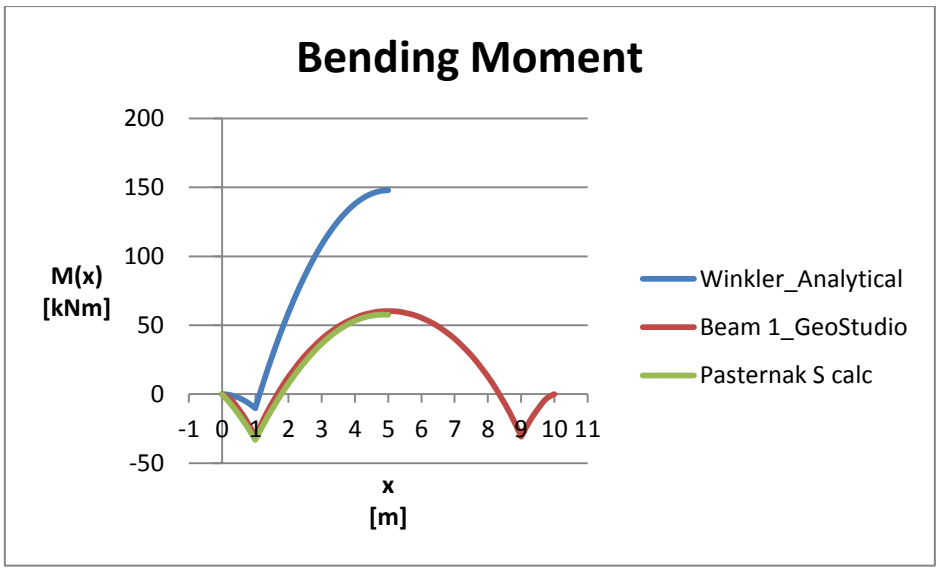

Figure 90: Bending moment obtained with Winkler (analytical), GeoStudio (FEM), Pasternak (analytical)

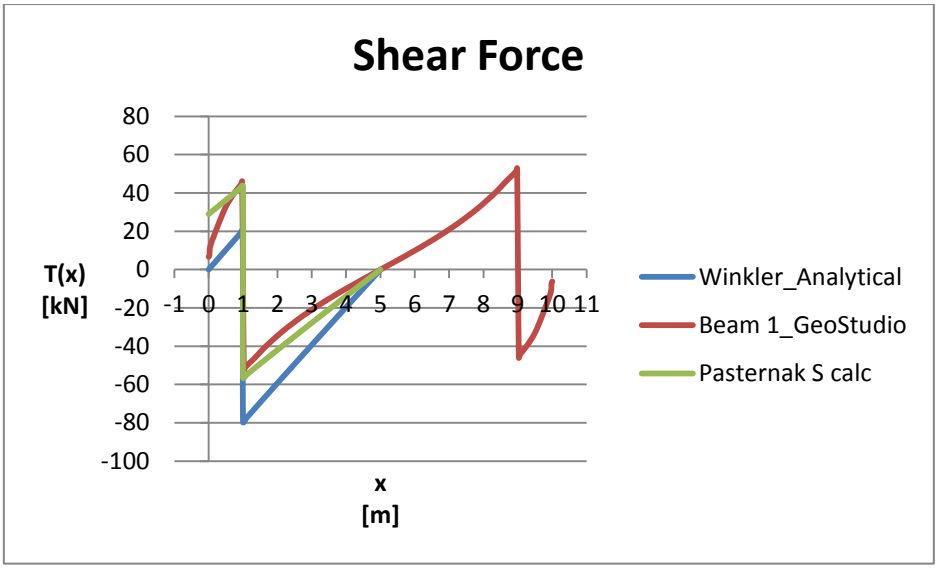

Figure 91: Shear force obtained with Winkler (analytical), GeoStudio (FEM), Pasternak (analytical)

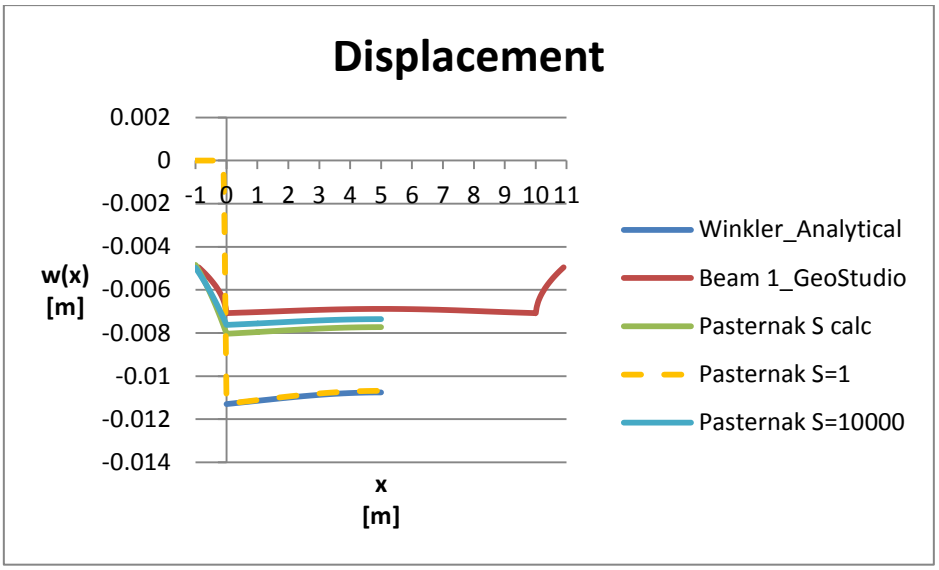

Figure 92: Displacement obtained with Winkler (analytical), GeoStudio (FEM), Pasternak (analytical)

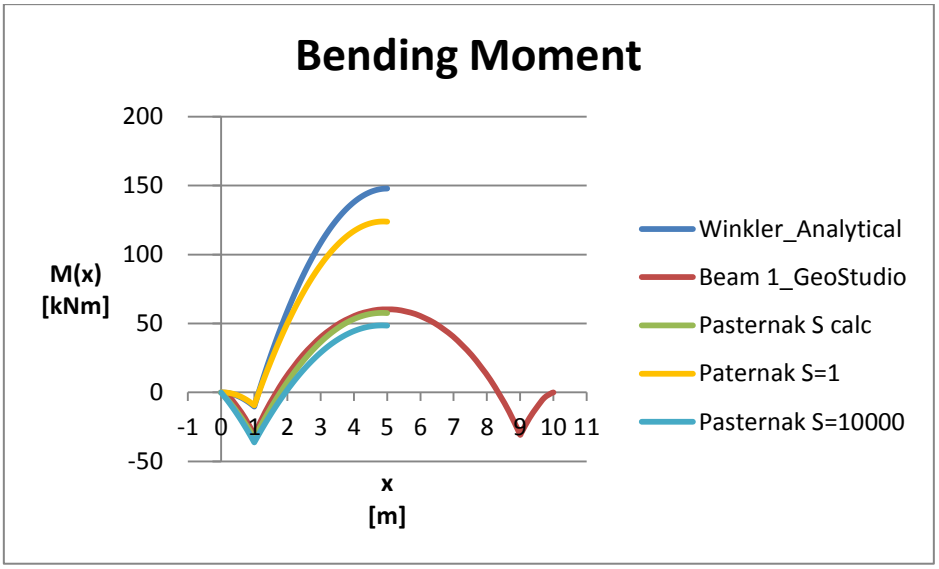

Figure 93: Bending moment obtained with Winkler (analytical), GeoStudio (FEM), Pasternak (analytical)

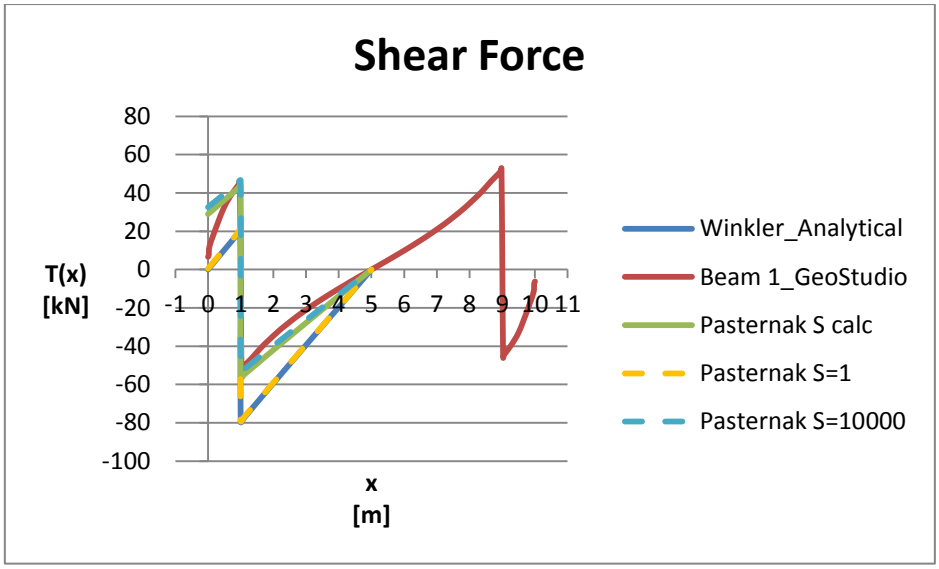

Figure 94: Shear force obtained with Winkler (analytical), GeoStudio (FEM), Pasternak (analytical)

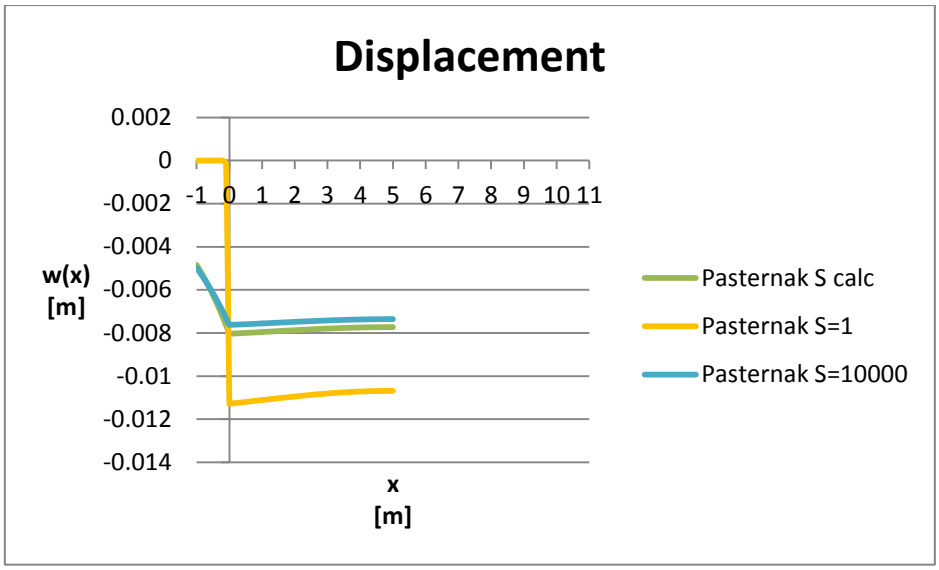

Figure 95: Displacement obtained with Winkler (analytical), GeoStudio (FEM), Pasternak (analytical)

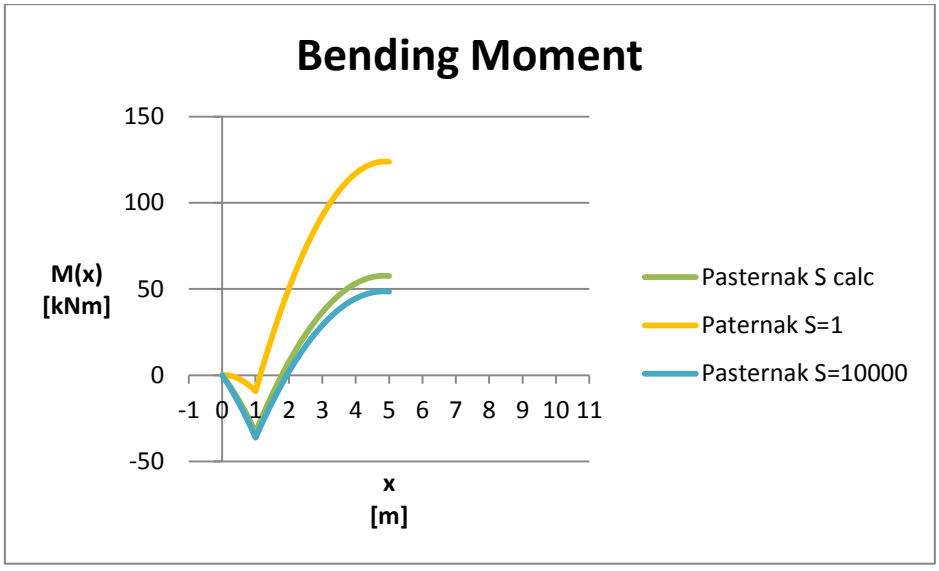

Figure 96: Bending moment obtained with Winkler (analytical), GeoStudio (FEM), Pasternak (analytical)

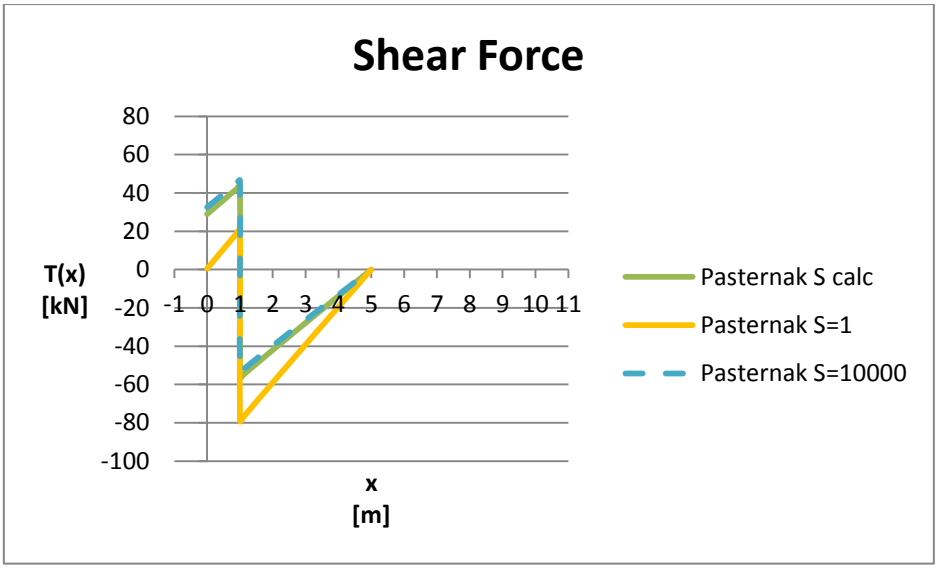

Figure 97: Shear obtained with Winkler (analytical), GeoStudio (FEM), Pasternak (analytical)

As it is easy to see, the solution with the Pasternak model (analytical) using the S calculated with the equation (44) better simulates the behavior of the continuum solution (GeoStudio, FEM) than the Winkler's solution (analytical). Pasternak model is useful to describe this kind of situation (long beam resting on elastic soil), but it is also helpful to study some interesting application that will be shortly described.

1.2.2.1 Pasternak – Symmetrical solution

In this application has been considered a symmetrical situation of a soil, with a distributed load applied on it to a length of 2 meters, and half a meter of free soil (not loaded) beside the two edges of the loaded soil: this model could describe the behavior of a loaded membrane (real as geosynthetics, or fictitious) resting on an elastic soil. The equations that describe the behavior of the "membrane" and of the ground around are the same used in chapter of the theoretical beam (in addiction there is the distributed load), but with some simplifications caused by the symmetry: in fact the equation of the membrane needs only two constants of integration (and not two for half membrane and other two for the other half)), and as for the free soil the equation needs one constant (no more two, that's to say the same situation of the theoretical beam) because in that way the displacement curve tends to infinite on the far side of the piece of soil, so the other constant can be placed equal to zero. This simplification provides a computational advantage.

On the left side of the loaded membrane the equation is

$$w_M(x) = C_{1\_M} e^{\sqrt{\frac{k}{S}}x} + C_{2\_M} e^{-\sqrt{\frac{k}{S}}x} + \frac{q}{k} \qquad (58)$$

and the equation of the unloaded part, left side, is

$$w_L(x) = C_{3\_M} e^{\sqrt{\frac{k}{S}}x} + C_{4\_M} e^{-\sqrt{\frac{k}{S}}x} \quad (59)$$

On the right side of the loaded membrane the equation is

$$w_M(x) = C_{1\_M} e^{\sqrt{\frac{k}{S}}x} + C_{2\_M} e^{-\sqrt{\frac{k}{S}}x} + \frac{q}{k} \quad (60)$$

and the equation of the unloaded part, right side, is

$$w_R(x) = C_{4\_M} e^{\sqrt{\frac{k}{S}}x} + C_{3\_M} e^{-\sqrt{\frac{k}{S}}x} \quad (61)$$

where k is the subgrade modulus and S is the membrane force.

Conditions for the four constants:

on the left end of the loaded area:

$$w_L(x)(x = -1) = w_M(x)(x = -1) \quad (62)$$

$$\frac{dw_L(x)}{dx}(x = -1) = \frac{dw_M(x)}{dx}(x = -1) \quad (63)$$

On the right end of the loaded area:

$$w_M(x)(x = 1) = w_R(x)(x = 1) \quad (64)$$

The last condition is satisfied placing:

$$C_{4\_M} = 0 \quad (65)$$

[7].

In the following graphics the trend of the displacement in function of k, q and S will be illustrated: for the values of "k" have been chosen the results of the previous calculations by the Winkler's method plus two arbitrary values of k = 5000 kN/m^3 and k = 10000 kN/m^3.

Table 6: Parameters for the solution; the implemented values are the chosen ones for one of the analyzed cases

L	k	ϕ'1	S	q	P1	P2	P1+P2	Δx
[m]	[kN/m^3]	[°]	[kN]	[kN/m]	[kN]	[kN]	[kN]	[m]
2	1824.063816	37	1000	-100	100	100	200	0.1

C1_M	C2_M	C3_M
0.0071	0.007102004	-0.0987

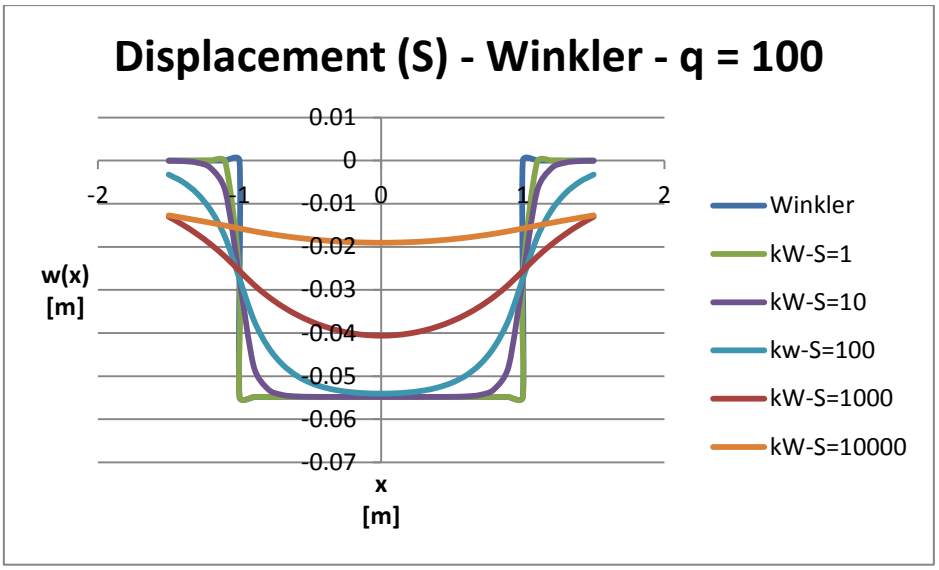

Figure 98: Displacement of the membrane varying S, k assumes the value adopted in the Winkler's solution and indicated in Table 6, q = 100 kN/m

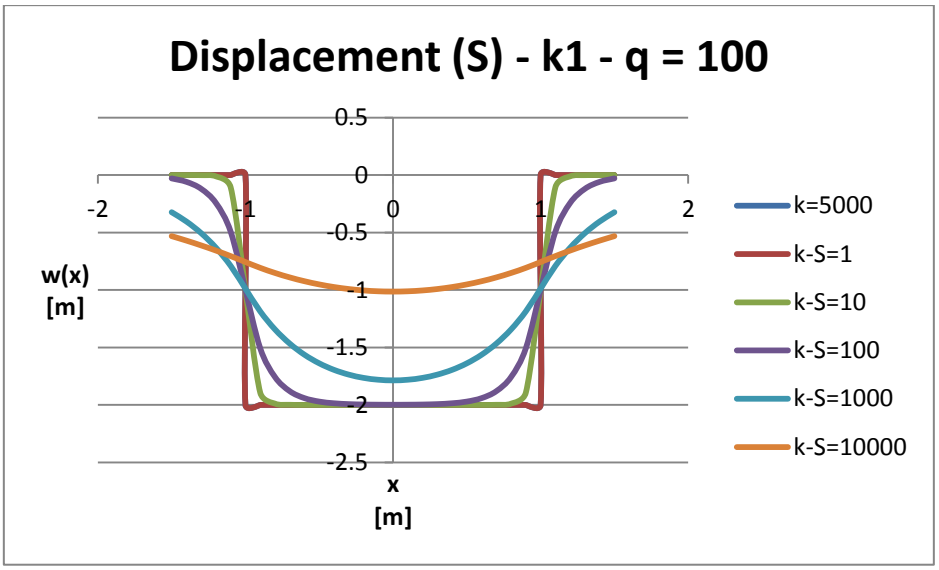

Figure 99: Displacement of the membrane varying S, k1 = 5000 kN/m^3, q = 100 kN/m

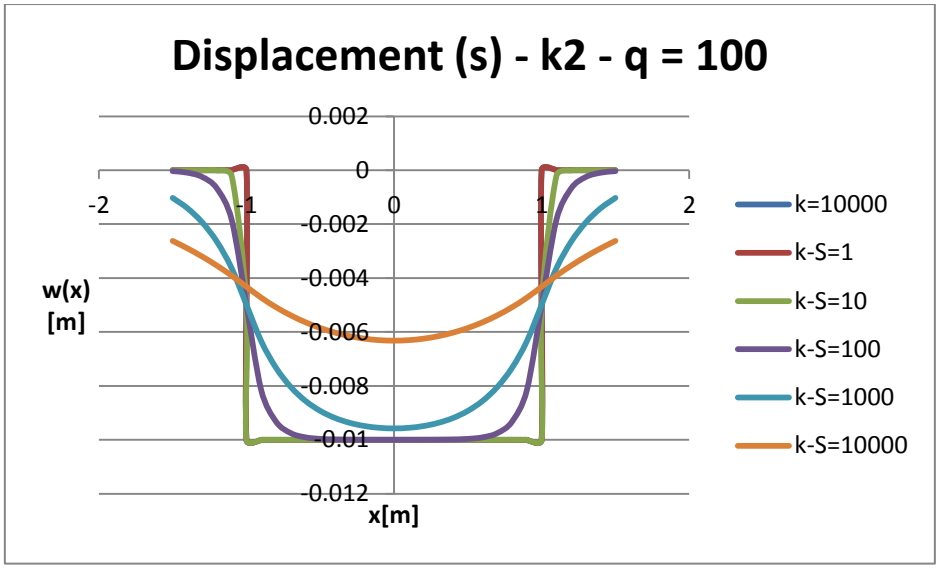

Figure 100: Displacement of the membrane varying S, k1 = 10000 kN/m³, q = 100 kN/m

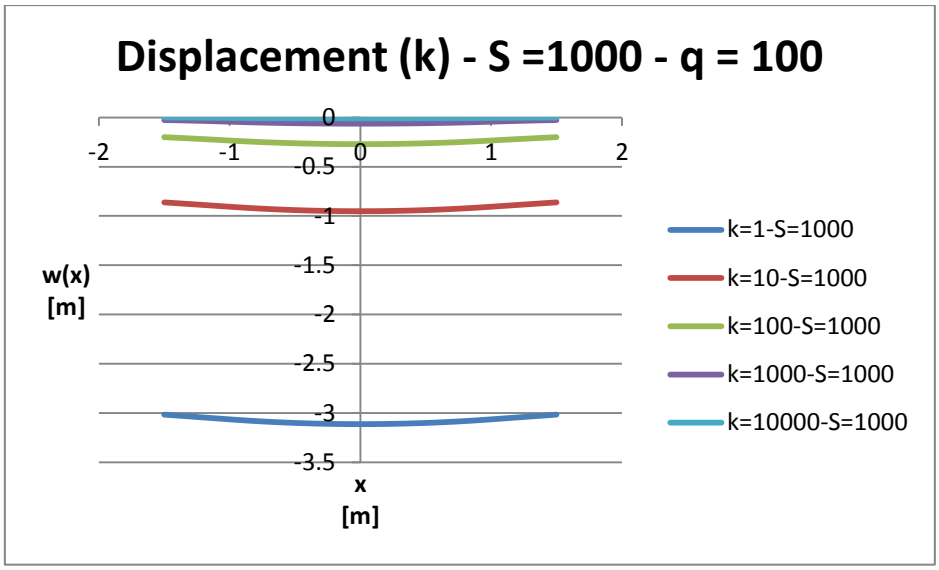

Figure 101: Displacement of the membrane varying k, S = 1000 kN, q = 100 kN/m

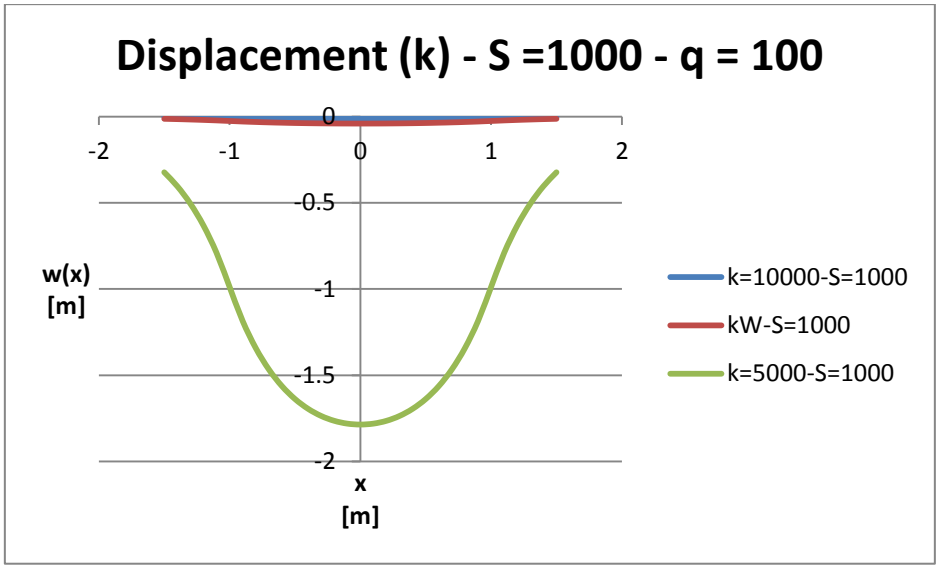

Figure 102: Displacement of the membrane varying k, S = 1000 kN, q = 100 kN/m

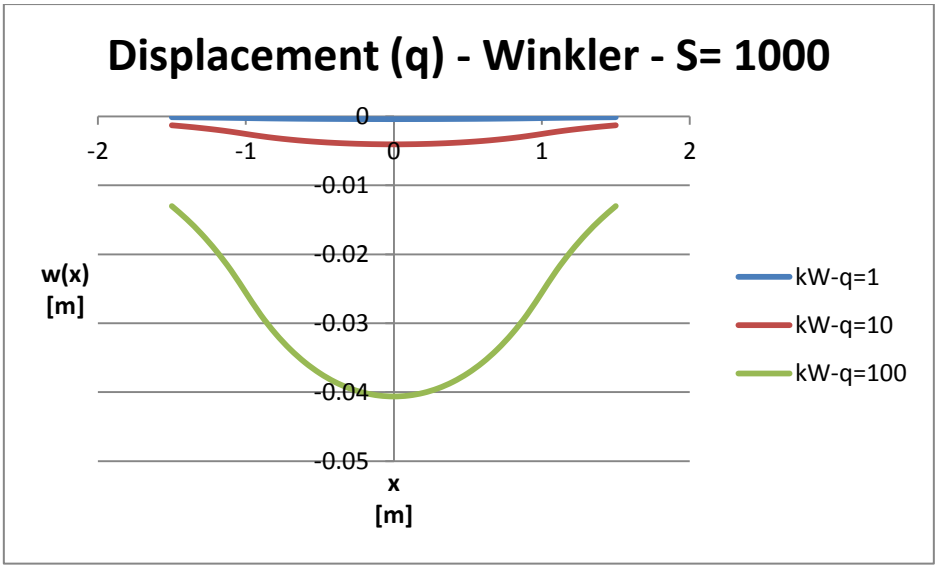

Figure 103: Displacement of the membrane varying q, k assumes the value adopted in the Winkler's solution and indicated in Table 6, S = 1000 kN

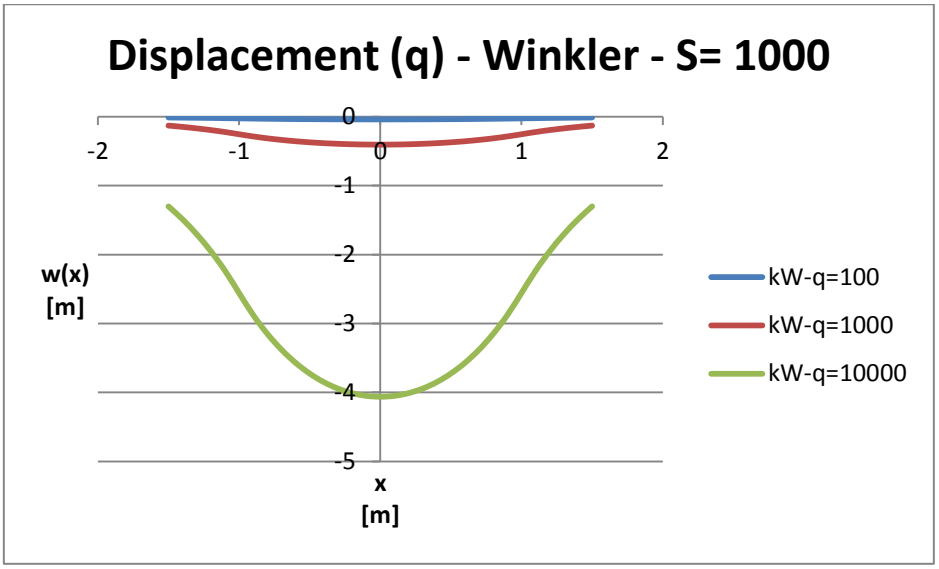

Figure 104: Displacement of the membrane varying q, k assumes the value adopted in the Winkler's solution and indicated in Table 6, S = 1000 kN

1.2.2.2 Pasternak – Reinforced soil

This example considers a part of ground of 3 m of length, with a distributed load applied on it. The soil has two different subgrade moduli: in fact on the two edges of this piece of ground, for 0.5 m on each side, has a ten times greater stiffness than the soil in the middle. This distribution of stiffness tries to simulate the situation that is possible to find when are used gravel columns in the soil, or piles, but always materials with greater stiffness than the soil. The geometry and the loads are symmetrical, so one can imagine a description similar to the one used in the previous chapter, with similar simplifications and advantages. As in the previous case, the model can show the behavior of a loaded membrane resting on an elastic

soil (with two different stiffnesses). So the equations that describe this application are the same used before, with the accuracy of using two different k. The simplifications caused by the symmetry permit to consider only half of the area (1.5 m), only two constants of integration for the part with "normal soil" and only two for the "reinforced soil" (so have been found the constants only for half of the considered zone, because in the other part the constants are the same because of the symmetry). On the left side of the loaded membrane resting on the normal soil the equation is

$$w_M(x) = C_{1\_M} e^{\sqrt{\frac{k}{S}}x} + C_{2\_M} e^{-\sqrt{\frac{k}{S}}x} + \frac{q}{k} \quad (66)$$

and the equation of the reinforced part, left side, is

$$w_L(x) = C_{3\_M} e^{\sqrt{\frac{kf}{S}}x} + C_{4\_M} e^{-\sqrt{\frac{kf}{S}}x} + \frac{q}{kf} \quad (67)$$

On the right side of the loaded membrane resting on the normal soil the equation is

$$w_M(x) = C_{1\_M} e^{\sqrt{\frac{k}{S}}x} + C_{2\_M} e^{-\sqrt{\frac{k}{S}}x} + \frac{q}{k} \quad (68)$$

and the equation of the reinforced part, right side, is

$$w_R(x) = C_{4\_M} e^{\sqrt{\frac{kf}{S}}x} + C_{3\_M} e^{-\sqrt{\frac{kf}{S}}x} + \frac{q}{kf} \quad (69)$$

where k is the subgrade modulus for the normal soil, kf the subgrade modulus for the reinforced soil and S is the membrane force.

Conditions for the four constants:

on the left end of the loaded area on the normal soil:

$$w_L(x)(x = -1) = w_M(x)(x = -1) \quad (70)$$

$$\frac{dw_L(x)}{dx}(x = -1) = \frac{dw_M(x)}{dx}(x = -1) \quad (71)$$

On the right end of the loaded area on the normal soil:

$$\frac{dw_M(x)}{dx}(x = 0) = 0 \quad (72)$$

On the left end of the loaded area on the reinforced soil:

$$\frac{dw_L(x)}{dx}(x = -1.5) = 0 \quad (73)$$

[7].

As in the previous application the following graphics illustrate the trend of the displacement in function of k, q and S: the results of the previous calculations by the Winkler's method plus two arbitrary values of k (k = 5000 kN/m^3, k = 10000 kN/m^3) have been used as "k" for the comparison.

Table 7: Parameters for the solution; the implemented values are the chosen ones for one of the analyzed cases

L	k	kf	ϕ'1	S	q	P1	P2	P1+P2
[m]	[kN/m^3]	[kN/m2]	[°]	[kN]	[kN/m]	[kN]	[kN]	[kN]
2	1824.064	18240.64	37	1000	-100	100	100	200

C_1	C_2	C_3	C_4
0.009328	0.009328	-0.77104	-2.1E-06

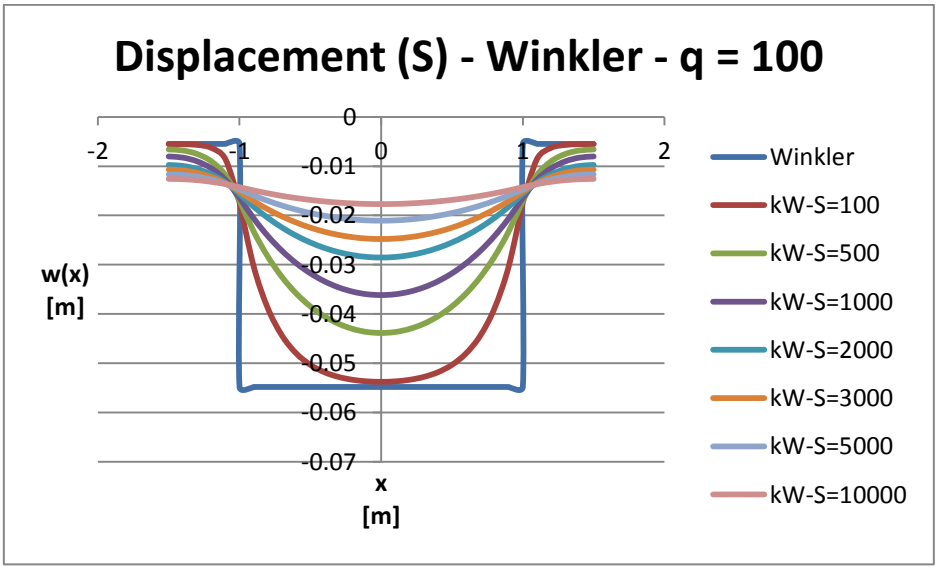

Figure 105: Displacement of the membrane varying S, k assumes the value adopted in the Winkler's solution and indicated in Table 7, q = 100 kN/m

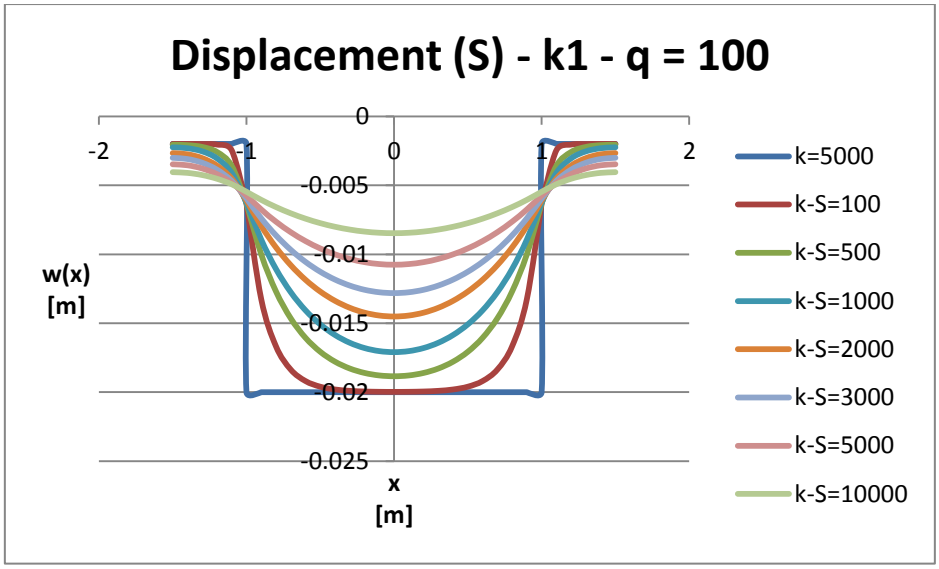

Figure 106: Displacement of the membrane varying S, k1 = 5000 kN/m², q = 100 kN/m

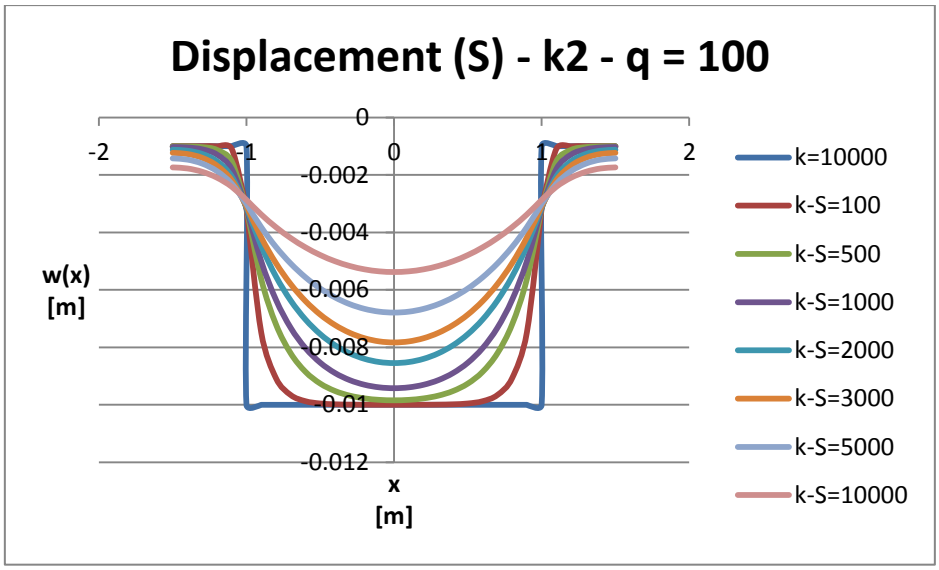

Figure 107: Displacement of the membrane varying S, k2 = 10000 kN/m², q = 100 kN/m

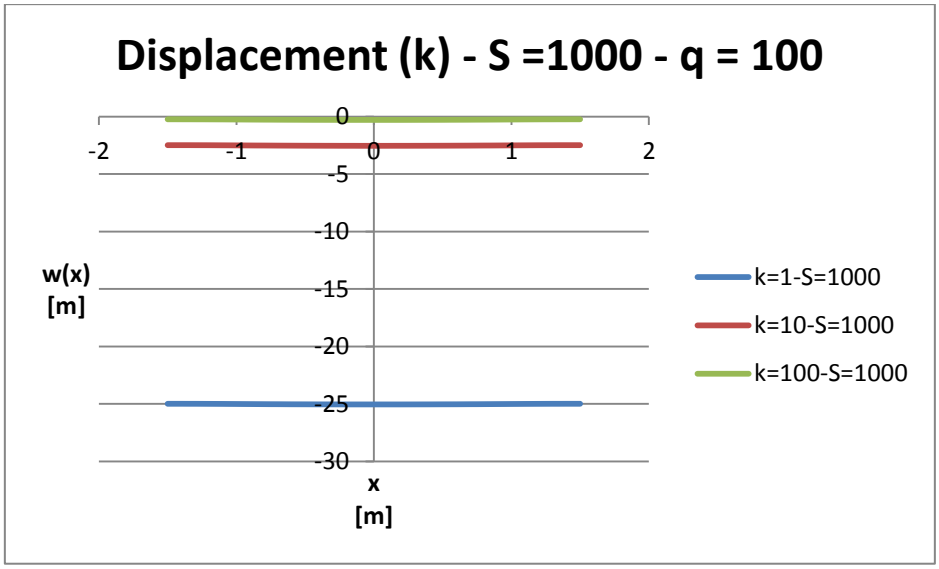

Figure 108: Displacement of the membrane varying k, S = 1000 kN, q = 100 kN/m

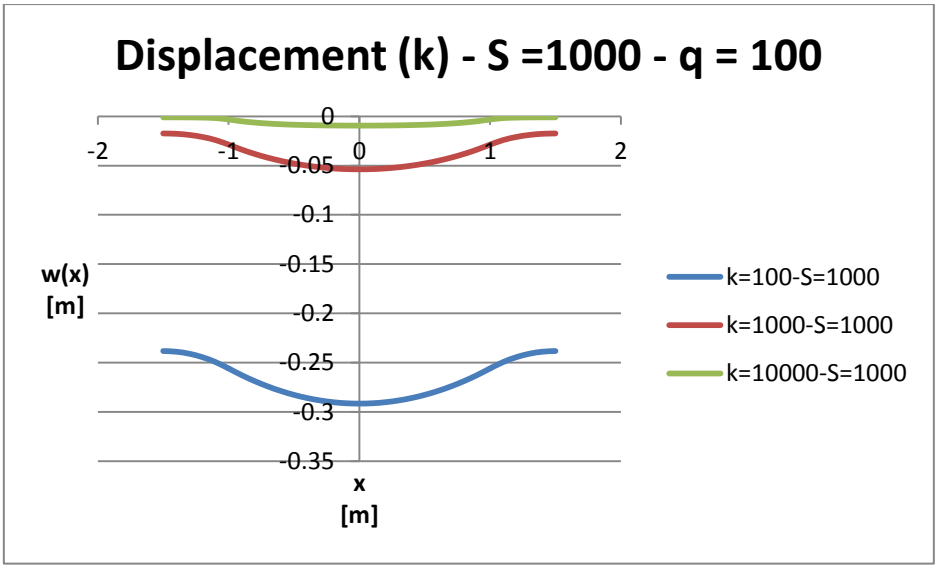

Figure 109: Displacement of the membrane varying k, S = 1000 kN, q = 100 kN/m

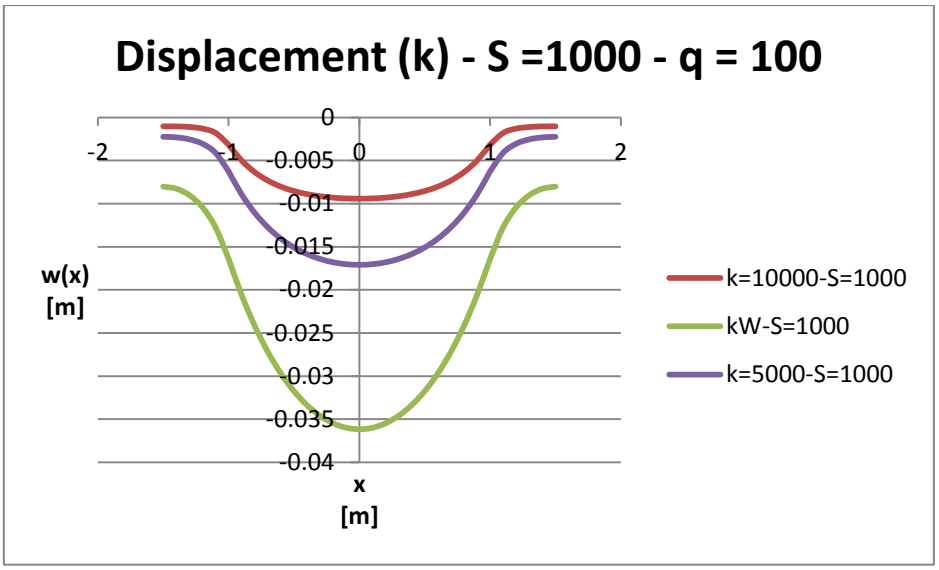

Figure 110: Displacement of the membrane varying k, S = 1000 kN, q = 100 kN/m

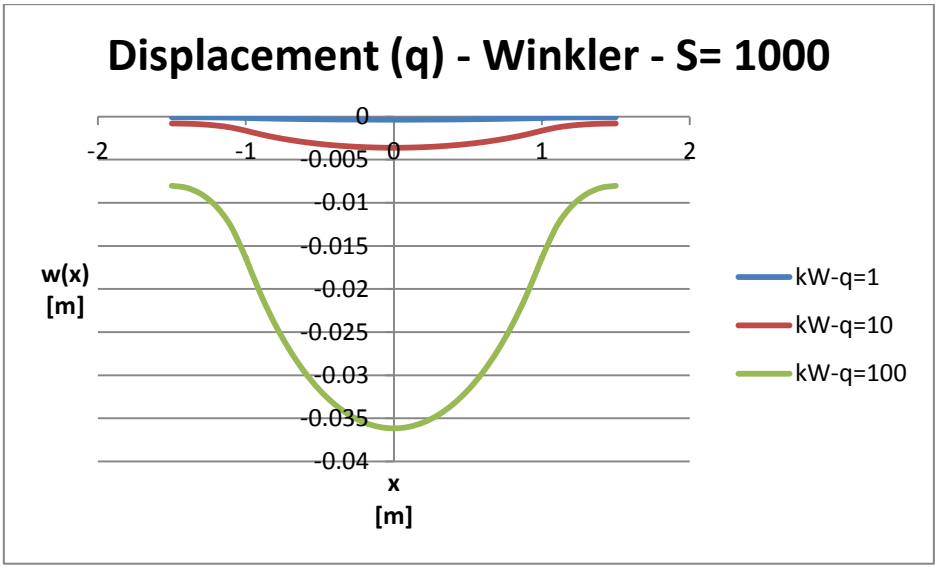

Figure 111: Displacement of the membrane varying q, k assumes the value adopted in the Winkler's solution and indicated in Table 7, S = 1000 kN

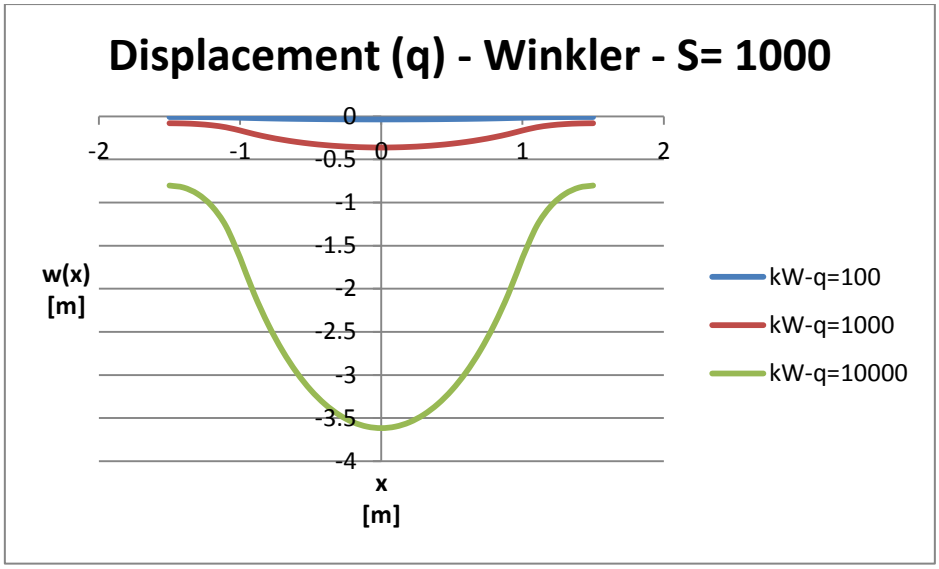

Figure 112: Displacement of the membrane varying q, k assumes the value adopted in the Winkler's solution and indicated in Table 7, S = 1000 kN

1.2.2.3 Pasternak – Finite difference

The third and probably most remarkable example deals with the situation analyzed in the second example but extended in a 2D loaded area, with deformative effects along the third axis (3D). First of all the equation of the membrane is similar to the one used in the previous chapter, but in this case represents a surface in two variables:

$$-S\left(\frac{\partial^2 w(x,y)}{\partial x^2}+\frac{\partial^2 w(x,y)}{\partial y^2}\right)+kw(x,y)=q(x,y) \quad (74)$$

where w is the displacement, k the subgrade modulus, q the load, S the membrane force.

This equation can be easily solved with the finite difference method applied on a spreadsheet. The 2D area the area has the shape of a square of 3 m from the side; in each of the four corners there is a square of 0.5 m from the side that represents the soil with greater stiffness (piles, gravel columns). The second derivative of a function f(x) can be approximated in this way:

$$\frac{d^2 f(x)}{dx^2} \Rightarrow \quad (75)$$

$$\Delta_0^2 f(x) = f(x+h) - 2f(x) + f(x-h) \quad (76)$$

where 0 is the center, h the step, Δ the variation.

The equation of the membrane has a second partial derivative, so the solution used in the spreadsheet is a little more complicated:

$$-S\left(\frac{1}{\Delta x^2}(L - 2C + R) + \frac{1}{\Delta x^2}(D - 2C + U)\right) + kw = q \qquad (77)$$

where Δx is placed equal to Δy (the discretization of the membrane along the two axis), L, C, R, D, U (respectively left, central, right, down, up) are the values of w in the cells nearby (and in) a selected cell, k is the subgrade modulus, S the membrane force, w and q are considered constants in the selected cell. In the cells where the stiffness is greater (in the corners) kf takes the place of k in the equation.

The equation of the membrane is valid in all the area, exept to the borders. Thus all the cells among the border must be placed equal to the cells that have (respectively) on the inner side of the left. This application has circular references, but you can set spreadsheet to find an iterative solution [7].

The 3D-graphics show the behavior of the membrane varying q, k (the value of "k" is the one obtained by the Winkler's method plus an arbitrary value of k = 10000 kN/m^3) and S.

Table 8: Parameters for the solution; the implemented values are the chosen ones for one of the analyzed cases

q	delta	kw	kf	S	cm	cf	p
[kN/m2]	[m]	[kN/m^3]	[kN/m^3]	[kN/m]	[-]	[-]	[m]
100	0.1	1824.064	18240.64	10000	0.249886	0.248865	0.0001

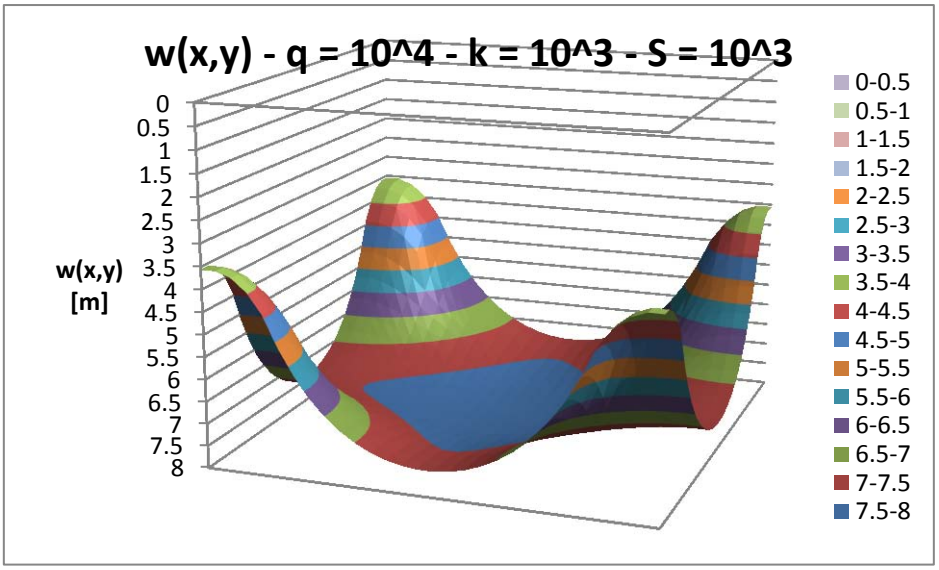

Figure 113: Displacement of the membrane for q = 10000 kN/m, k = 1000 kN/m^3, S = 1000 kN/m

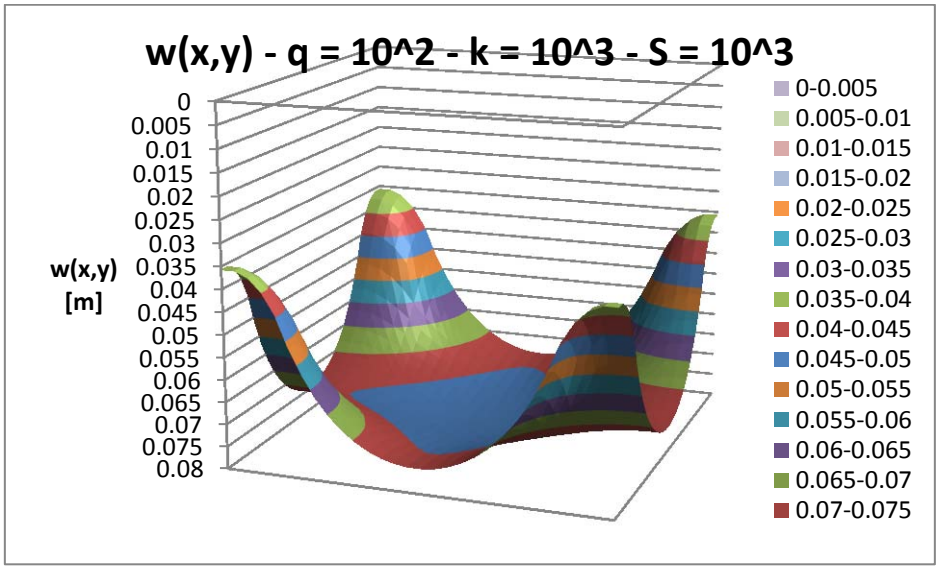

Figure 114: Displacement of the membrane for q = 10000 kN/m, k = 1000 kN/m³, S = 1000 kN/m

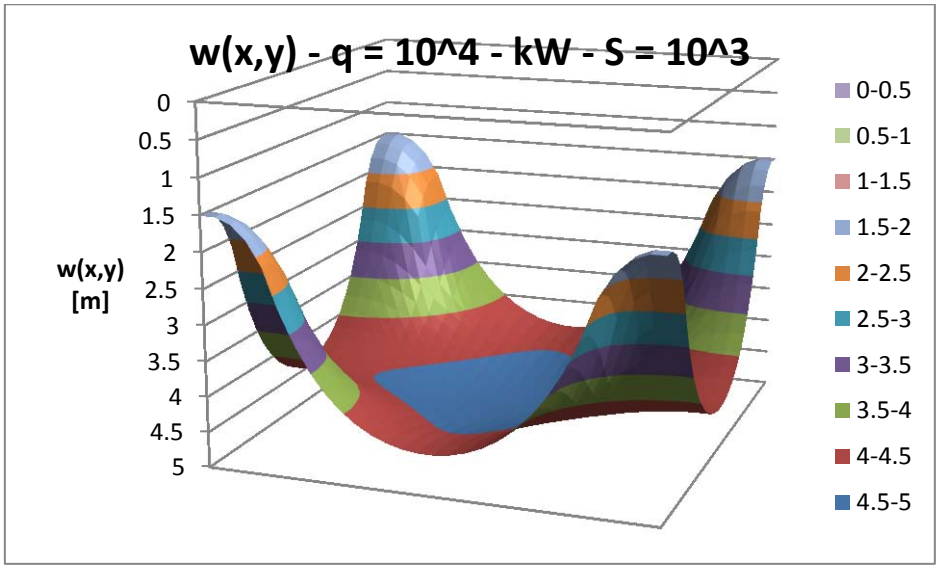

Figure 115: Displacement of the membrane for q = 10000 kN/m, k assumes the value adopted in the Winkler's solution and indicated in Table 8, S = 1000 kN

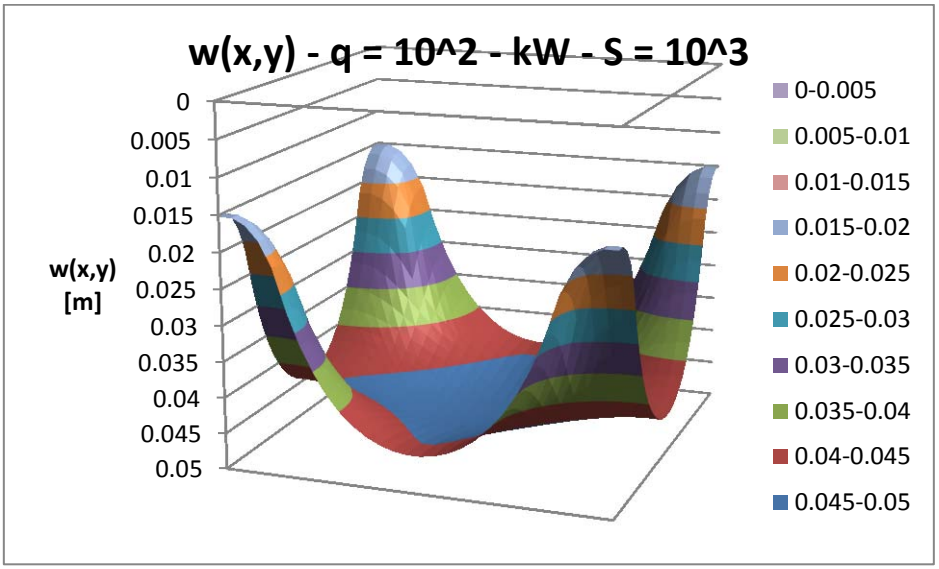

Figure 116: Displacement of the membrane for q = 100 kN/m, k assumes the value adopted in the Winkler's solution and indicated in Table 8, S = 1000 kN/m

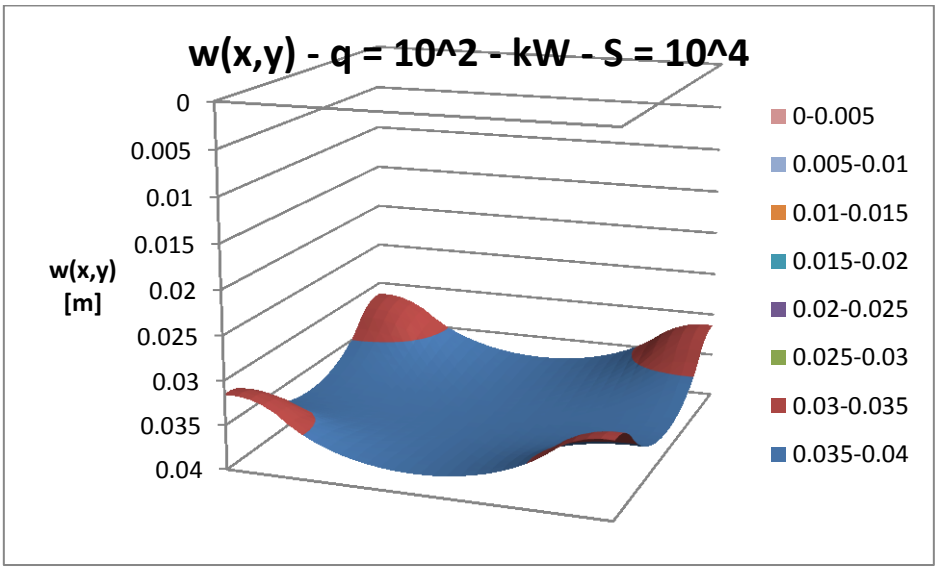

Figure 117: Displacement of the membrane for q = 100 kN/m, , k assumes the value adopted in the Winkler's solution and indicated in Table 8, S = 10000 kN/m

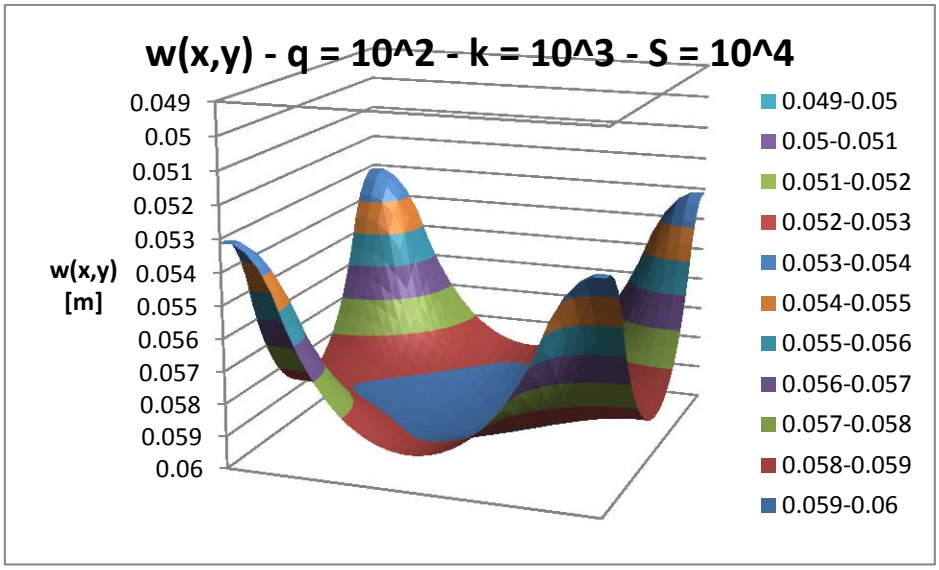

Figure 118: Displacement of the membrane for q = 100 kN/m, k = 1000 kN/m³, S = 10000 kN/m

1.3 Linear elastic versus elastic – plastic model

1.3.1 Theoretical introduction

In this chapter will be introduced a new FEM program in order to analyze the same problem studied in the former chapters, but changing the constitutive model from linear elastic into elastic-plastic: the program is Midas GTS, and the adopted constitutive model is Mohr-Coulomb. The purpose is to highlight the differences that occur between the two models, focusing on the behavior of the soil changing the constitutive parameters and in particular understand if the choice of the elastic model for the former analyses is suitable or not; that's to say that in the following chapter it has been verified until which value of the ratio between the load and the strength of the material an elastic model could be replace an elastic-plastic model.

Linear elastic model is the simplest constitutive model, its coefficients are the elastic modulus E and the Poisson's ratio ν. In 3D analysis the stress-strain relationship is expressed by the equation (78).

$$\begin{Bmatrix} \sigma_x \\ \sigma_y \\ \sigma_z \\ \tau_{xy} \\ \tau_{yz} \\ \tau_{zx} \end{Bmatrix} = \frac{E}{(1+\nu)(1-2\nu)} \begin{bmatrix} 1-\nu & \nu & \nu & & & \\ \nu & 1-\nu & \nu & & 0 & \\ \nu & \nu & 1-\nu & & & \\ & & & \frac{1-2\nu}{\nu} & & \\ & 0 & & & \frac{1-2\nu}{\nu} & \\ & & & & & \frac{1-2\nu}{\nu} \end{bmatrix} \begin{Bmatrix} \varepsilon_x \\ \varepsilon_y \\ \varepsilon_z \\ \gamma_{xy} \\ \gamma_{yz} \\ \gamma_{zx} \end{Bmatrix} \quad \textbf{(78)}$$

In 2D analyses $\tau_{yz} = \tau_{zx} = \gamma_{yz} = \gamma_{zx} = 0$, and especially for plain strain analyses $\varepsilon_z = 0$.

The parameter ν represents the pure volumetric strain, and as it approaches 0.5 the volumetric strain becomes close to 0 (incompressibility): in order to not have numerical problems is programs usually the assumed value is $\nu = 0.49$.

In this model the strain is directly proportional to the stress (Figure 119); the slope of linear curve is constant and depending on E and ν.

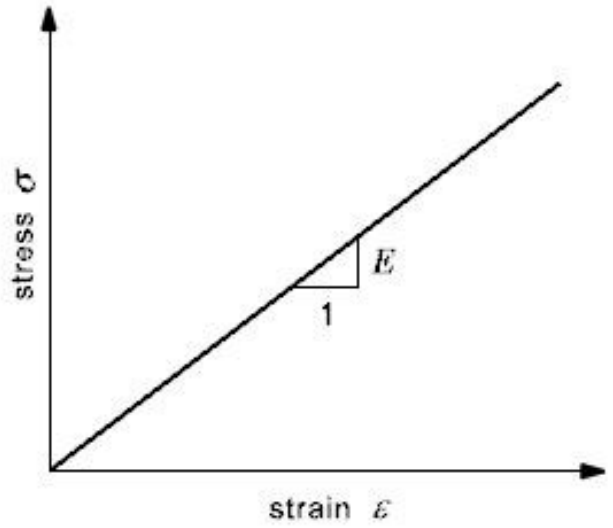

Figure 119: Stress-strain relationship of linear elastic model [8]

Generally the elastic model describes the behavior of the soil immediately after the load is applied and for small deformation. This method based on the Hook's Law is highly used for simple and preliminary analysis. The stress-strain relationship of soil is very complex: it depends on the material composition, porosity, stress history and loading method and exhibits a nonlinear material characteristics: it is very difficult to approximate soil as an elastic material. For this reason the key parameter, E, must be clearly defined to adequately replace the real behavior of soil.

Linear elastic analysis usually refers to deformability of the ground whereas elastic-plastic analysis refers either to deformability or instability of ground. Instability is determined by the shear strength of a material, deformability by both shear strength and elastic properties. If the load is greater of the shear strength capacity of the ground, some areas could reach the failure limit (plastic state), confined yield zones, surrounded by elastic zones; anyway some local failures do not necessarily cause a global failure. An elastic-plastic model distinguishes between reversible (elastic) and irreversible (plastic) deformation. The yield function defines the stress-condition at which deformation may occur. If the yield function is not satisfied the deformations will be fully elastic.

In the stress-strain relationship of an elastic and perfectly plastic model the stress is directly proportional to strain until the yield point after which the curve becomes completely horizontal (Figure 120).

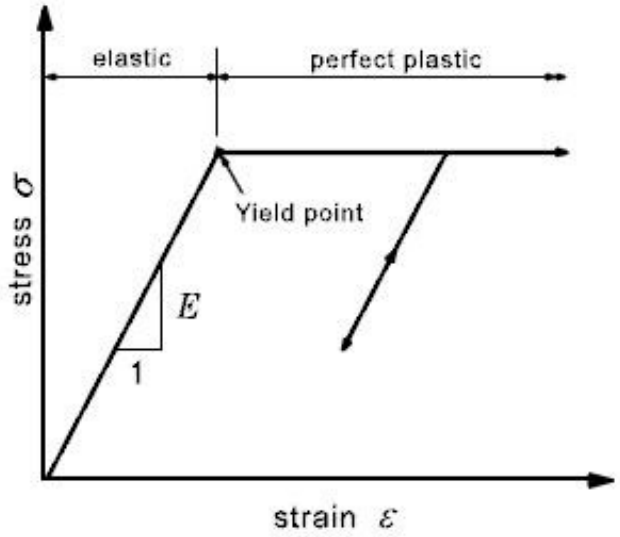

Figure 120: Stress-strain relationship of elastic-plastic model [8]

The parameters that define the model are the elastic modulus E, the Poisson's ratio ν, the cohesion c, the friction angle φ, the dilatancy angle ψ.

Usually the deformation caused by a load is composed by components: elastic and plastic strain.

$$\underline{\varepsilon} = \underline{\varepsilon}^{e} + \underline{\varepsilon}^{p} \quad \textbf{(79)}$$

Where $\underline{\varepsilon}$ is the total strain, $\underline{\varepsilon}^{e}$ is the elastic strain, $\underline{\varepsilon}^{p}$ is the plastic strain.

Some concepts are important to define the constitutive equations in plasticity: yield criteria (set the starting point of plastic deformation), flow rule (define plastic deformation), hardening rule (define deformation hardening)

The yield function (or loading function), F, which defines the limit of the elastic response range of a material is defined:

$$F\left(\underline{\sigma}, \underline{\varepsilon}^{p}, k\right) = \underline{\sigma}^{p}\left(\underline{\sigma}, \underline{\varepsilon}^{p}\right) - k\left(\varepsilon_{p}\right) \leq 0 \quad \textbf{(80)}$$

In plasticity theory the yield function can't be a positive value. When yielding occurs, the stress state is modified by accumulating plastic strains until the yield function is reduced to zero. This process is known as the "Plastic Corrector" phase or "Return Mapping".

Where σ, σ_e, k, ε^p are the current stress, the equivalent or effective stress, hardening factor, equivalent plastic strain respectively.

The plastic deformation that uses the plastic rule shown in is expressed by the following equations:

$$\mathrm{d}\,\underline{\varepsilon}^{\mathrm{p}} = \mathrm{d}\,\lambda\,\frac{\partial \mathrm{g}}{\partial \underline{\sigma}} = \mathrm{d}\,\lambda\,\mathbf{b} \tag{81}$$

Where $\partial \mathrm{g}/\partial \underline{\sigma}$ is the direction of plastic straining and $\mathrm{d}\lambda$ the plastic multiplier that defines the magnitude of plastic straining.

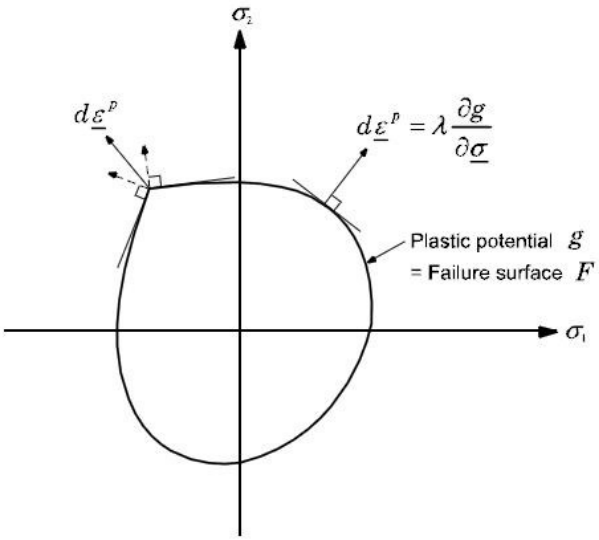

Figure 121: Geometric illustration of associated flow rule and singularity [8]

The function g is the "Plastic potential", usually defined in terms of stress invariants. If g is equal to F it is termed as "Associated flow rule" and the direction of the plastic strain vector is orthogonal to the yield surface; if g and F are unequal it is referred as "Non-associated flow rule". The former can be expressed by the following equation:

$$\mathrm{d}\,\underline{\varepsilon}^{\mathrm{p}} = \mathrm{d}\,\lambda\,\frac{\partial \mathrm{F}}{\partial \underline{\sigma}} = \mathrm{d}\,\lambda\,\mathbf{a} \tag{82}$$

Special consideration is required if singular points (Figure 121) occur at a corner or flat surface (impossibility to define the plastic flow path).

The equation (83) is the standard constitutive equation. Stress increments are determined by the elastic part of the strain increments.

$$\mathrm{d}\,\underline{\sigma} = \mathbf{D}^{\mathrm{e}}\left(\mathrm{d}\,\underline{\varepsilon} - \mathrm{d}\,\underline{\varepsilon}^{\mathrm{p}}\right) = \mathbf{D}^{\mathrm{e}}\left(\mathrm{d}\,\underline{\varepsilon} - \mathrm{d}\,\lambda\,\mathbf{a}\right) \tag{83}$$

Where $\mathbf{D}^{\mathrm{e}}$ is the elastic constitutive matrix. The following consistency condition needs to be satisfied so as the stresses are always maintained on the yield surface. Therefore the equation (93) allows to calculate the infinitesimal stress increments.

$$\mathrm{d}\,\underline{\sigma} = \mathbf{C}\,\mathrm{d}\,\underline{\varepsilon} - \mathrm{d}\,\lambda\,\mathbf{C}\,\mathbf{a} = \left(\mathbf{D}^{\mathrm{e}} - \frac{\mathbf{D}^{\mathrm{e}}\mathbf{a}\mathbf{a}^{\mathrm{T}}\mathbf{D}^{\mathrm{eT}}}{\mathbf{a}^{\mathrm{T}}\mathbf{D}^{\mathrm{e}}\mathbf{a} + \mathrm{h}}\right)\mathrm{d}\,\underline{\varepsilon} \tag{84}$$

Using the full Newton-Raphson iteration procedure and a consistent stiffness matrix the convergence can be much faster due to the second-order convergence characteristic of the aforementioned method.

$$\mathrm{d}\,\underline{\sigma} = \mathbf{C}\,\mathrm{d}\,\underline{\varepsilon} - \mathrm{d}\,\lambda\,\mathbf{C}\,\mathbf{a} - \lambda\,\mathbf{C}\,\frac{\partial \mathbf{a}}{\partial \underline{\sigma}}\,\mathrm{d}\,\underline{\sigma} = \left(\mathbf{R} - \frac{\mathbf{R}^{\mathrm{e}}\mathbf{a}\mathbf{a}^{\mathrm{T}}\mathbf{R}^{\mathrm{eT}}}{\mathbf{a}^{\mathrm{T}}\mathbf{R}^{\mathrm{e}}\mathbf{a} + \mathrm{h}}\right)\mathrm{d}\,\underline{\varepsilon} \tag{85}$$

Where

$$\mathbf{R} = \left(\mathbf{I} + \mathrm{d}\,\lambda\,\mathbf{D}^{\mathrm{e}}\,\frac{\partial \mathbf{a}}{\partial \underline{\sigma}}\right)^{-1} \tag{86}$$

$$\mathbf{D}^{\mathrm{e}} = (\mathbf{I} + \mathrm{d}\,\lambda\,\mathbf{D}^{\mathrm{e}}\,\mathbf{a})^{-1}\,\mathbf{D}^{\mathrm{e}} \tag{87}$$

In the elastic-plastic analyses carried out in this chapter (and also using GeoStudio and Plaxis in chapter 2) the Mohr-Coulomb failure criterion (1900) has been adopted; it is expressed by:

$$|\tau| = \mathrm{f}(\sigma) \tag{88}$$

The limiting stress state, τ_{s}, in a plane is only related to the normal stress, σ, in the same plane. The failure envelope expressed by the equation (88) is experimentally determined. The Mohr's criterion affirms that a material fails when the largest Mohr's circle is tangent to the envelope. For this reason no effect on the failure condition is due to the intermediate principal stress σ_{i} (σ_1, σ_2, σ_3).

The straight line defined by equation (89) represents the simplest representation of the Mohr's failure envelope:

$$|\tau| = \mathrm{c} + \sigma \tan\varphi \tag{89}$$

Where c is the cohesion and φ the friction angle.

The Mohr-Coulomb failure criterion is usually described by the equation (98).

There are three limitations in using the Mohr-Coulomb criterion. Firstly, when the failure envelope is reached by the largest Mohr's circle the intermediate principal stress σ_{i} (σ_1, σ_2, σ_3) doesn't influence the failure stress: this is inconsistent with experimental results. Secondly, the meridians and failure envelop of the Mohr's circle are straight lines and independent of strength parameter (φ) and hydraulic (or confining) pressure (Figure 122)Figure 122:: the precision of the criterion is

good for limited hydraulic pressure, but it decreases by increasing the hydraulic pressure area. Numerical errors may occur due to the discontinuity of the yield surface (that is not smooth) at the corner. Lastly, the Mohr-Coulomb cannot describe the compaction of soil.

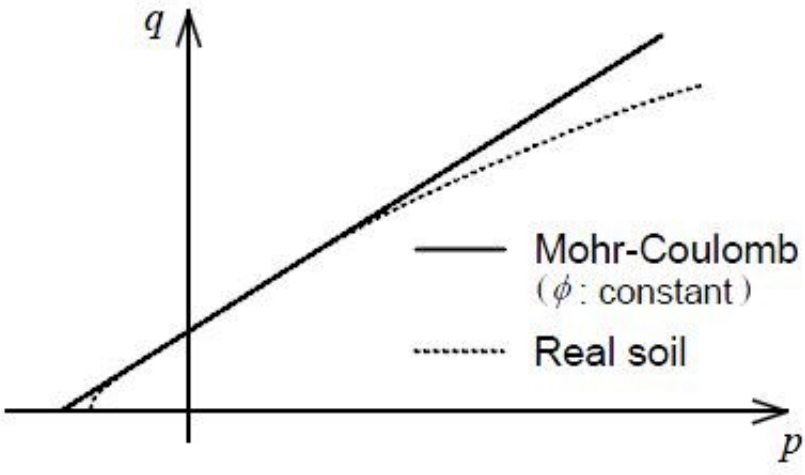

Figure 122: Schematization of yield function [9].

Despite this limitations, adopting this criterion within practical hydraulic pressure limits leads to relatively good results; it is a widely used criterion to model granular materials (such as soil and concrete) due to its precision and simplicity and has been successfully used in geotechnical engineering; assuming this model the solutions in nonlinear analyses are reliable.

The Mohr-Coulomb equation can also be expressed in terms of the principle stresses ($\sigma_1 \leq \sigma_2 \leq \sigma_3$), in terms of stress invariants J_1, J_2 and θ_0, or in terms of the variables ξ, ρ and θ_0.

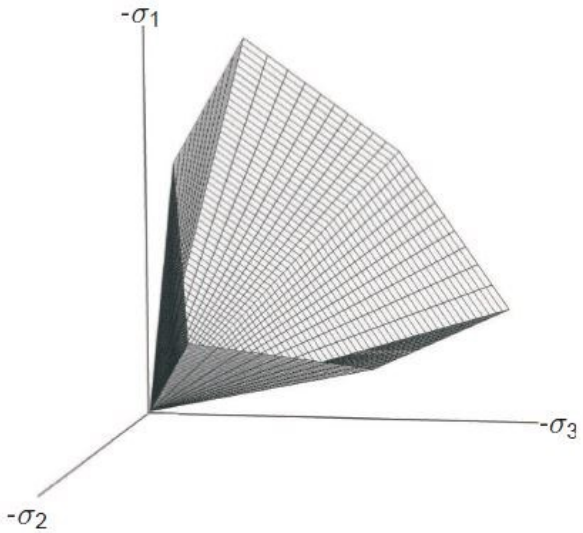

Figure 123: The Mohr-Coulomb yield surface in principal stress space (c=0) [10]

In the following chapter the applications of this model will be carried out [9], [8], [10].

1.3.2 Overview of the results

In this chapter have been analyzed the behavior of the same model studied in chapter 0 but adopting an elastic plastic constitutive model. The aim is to verify if the previous model is adequate to describe the system of loaded beam resting on the soil for the given set of conditions. The used program is Midas GTS.

Table 9: Parameters of the soils and of the beam (Mohr-Coulomb constitutive model)

SAND							
H	γ	ϕ	c	ν	ψ	Es	K_0
[m]	[kN/m^3]	[°]	[kPa]	[-]	[°]	[kPa]	[-]
5	18	37	0	0.3	5	37x10^3	0.5
CLAY							
H	γ	ϕ	c	ν	ψ	Es	K_0
[m]	[kN/m^3]	[°]	[kPa]	[-]	[°]	[kPa]	[-]
5	20	25	0	0.3	0	9x10^3	0.5

BEAM						
Eb	L	A	J	P1	P2	q
[kPa]	[m]	[m^2]	[m^4]	[kN]	[kN]	[kN/m]
30x10^6	10	1	0.083333	100	100	20

The mesh is composed by 4-noded quadrilateral elements (four integration points) and 3-noded triangular elements (one integration point), that's to say "linear elements" with "linear interpolation". The first type of elements leads to accurate displacement and stress result, whereas the second type provides poor accuracy of stresses, the displacements are good: the geometry and the system beam-loads is not so detailed or complex, so these elements are suitable to the problem, furthermore the use of "quadratic elements" could lead to a rigid behavior not consistent with the real soil.

The used analyses is "construction stage", that's to say that first the "in situ analysis" has been performed by using the "K_0 method" which allows to determine the stresses within the soil caused by the self-weight of ground before the "activation" of loads, then the displacements (by choosing an option in the program) have been deleted (in fact a new parameter which wasn't considered in the elastic method is the non-dimensional quantity $K_0 = \sigma_h / \sigma_v$, where σ_h and σ_v the horizontal and the vertical stress within the ground respectively). The second step is the activation of the loads and the consequent analysis.

The iteration method adopted is the "Newton-Raphson method", the load increment is the "equidistant load step", the convergence criterion is "force norm ratio": all these parameters are summarized in Figure 124.

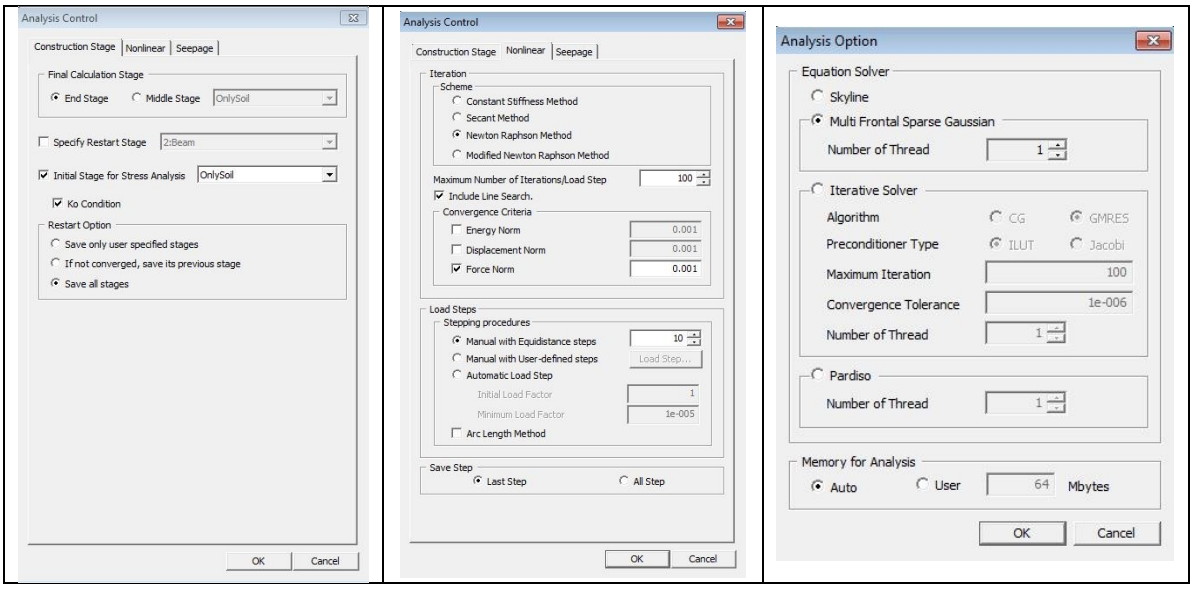

Figure 124: Midas GTS analysis set up

A comparison between elastic model and elastic-plastic model (both performed by Midas GTS) have been performed, by using for the second type a cohesion c = 0.1 Kpa (the "0" value causes numerical error in the calculation of the stiffness matrix), and by varying the entity of loads (from two forces of 100 kN each to two forces of 20000 kN each): the purpose is to verify if the behavior of the soil is still elastic or turned into elastic-plastic, in the latter case the model assumed in chapter 0 would be incorrect. In the following graphics (Figure 125, Figure 126) one can see the displacement of the beam for both elastic and elastic-plastic case (with c = 0.1 kPa) by varying the entity of load.

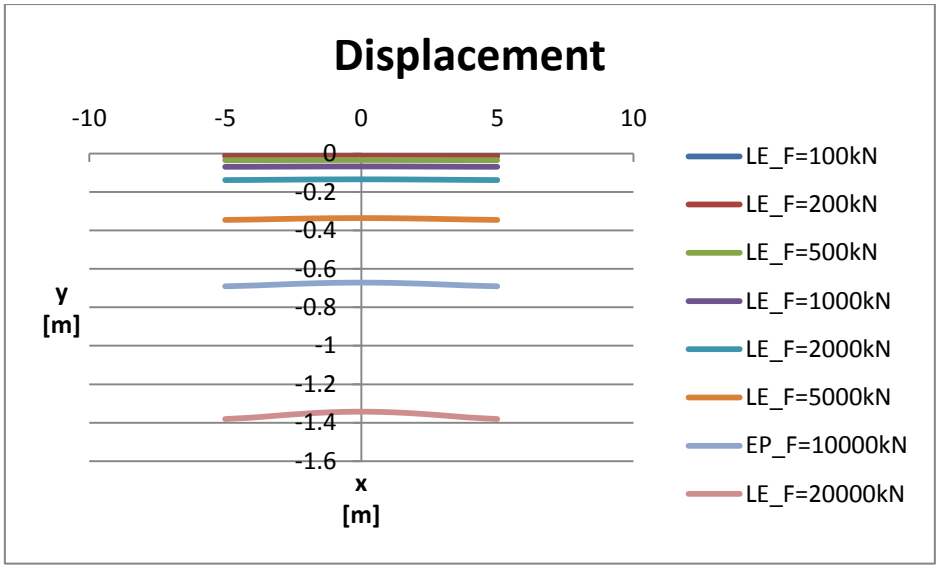

Figure 125: Displacement of the beam on linear elastic soil by varying the entity of load

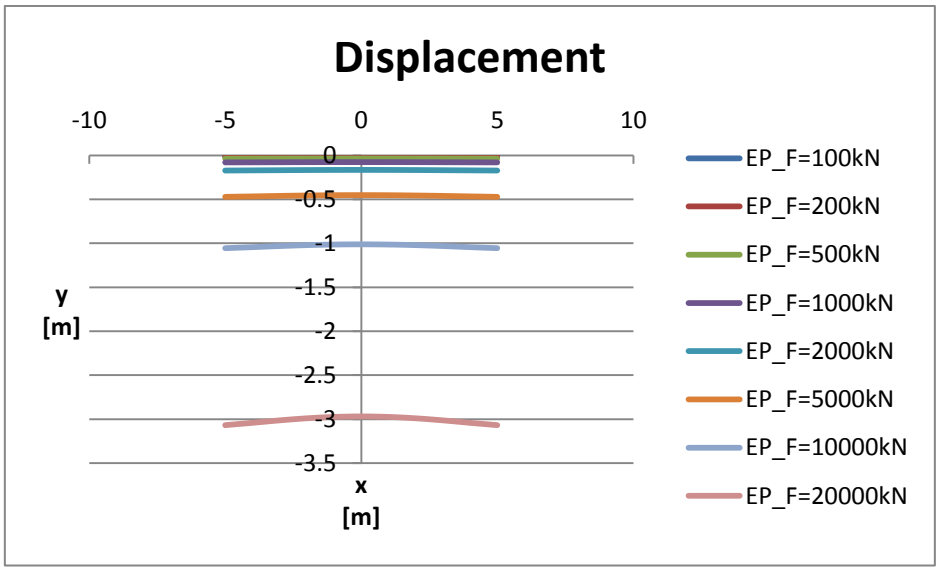

Figure 126: Displacement of the beam on elastic-plastic soil (c=0.1 kPa) by varying the entity of load

As it is easy to see for the load "F = 100 kN" (that's to say two forces of 100 kN each), the assumed load in chapter 0, the behavior seems to be similar either for elastic or elastic-plastic model. In order to prove this hypothesis the displacement of two nodes along the symmetry axis of the beam has been calculated: the load has been varied with the same modality as the previous analysis, both for the elastic model that the elastic-plastic model. The first point is located 1 m below ground level (in the sandy soil), the second 6 m below the ground level (in the clay soil). The following force-displacement graphics (from Figure 127 to Figure 131) illustrate the trend of the solution. One can see the level of plasticity of soil in the following screenshots from Figure 132 to Figure 135: in the first image only some plastic points appear under the right force (one can notice the asymmetry of the response

of the soil, probably because of a numerical error in the post processing procedure, Figure 132) under a load of two forces of 100 kN each. In the second image (Figure 133) appear the first plastic points in the clay soil under a load of two forces 600 kN each. In the third image (Figure 134) appear plastic points around the node (in clay) considered in the analysis (6 m below the ground level, along the axis of symmetry of the beam) under a load of two forces of 2000 kN each. The fourth image shows the spread of plasticity in the clay soil under a load of two forces of 5000kN each.

For this reason it's possible to say that the behavior of the point of in clay is elastic until a load of two forces of 2000 kN is applied when plasticity occurs. From the graphics force-displacement the point in sand seems to behave like the one in sand, that's to say that is seems to gradually plasticize: in the screenshots this phenomenon doesn't appear, probably because a numerical error in the post processing procedure.

Anyway the important achievement is that the soil (sand and clay) is surely in an elastic state for a load of two forces of 100 kN each and consequently the model used in the chapter 0 is suitable to characterize the issue described.

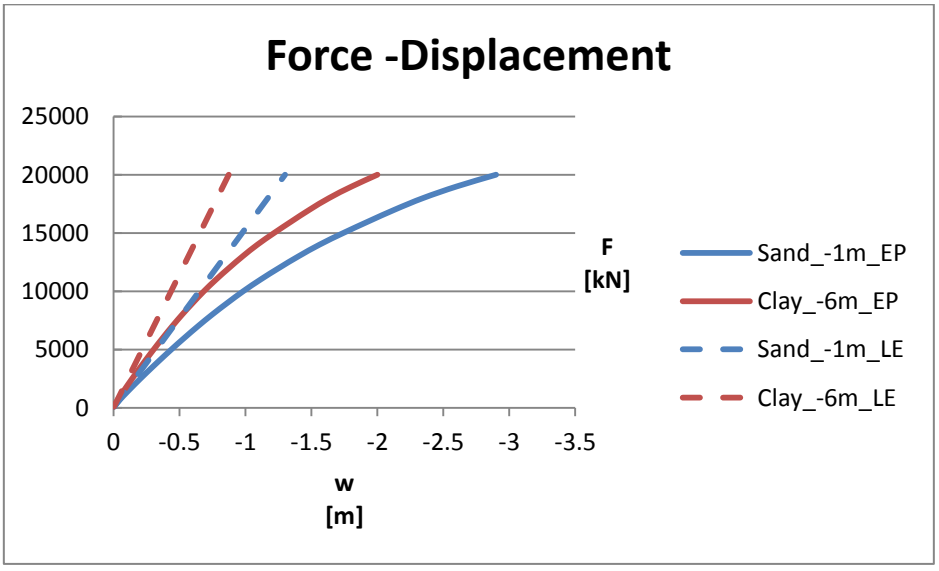

Figure 127: Force-displacement graphic of the two points in sand and clay, linear elastic constitutive model and elastic-plastic constitutive model

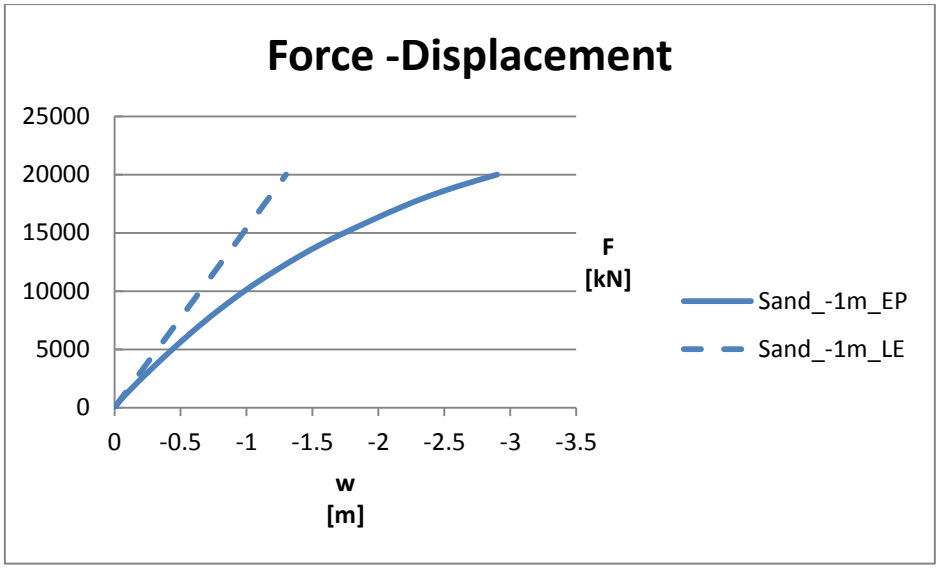

Figure 128: Force-displacement graphic of the point in sand, linear elastic and elastic-plastic constitutive model

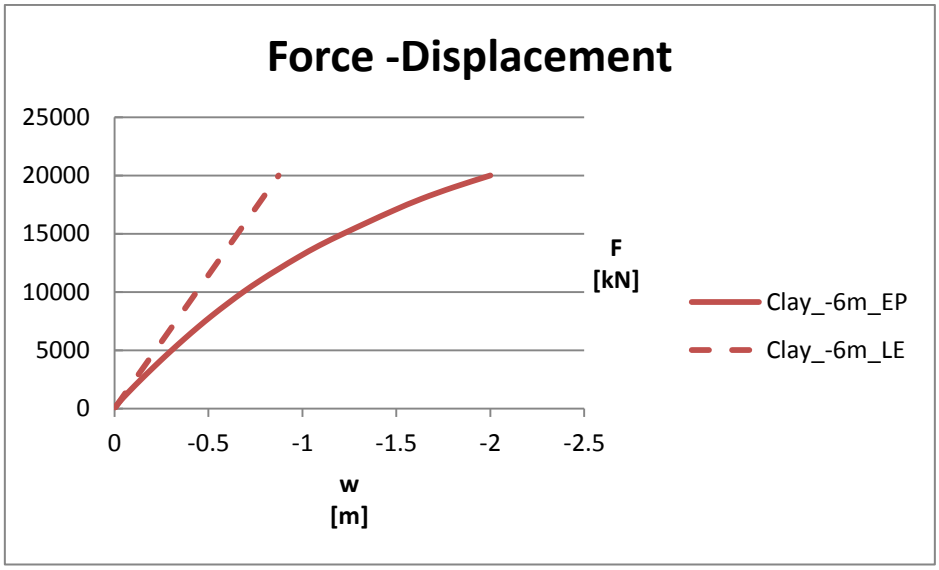

Figure 129: Force-displacement graphic of the point in clay, linear elastic and elastic-plastic constitutive model

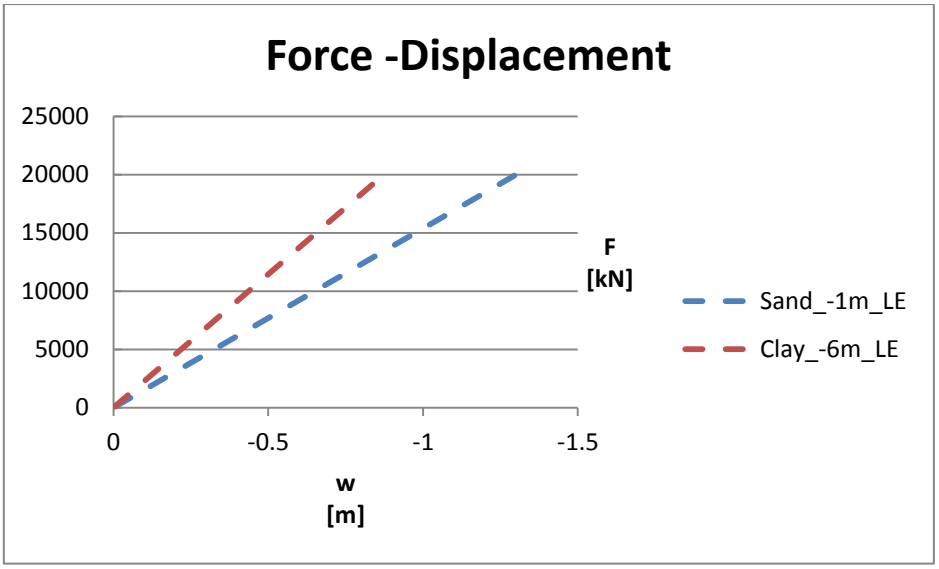

Figure 130: Force-displacement graphic of the two points in sand and clay, linear elastic constitutive model

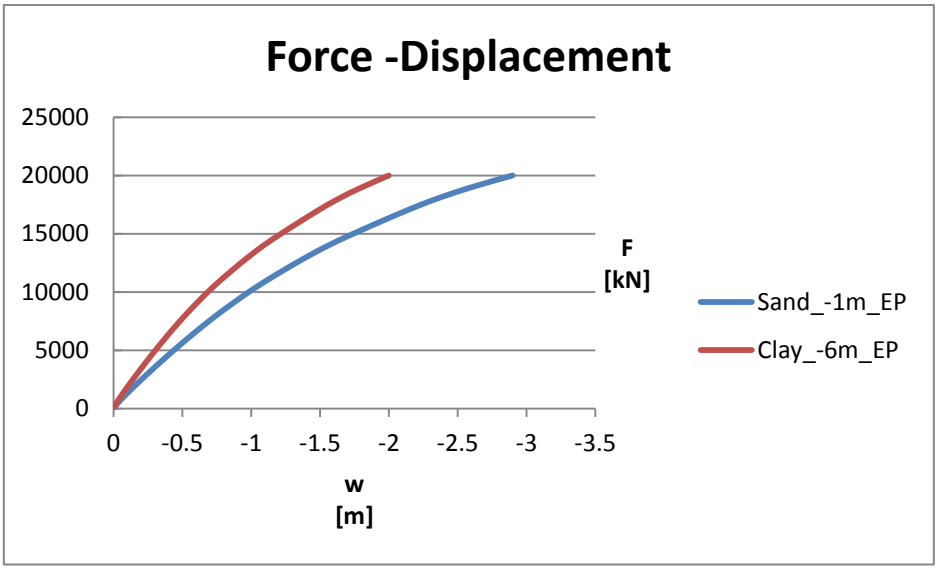

Figure 131: Force-displacement graphic of the two points in sand and clay, elastic-plastic constitutive model

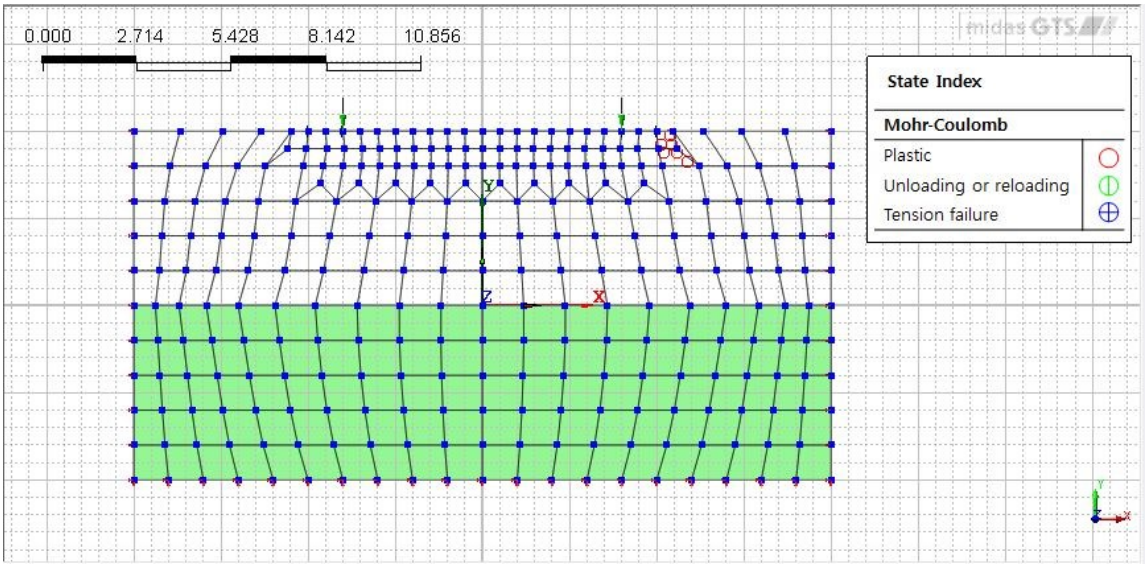

Figure 132: Plastic points under a load of two forces of 100 kN each

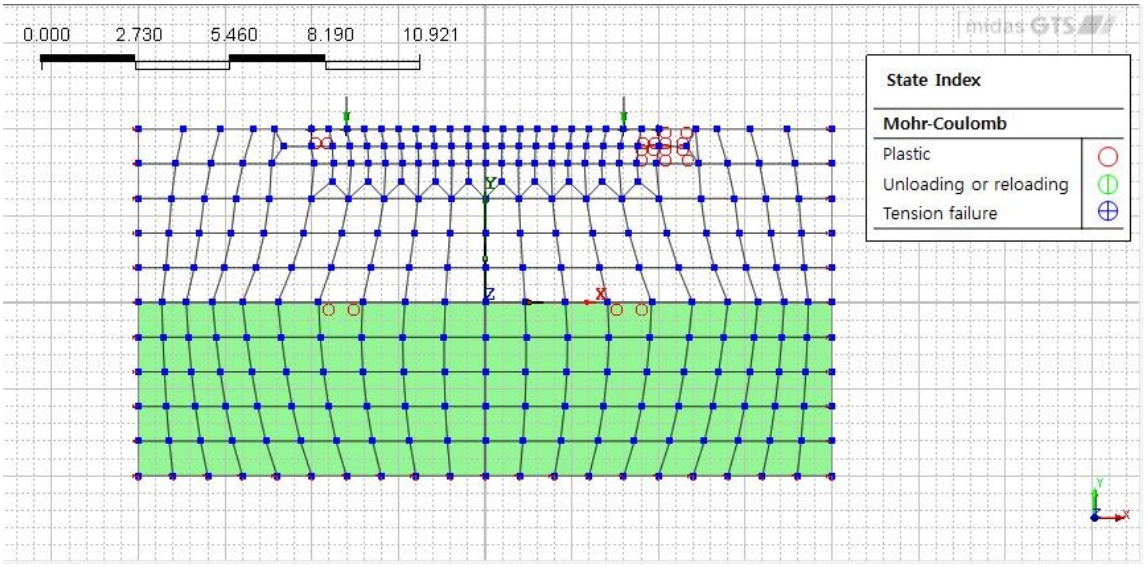

Figure 133: Plastic points under a load of two forces of 600 kN each

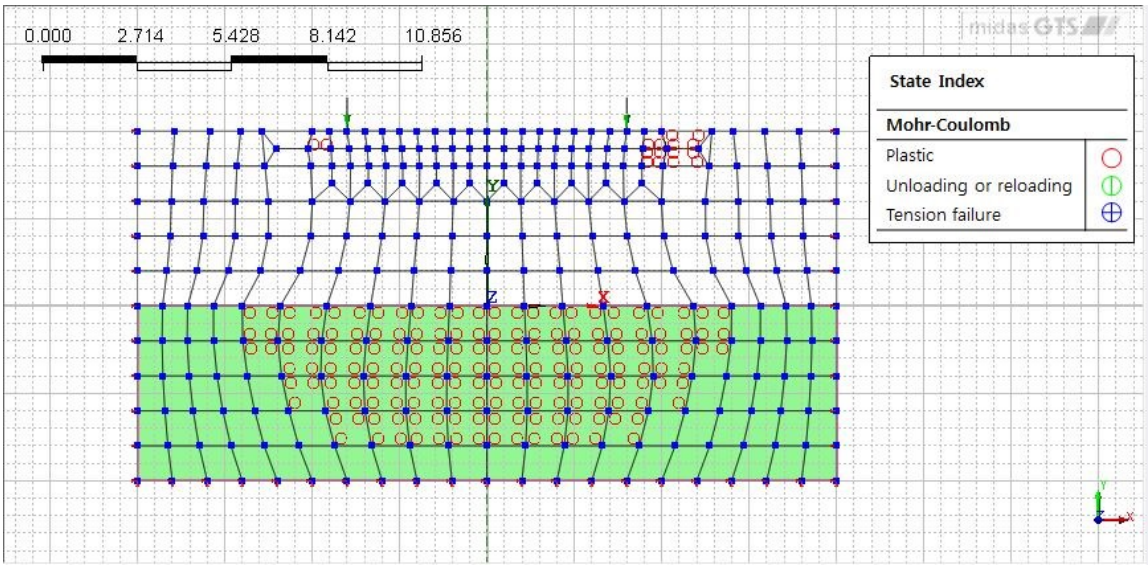

Figure 134: Plastic points under a load of two forces of 2000 kN each

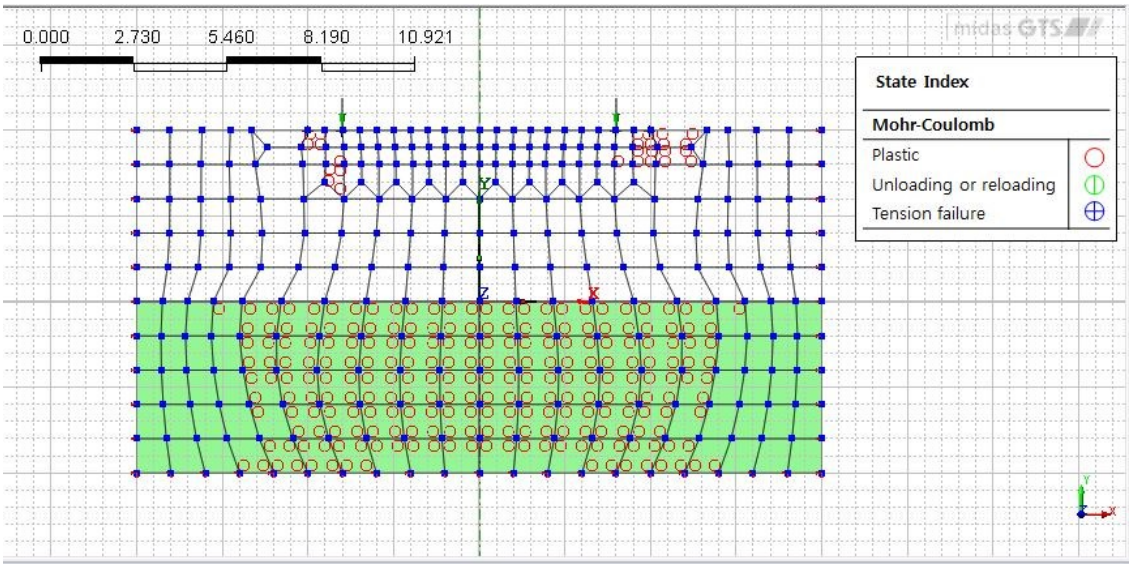

Figure 135: Plastic points under a load of two forces of 5000 kN each

In order to have a whole description of the behavior of the points of in sand and clay under the three topic loads described before (100 kN, 2000 kN and 5000 kN) screenshots of some characteristics of the model will be shown in the following pages; in addiction for every load with graphics will be shown the trend of the displacement of the beam, the displacement of the points along the axis of symmetry, the stress SYY below the left force, the mid-point of the beam, the right either for the elastic model or for the elastic-plastic one varying the cohesion (from c = 0.1 kPa to 20 kPa). Increasing the load the soil diverges from the elastic behavior, and consequently the displacement and the stress increase. The variation of the cohesion modifies the response of the soil but not significantly than the elastic model.

Remarkable is the trend of the bending moment and of the shear force of the beam (from Figure 175 to Figure 177): as for the other characteristics of the model also this stress parameters diverge from the elastic solution.

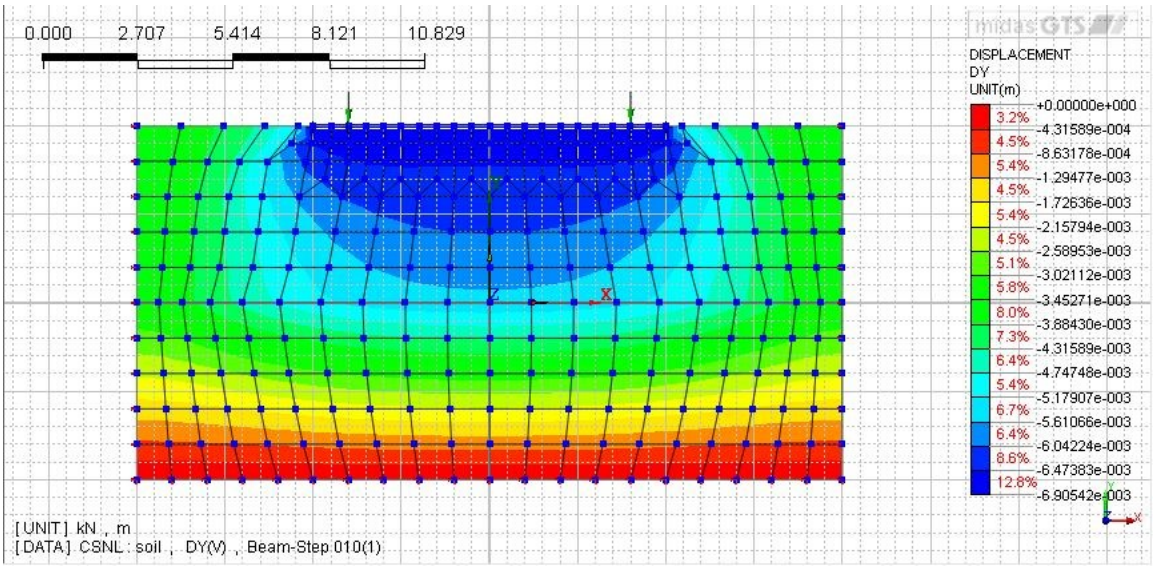

Figure 136: Displacement DY, F=100 kN, linear elastic

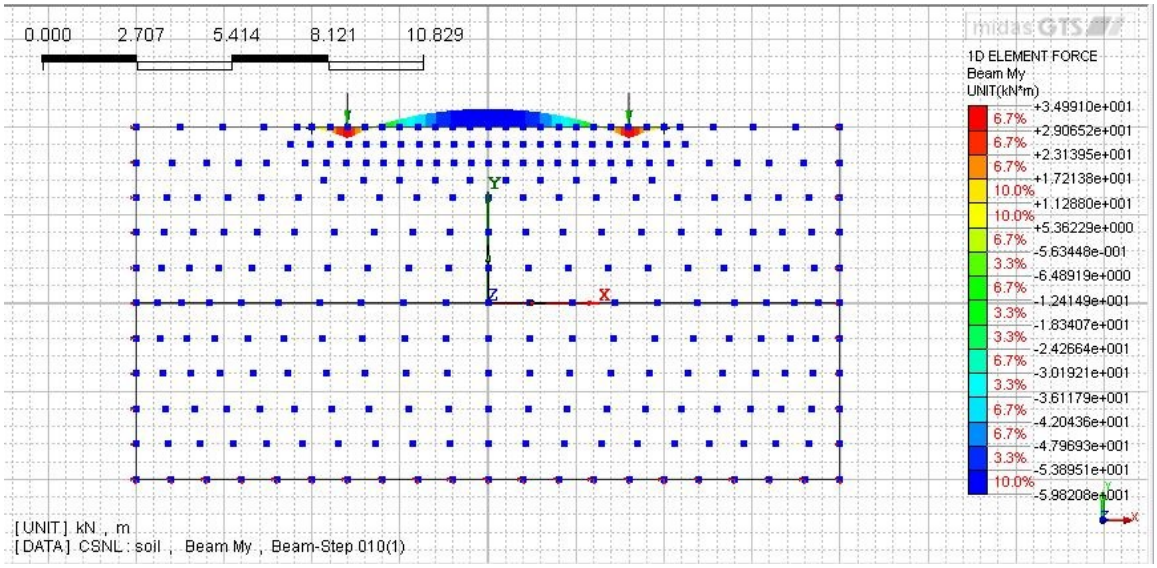

Figure 137: Bending moment, F=100 kN, linear elastic

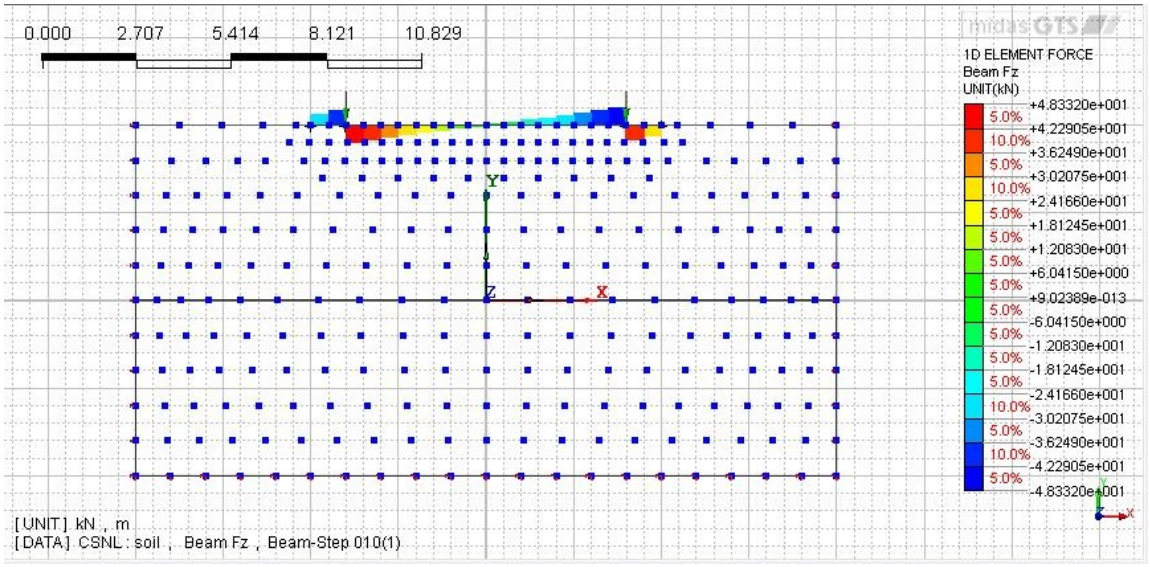

Figure 138: Shear force, F=100 kN, linear elastic

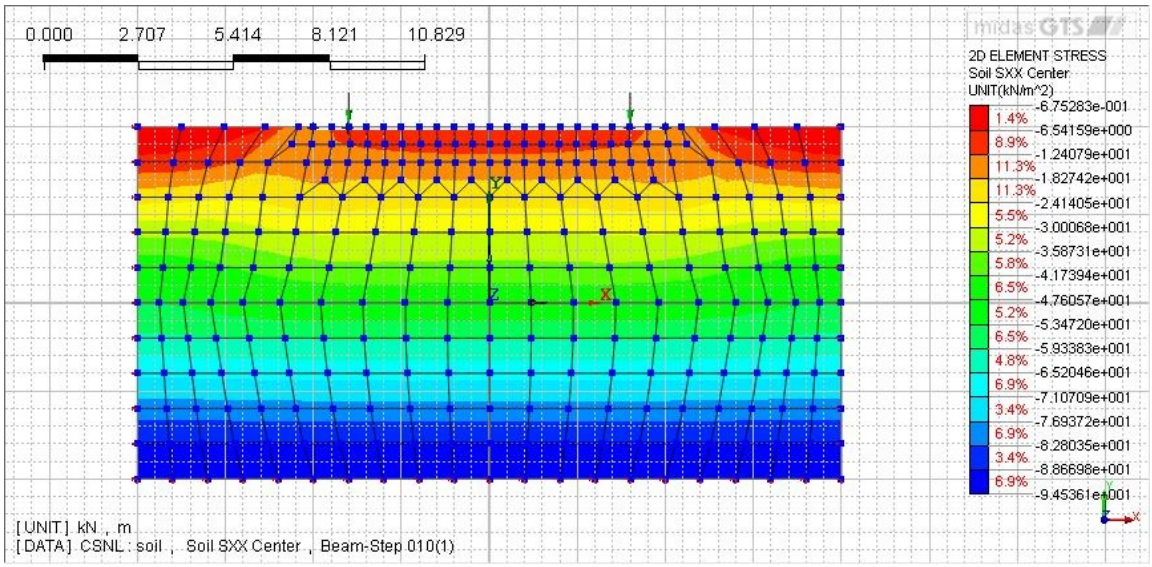

Figure 139: Stress SXX, F=100 kN, linear elastic

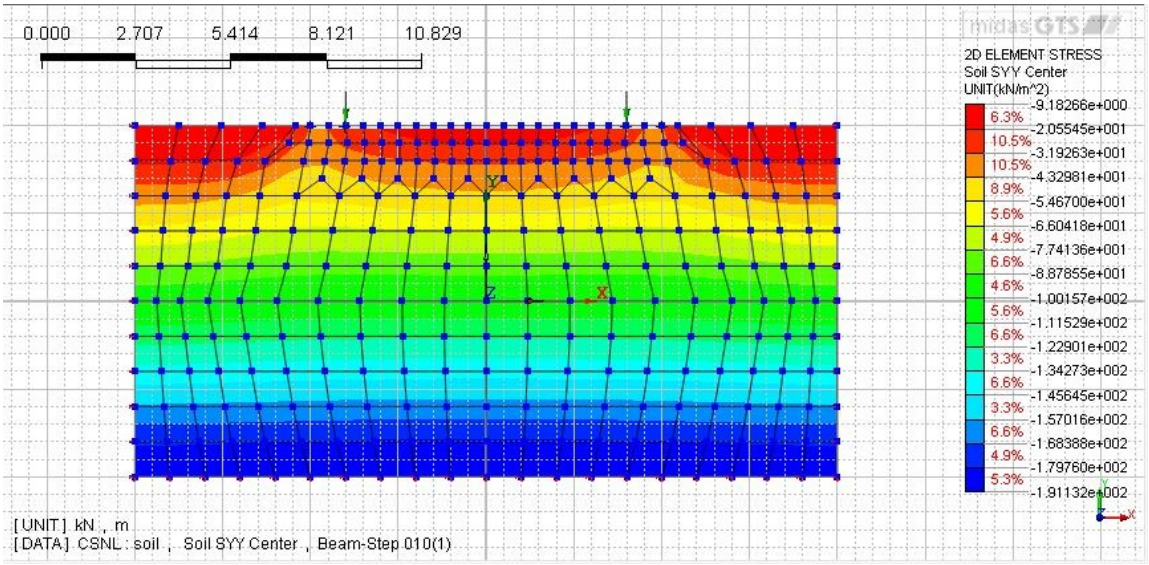

Figure 140: Stress SYY, F=100 kN, linear elastic

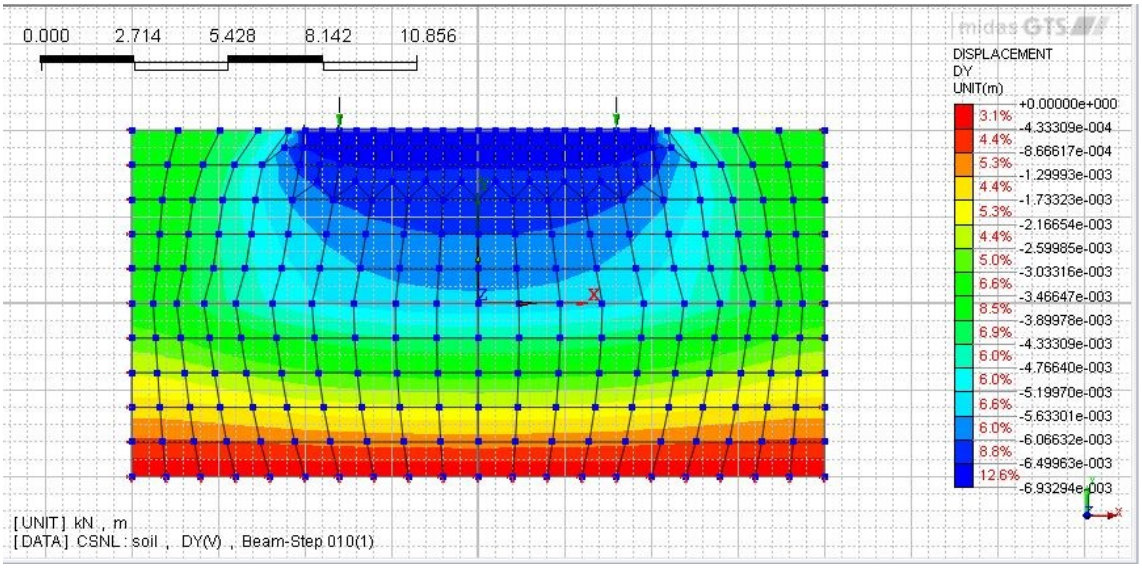

Figure 141: Displacement DY, F=100 kN, elastic plastic, c=0.1 kPa

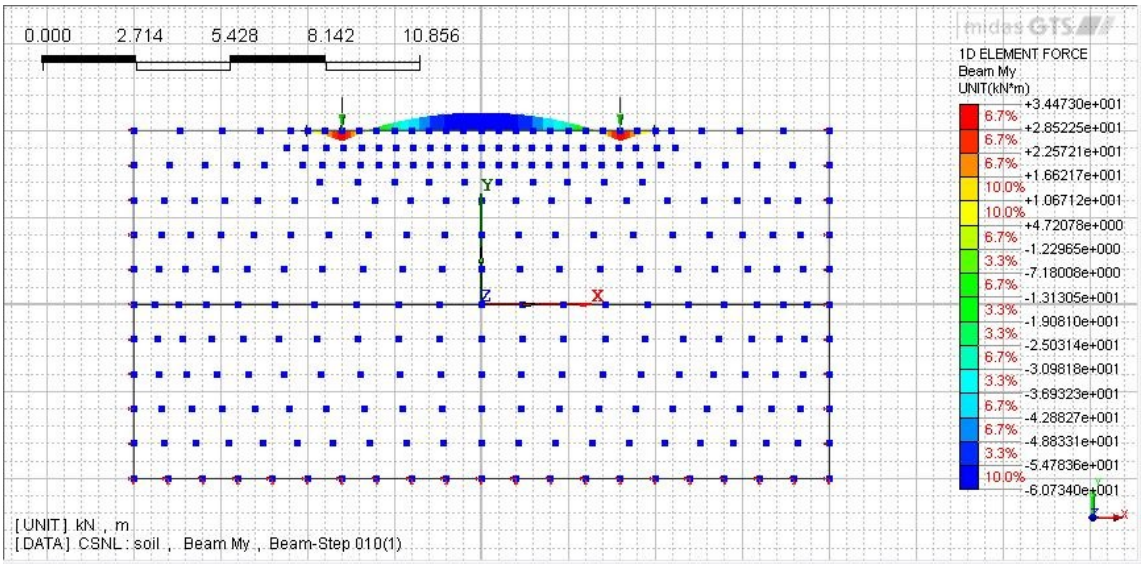

Figure 142: Bending moment, F=100 kN, elastic plastic, c=0.1 kPa

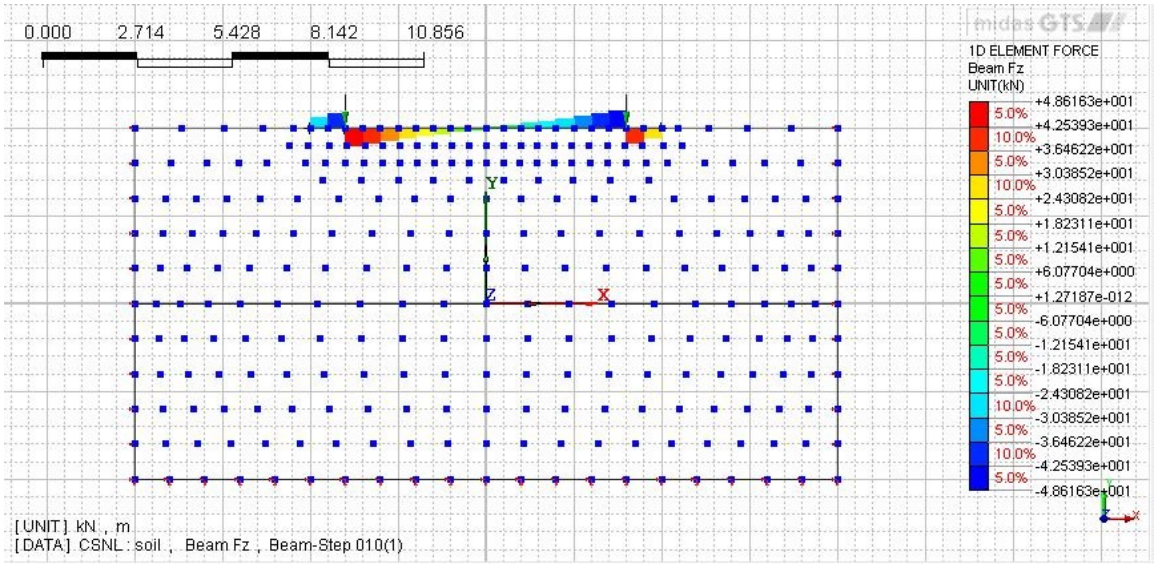

Figure 143: Shear force, F=100 kN, elastic plastic, c=0.1 kPa

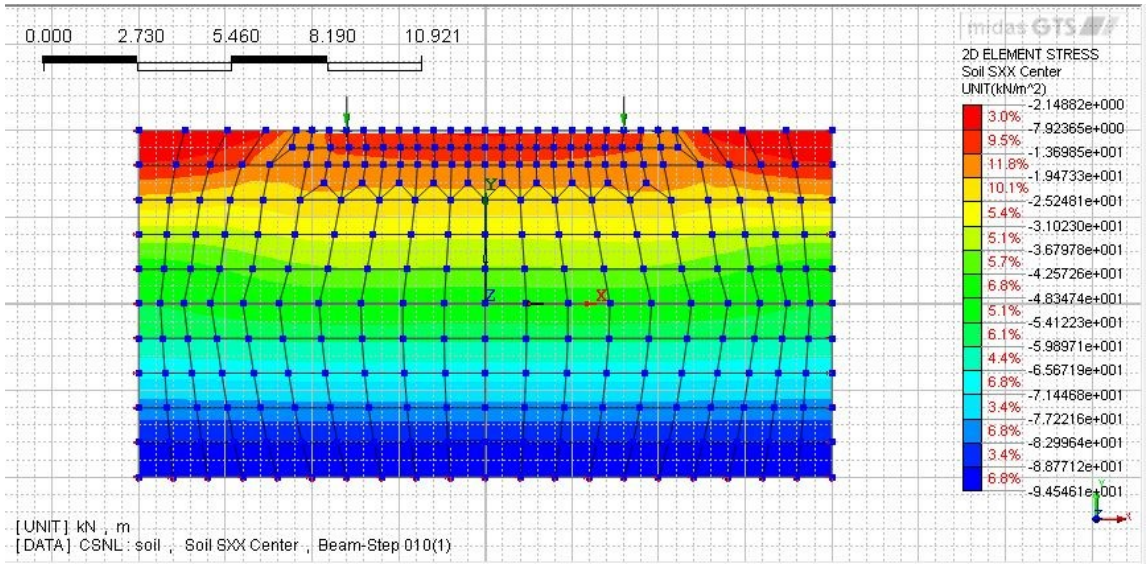

Figure 144: Stress SXX, F=100 kN, elastic plastic, c=0.1 kPa

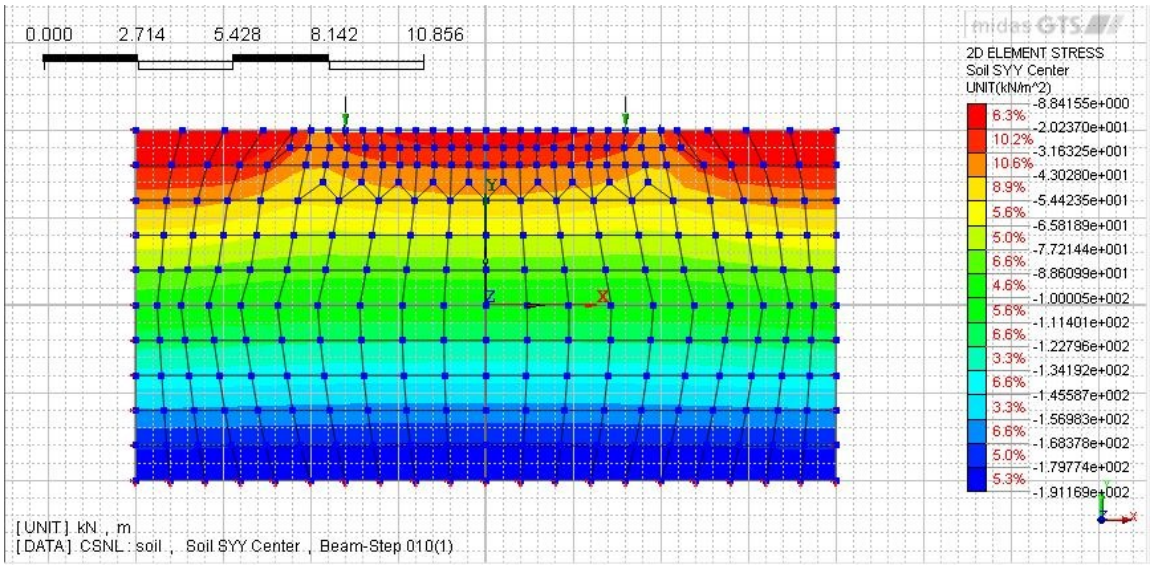

Figure 145: Stress SYY, F=100 kN, elastic plastic, c=0.1 kPa

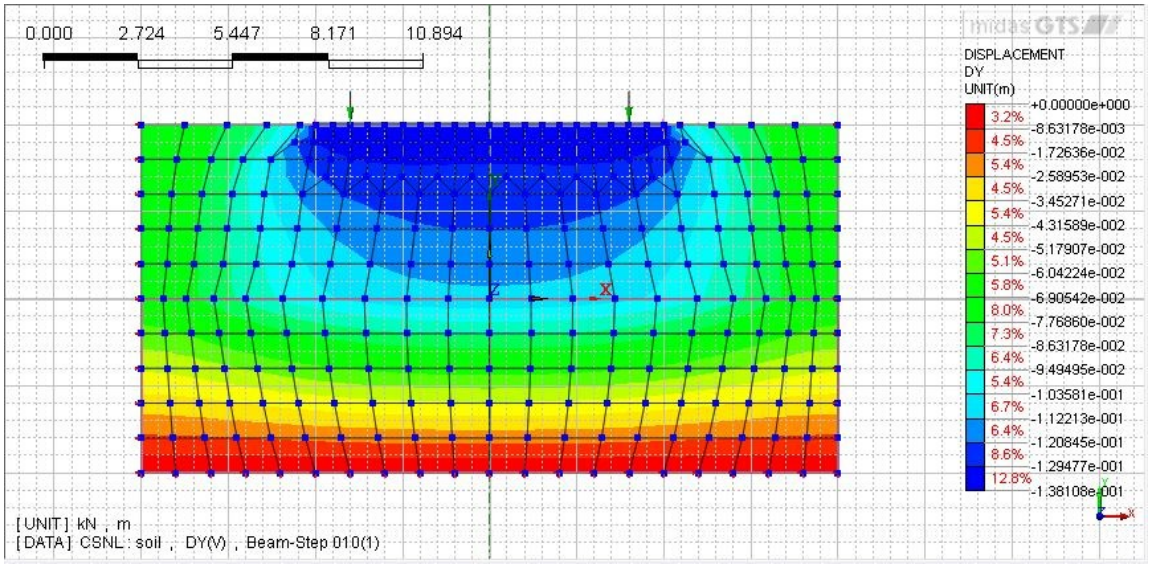

Figure 146: Displacement DY, F=2000 kN, linear elastic

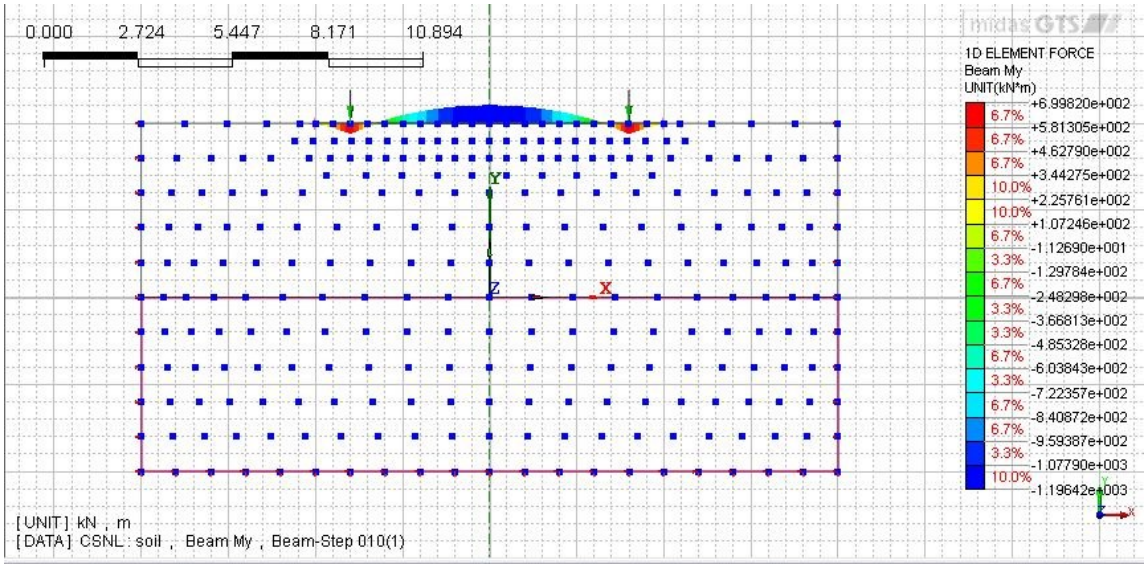

Figure 147: Bending moment, F=2000 kN, linear elastic

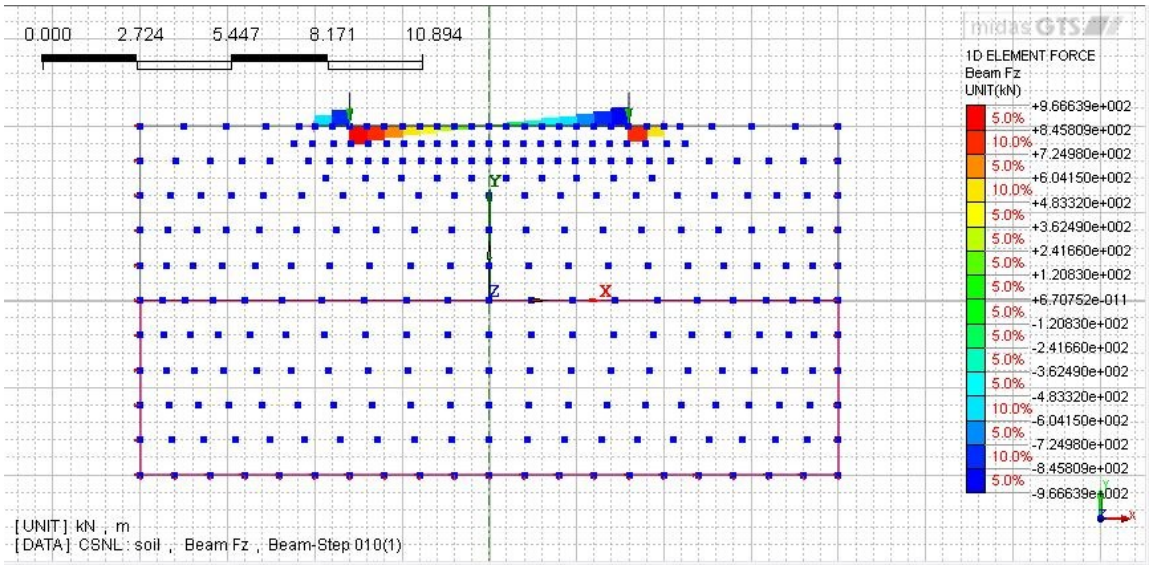

Figure 148: Shear force, F=2000 kN, linear elastic

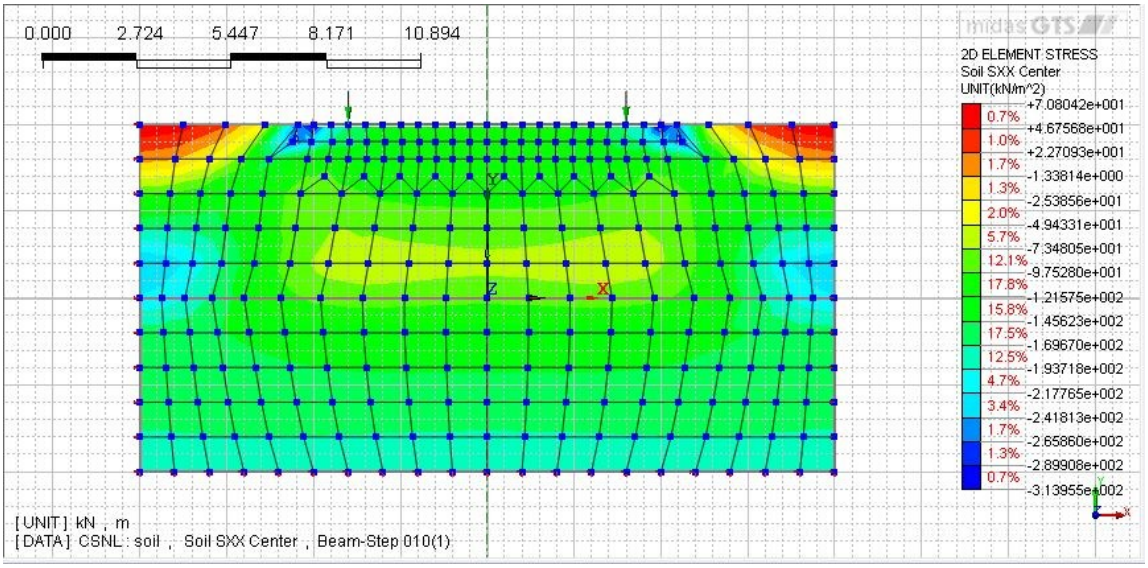

Figure 149: Stress SXX, F=2000 kN, linear elastic

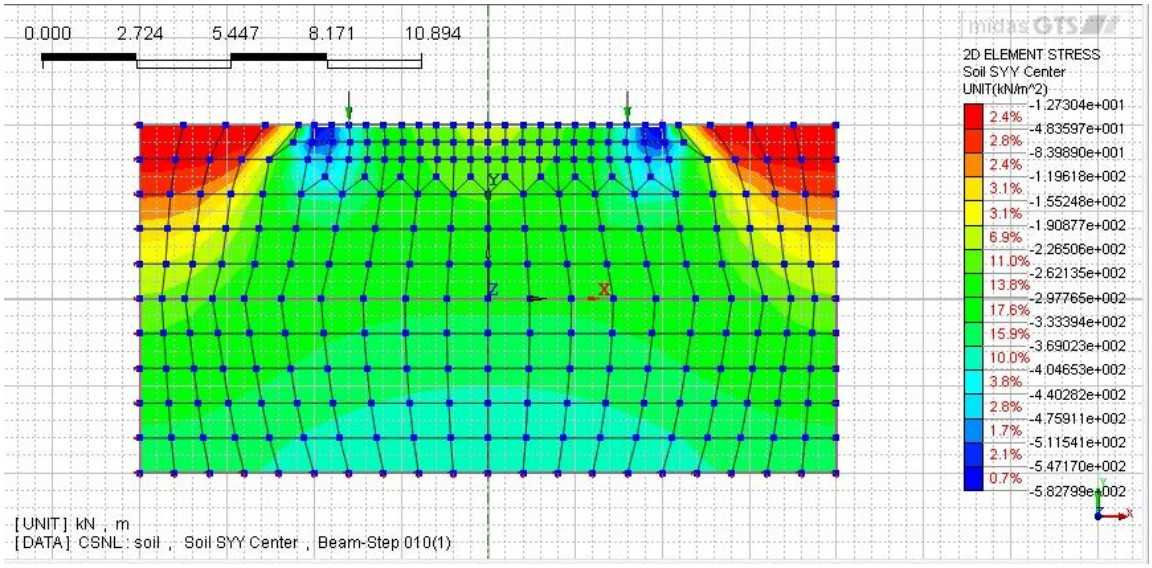

Figure 150: Stress SYY, F=2000 kN, linear elastic

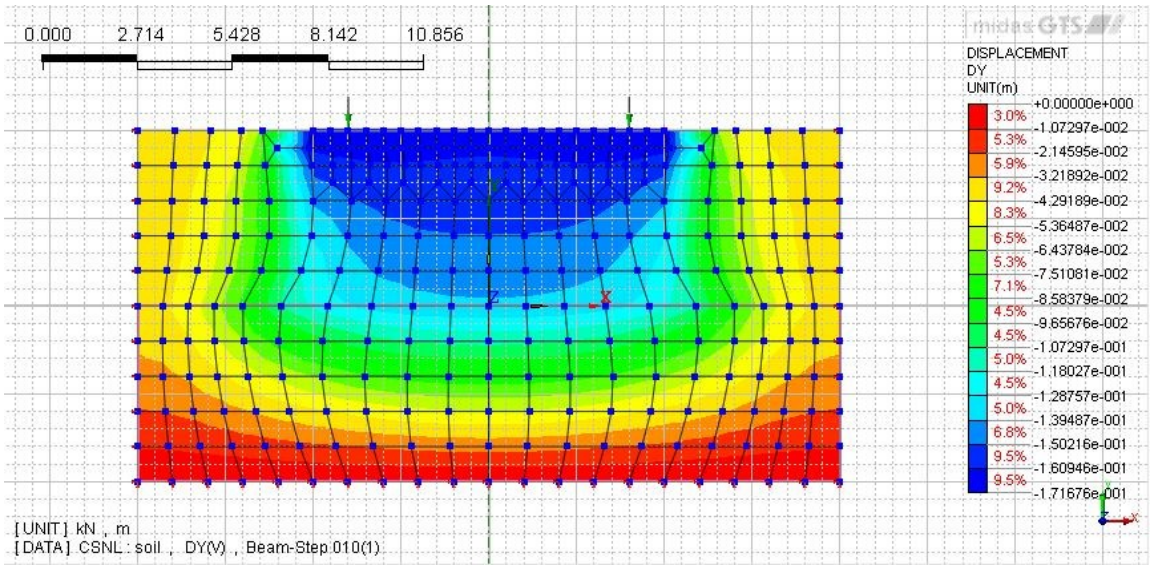

Figure 151: Displacement DY, F=2000 kN, elastic plastic, c=0.1 kPa

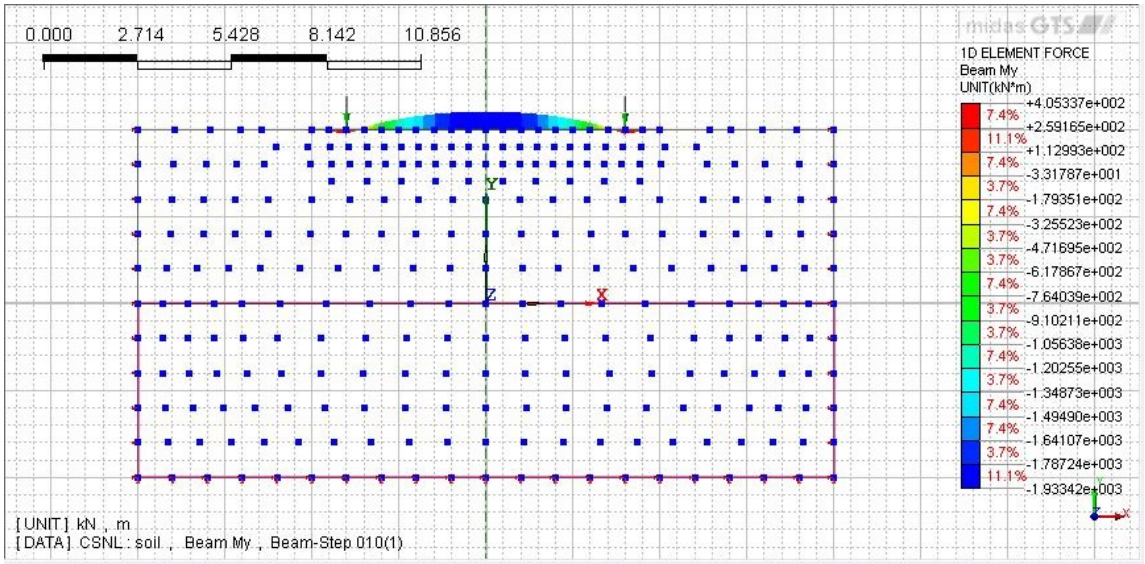

Figure 152: Bending moment, F=2000 kN, elastic plastic, c=0.1 kPa

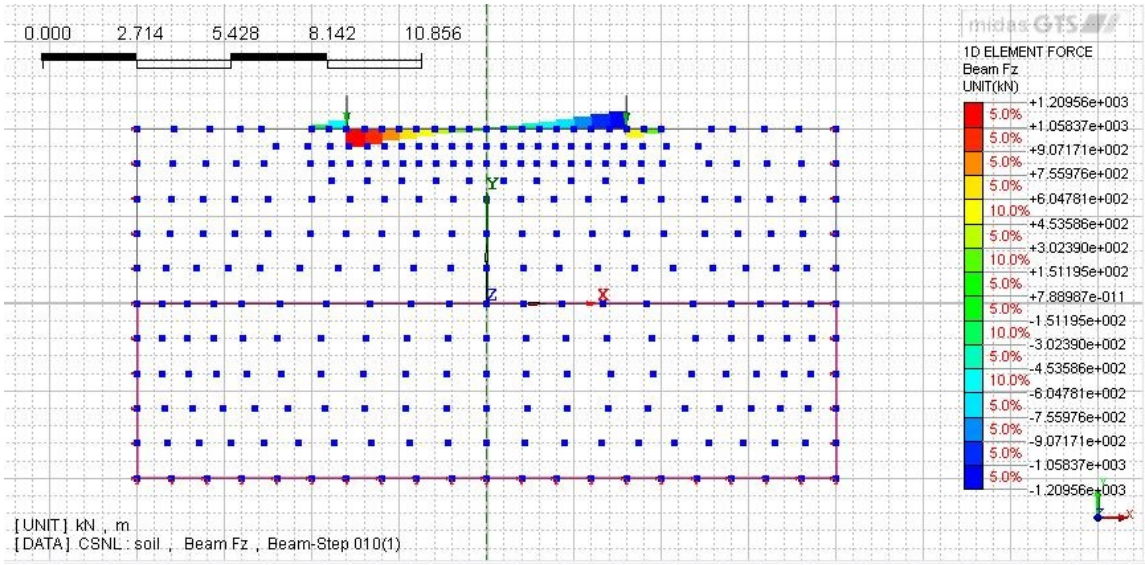

Figure 153: Shear force, F=2000 kN, elastic plastic, c=0.1 kPa

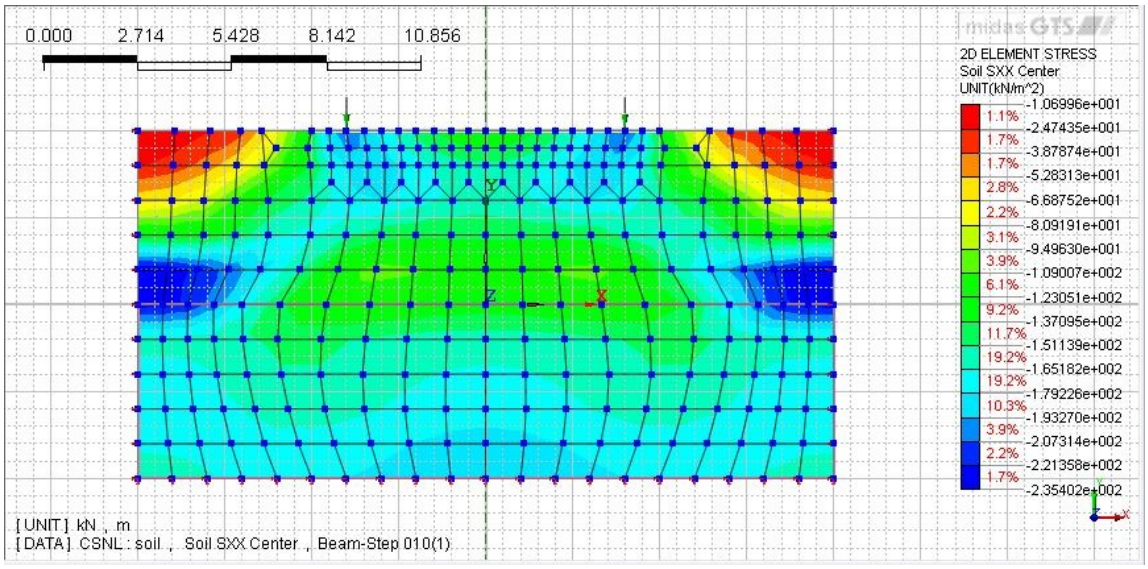

Figure 154: Stress SXX, F=2000 kN, elastic plastic, c=0.1 kPa

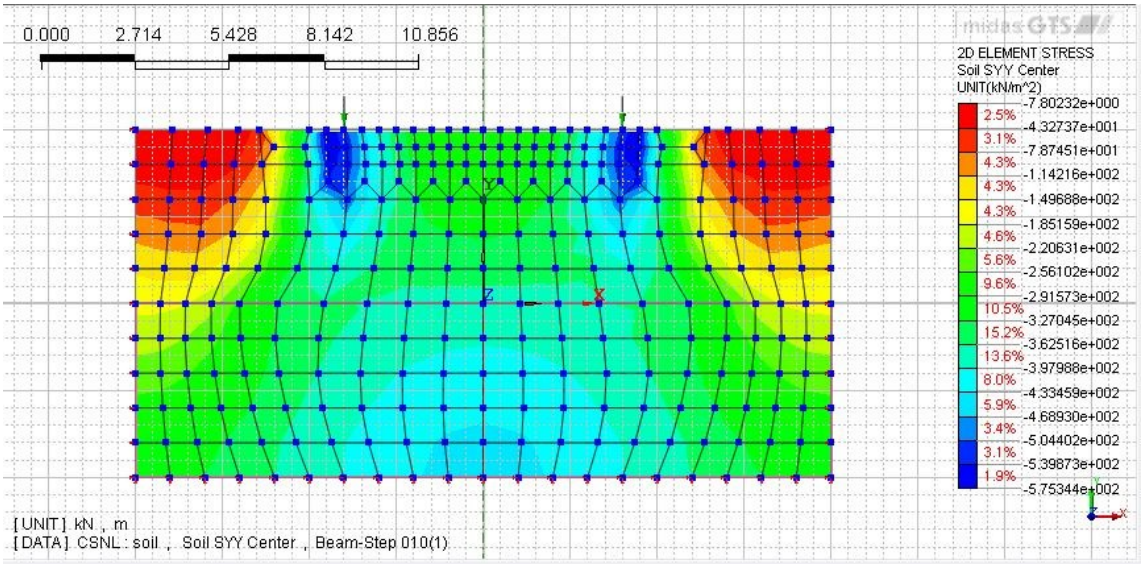

Figure 155: Stress SYY, F=2000 kN, elastic plastic, c=0.1 kPa

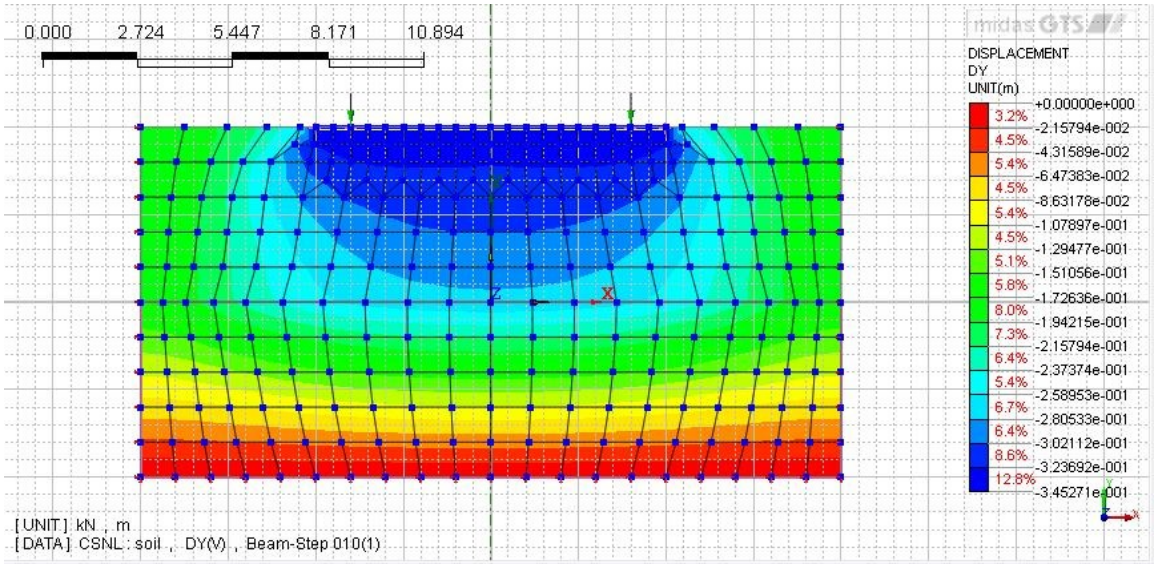

Figure 156: Displacement DY, F=5000 kN, linear elastic

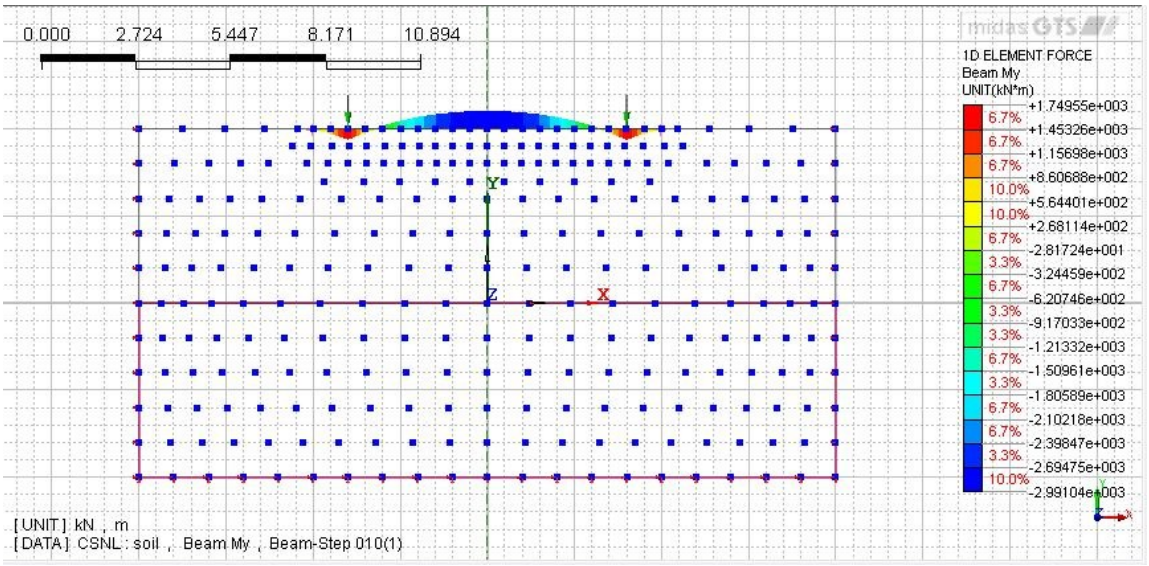

Figure 157: Bending moment, F=5000 kN, linear elastic

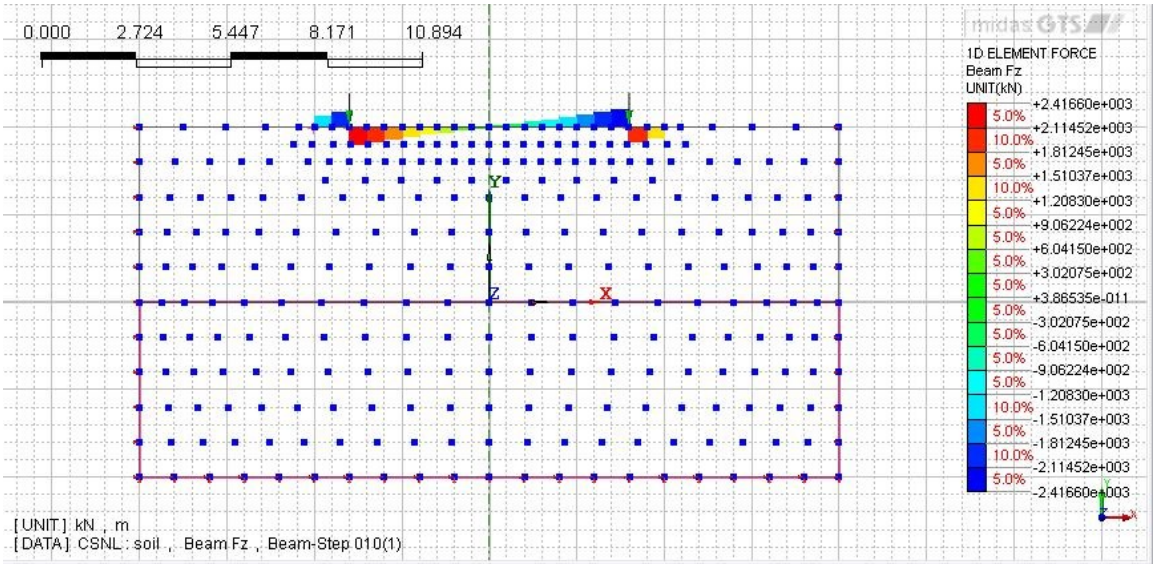

Figure 158: Shear force, F=5000 kN, linear elastic

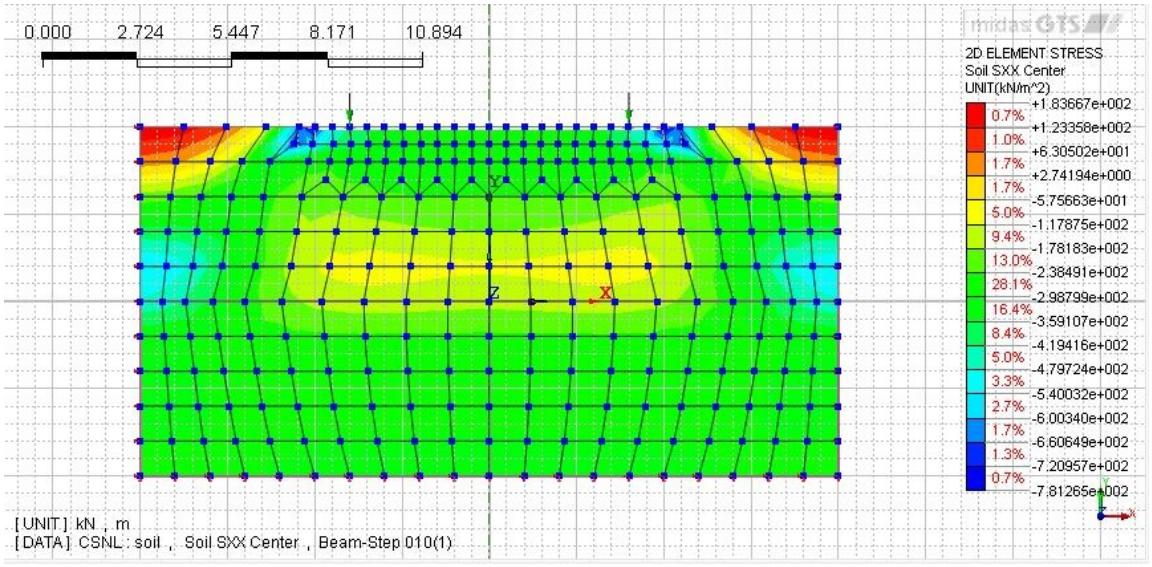

Figure 159: Stress SXX, F=5000 kN, linear elastic

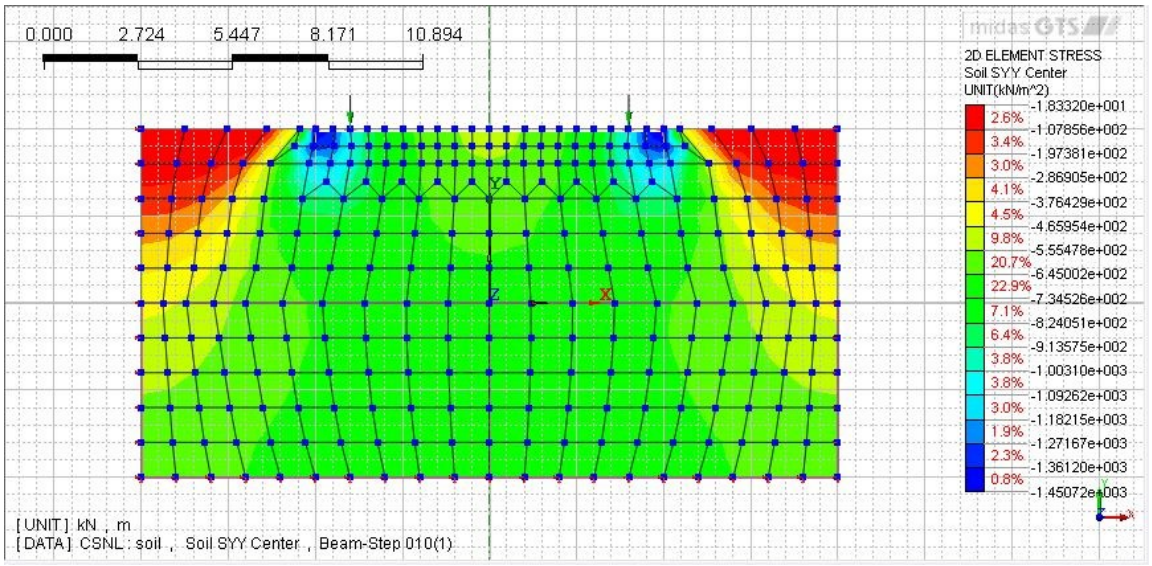

Figure 160: Stress SYY, F=5000 kN, linear elastic

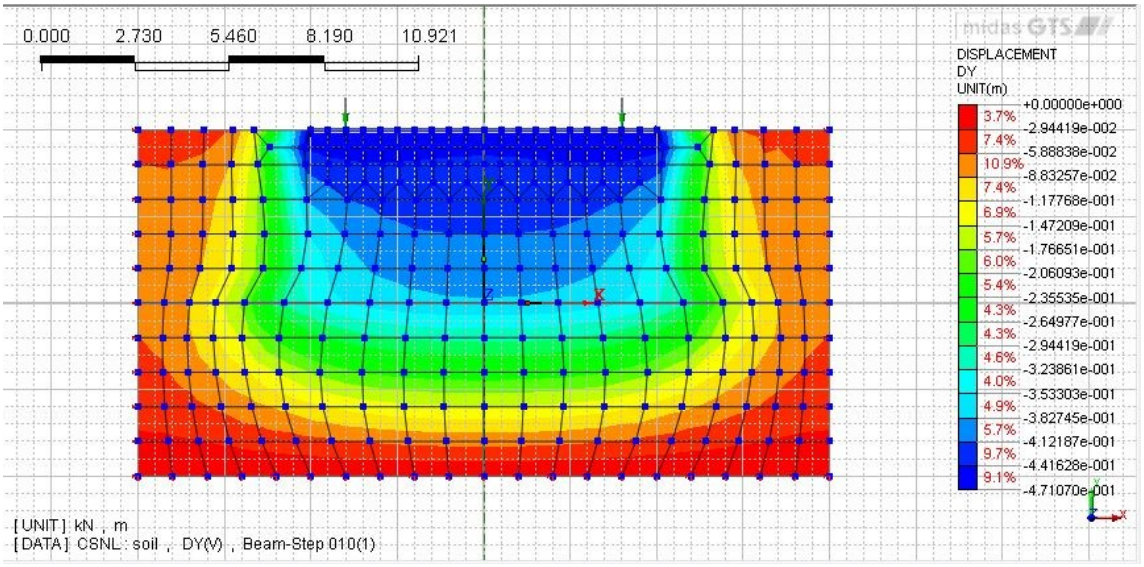

Figure 161: Displacement DY, F=5000 kN, elastic plastic, c=0.1 kPa

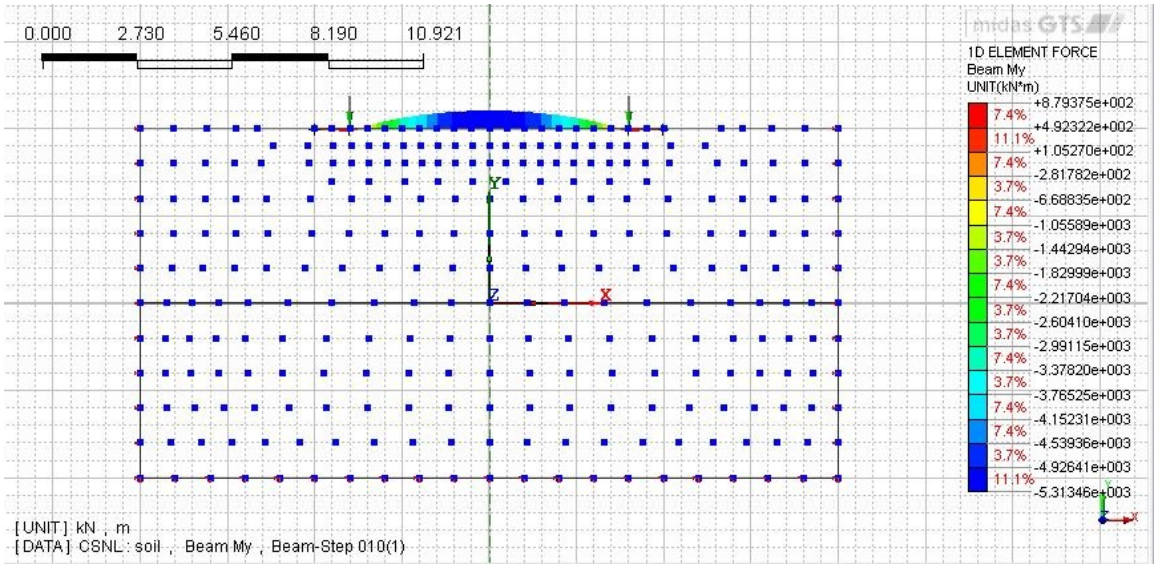

Figure 162: Bending moment, F=5000 kN, elastic plastic, c=0.1 kPa

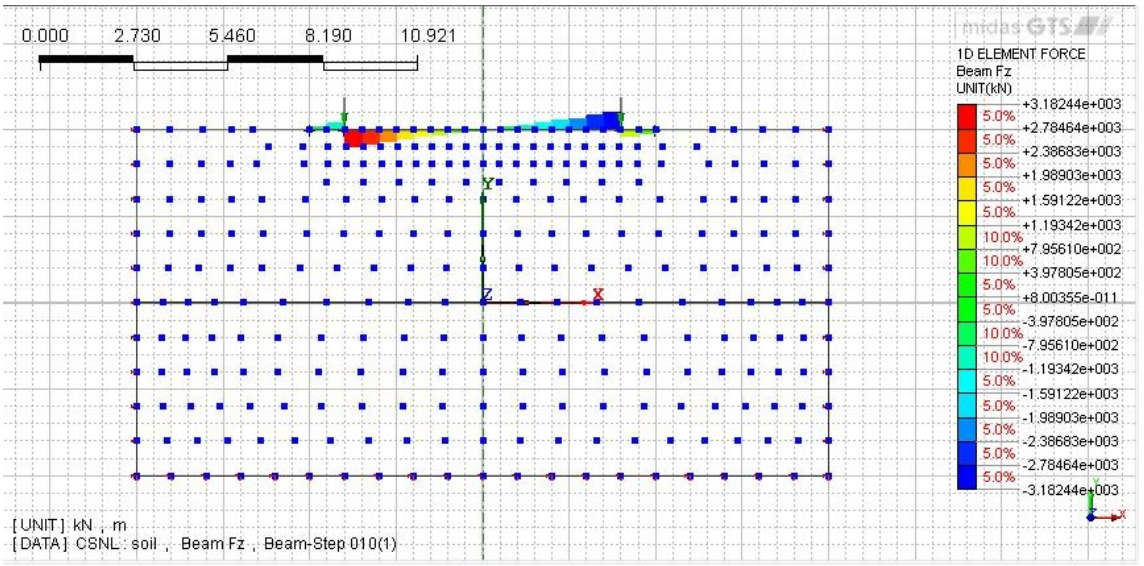

Figure 163: Shear force, F=5000 kN, elastic plastic, c=0.1 kPa

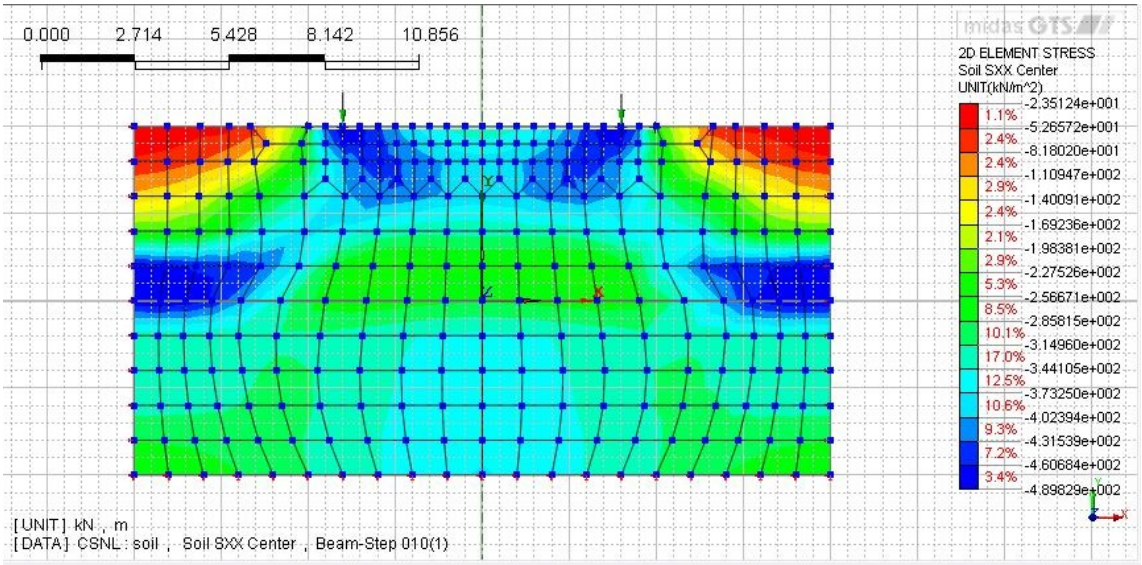

Figure 164: Stress SXX, F=5000 kN, elastic plastic, c=0.1 kPa

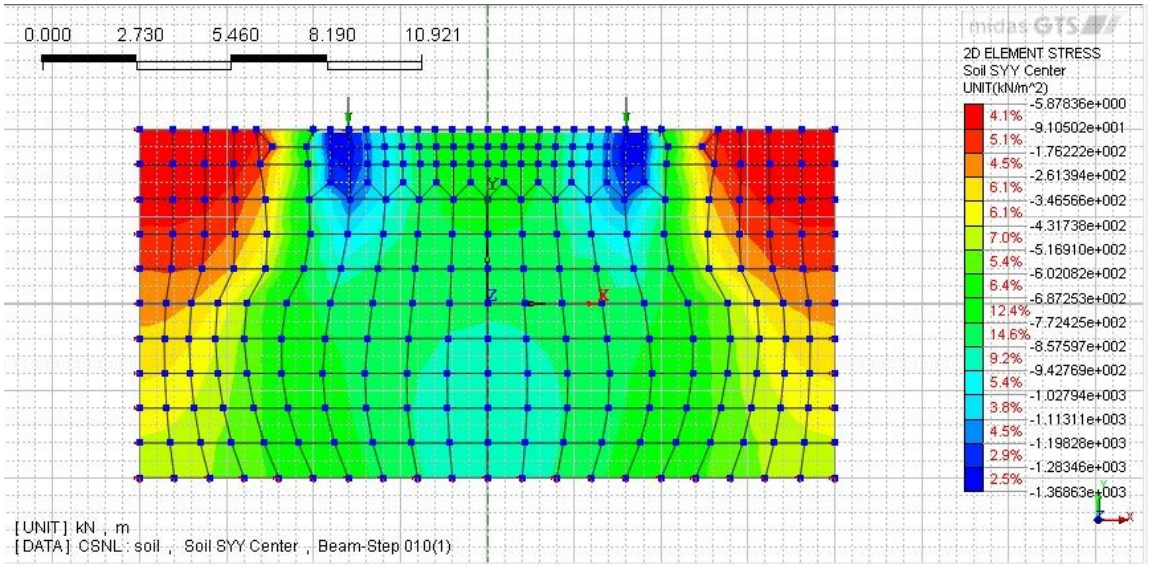

Figure 165: Stress SYY, F=5000 kN, elastic plastic, c=0.1 kPa

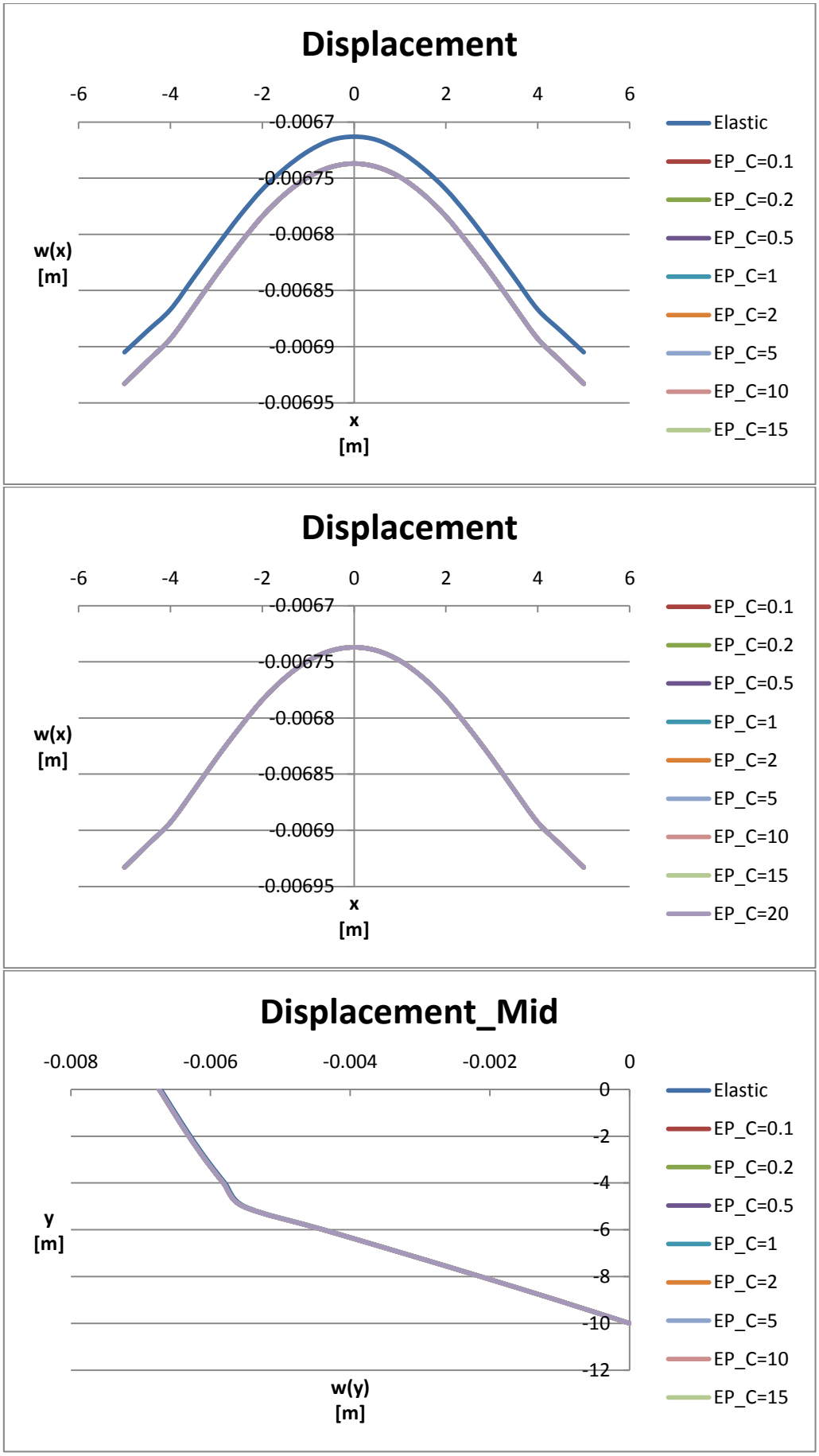

Figure 166: Displacement of the beam and of the nodes along the axis of symmetry, F=100 kN

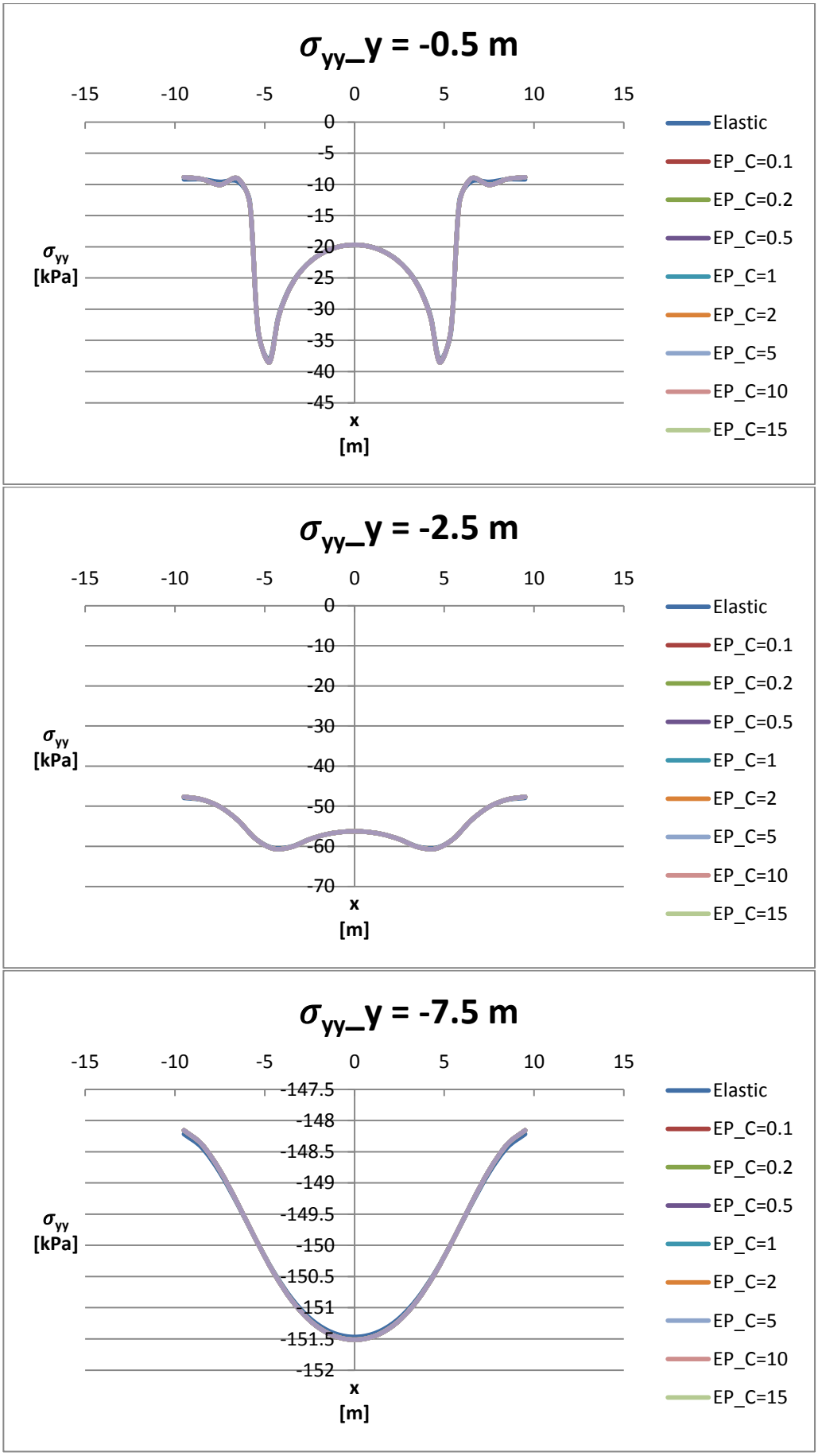

Figure 167: Stress SYY calculated at 0.5 m, 2.5 m, 7.5 m below the ground level, F=100 kN

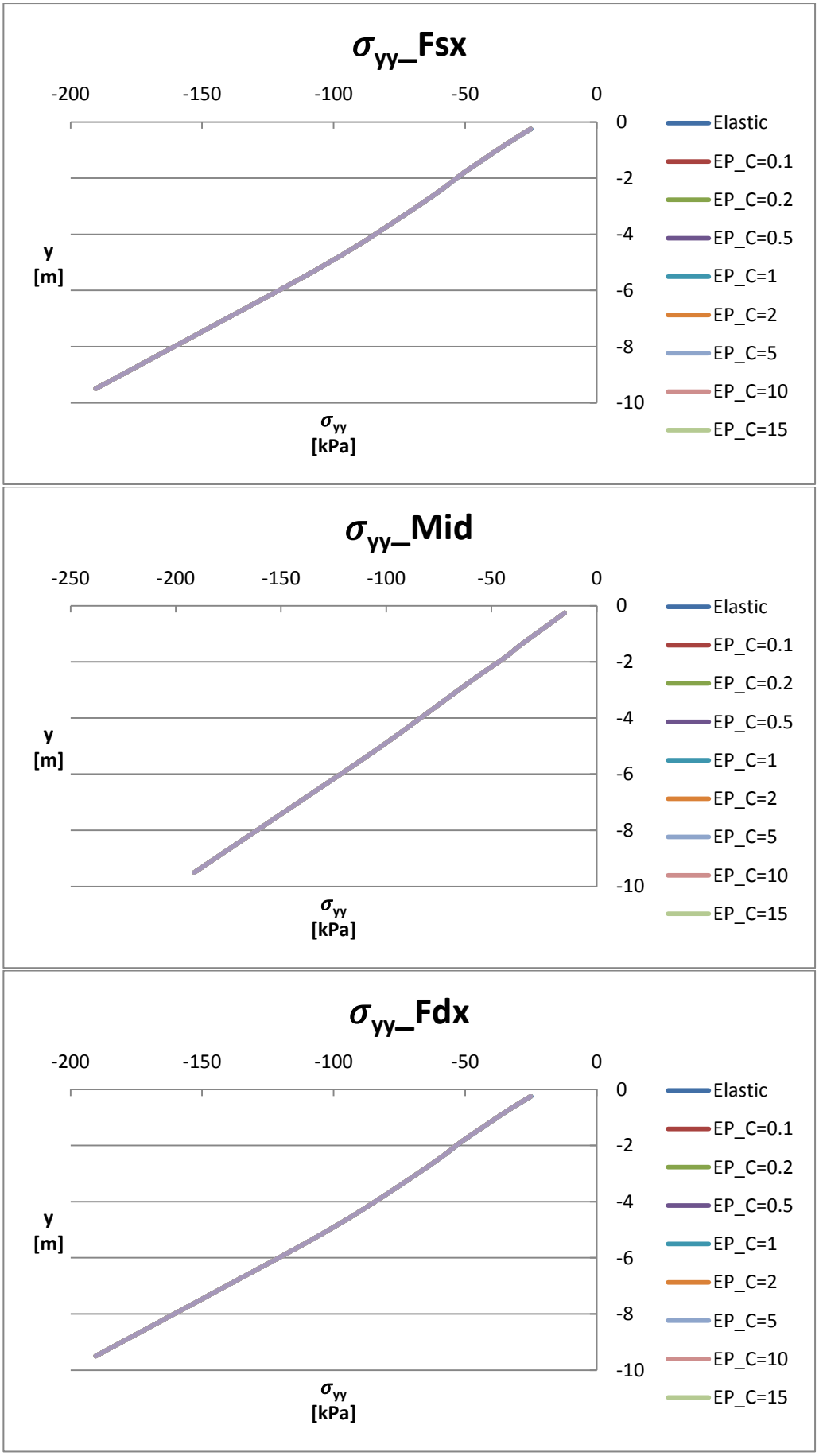

Figure 168: Stress SYY calculated below the left force,the mid-point of the beam,the right force, F=100 kN

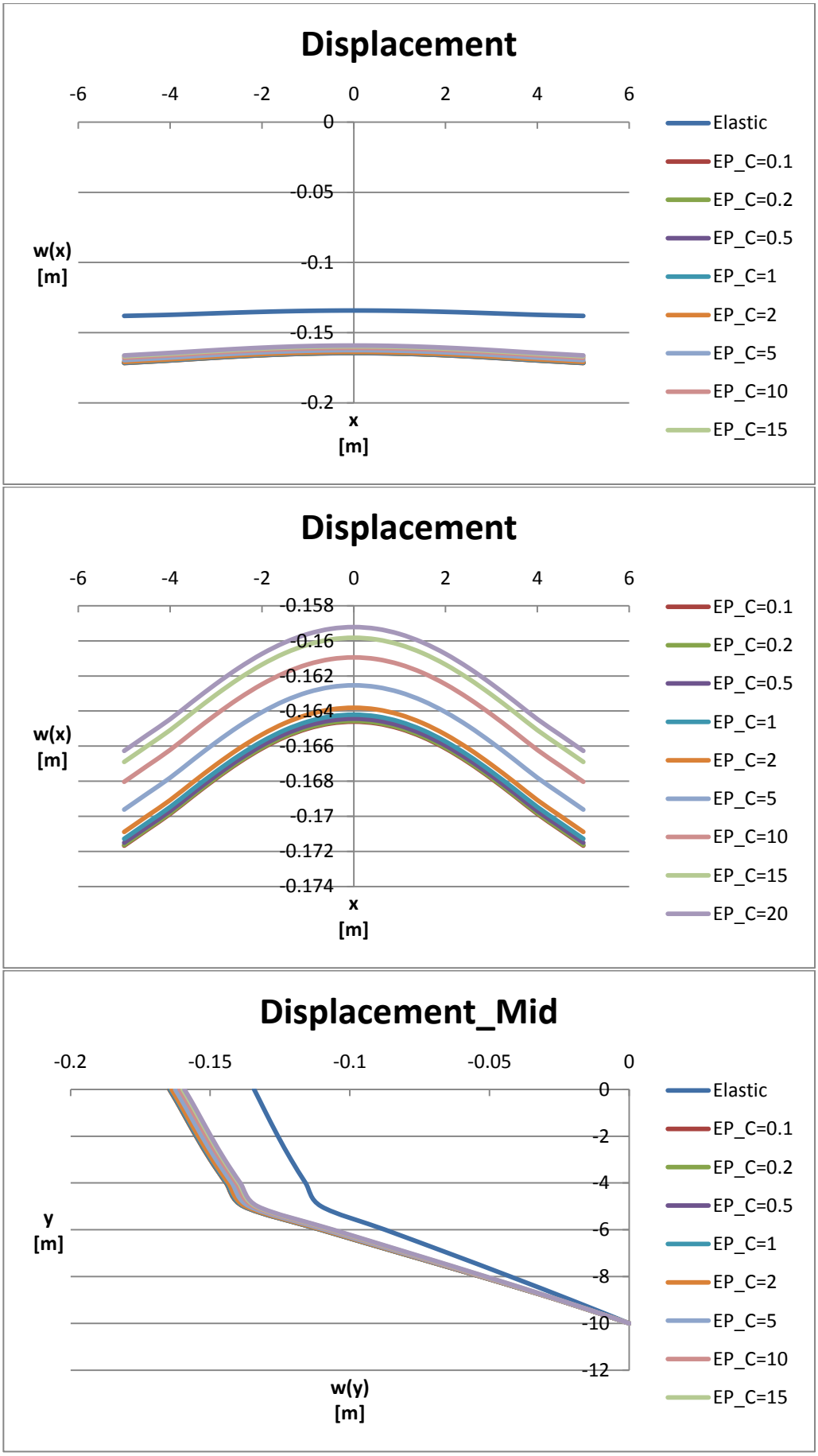

Figure 169: Displacement of the beam and of the nodes along the axis of symmetry, F=2000 kN

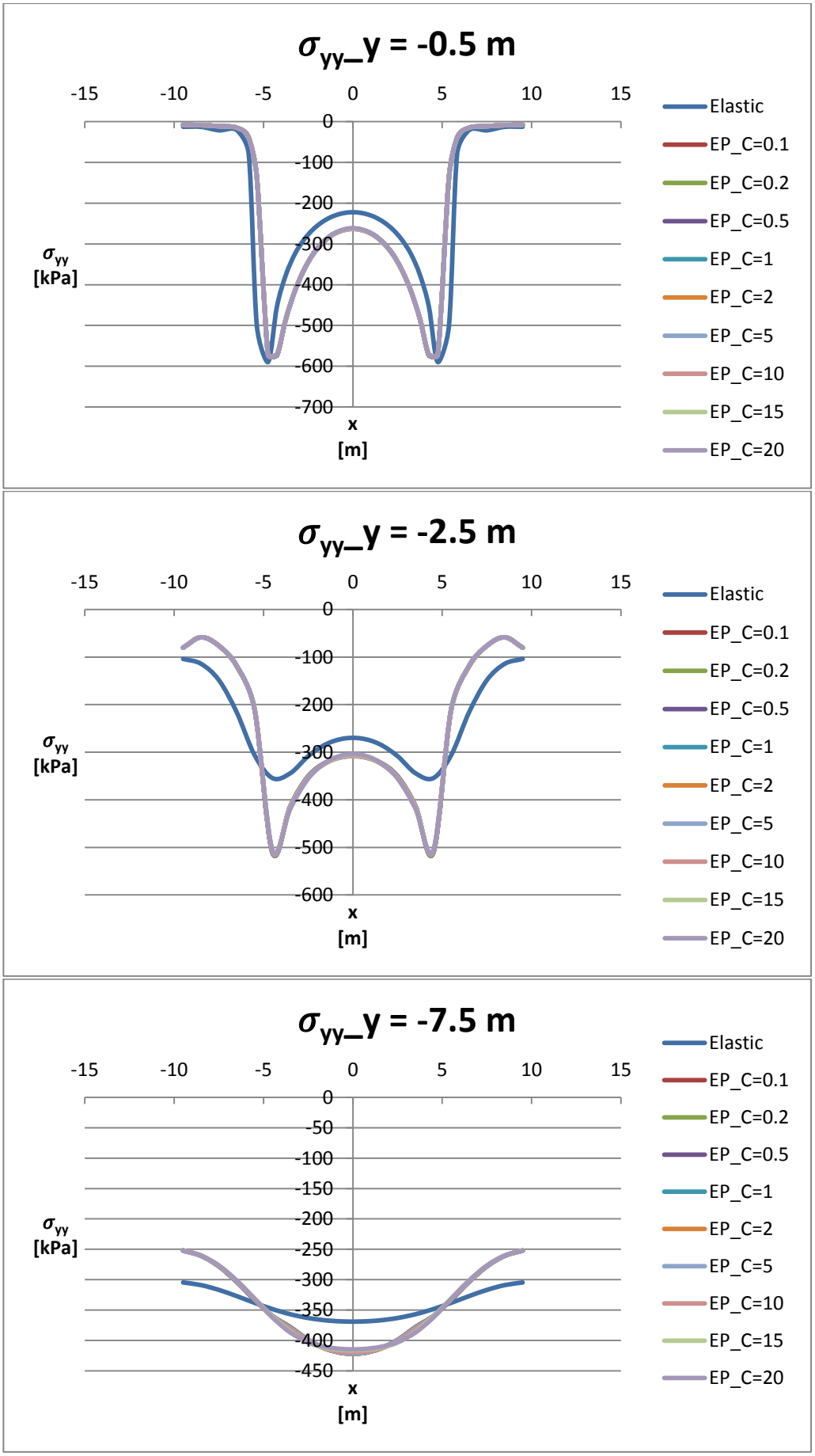

Figure 170: Stress SYY calculated at 0.5 m, 2.5 m, 7.5 m below the ground level, F=2000 kN

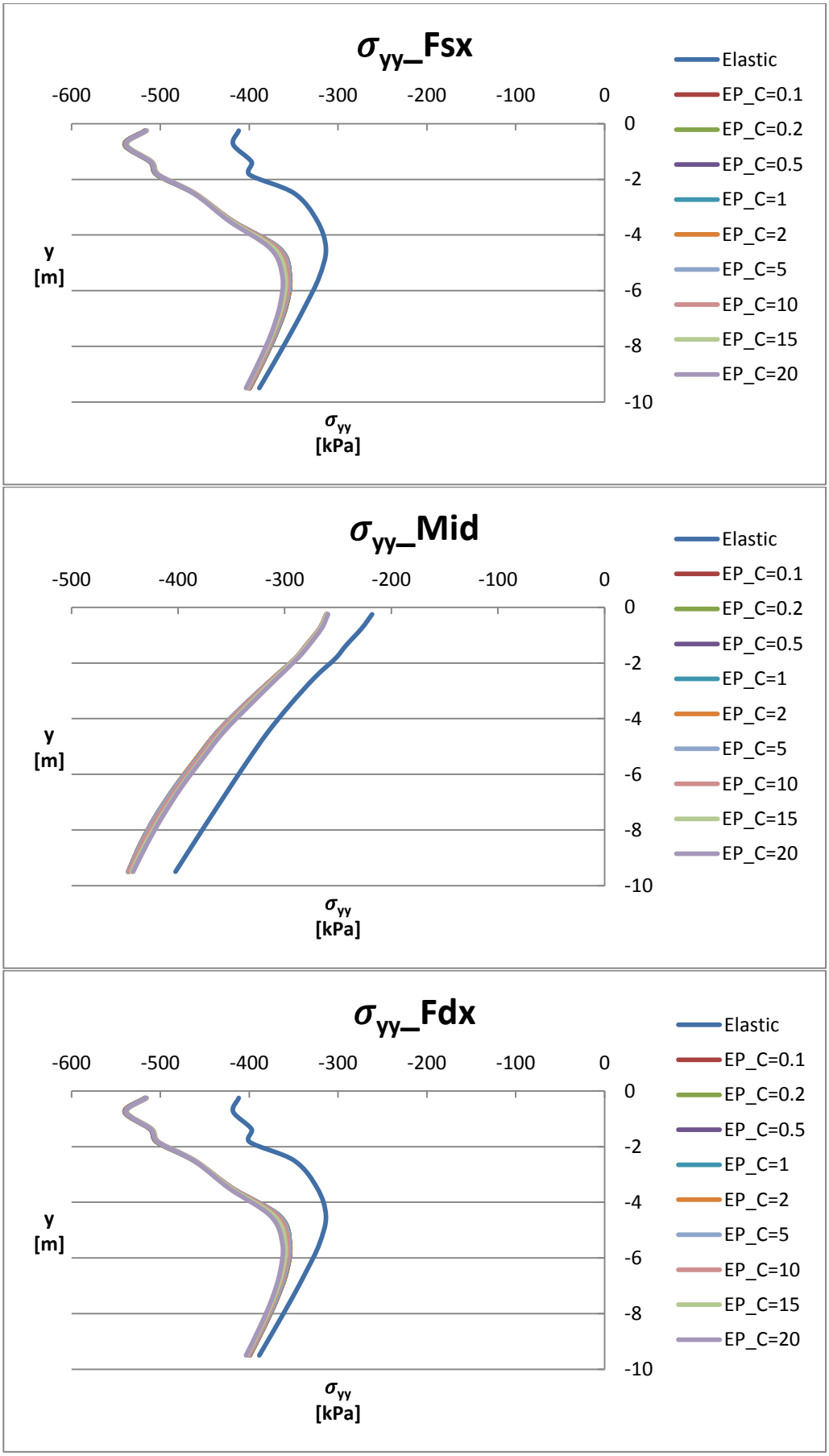

Figure 171: Stress SYY calculated below the left force, the mid-point of the beam, the right force, F=2000 kN

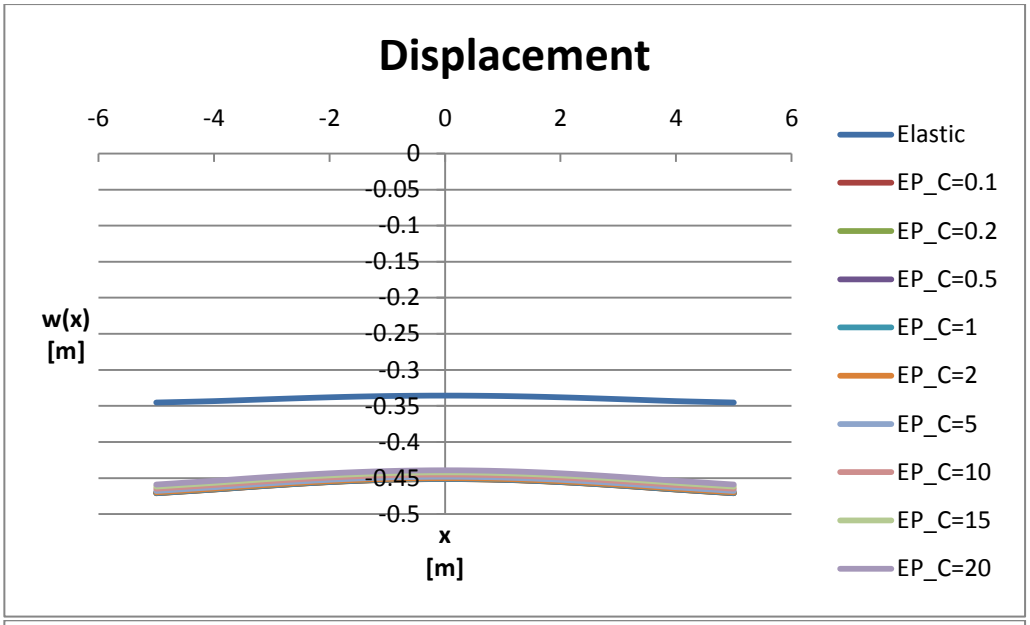

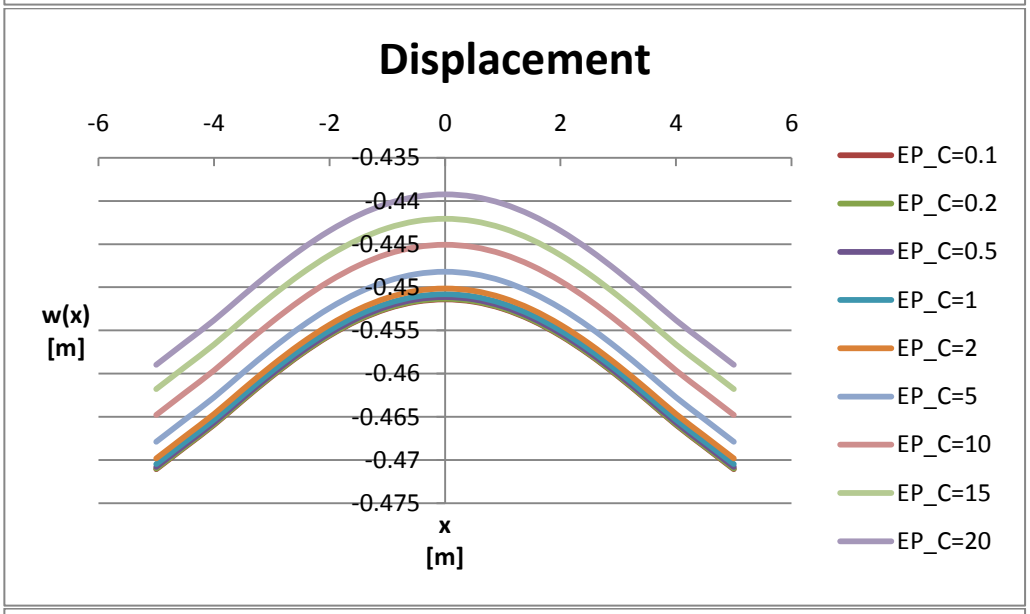

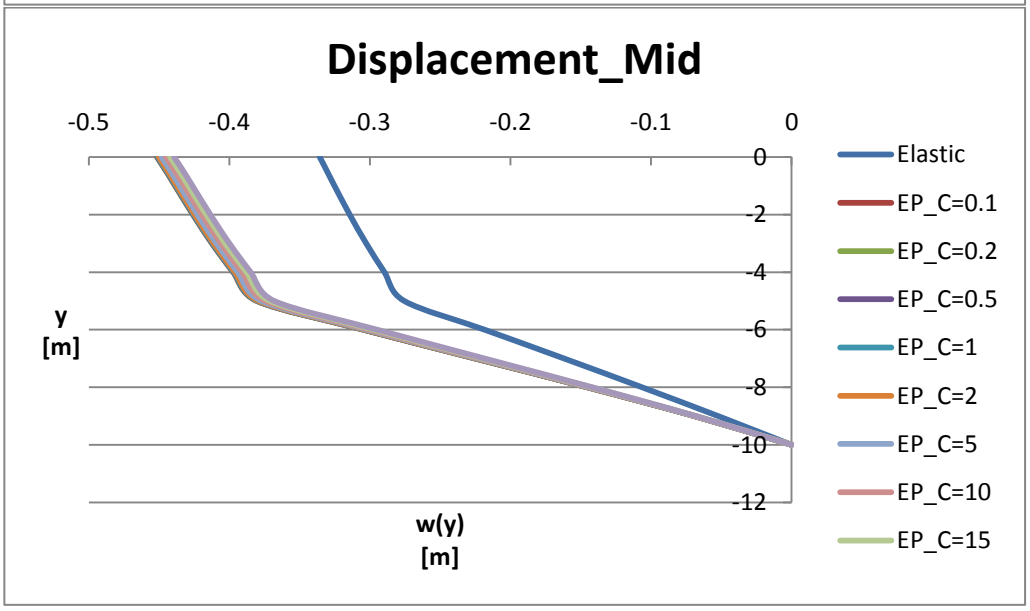

Figure 172: Displacement of the beam and of the nodes along the axis of symmetry, F=5000 kN

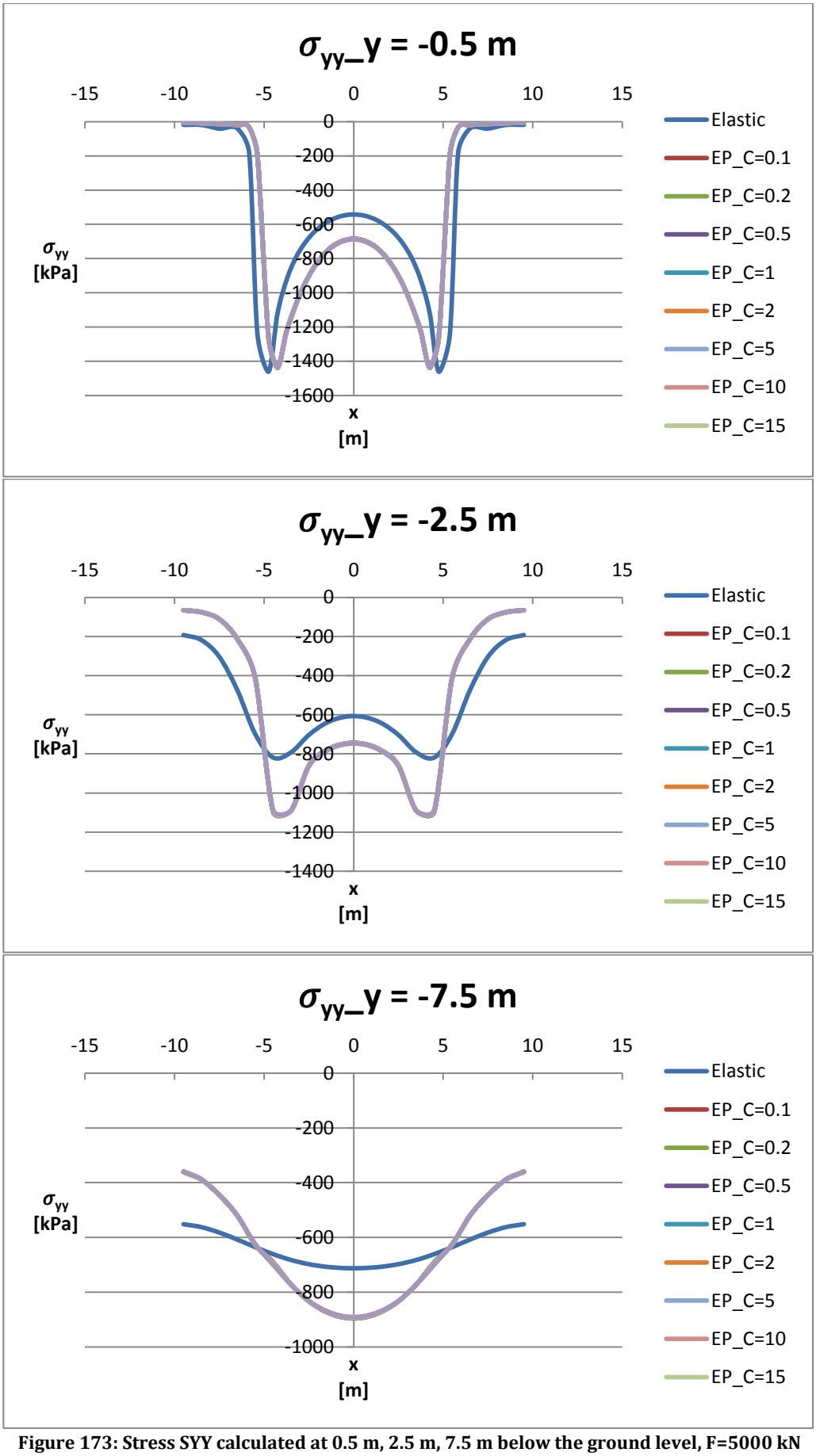

Figure 173: Stress SYY calculated at 0.5 m, 2.5 m, 7.5 m below the ground level, F=5000 kN

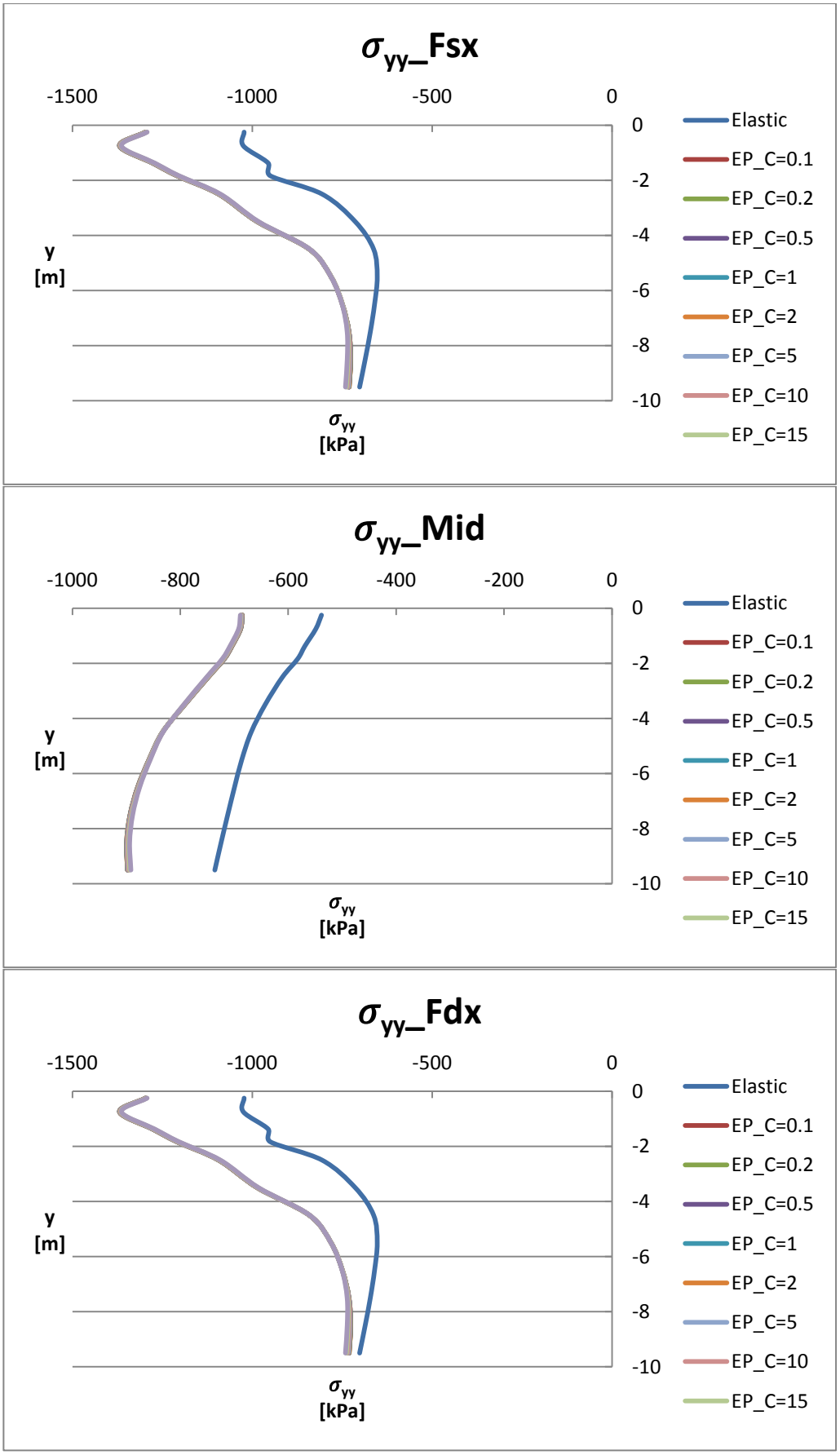

Figure 174: Stress SYY calculated below the left force, the mid-point of the beam, the right force, F=5000 kN

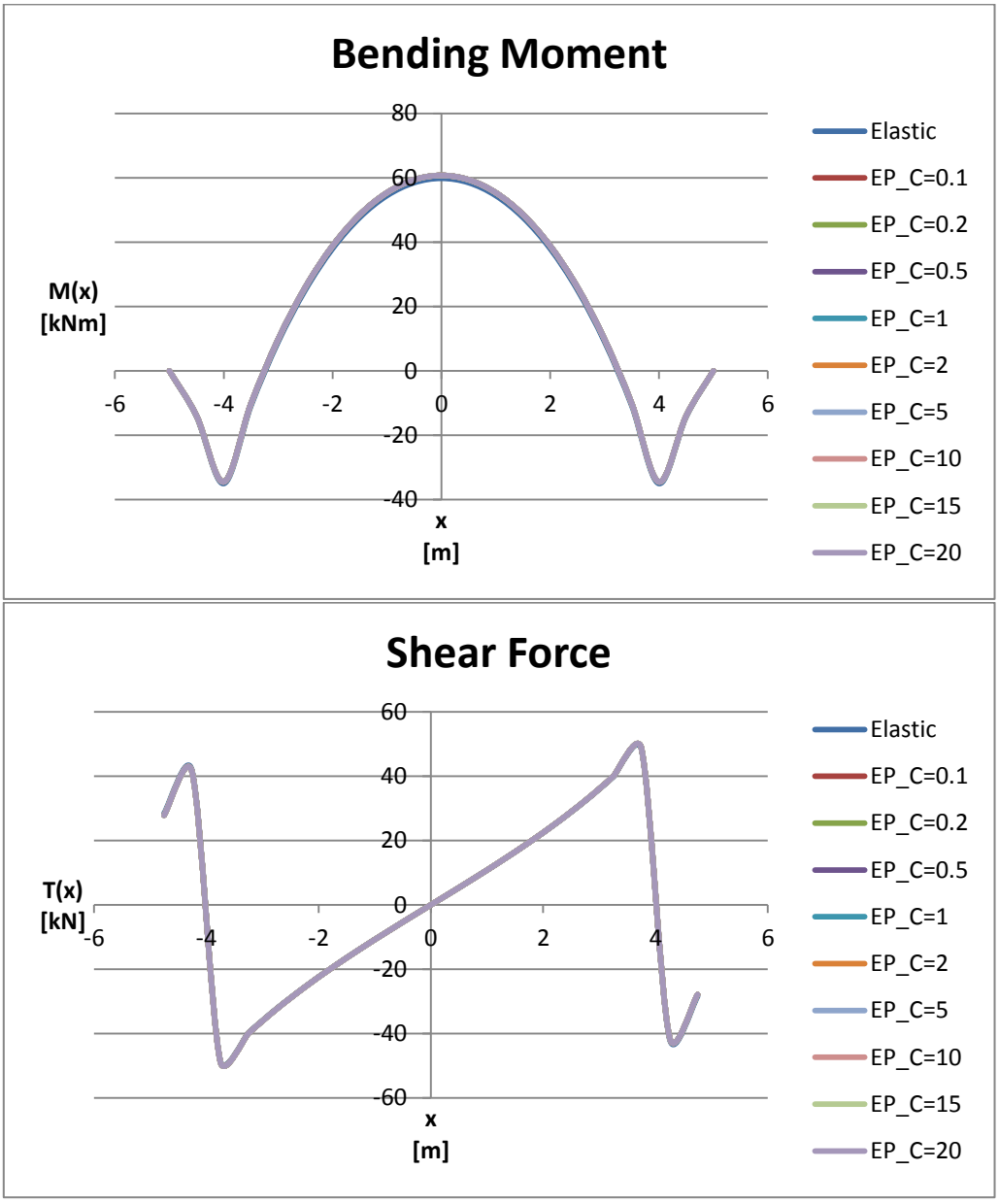

Figure 175: Bending moment and shear force, F=100 kN

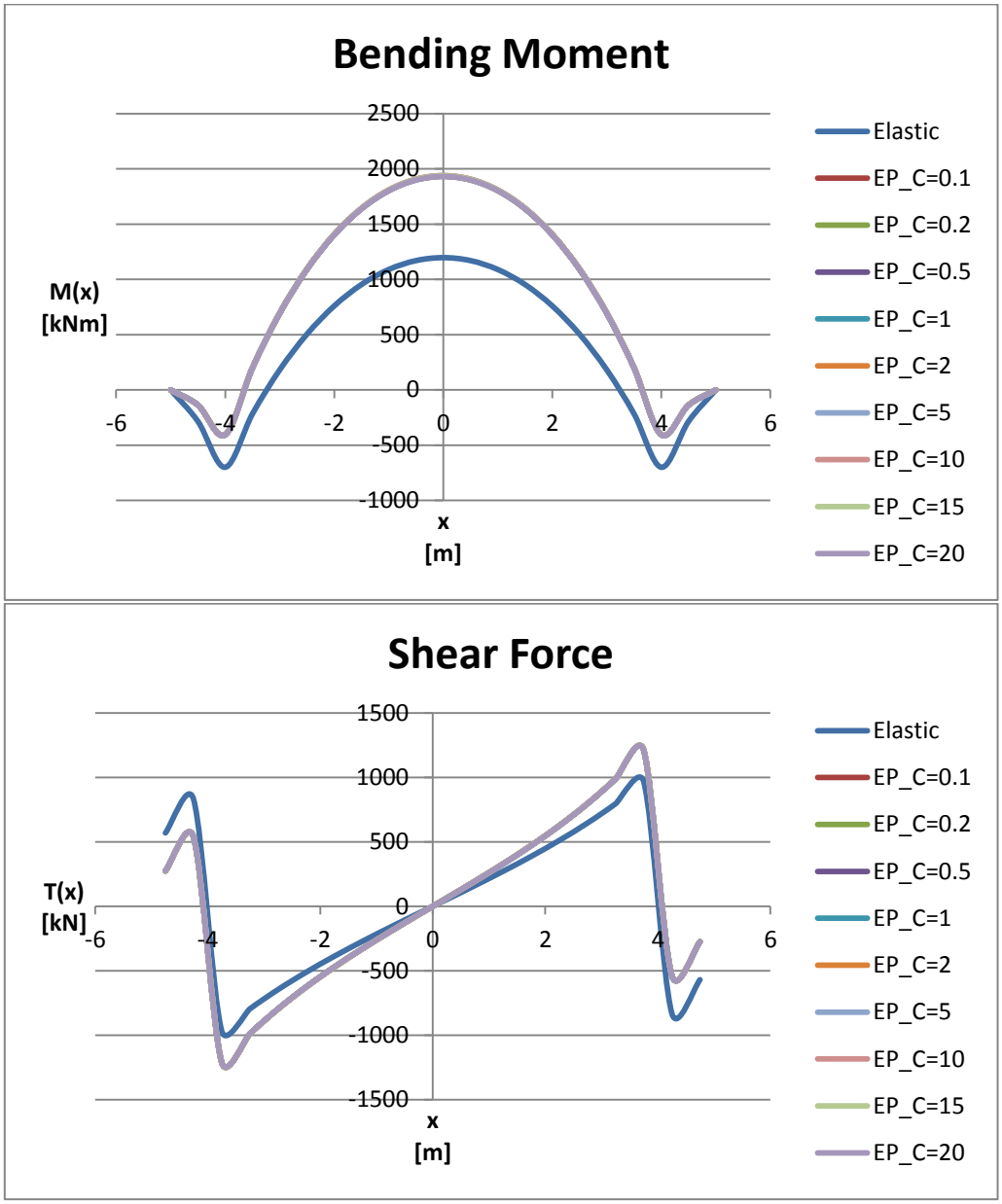

Figure 176: Bending moment and shear force, F=2000 kN

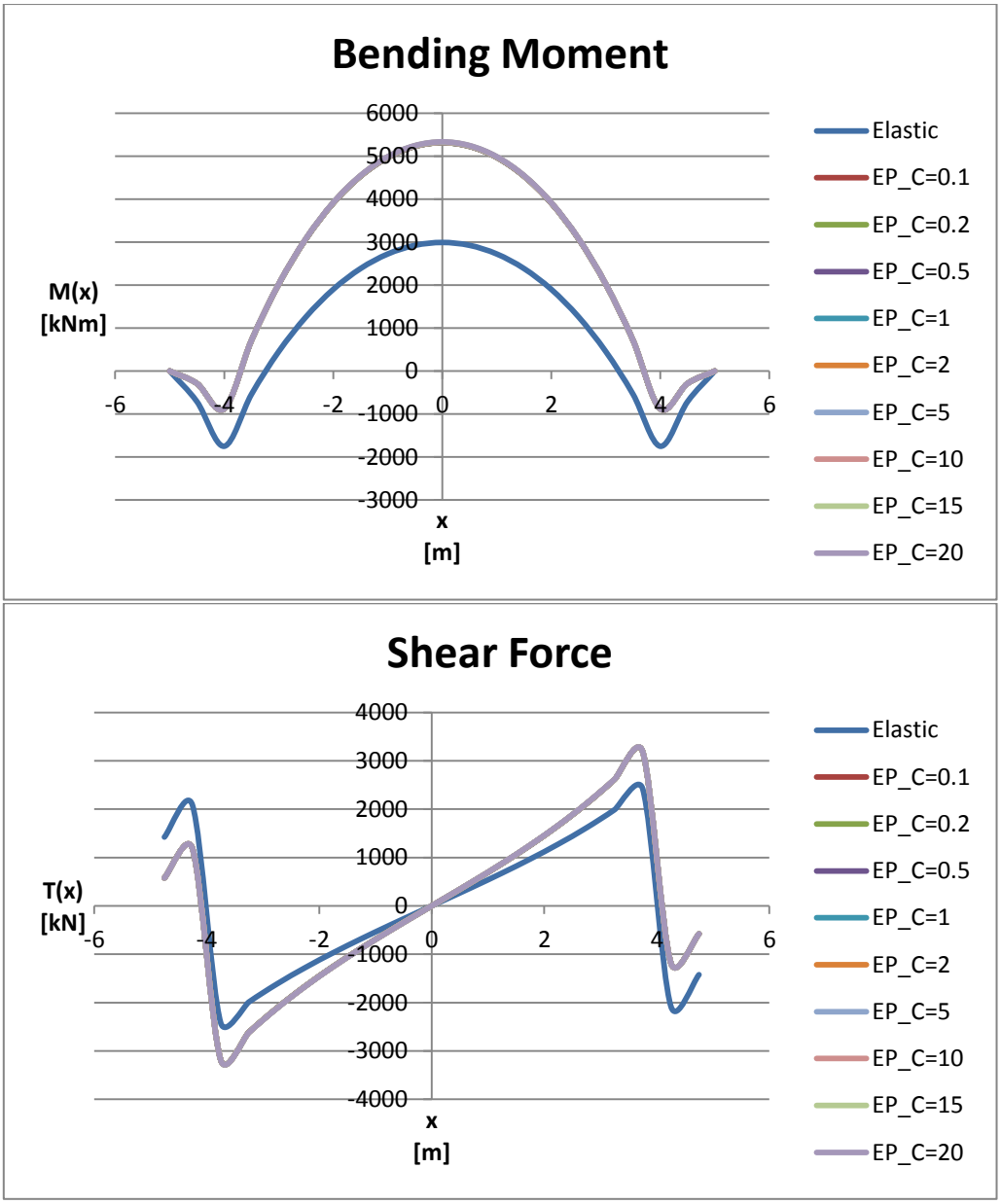

Figure 177: Bending moment and shear force, F=5000 kN

[11], [12], [13], [8].

2 Vertical structures

2.1 Introduction

The interaction between soil and structure can also be studied in vertical elements, such as sheet pile retaining walls. In this case the interaction is very complicated because the soil has the dual purpose of loading the structure on the active side of the sheet pile and support it on the passive side, in fact it has a portion embedded in the soil. That's why a part from the FEM techniques, the other kind of methods are based on empirical or empirically based factors and a theoretically correct solution can't be achieved.

The design of a retaining wall needs two sets of calculation, one to achieve the equilibrium of the structure, the other to determine, from the values of bending moments and shear forces obtained from equilibrium, the characteristics of the structure. Generally retaining walls can be divided into two categories: cantilever and supported walls. The first type requires a sufficient embedment, that's to say the fixity of the toe, and this attribute depends on the penetration into the ground. The second type, either tied or strutted, shares the supporting role between soil and supporting members. Usually the effectiveness of a cantilever depends on its "acceptable deflection under load". The height determines whether it is more effective a cantilever or a propped wall. The design of the wall must be carried out taking into account either the Ultimate Limit State or the Serviceability Limit State: the latter is important when the deflection of the wall and the movement of the ground are significant.

The designer has also to decide either to use free earth model or fixed earth model for the toe of the wall, and the difference between the two assumptions is based on the influence that the depth of embedment has on the wall deflection. A wall designed as a free earth support behaves like a supported vertical beam, the toe is allowed to rotate and not to translate; a tie or a prop on the top could be the other support; this kind of model, for a given set of conditions, requires less depth of embedment but the beam has a maximum for bending moment. A fixed earth support avoids either translation or rotation of the toe, so it acts like a propped cantilever (fixed end); the upper support could be provided by a prop or a tie. In this case the maximum bending moment along the beam decreases but the toe fixity creates a fixed end moment in the wall and an increase of the depth of embedment of the beam is required. This design approach must be adopted when the end of the sheet pile is fixed and the embedment in the soil provides the support of the wall. No failure mechanism exists to check the stability of the sheet piles once the fixed earth support is assumed, but many empirical approach have been studied. Both methods are valid only if support is provided over the middle of the retained height.

An important topic of wall design is the distribution of pressures and the bending moment reduction. In fact the triangular distribution of earth pressure is a simplification that doesn't take into account the interaction between soil and structure, feature that influences the distribution of bending moments and shear forces along the wall, and of earth pressure itself. The soil and the flexibility of the wall influence this reduction and this deflection of the wall causes a movement away from the soil (between the embedded part and the position of the support). This movement could cause an arching effect within the soil: the internal capabilities are improved and the pressure on the wall decreases. A reduction of the maximum bending moment and an increase of the reaction in the support obviously occurs: in fact, usually, the reaction calculated by a soil structure interaction is higher than that obtained by a limit equilibrium analysis. This arching effect could not be taken into account (or can be but with caution) in vibrational situation, stratified soils, yielding of the support or movement of the toe. Programs based on soil-structure interaction automatically take into account the arching effect on bending moment, thus for a calculation by simple equilibrium is it recommended to increase the load of a certain percentage on the support.

Anyway the pressure on the wall that is commonly assumed, with its simplified triangular shape, doesn't take into account the movement of the wall (this lack nevertheless gives a conservative solution), which caused a decrease of pressure where it is large, and an increase where it is small: features that can be seen with a computer program. The shape of pressure can be further improved by a program based on the interaction between soil and structure, and the modification would be an increase of the passive pressure and a decrease of the active. As said previously it's also important to keep in mind that the deflection is a function either of the section and the material of the wall or the compression of the soil in a passive/active state: that's to say that a stiff wall with less props could be as effective as a flexible wall with more props. Thus when the soil-structure interaction is taken into account a flexible wall solution could be more cost effective than one based on a stiff wall, because a reduction in strength demand occurs so the required bending moment section is minimized [14].

In this chapter will be described some different approaches that can be used to study a retaining sheet pile wall. The first will be the classic method, it is highly simplified but can give some general indication about the length of the wall. A second approach will be a computational program based on dependent pressures. The last approach will be an analysis done with two FEM programs. The case study will be an excavation by a sheet pile: the parameters of the soil and of the structure have been chosen in an arbitrary manner and only for schematic purpose, the water table is not taken into account. Each approach will analyze two different conditions: a granular soil and a cohesive soil, for both of them will be offered a comparison between the different assumed methods.

All these descriptions will be made in the proper chapters.

2.2 Classic method - Theoretical introduction

The aim of this method is to find the required length of the wall to achieve equilibrium of the structure: the soil has been assumed to be at the yielding limit state so the theory of Rankine for rigid-plastic material has been assumed. The adopted failure criterion for the soil is that of Mohr-Coulomb.
The vertical pressure in the ground is:

$$\sigma_v = \sum(\gamma_i \ h_i) + \ q \tag{90}$$

where q is the load [kN/m^2], h_i the thickness of the layer, γ_i the self-weight of the i-th layer; for a system where there are layers of soil below the water table (it won't be take into account in this work) shall be used the effective weight γ'_i expressed by the formula:

$$\gamma'_i = \gamma_i - \gamma_{H2O} \tag{91}$$

where γ_{H2O} is the self-weight of water (assumed 9.81 kN/m^3).

The active horizontal pressure is calculated by the following formula:

$$\sigma_h = \sigma_v \, K_a - 2c\sqrt{K_a} \tag{92}$$

In this formula σ_v is the vertical stress from the weight of the soil, c is the cohesion, and K_a is the coefficient of Rankine active pressure. It amounts to:

$$K_a = \tan^2\left(\frac{\pi}{4} - \frac{\varphi}{2}\right) \tag{93}$$

where φ is the angle of internal friction of the soil.

The passive horizontal pressure is:

$$\sigma_h = \sigma_v \, K_p + 2c\sqrt{K_p} \tag{94}$$

where σ_v and c are as above the vertical stress from the weight of the soil and the cohesion respectively; K_p is the coefficient of Rankine passive pressure. It amounts to:

$$K_p = \tan^2\left(\frac{\pi}{4} + \frac{\varphi}{2}\right) \quad \textbf{(95)}$$

where φ is the angle of internal friction of the soil.

This method has been applied to the problem under consideration using a spreadsheet. As said before, the purpose is to achieve equilibrium by varying the length of the wall, that's to say by trial and correction. One enters the value of the depth of embedding in the spreadsheet: immediately the bending moment about the toe is calculated: the length can be assumed as correct when passive moment is slightly greater than the active moment.

Where the area of the active pressure below the ground level is equal to the area of the passive pressure below the ground level, the shear force is equal to zero. The sum of the values of the bending moments about and above the level of zero shear gives the value of maximum bending moment. With the spreadsheet it's also possible to have the trend of the bending moment along the wall.

A suggestion for the design in order to find the proper penetration depth of the pile is to increase by 20% the depth below the point where passive and active pressure are equal. [7], [15], [14].

2.3 Dependent pressures method - Theoretical introduction

This approach assumes that the soil in the vicinity of the wall behaves as ideally elastic-plastic Winkler material; the method is based on the Winkler model of subgrade reaction modulus that characterizes the behavior of the material in the elastic region: by exceeding the limit of deformation that occurs when passive pressure is reached, the soil behaves as ideally plastic material; the parameter k_h is the stiffness on an ideal elastic support, so as for the horizontal beam, and a system of these "springs" replaces the reaction of the soil in contact with the wall. It has been assumed that the wall is an elastic beam and the horizontal elastic reaction of the soil is equal to the horizontal displacement at that point multiplied by k_h:

$$p_x = k_h\, x \quad \textbf{(96)}$$

And

$$x = x(z) \quad \textbf{(97)}$$

The k_h parameter isn't the Winkler coefficient for horizontal foundation, it doesn't have a physical meaning and it depends on the stiffness and the geometry of the wall and on the condition of the soil. As the in-situ methods can't define a value of k_h, either empirical or theoretical methods have been developed, the latters based on the classic theory of elasticity: some of these are Terzaghi's method, Chadeisson and Monnet method, Menard and Bourdon method.

In this work has been used a program based on Chadeisson and Monnet method: its aim is to calculate the displacement with which the soil reaches the limit of passive pressure defined by Rankine. The k_h evaluated by this empirical method depends on the shear force of the soil by the parameters φ' and c' (the adopted failure criterion is that of Mohr-Coulomb), and on the stiffness of the wall; for given subsoil:

$$k_h = \left[20\ EI \left(\frac{K_p\ \gamma \left(1 - \frac{K_0}{K_p}\right)}{dr_0} \right)^4 \right]^{\frac{1}{5}} + A_p\ c' \frac{\tan \frac{c'}{c_0}}{dr_0} \qquad \textbf{(98)}$$

where γ is the self-weight of soil, K_p the passive pressure coefficient, K_0 the pressure coefficient at rest, dr_0 the characteristic displacement (0.015 m), c' the effective cohesion, A_p the coefficient allowing for soil cohesion, c_0 is equal to 30 kPa

The formulae used in this method to determine the pressure along the wall are the same as those used for the classic method, and the coefficient of active and passive pressure are defined by the theory of Rankine: so all the formulae showed in the chapter concerning the classic method are still valid in this one.

In addition the constitutive equation of the beam with small displacement is required:

$$\frac{d^2x(z)}{dz^2} = -\frac{M(z)}{EI} \qquad \textbf{(99)}$$

where x(z) is a function of displacement, M(z) is the bending moment, EI is the flexural rigidity of the beam.

This formula combined with the load function

$$\frac{d^2M(z)}{dz^2} = -p_r(z) \qquad \textbf{(100)}$$

Gives

$$\frac{d^4x(z)}{dz^4} = \frac{p_r(z)}{EI} \qquad \textbf{(101)}$$

Taking into account the elastic reaction of the soil the previous equation is extended in the following way

$$\frac{d^4x(z)}{dz^4} + k_h\, x = \frac{p_r(z)}{EI} \tag{102}$$

where k_h is the coefficient of elasticity defined in the chapter.

It has been assumed that the value of the pressure acting on the wall may vary between the two bounds of passive or active pressure, but without falling outside of them, and that the acting pressure on an undeformed structure is the pressure at rest. For a deformed structure the pressure is

$$\sigma = \sigma_r - k_h w \tag{103}$$

$$\sigma = \sigma_a \text{ for } \sigma < \sigma_a \tag{104}$$

$$\sigma = \sigma_p \text{ for } \sigma > \sigma_p \tag{105}$$

where σ_r is the pressure at rest, k_h is the modulus of subsoil reaction, w is the deformation of structure, σ_a is the active earth pressure, σ_p is the passive earth pressure.

The computational procedure starts with the pressure at rest acting on the wall and the k_h assigned to all the system of supports (Figure 178:).

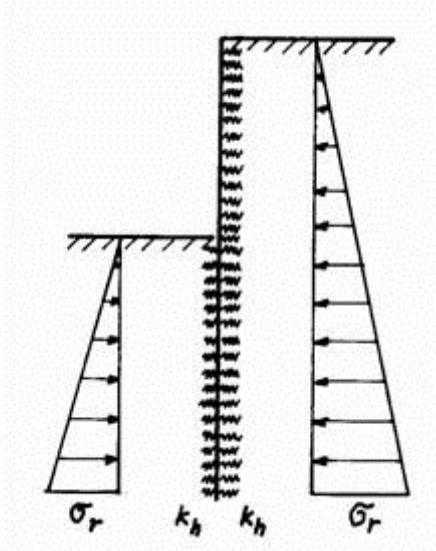

Figure 178: 1st step of the computational procedure [7]

The following step requires that the program to check the locations at which the condition for allowable magnitudes of pressures acting on the wall is satisfied or violated. In the latter case the value of $k_h = 0$ has been assigned, and the wall is loaded by active or passive pressure

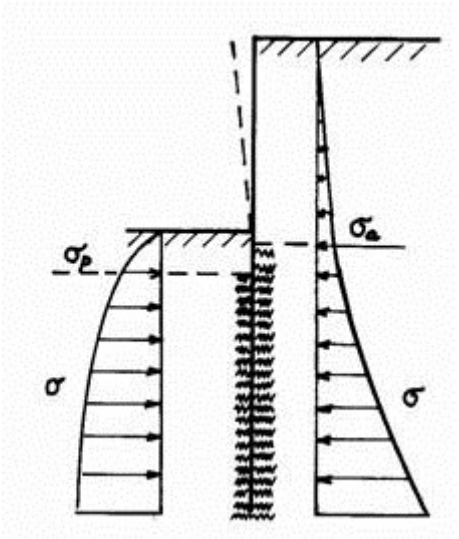

Figure 179: 2nd step of the computational procedure [7]

The above iteration procedure continues until all required conditions are satisfied.

In analyses of subsequent stages of construction the program accounts for plastic deformation of the wall. This is also the reason for specifying individual stages of construction that comply with the actual construction process. The program based on this method and used in the analyses is SheetPile2.0. [7], [16], [17], [15], [18].

2.4 FEM solution - Theoretical introduction

As said before the third approach that has been used for the case study is a calculation by finite element method programs. To better understand the problems related with the modeling of soil-structure interaction the analysis has been carried out by two different programs: GeoStudio and Plaxis. The latter has been used with two different modalities.

The solution is highly influenced by the modeling procedure, and elements which have been properly created to replace the interaction are the key for a better result: thus a comparison between different programs is necessary to analyze this feature.

A significant issue is also the construction by stage that either in GeoStudio or in Plaxis has been taken into account. The “in situ analysis” for the former and the “initial analysis” for the latter are followed by a “load-deformation analysis” and a

"phase-1" respectively: these "two-phase" analyses allow the system soil-structure to simulate the actual excavation. The first phase occurs before the excavation and the second one after it: the latter stage is based on the values of deformation and stress obtained from the former one, in this way the sequence of staged construction develops like a common time continuum. In first phase the gravity is applied to the elements through the material self-weight, in order so simulate the existing state of stress. In the second phase loads are applied as boundary conditions and the new state of stress is implemented. The simulation is performed by adding or removing elements from the mesh, that's to say activating or deactivating regions. The soil has been set as an elastic-plastic material (Mohr-Coulomb model, see chapter 1.3.1) [5], [19].

2.4.1 Plaxis solution

In Plaxis the soil has been set up as an linear elastic perfectly-plastic material, and the failure criterion that has been adopted is that of Mohr-Coulomb (chapter 1.3.1), thus the parameters that define the material are (1.3.1) the Young's modulus E [kN/m^2], the Poisson's ratio ν [-], the cohesion c [kN/m^2], the friction angle φ [°], the dilatancy ψ [°]

The issue has been analyzed as a plane strain model, thus the finite elements have two dimensions and with two translational degree of freedom per node.

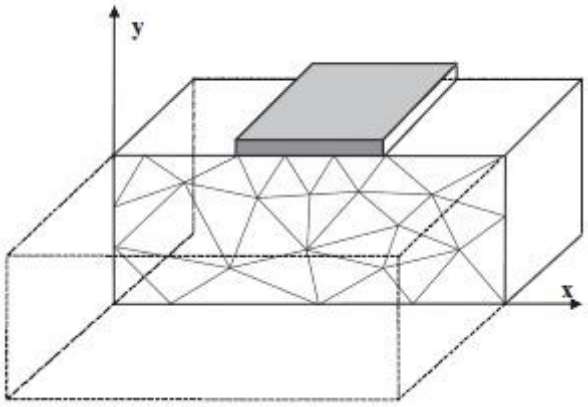

Figure 180: Example of a plain strain [19]

A "coarse" element distribution has been set up, it's enough to have an accurate solution as a first approach: as will be explained in the following chapters this distribution will be turned into a "medium" or "fine" one according to the requirement. The average element I_e size is assumed equal to:

$$I_e = \sqrt{\frac{(x_{max} - x_{min})(y_{max} - y_{min})}{n_c}} \quad \textbf{(106)}$$

Where x_{max}, x_{min}, y_{max}, x_{min} are the geometry dimensions of the mesh, and n_c is a value that takes into account the global coarseness

Very coarse:	$n_c = 25$	Around 75 elements
Coarse:	$n_c = 50$	Around 150 elements
Medium:	$n_c = 100$	Around 300 elements
Fine:	$n_c = 200$	Around 600 elements
Very fine:	$n_c = 400$	Around 1200 elements

Figure 181: Global coarseness [19]

The element that has been used is the default 15-node triangle for the first analyses and changed into a 6-node triangle in the subsequent ones: for the first one the displacements are obtained by an interpolation of the fourth order, and twelve Gauss points (stress points) are involved in the numerical integration; for the second one the displacements are obtained by an interpolation of the second order, and three Gauss points (stress points) are involved in the numerical integration. The 15 – node triangle provides high quality stress results for difficult problems, the 6 – node triangle provides good results in standard deformation analyses.

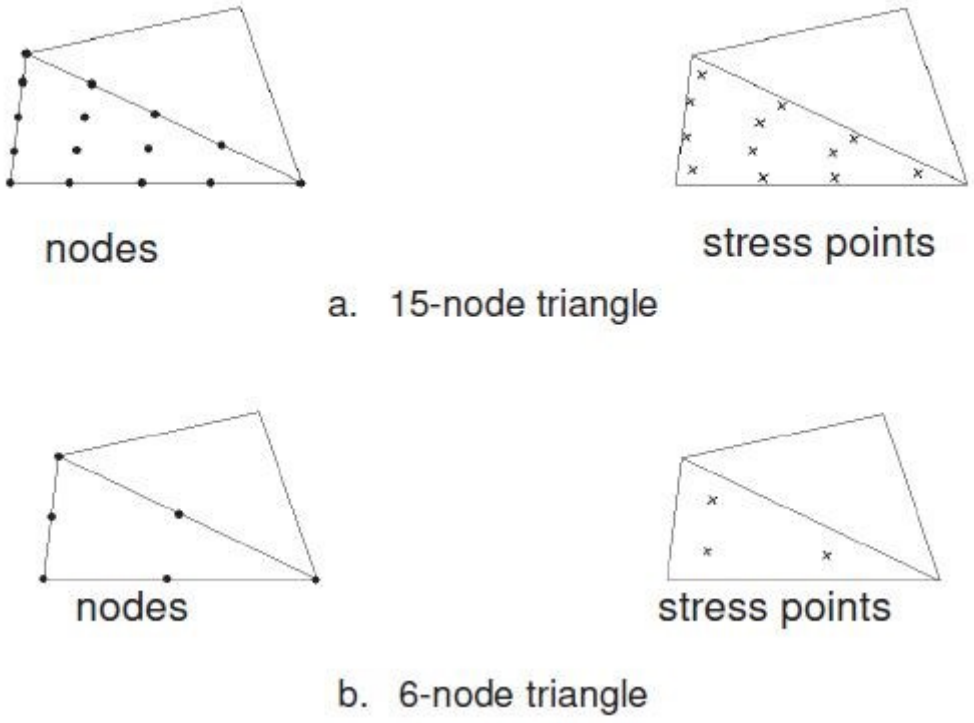

Figure 182: Distribution of nodes and Gauss points [19].

A particular element must be described with more accuracy: the interface. This peculiar feature of Plaxis has a fundamental importance in the analysis, in fact it

takes into account the soil-structure interaction. A fictitious thickness defines the material properties of this element. The elastic deformation increases with the thickness: generally a little deformation is required for an interface, but you must consider that a too little thickness may ill-condition the numerical process. The parameter of the interface is Ri: "Rinter: this parameter relates the strength of the soil to the strength in the interfaces" [20]; "Hence, using the entered Rinter-value gives a reduced interface friction and interface cohesion (adhesion) compared to the friction angle and the cohesion in the adjacent soil" [20].

The equations are:

$$\tan \varphi_{interface} = R_{inter} \tan \varphi_{soil} \leq \tan \varphi_{soil} \quad \textbf{(107)}$$

$$c_{inter} = R_{inter} c_{soil} \quad \textbf{(108)}$$

$$\psi_i = 0° \text{ for } R_{inter} < 1, \text{otherwise } \psi_i = \psi_{soil} \quad \textbf{(109)}$$

An elastic-plastic model is used to describe the relationship between soil and structure, and the Coulomb criterion is used to distinguish the elastic behavior from the plastic one. The interface to remain elastic:

$$|\tau| < \sigma_n \tan \varphi_i + c_i \quad \textbf{(110)}$$

And to behave as a plastic material:

$$|\tau| = \sigma_n \tan \varphi_i + c_i \quad \textbf{(111)}$$

Where σ_n is the effective normal stress, τ the shear stress, φ_i and c_i are the friction angle and the cohesion of the soil.

The shear and compression moduli are related by the expressions:

$$E_{oed,i} = 2G_i \frac{1 - \nu_i}{1 - 2\nu_i} \quad \textbf{(112)}$$

$$G_i = R_{inter}^2 G_{soil} < G_{soil} \quad \textbf{(113)}$$

$$\nu_i = 0.45 \quad \textbf{(114)}$$

A 15-nodes soil element is connected to the corresponding interface element by five points; thus an interface element requires two pairs of five nodes to be define (one

pair for each side). A 6-nodes soil element is connected to the corresponding interface element by three points; thus an interface element requires two pairs of three nodes to be define (one pair for each side). This element has zero thickness because in the FEM formulation two nodes pair have the same coordinates. The Newton-Cotes integration allow to obtain the stiffness matrix of the interface element; the 10-node interface element uses five Newton-Cotes stress points while the 6-node interface element uses five Newton-Cotes stress points and for both of them these coincide with a node pairs.

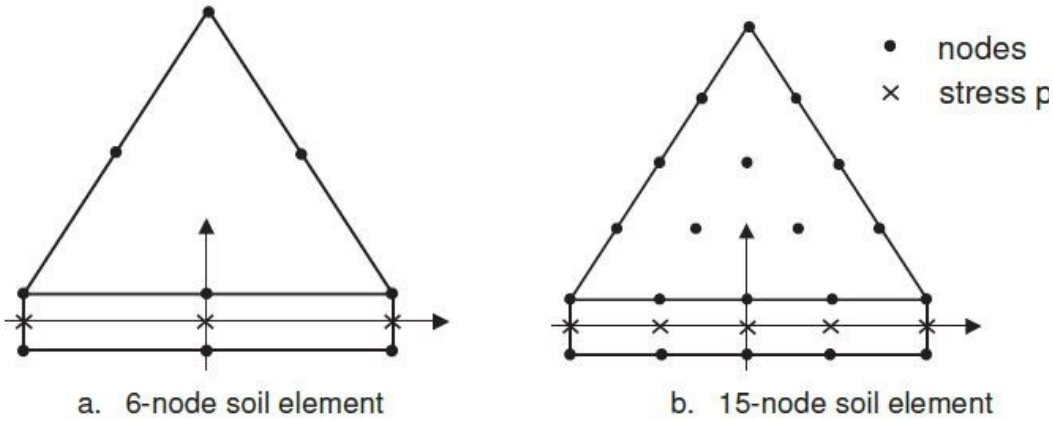

Figure 183: Distribution of nodes and stress points on an interface element [19]

This element reproduces the soil-structure interaction because allows the sliding between the two surfaces, issue that is not taken into account without the interface element because the points are chained together [19], [20].

2.4.2 GeoStudio solution

As for the previous program, in the analyses performed by GeoStudio the soil has been assumed as linear elastic perfectly-plastic material, with a Mohr-Coulomb yield criterion (chapter 1.3.1). Hence the parameters required by the model are the same as those described in the former chapter. The model is a plane strain, the same as Plaxis.

The mesh is composed by 6-noded triangles, thus the integration points (and the integration orders) are three. This mesh have been chosen in order to have a homogeneous comparison with Plaxis (as said in the previous chapter the 15-nodes triangle element used for the first calculation with Plaxis will be turned to a 6-nodes triangle for the comparison with GeoStudio).

The size of the elements has been modified (in some strategic points for instance) in order to have a better discretization. An interface has been generated along the structure and it describes the friction properties between soil and structure. Material properties (elastic-plastic behavior, with the parameters that are required) have been assigned to the interface. However the thickness of this element doesn't

have a physical meaning and it isn't taken into account in the solution. This interface is important for the solution, but it doesn't have the properties that are specified in Plaxis. The results indeed are highly dependent on the stiffness of the interface material and on the other parameters that will be specified in the proper chapter. In order to have a homogeneous comparison with Plaxis the parameters of the interface in GeoStudio are calculated by the suggested formulae of chapter 2.4.1, these formulae could relate the two programs [5].

2.5 Overview of the results –Sand

2.5.1 Introduction: searching for the length to compare

In order to have an uniform length of the sheet pile that allows the expected comparison, it is necessary to choose the best solution, that's to say to compare the solutions obtained by different approaches for a given set of conditions, and decide which of them could be the suitable one. The first length that provides an acceptable solution for the "Classic Method" is 7 m (it's important to remember that this method gives a simplified solution, so it is reasonable to use a "minimum value" obtained by a more precise approach). The minimum value for Sheetpile2.0 is 7.5 m, but the displacement is 8.43 cm. The minimum value for Plaxis is 8.5 m, but the displacement is 1.395 cm (peak value). GeoStudio in this case is considered a "comparison program". Plaxis provides an acceptable solution (0.957 cm) with a 10 m length sheet pile, and the length to be analyzed will be chosen by varying the length of the sheet pile adopting this program. Using a 12 m length sheet pile the maximum displacement is 0.923 cm, from 13 m on there isn't a significant improvement of the performance. In order to compare two different behaviors have been chosen two different "comparison lengths" for the sheet pile: the first one is close to the instability (9 m), the second one widely ensures the equilibrium (12 m). The solution by Plaxis has been obtained by assuming a "coarse" distribution of the mesh, that's to say that around 150 elements compose the mesh (2.4.1). The average element size, I_e, for the assumed geometry of the model is I_e = 4 m. In order to have a coherent comparison with GeoStudio it is necessary to have the same characteristics of the mesh in both programs, but with this number and dimension of elements GeoStudio can't ensure an adequate solution. For this reason the choice of the length of the sheet pile has been made using a "coarse" mesh in Plaxis; then, for the chosen lengths, in order to compare the results from the different approaches, the mesh of Plaxis has been changed into a "medium" mesh with around 300 elements and I_e = 2.8 m for the solution with the 9 m length sheet pile. The elements of Plaxis have been changed too, from 15-nodes triangle to 6 -nodes triangles because GeoStudio supports only this second kind of elements. In the following graphics (Figure 186) one can notice how this change doesn't significantly modify the solution.

For the second comparison (12 m) instead of GeoStudio a different solution by Plaxis has been assumed; in this case the mesh has been set "fine" (around 600 elements and I_e = 2 m) keeping a 6-nodes triangle element, the value of R_i is changed from R_i = 0.8 into R_i = 1 ("rigid"): this situation simulates the lack of the interface (only soil and plate).

In the following graphic and table one can notice how the displacement varies changing the length of the sheet pile (Plaxis solution): the chosen solutions represent behaviors either close to stability or close to instability.

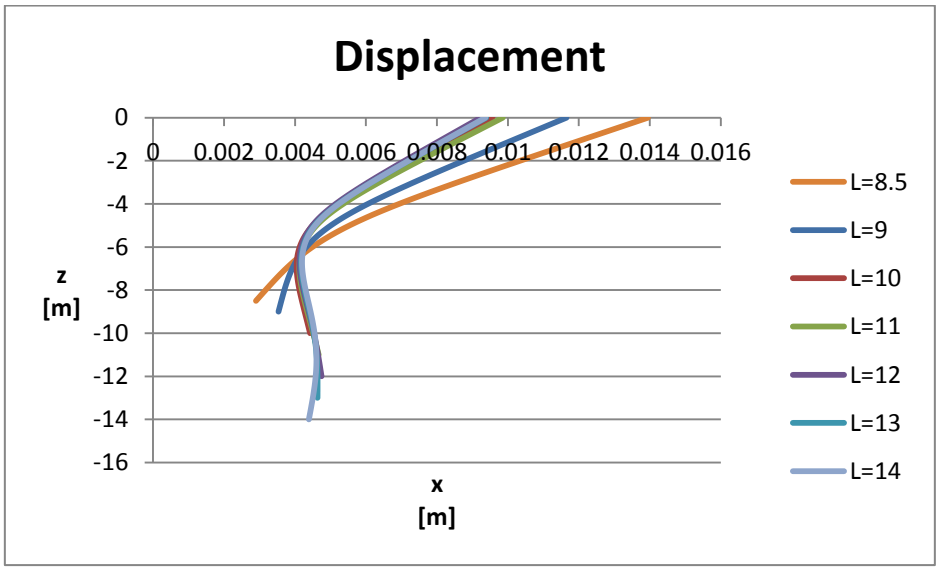

Figure 184: Horizontal displacement of the sheet pile varying its length

Table 10: Maximum and minimum values of the displacement of the sheet pile varying its length, absolute and relative difference of displacement between sheet piles with different lengths

DISPLACEMENT [m]							
MAXIMUM							
L =8.5	L = 9	L = 10	L = 11	L = 12	L = 13	L = 14	L = 15
0.013949	0.011653	0.009567	0.009856391	0.009234	0.009391	0.009367	0.009413
ABS_DIFF	16%	31%	29%	34%	33%	33%	33%
REL_DIFF	16%	18%	-3%	6%	-2%	0%	0%
MINIMUM							
L =8.5	L = 9	L = 10	L = 11	L = 12	L = 13	L = 14	L = 15
0.002899	0.003534	0.004046	0.004120155	0.004126	0.004172	0.004198	0.004022
ABS_DIFF	-22%	-40%	-42%	-42%	-44%	-45%	-39%
REL_DIFF	-22%	-14%	-2%	0%	-1%	-1%	4%

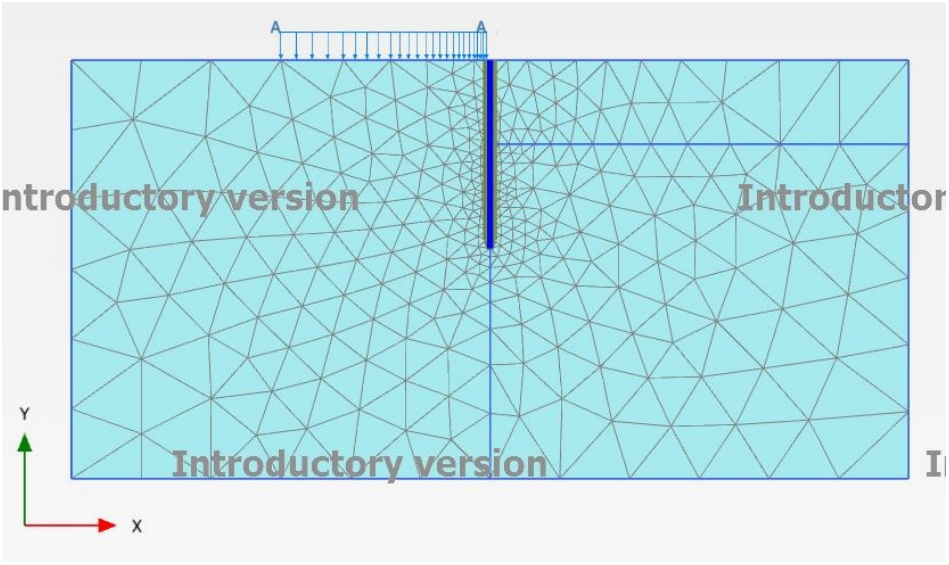

Figure 185: The mesh: "coarse" with tri-15 elements used at the beginning for the choice of the sheet pile's length

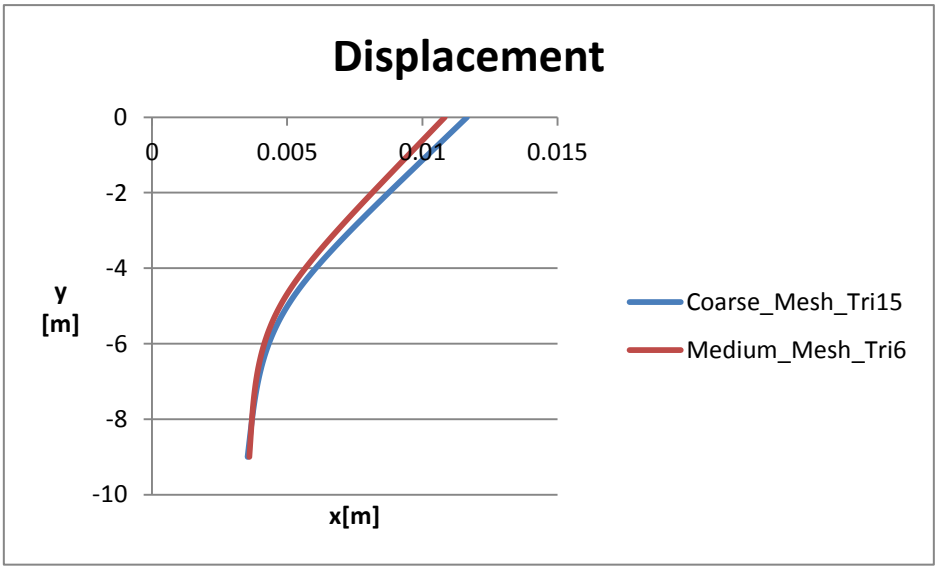

Figure 186: Displacement of a sheet pile of 9 m in sand using Plaxis with: coarse mesh and tri-15 elements, medium mesh and tri-6 elements

Table 11: Maximum and minimum values of the displacement in the sheet pile of 9 m in sand using Plaxis with a coarse mesh and tri-15 elements, and with a medium mesh and tri-6 elements, absolute difference

DISPLACEMENT [m]			
MAXIMUM		MINIMUM	
COARSE	MEDIUM	COARSE	MEDIUM
0.01165	0.01083	0.00353	0.00360
ABS_DIFF	7%	ABS_DIFF	-2%

2.5.2 Classic Method – Sand - 1st case (9 m) results

As said in the previous chapter, this method considers the wall as a rigid element, so the parameters of the sheet pile aren't required, a part from the length that must be varied with a method of trial and correction until the equilibrium is achieved (see chapter 2.2). The only comparable stress parameter that this method provides is the bending moment.

Table 12: Parameters required in the Classic Method

SAND						SP
H	γ	ϕ	c	q	dex	L
[m]	[kN/m^3]	[°]	[kPa]	[kN/m]	[m]	[m]
20	18	37	0	10	4	9

Where H is thickness of the layer, γ the self-weight of sand, φ the angle of friction of sand, c the cohesion of sand, q is the load, dex the excavation, L the final length that is required for equilibrium.

These are the graphics obtained by this approach. As the minimum required length to have equilibrium is 7 m, the trend of the bending moment is taken into account only within this length and not for the remaining part of the sheet pile (Figure 189).

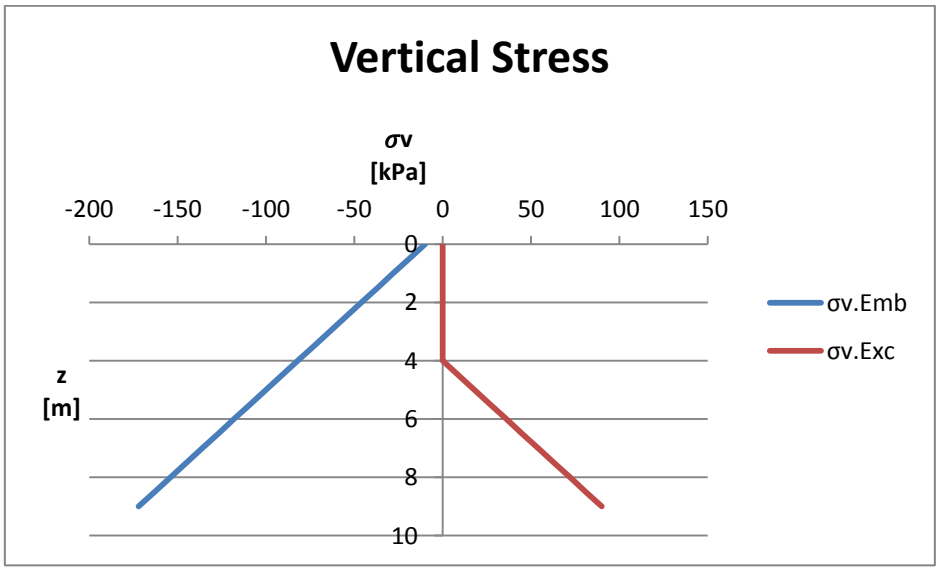

Figure 187: Vertical stress along a sheet pile of 9 m in sand using the Classic Method

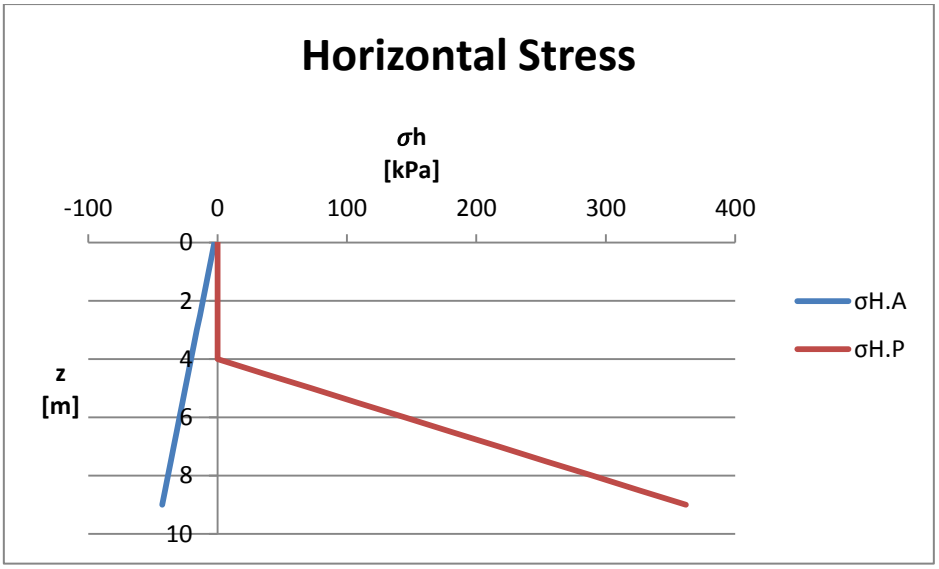

Figure 188: Horizontal stress along a sheet pile of 9 m in sand using the Classic Method

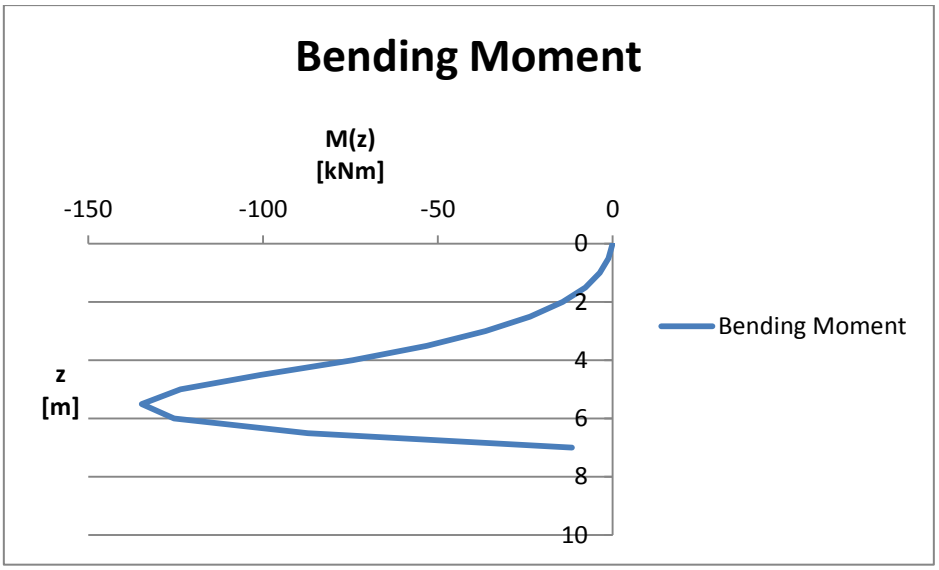

Figure 189: Bending moment of a sheet pile of 9 m in sand using the Classic Method

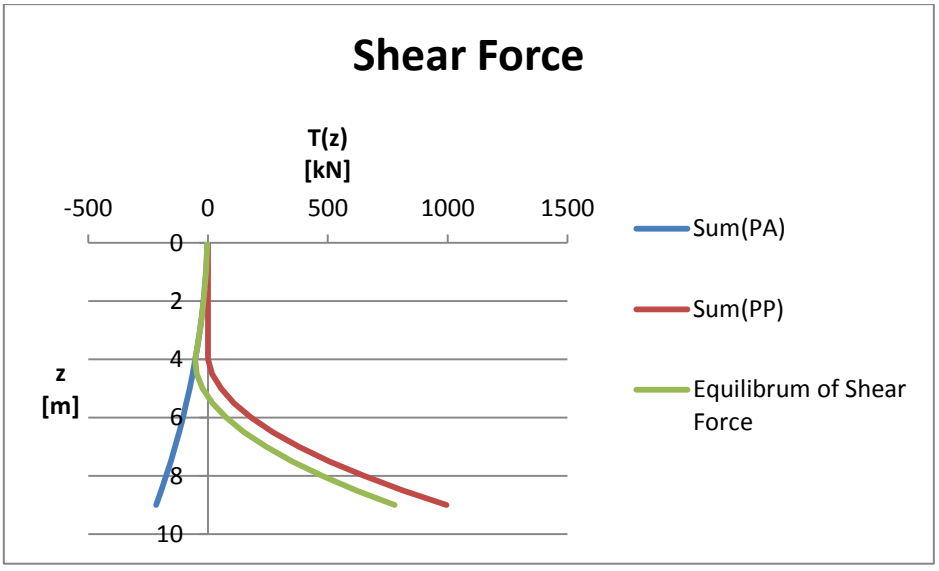

Figure 190: Shear force of a sheet pile of 9 m in sand using the Classic Method

2.5.3 SheetPile2.0 – Sand - 1st case (9 m) results

This program, based on the dependent pressure method, gives the values of displacement, angle of rotation, bending moment, shear force and reaction.

Table 13: Parameters required in SheetPile2.0

SAND							SHEET PILE		
H	γ	ϕ	c	q	dex	dwl	t	Ep	L
[m]	[kN/m^3]	[°]	[kPa]	[kN/m]	[m]	[m]	[m]	[kPa]	[m]
20	18	37	0	10	4	0	0.5	20x10^6	9

Where H is thickness of the layer, γ the self-weight of sand, φ the angle of friction of sand, c the cohesion of sand, q is the load, dex the excavation, dwl the depth of the groundwater level, t , Ep and L are the thickness, the elastic modulus and the length of the sheet pile respectively.

This is the graphic interface of the program.

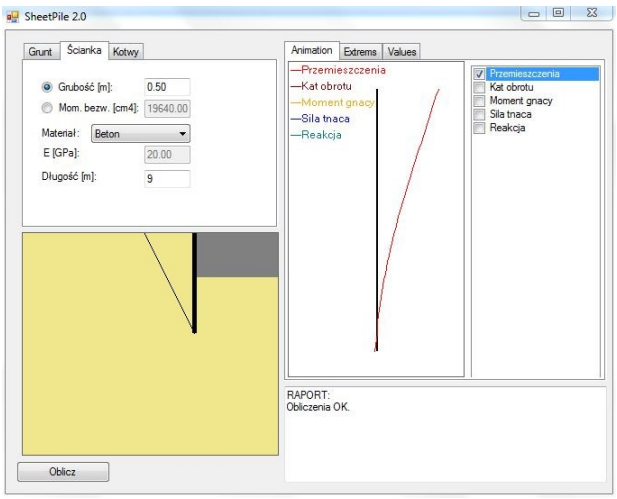

Figure 191: Graphic interface of SheetPile2.0

The following graphic shows the value of the displacement obtained with a 7.5 m sheet pile, the minimum length that ensures a solution with this program: the value is too high to be acceptable.

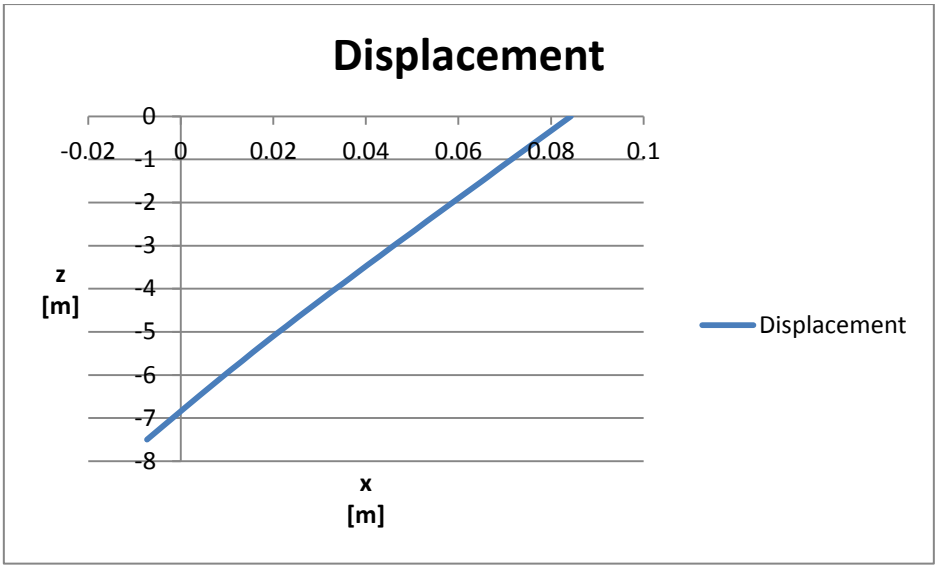

Figure 192: Displacement of a sheet pile of 7.5 m in sand using SheetPile2.0

The following graphics consider the chosen length: 9 m.

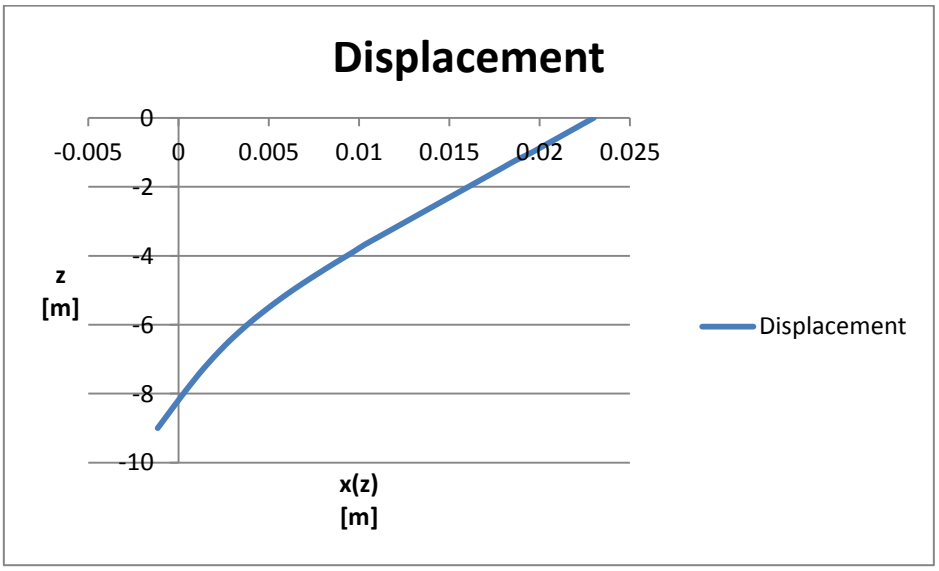

Figure 193: Displacement of a sheet pile of 9 m in sand using SheetPile2.0

Table 14: Maximum and minimum values of the displacement in the sheet pile of 7.5 m and in the sheet pile of 9 m in sand using SheetPile2.0, absolute difference

DISPLACEMENT [m]			
MAXIMUM		MINIMUM	
SP2.0-7.5m	SP2.0-9m	SP2.0-7.5m	SP2.0-9m
0.08430	0.02300	-0.00728	-0.00115
ABS_DIFF	73%	ABS_DIFF	84%

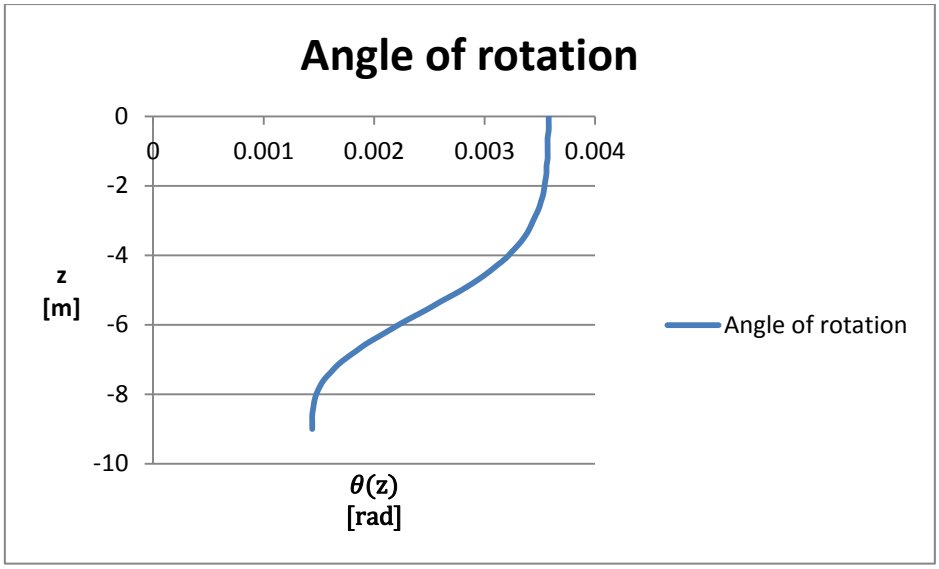

Figure 194: Angle of rotation of a sheet pile of 9 m in sand using SheetPile2.0

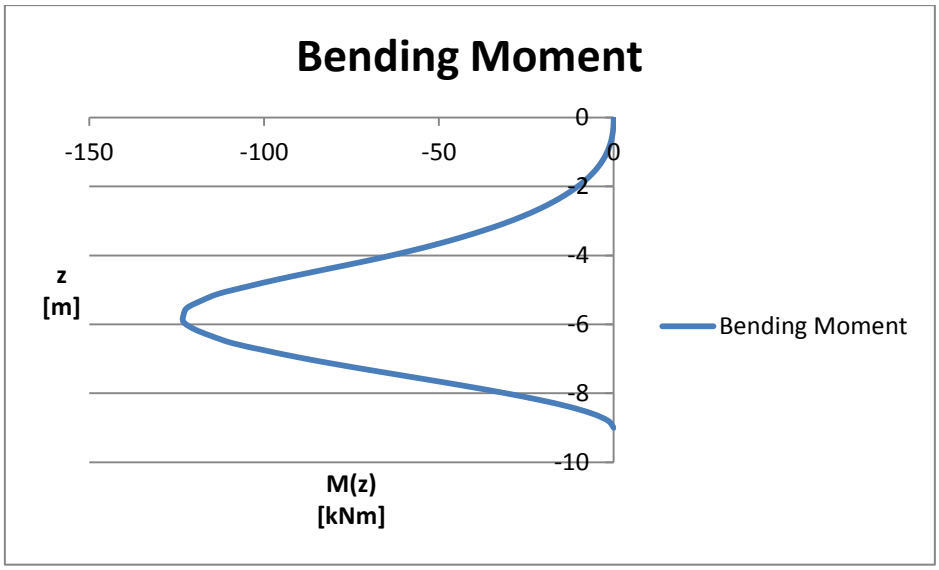

Figure 195: Bending moment of a sheet pile of 9 m in sand using SheetPile2.0

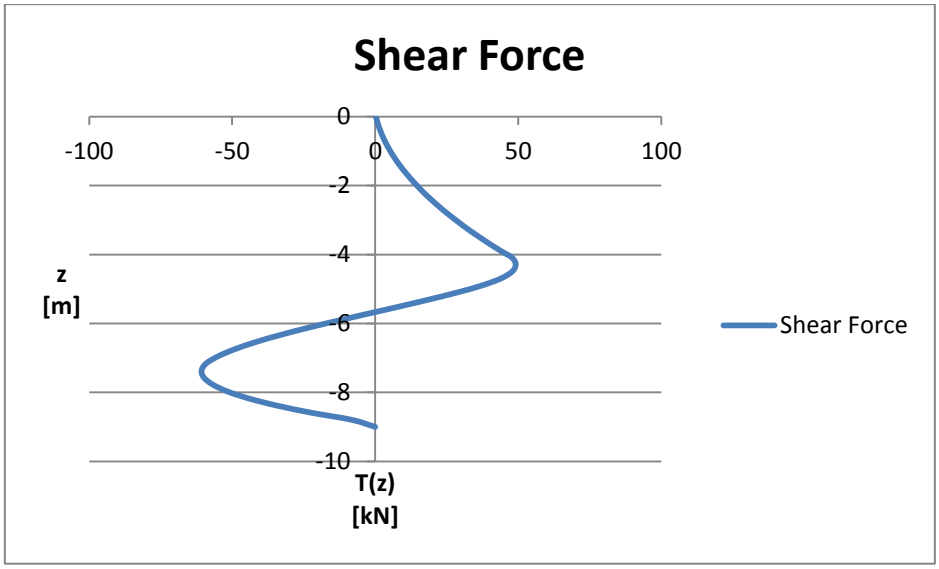

Figure 196: Shear force of a sheet pile of 9 m in sand using SheetPile2.0

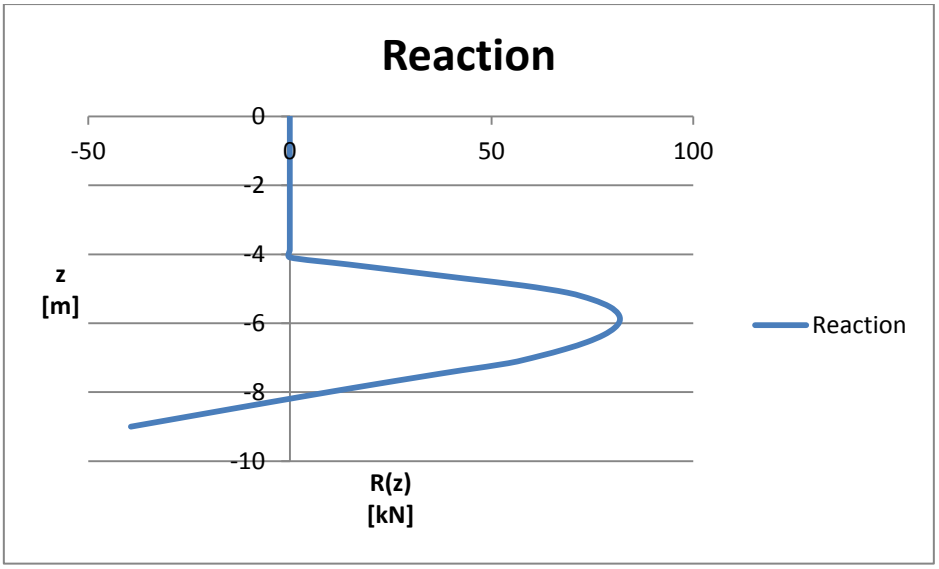

Figure 197: Reaction of a sheet pile of 9 m in sand using SheetPile2.0

2.5.4 Plaxis – Sand - 1st case (9 m) results

Plaxis provides an accurate solution for this kind of problems, in particular because of its geometry issue "interface" which adequately represents the interaction between soil and sheet pile. The assumed model is represented in the following image.

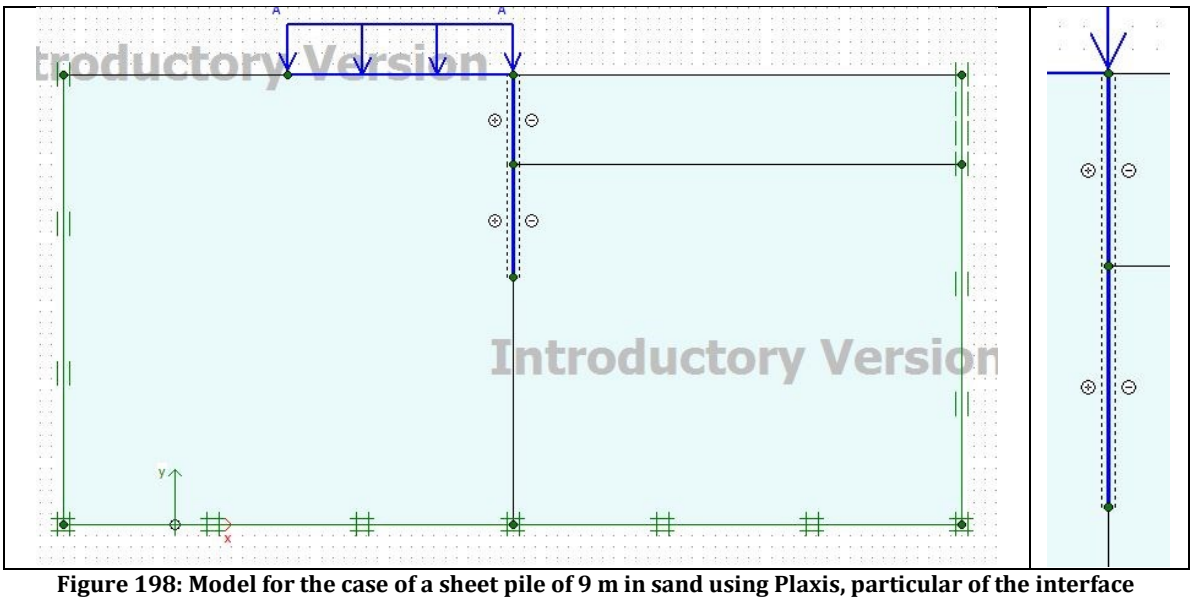

Figure 198: Model for the case of a sheet pile of 9 m in sand using Plaxis, particular of the interface

The generated mesh (Figure 199) is a medium element distribution.

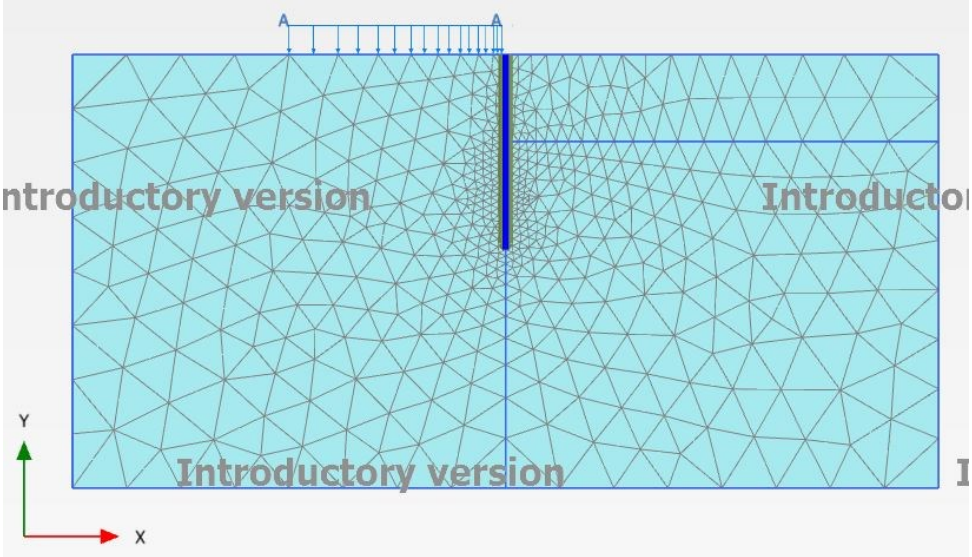

Figure 199: The mesh: "medium" with tri-6 elements

These are the main characteristics of the model.

Table 15: Parameters required in Plaxis

SAND								
H	γ	ϕ	c	ν	ψ	Es	q	dex
[m]	[kN/m^3]	[°]	[kPa]	[-]	[°]	[kPa]	[kN/m]	[m]
20	18	37	0	0.3	5	37x10^3	10	4

SHEET PILE					IF
L	w	EA	EJ	ν	Ri
[m]	[kN/m/m]	[kN/m]	[kNm^2]	[-]	[-]
9	12.5	10x10^6	208333.3	0.3	0.8

Where H is thickness of the layer, γ the self-weight of sand, φ the angle of friction of sand, c the cohesion of sand, ν the Poisson's ratio, ψ the dilatation angle, Es elastic modulus of the soil, q is the load, dex the excavation, L, w, EA, EJ, ν are the length, the weight of 1m^2, the axial stiffness, the flexural rigidity (bending stiffness), the Poisson's ratio of the sheet pile respectively, Ri is a parameter of the interface (2.4.1).

The results obtained by this program will be exposed in the following screenshots.

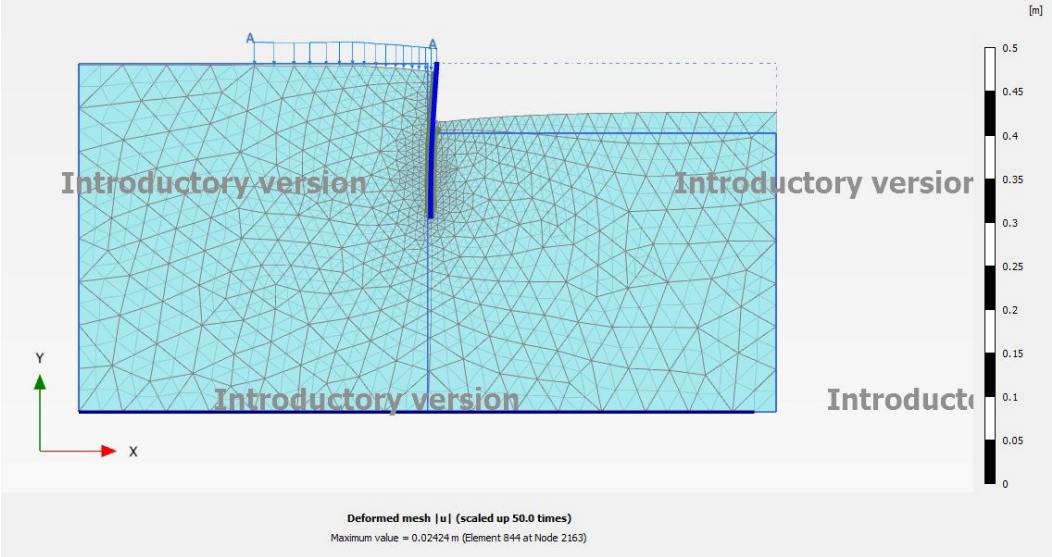

Figure 200: Deformed mesh for the case of a sheet pile of 9 m in sand using Plaxis

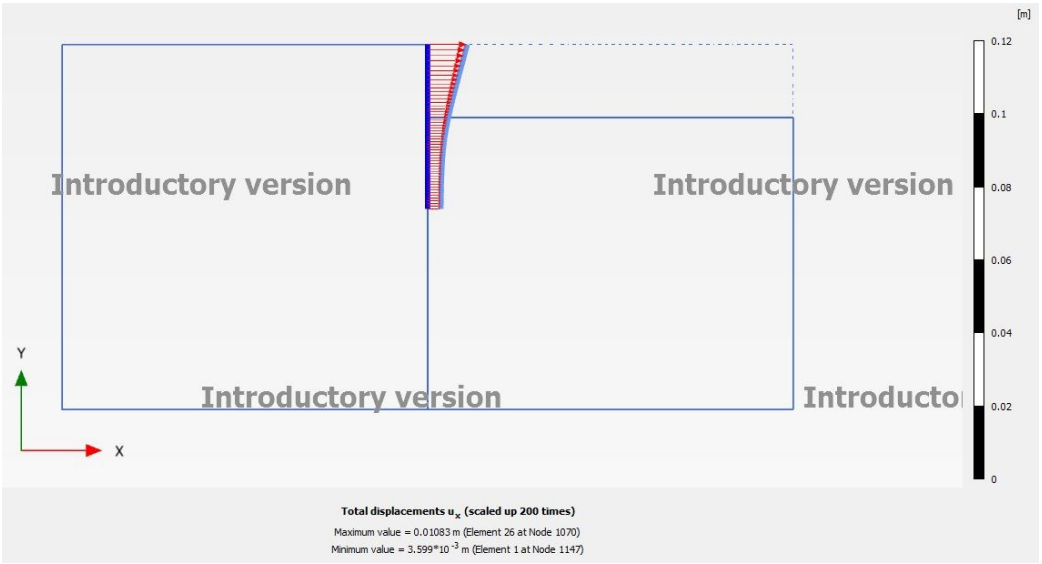

Figure 201: Displacement u_x of a sheet pile of 9 m in sand using Plaxis

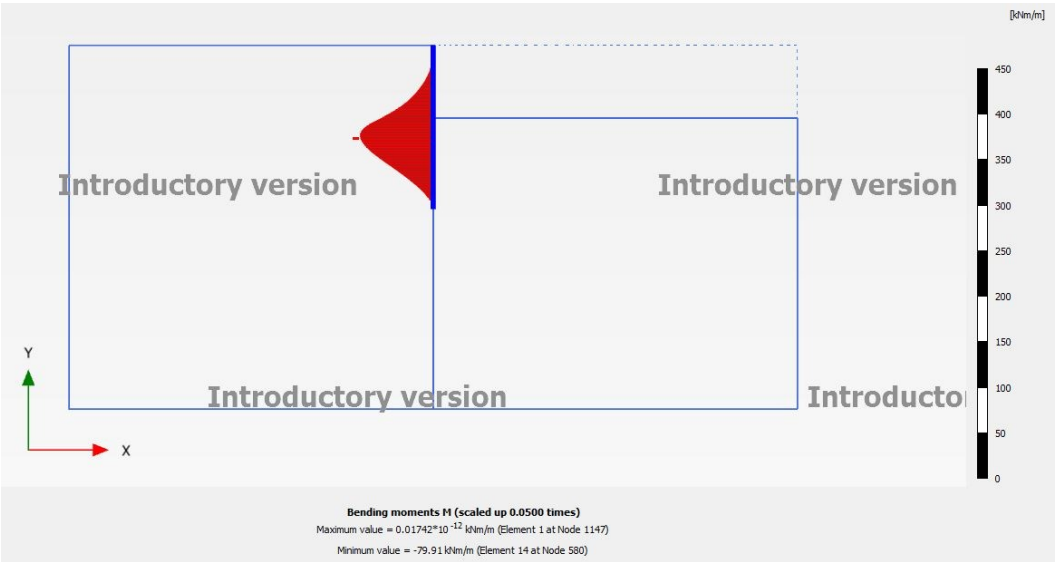

Figure 202: Bending moment of a sheet pile of 9 m in sand using Plaxis

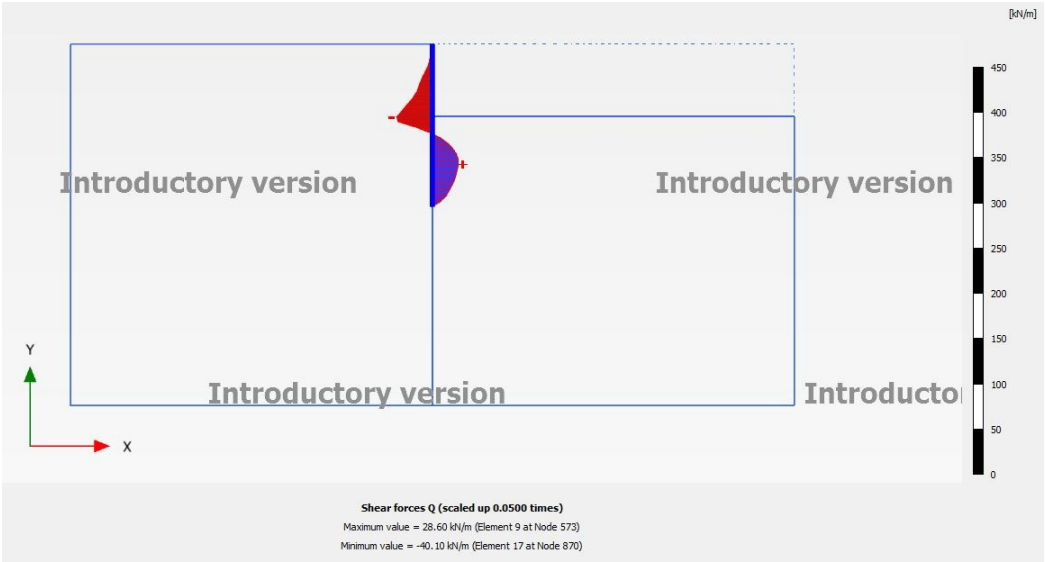

Figure 203: Shear force of a sheet pile of 9 m in sand using Plaxis

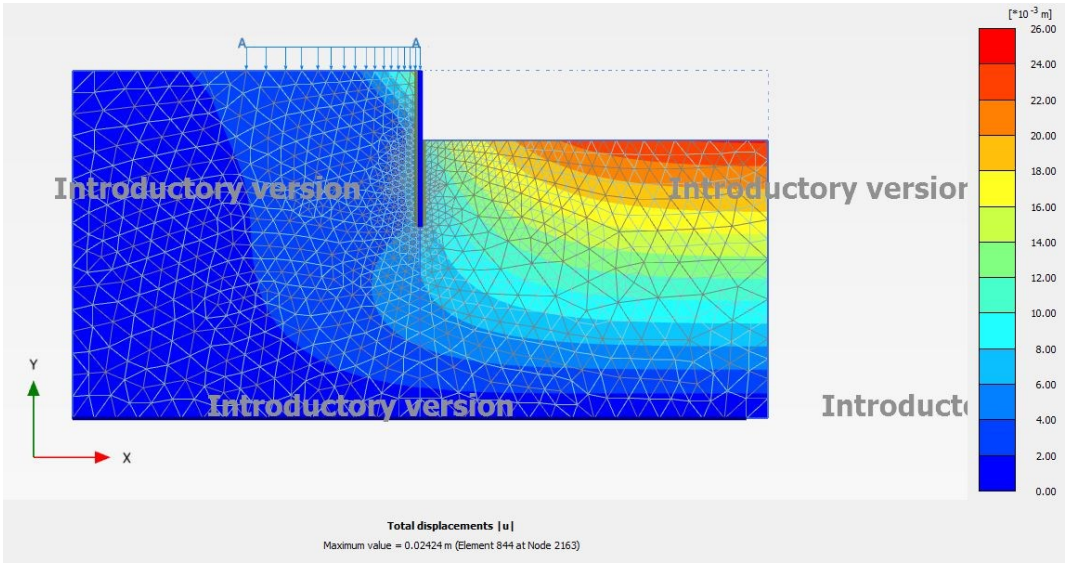

Figure 204: Total displacement u for the case of a sheet pile of 9 m in sand using Plaxis

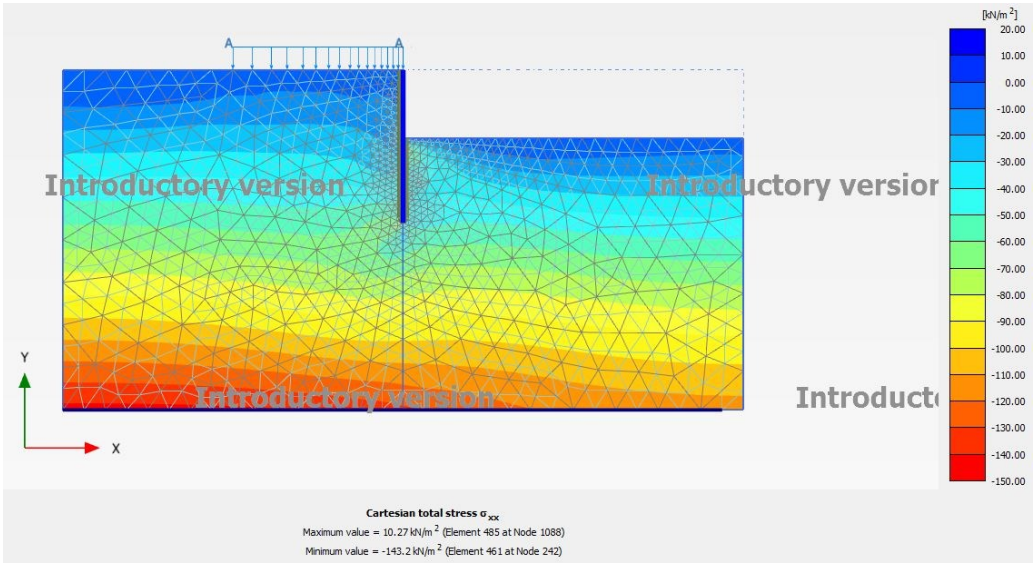

Figure 205: Total stress σ_{xx} for the case of a sheet pile of 9 m in sand using Plaxis

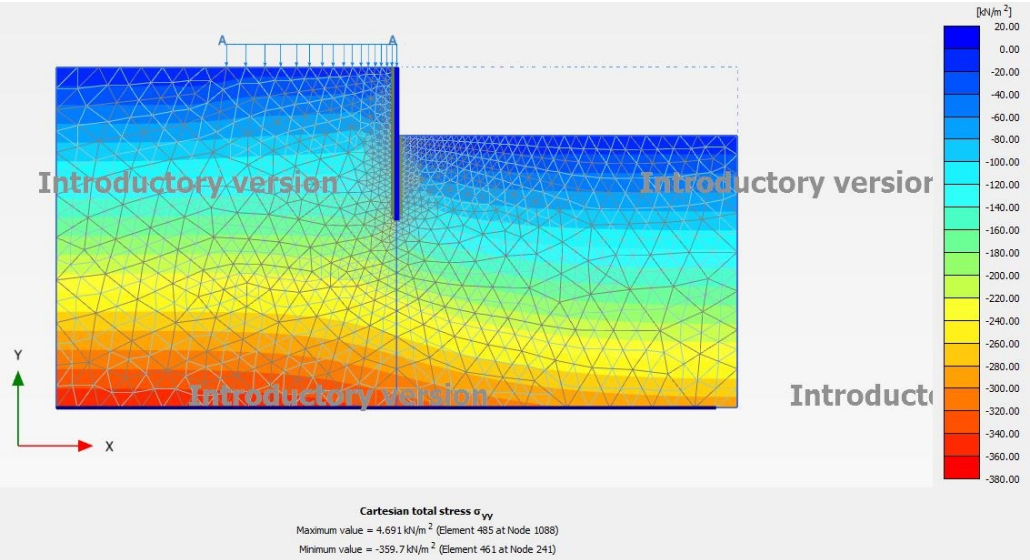

Figure 206: Total stress σ_{yy} for the case of a sheet pile of 9 m in sand using Plaxis

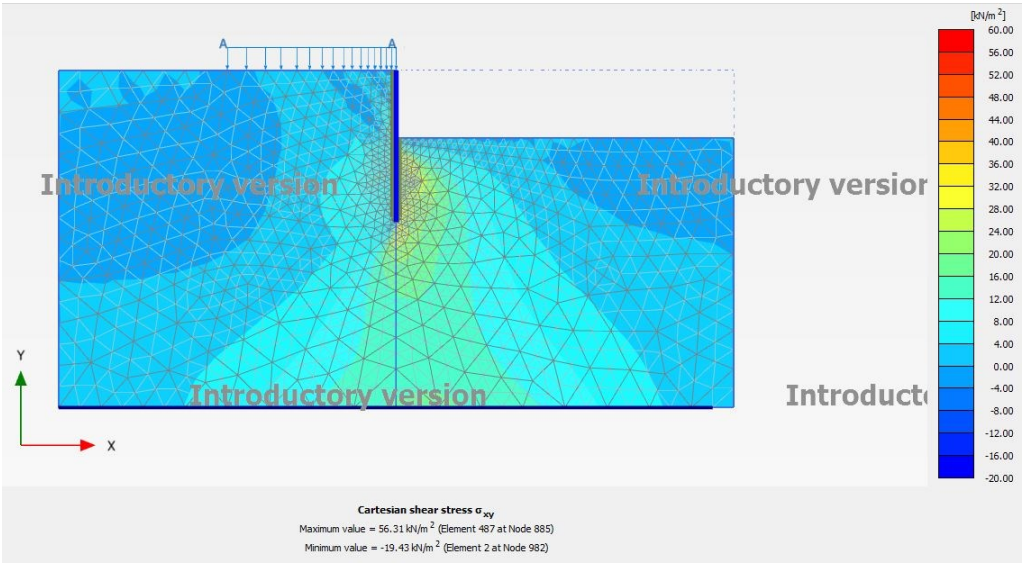

Figure 207: Total stress σ_{xy} for the case of a sheet pile of 9 m in sand using Plaxis

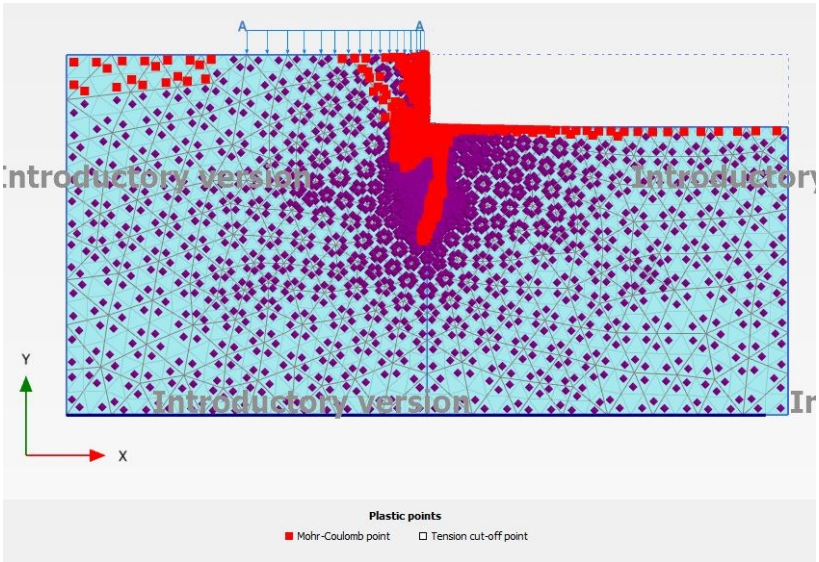

Figure 208: Plastic points for the case of a sheet pile of 9 m in sand using Plaxis

2.5.5 GeoStudio – Sand - 1st case (9 m) results

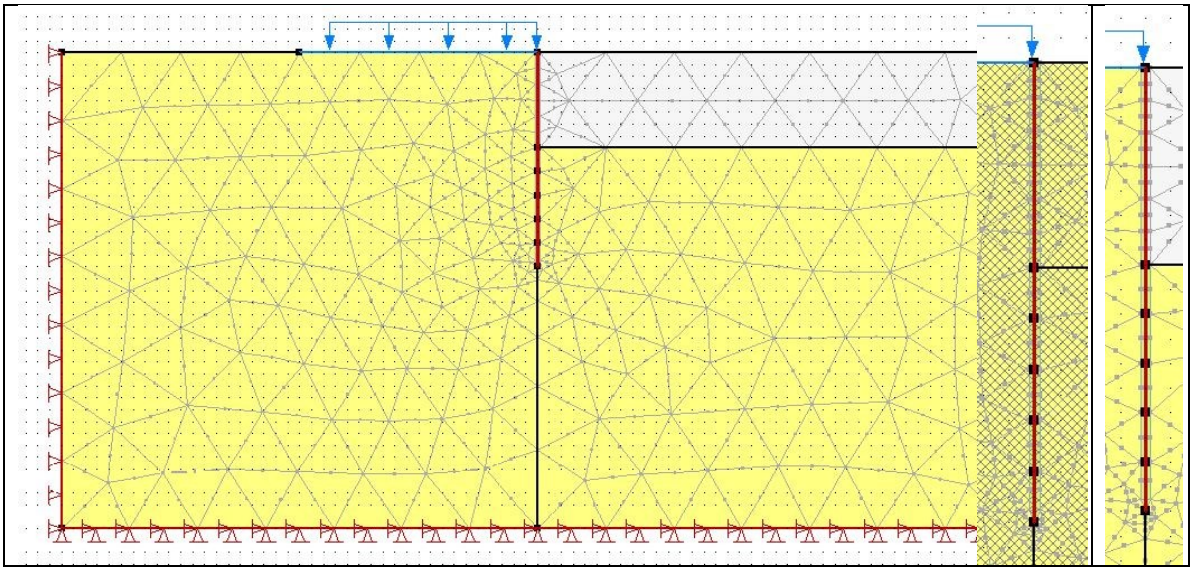

Figure 209: Model for the case of a sheet pile of 9 m in sand using Plaxis, particulars of the interface

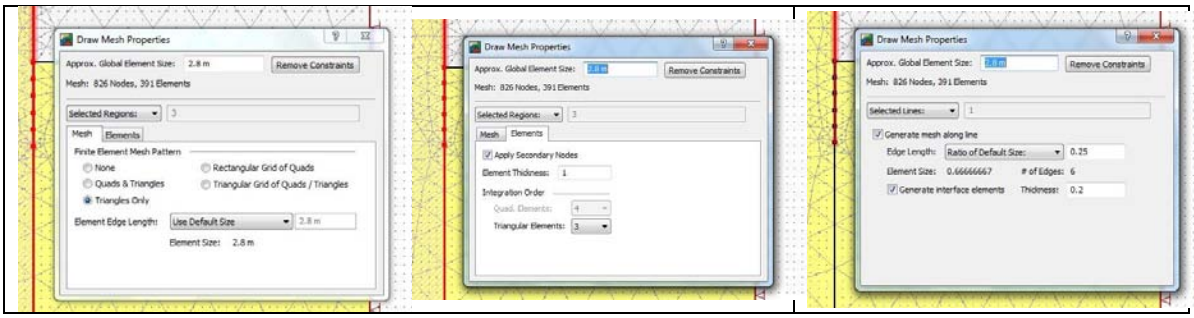

Figure 210: Set up of the mesh

The mesh is composed by 826 nodes and 391 elements, the elements are tri-6, the approximate element size is 2.8 m.

Table 16: Parameters required in GeoStudio

SAND								
H	γ	ϕ	c	ν	ψ	Es	q	dex
[m]	[kN/m^3]	[°]	[kPa]	[-]	[°]	[kPa]	[kN/m]	[m]
20	18	37	0	0.3	5	37x10^3	10	4

SHEET PILE				
t	Ep	L	A	J
[m]	[kPa]	[m]	[m^2]	[m^4]
0.5	20x10^6	9	0.5	0.010417

INTERFACE					
γ	ϕ	c	ν	ψ	Ei
[kN/m^3]	[°]	[kPa]	[-]	[°]	[kPa]
18	31	0	0.45	0	9107.2

Where H is thickness of the layer, γ the self-weight of sand, φ the angle of friction of sand, c the cohesion of sand, ν the Poisson's ratio, ψ the dilatation angle, Es elastic modulus of the soil, q is the load, dex the excavation, t, Ep, L, A, J are the thickness, the elastic modulus, the length, the area, the moment of inertia of the sheet pile respectively, γ, φ, c, ν, ψ, Ei are self-weight, the angle of friction, the cohesion, the Poisson's ratio, the dilatation angle, elastic modulus of the interface respectively.

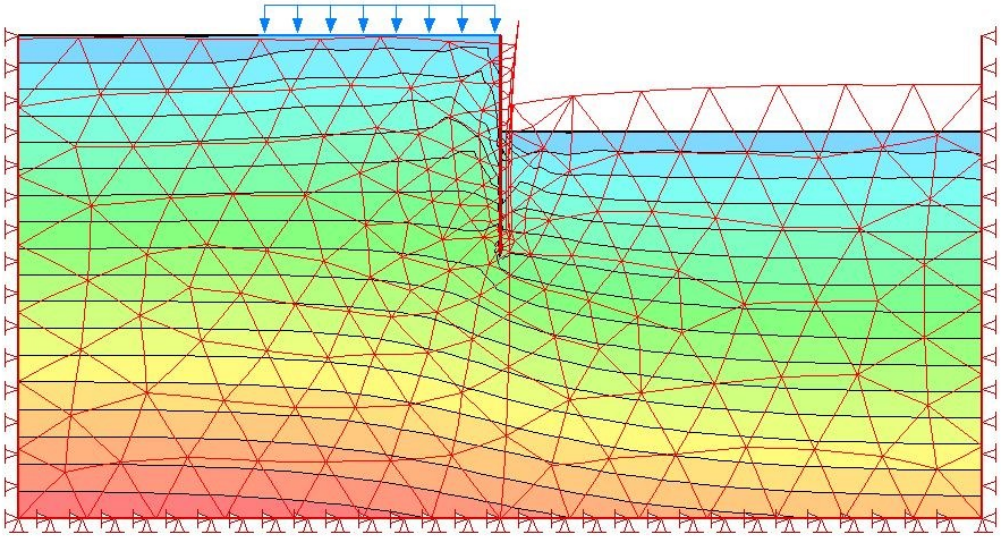

Figure 211: Deformed mesh for the case of a sheet pile of 9 m in sand using GeoStudio

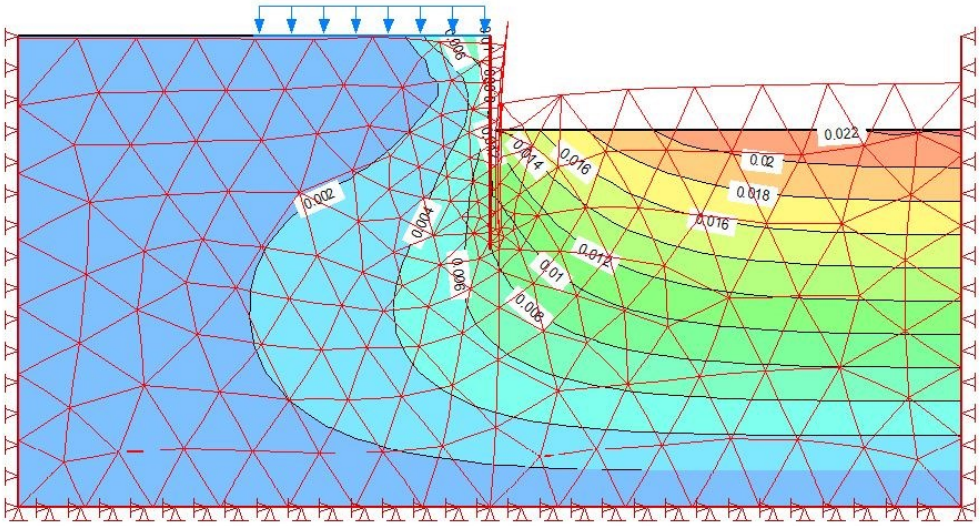

Figure 212: Total displacement u_{xy} for the case of a sheet pile of 9 m in sand using GeoStudio

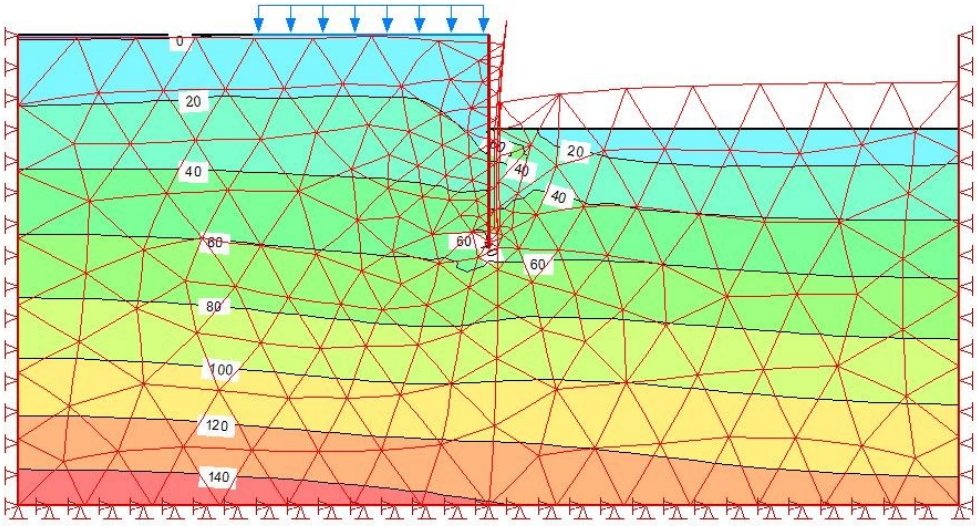

Figure 213: Total stress σ_{xx} for the case of a sheet pile of 9 m in sand using GeoStudio

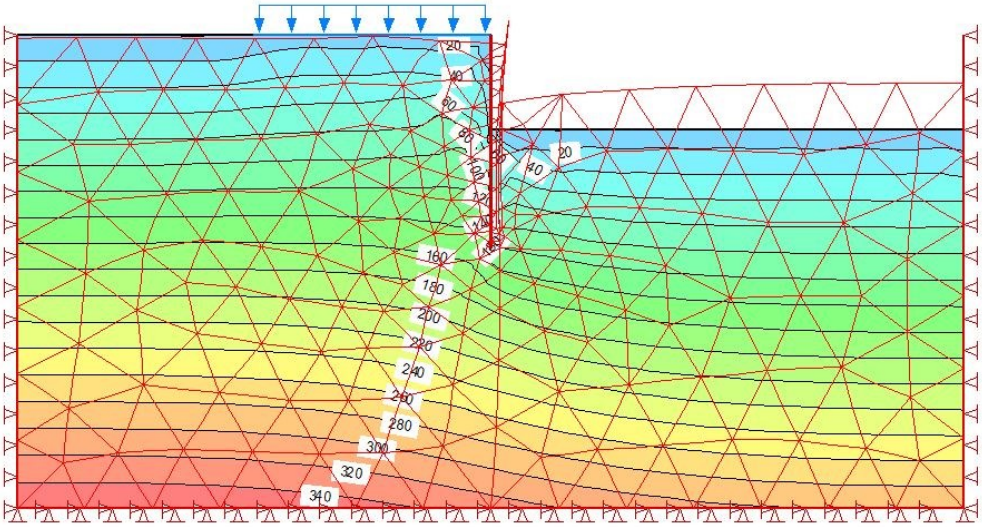

Figure 214: Total stress σ_{yy} for the case of a sheet pile of 9 m in sand using GeoStudio

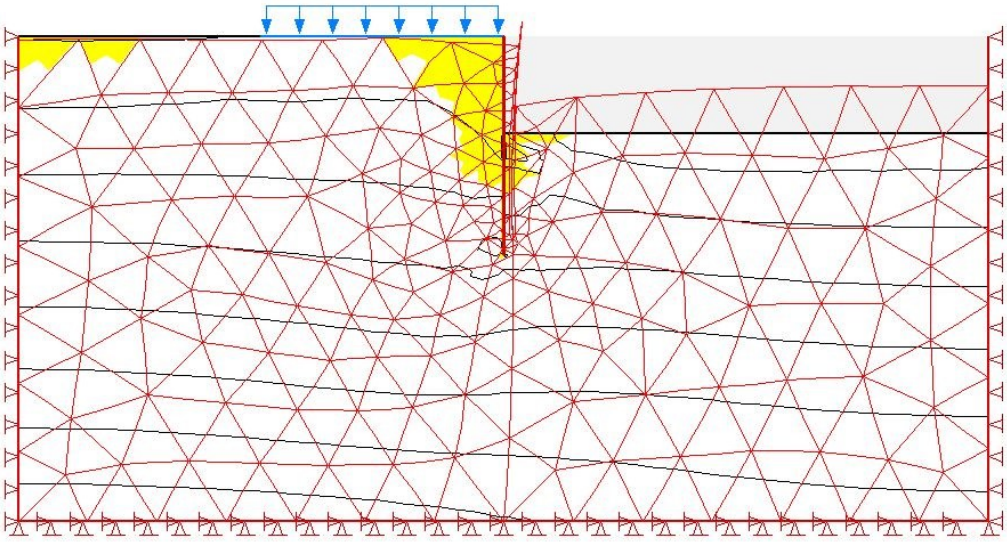

Figure 215: Plastic points for the case of a sheet pile of 9 m in sand using GeoStudio

2.5.6 Sand – 1st case (9 m) comparison

The values obtained by SheetPile2.0 and by the Classic Method (that provides only the bending moment) can be considered conservative and useful for a preliminary evaluation of the parameters, whereas the FEM solutions can be chosen as more coherent with the real behavior of the soil-structure system. Regarding the bending moment obtained with the Classic Method (see chapter 2.5.2): as the minimum required length to have equilibrium is 7 m, the trend of the bending moment is taken into account only within this length and not for the remaining part of the sheet pile (Figure 217).

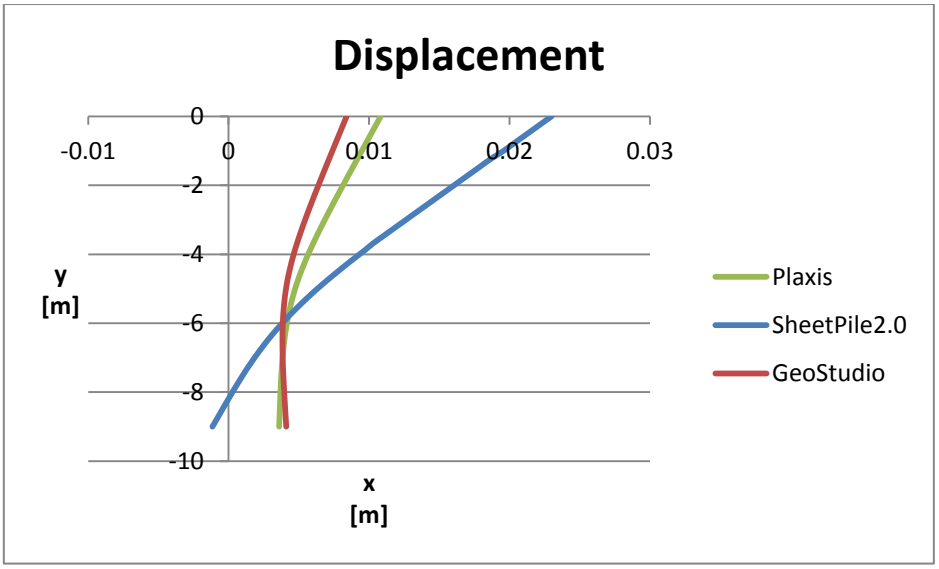

Figure 216: Displacement of a sheet pile of 9 m in sand using Plaxis, SheetPile2.0, GeoStudio

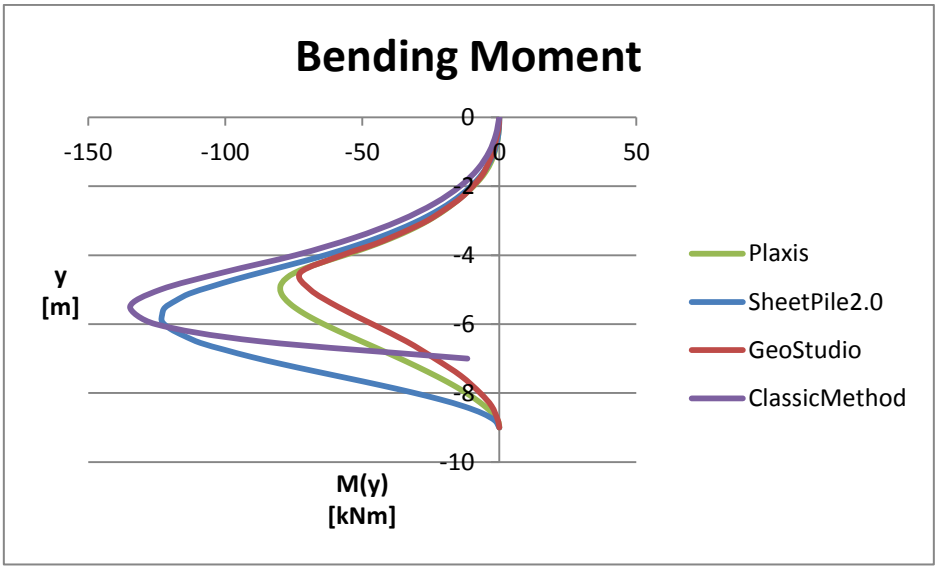

Figure 217: Bending moment of a sheet pile of 9 m in sand using Plaxis, SheetPile2.0, Geostudio, the Classic Method

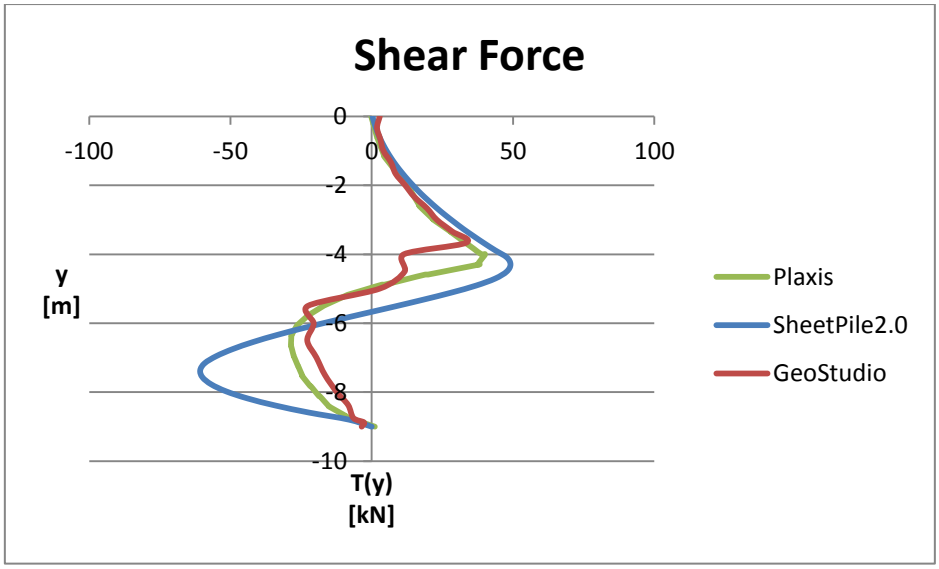

Figure 218: Shear force of a sheet pile of 9 m in sand using Plaxis, SheetPile2.0, Geostudio

Table 17: Maximum and minimum values of the displacement, bending moment, shear force in the sheet pile of 9 m in sand using Plaxis, SheetPile2.0, GeoStudio and the Classic method, absolute difference

DISPLACEMENT [m]							
MAXIMUM				MINIMUM			
Plaxis	SP2.0	GS	CM	Plaxis	SP2.0	GS	CM
0.010832	0.02303	0.008406	-	0.003599	-0.00115	0.003836	-
ABS_DIFF	-113%	22%	-	ABS_DIFF	132%	-7%	-
BENDING MOMENT [kNm]							
MAXIMUM				MINIMUM			
Plaxis	SP2.0	GS	CM	Plaxis	SP2.0	GS	CM
1.74E-14	0	5.82E-11	0	-79.9085	-123.373	-72.5062	-134.696
ABS_DIFF	-	-	-	ABS_DIFF	-54%	9%	-69%
SHEAR FORCE [kN]							
MAXIMUM				MINIMUM			
Plaxis	SP2.0	GS	CM	Plaxis	SP2.0	GS	CM
40.0987	49.13711	33.39534	-	-28.6003	-60.7047	-22.8175	-
ABS_DIFF	-23%	17%	-	ABS_DIFF	-112%	20%	-

2.5.7 Classic Method – Sand – 2nd case (12 m) results

The only parameter that has been changed from the 1st case is the length of the sheet pile "L", from L = 9 m into L = 12 m. The other parameters are the same as chapter 2.5.2. The results are exposed in the following graphics. As the minimum required length to have equilibrium is 7 m, the trend of the bending moment is taken into account only within this length and not for the remaining part of the sheet pile (Figure 221)

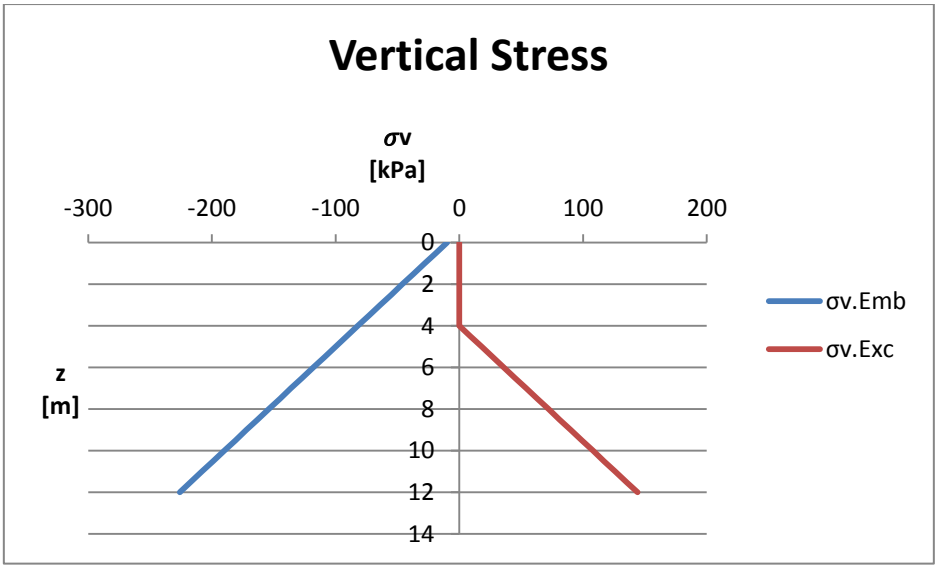

Figure 219: Vertical stress along a sheet pile of 12 m in sand using the Classic Method

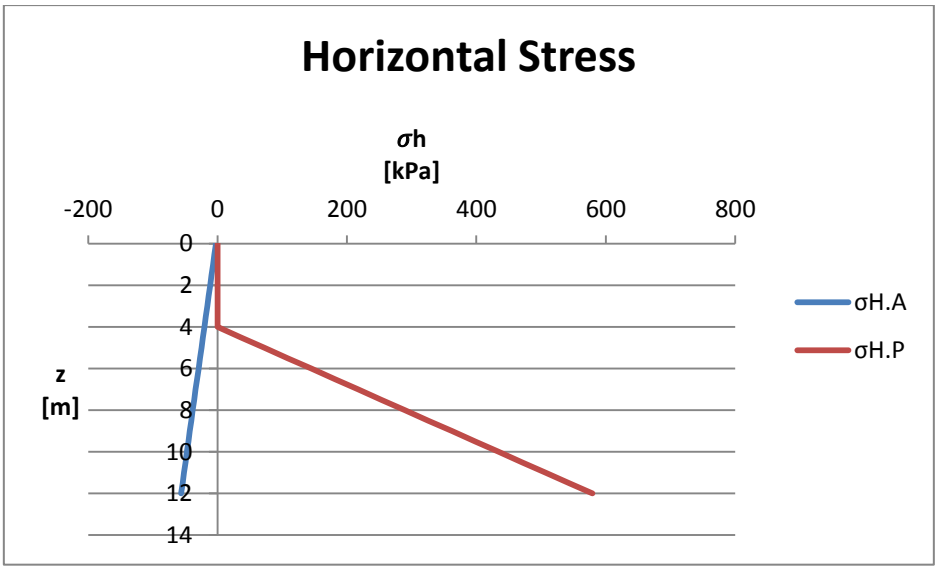

Figure 220: Horizontal stress along a sheet pile of 12 m in sand using the Classic Method

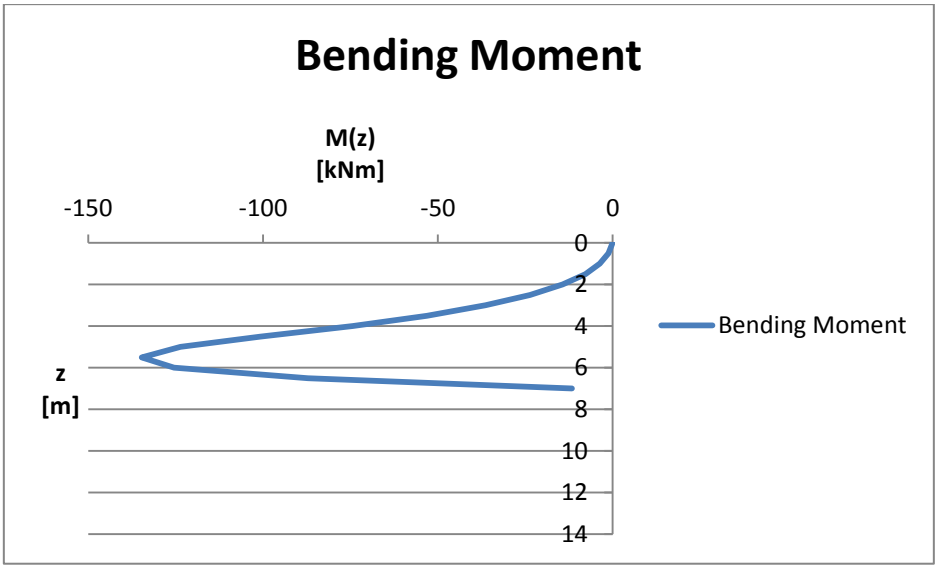

Figure 221: Bending moment of a sheet pile of 12 m in sand using the Classic Method

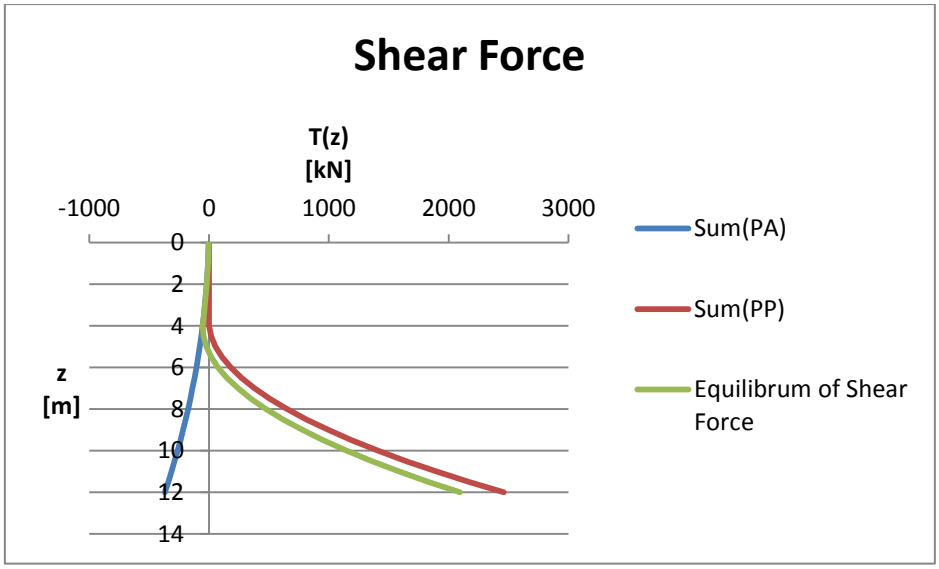

Figure 222: Shear force of a sheet pile of 12 m in sand using the Classic Method

2.5.8 SheetPile2.0 – Sand – 2nd case (12 m) results

The only parameter that has been changed from the 1st case is the length of the sheet pile "L", from L = 9 m into L = 12 m. The other parameters are the same as chapter 2.5.3. The results are exposed in the following graphics.

Table 18: Maximum and minimum values of the displacement in the sheet pile of 7.5 m and in the sheet pile of 12 m in sand using SheetPile2.0, absolute difference

DISPLACEMENT [m]			
MAXIMUM		MINIMUM	
SP2.0-7.5m	SP2.0-12m	SP2.0-7.5m	SP2.0-12m
0.08430	0.01820	-0.00728	0.00095
ABS DIFF	78%	ABS DIFF	113%

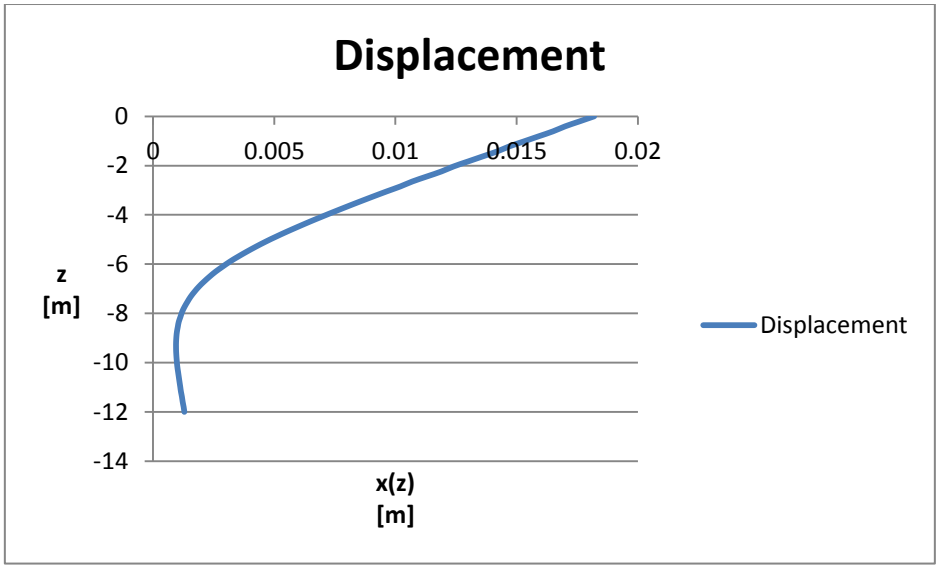

Figure 223: Displacement of a sheet pile of 12 m in sand using SheetPile2.0

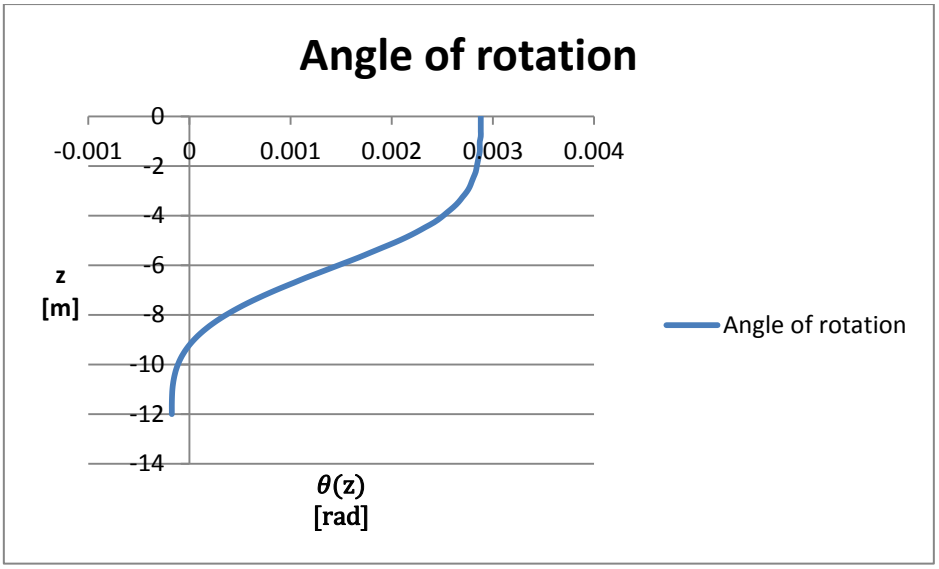

Figure 224: Angle of rotation of a sheet pile of 12 m in sand using SheetPile2.0

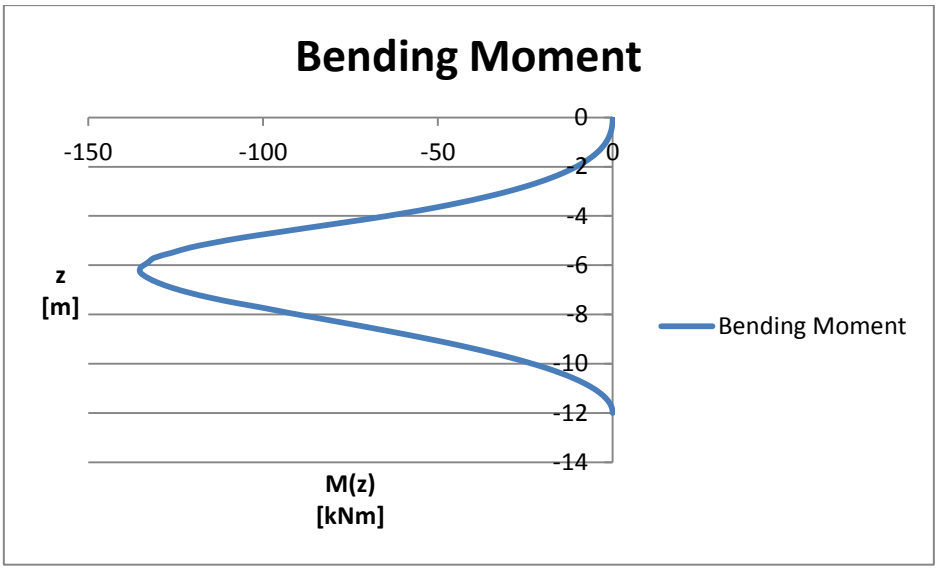

Figure 225: Bending moment of a sheet pile of 12 m in sand using SheetPile2.0

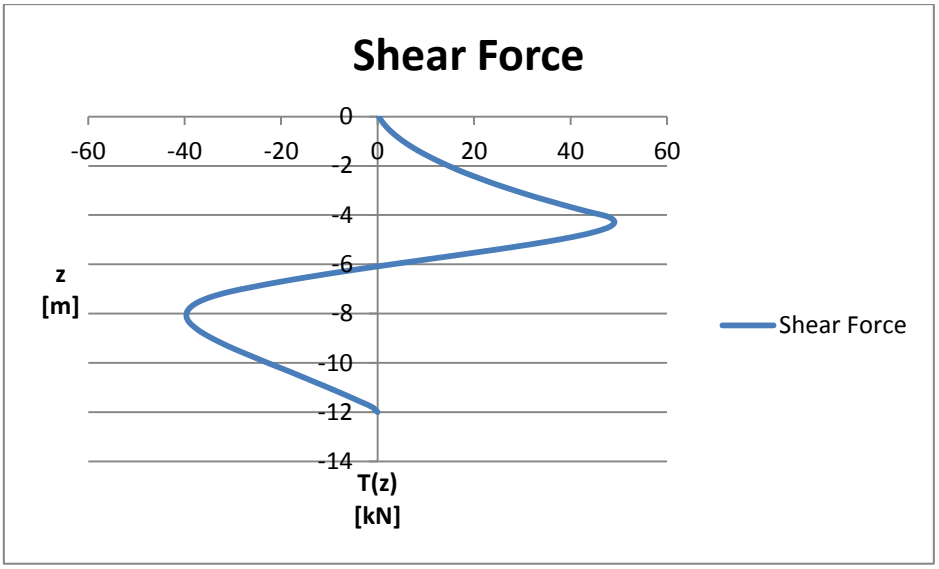

Figure 226: Shear force of a sheet pile of 12 m in sand using SheetPile2.0

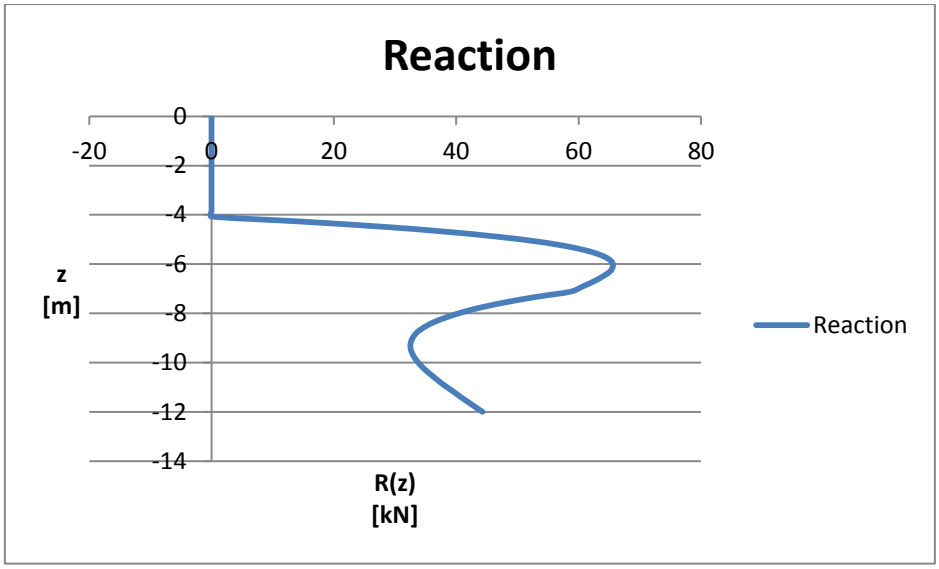

Figure 227: Reaction of a sheet pile of 12 m in sand using SheetPile2.0

2.5.9 Plaxis – Sand – 2nd case (12 m) results

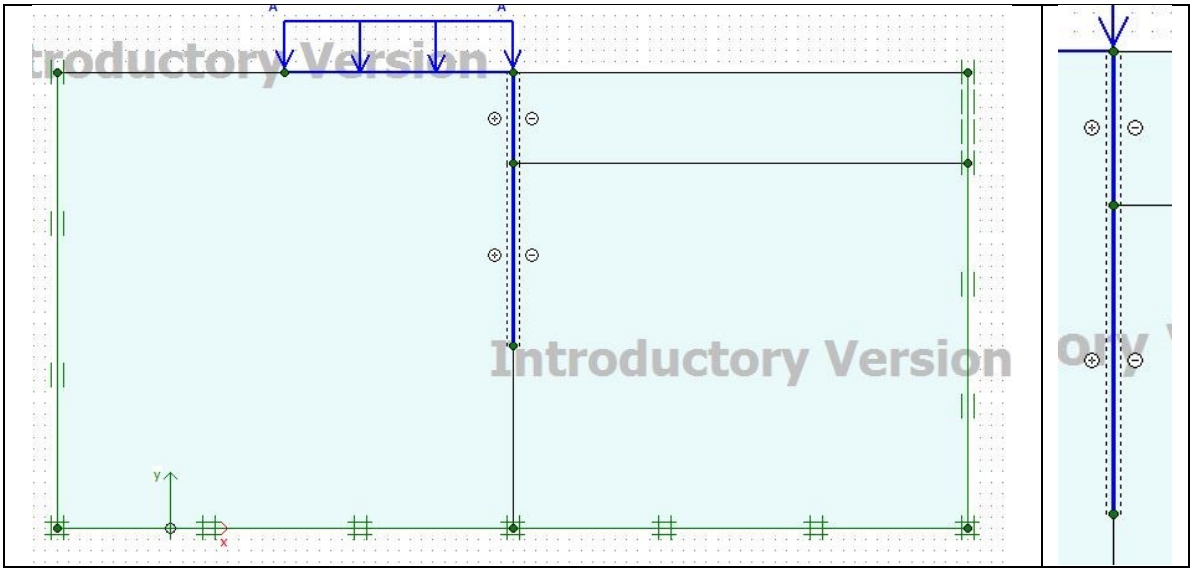

Figure 228: Model for the case of a sheet pile of 12 m in sand using Plaxis, particular of the interface

The only parameter that has been changed from the 1st case is the length of the sheet pile "L", from L = 9 m into L = 12 m. The other parameters are the same as chapter 2.5.4. The generated mesh (Figure 200) is a fine element distribution. The results are illustrated in the following screenshots.

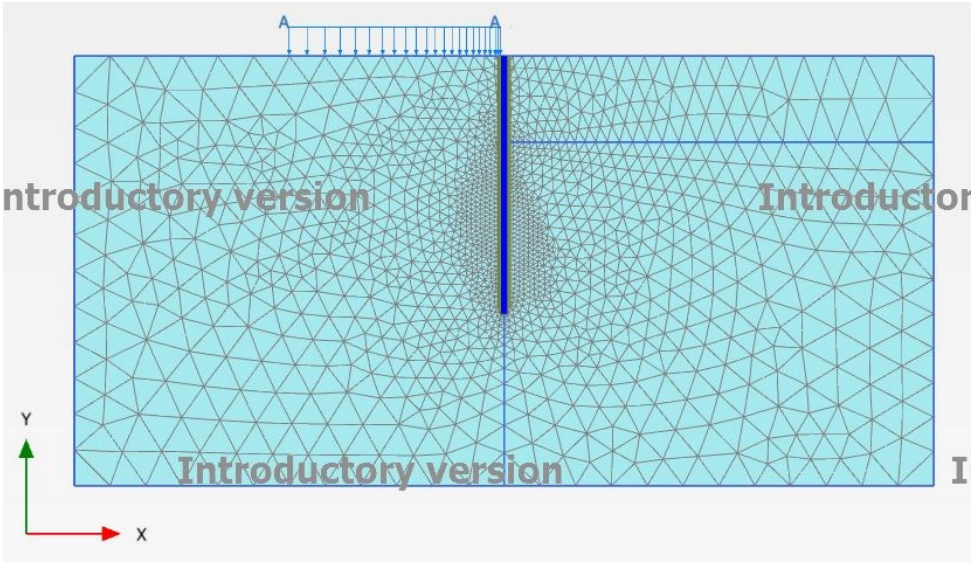

Figure 229: The mesh: "fine" with tri-6 elements

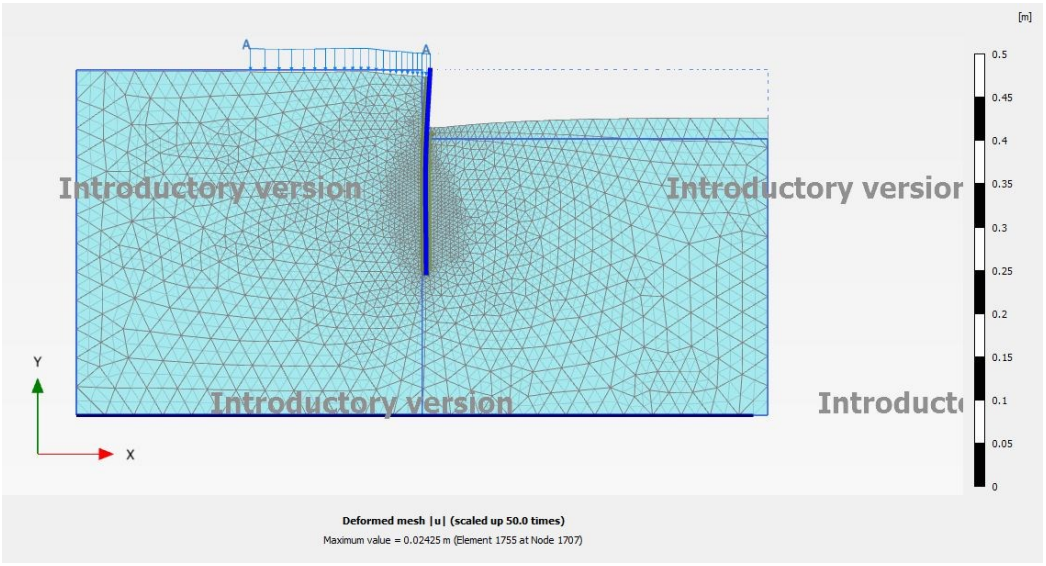

Figure 230: Deformed mesh for the case of a sheet pile of 12 m in sand using Plaxis

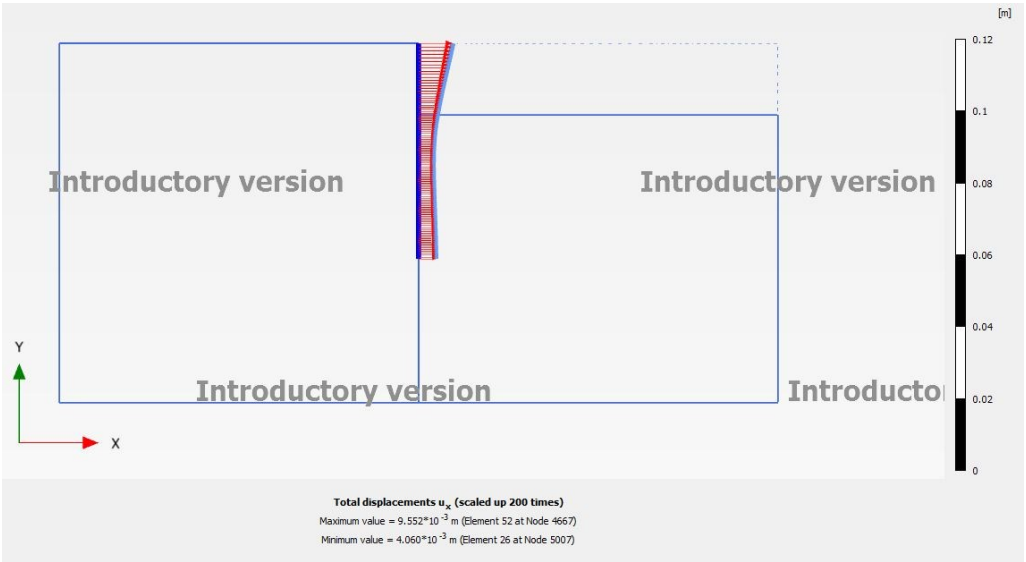

Figure 231: Displacement u_x of a sheet pile of 12 m in sand using Plaxis

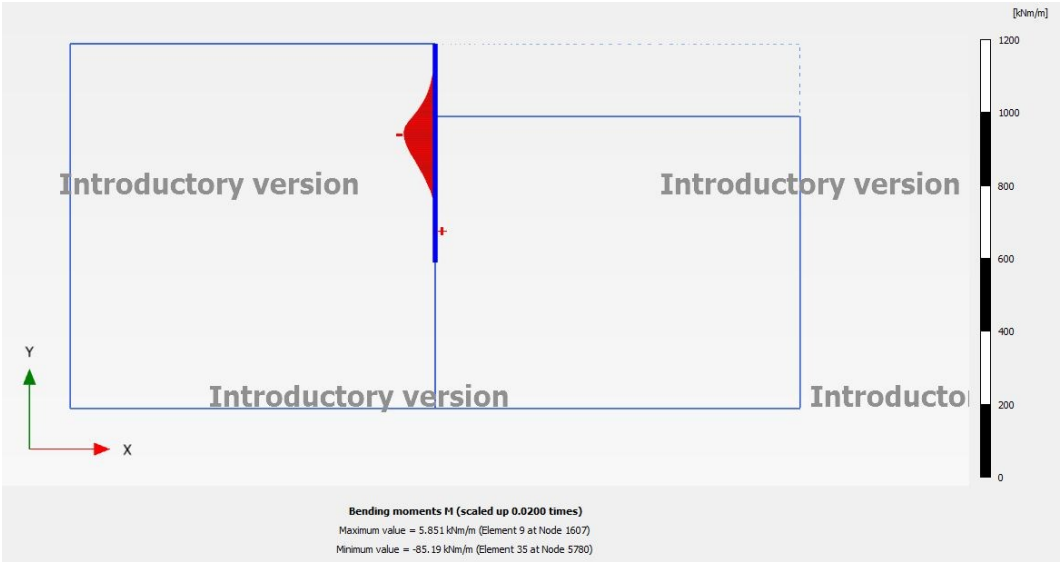

Figure 232: Bending moment of a sheet pile of 12 m in sand using Plaxis

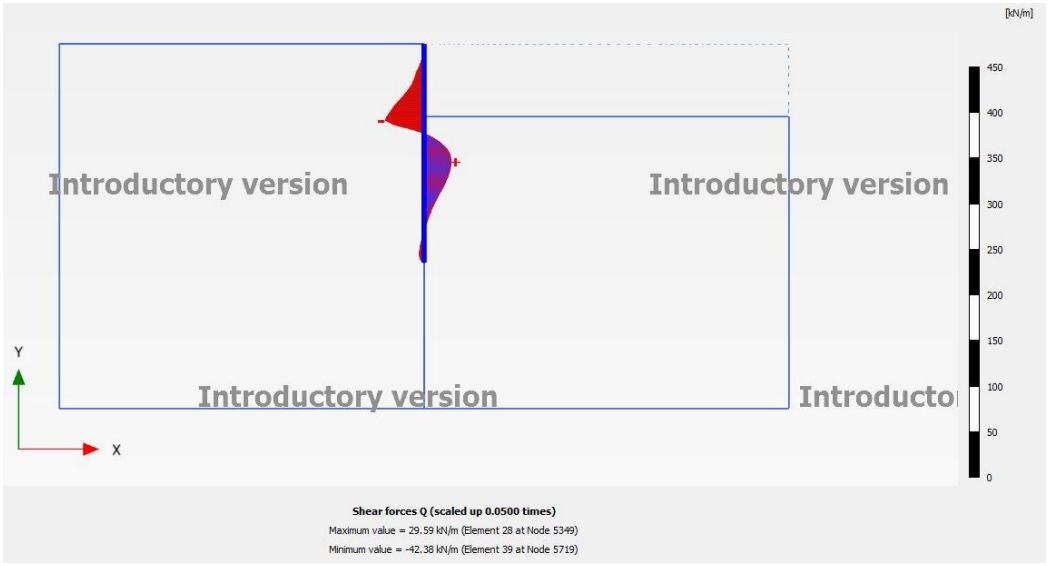

Figure 233: Shear force of a sheet pile of 12 m in sand using Plaxis

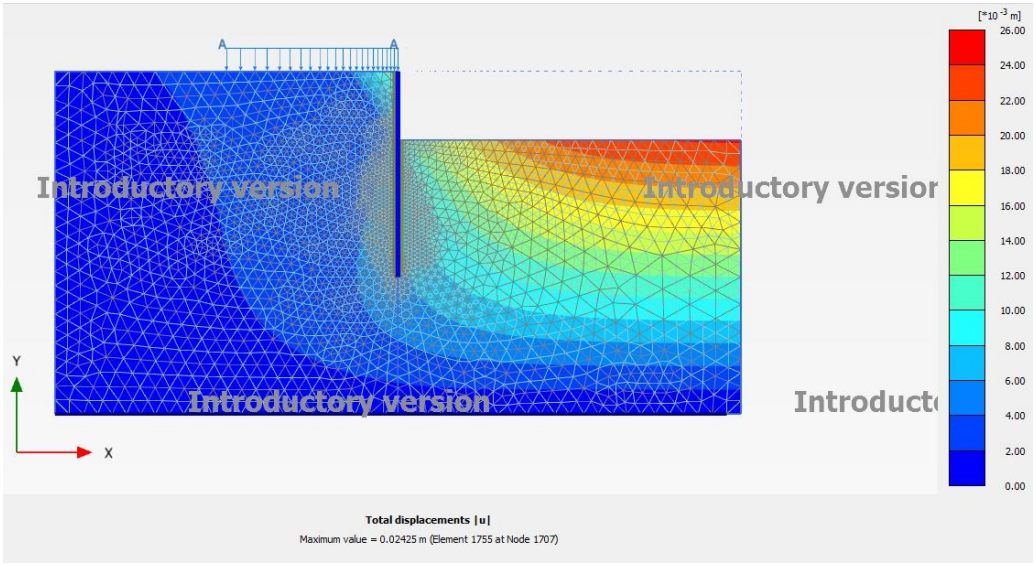

Figure 234: Total displacement u for the case of a sheet pile of 12 m in sand using Plaxis

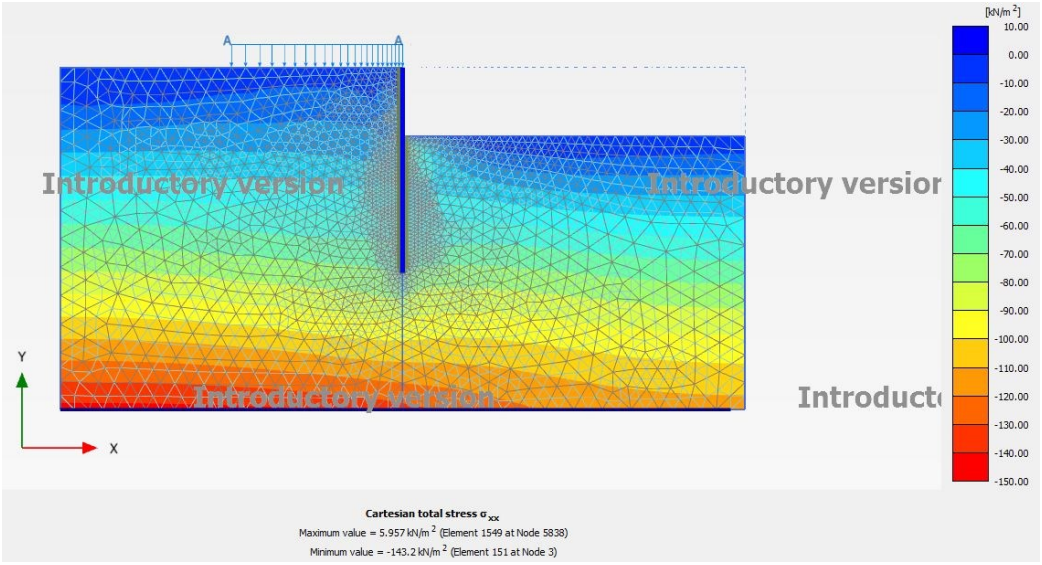

Figure 235: Total stress σ_{xx} for the case of a sheet pile of 12 m in sand using Plaxis

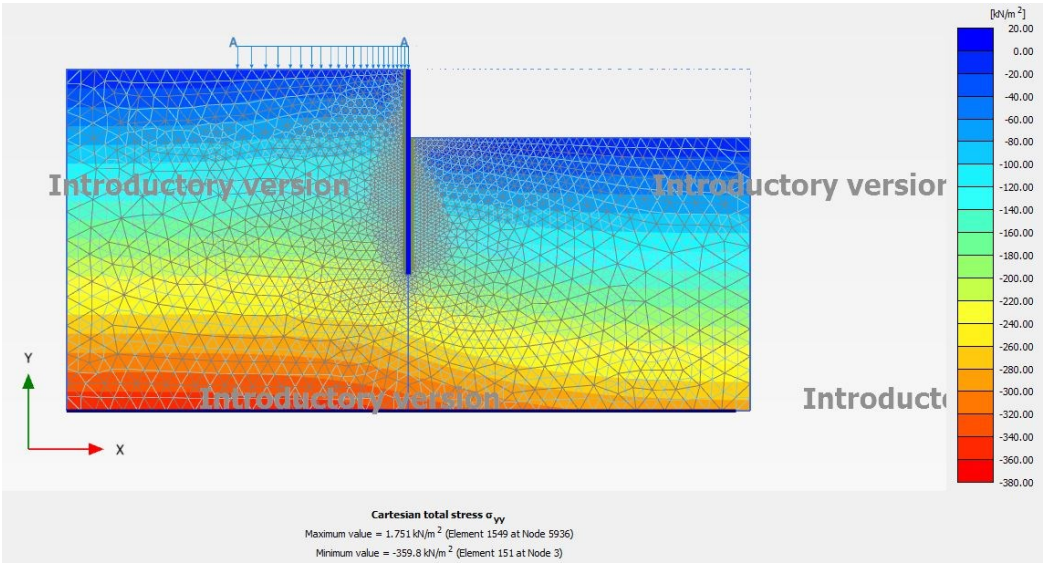

Figure 236: Total stress σ_{yy} for the case of a sheet pile of 12 m in sand using Plaxis

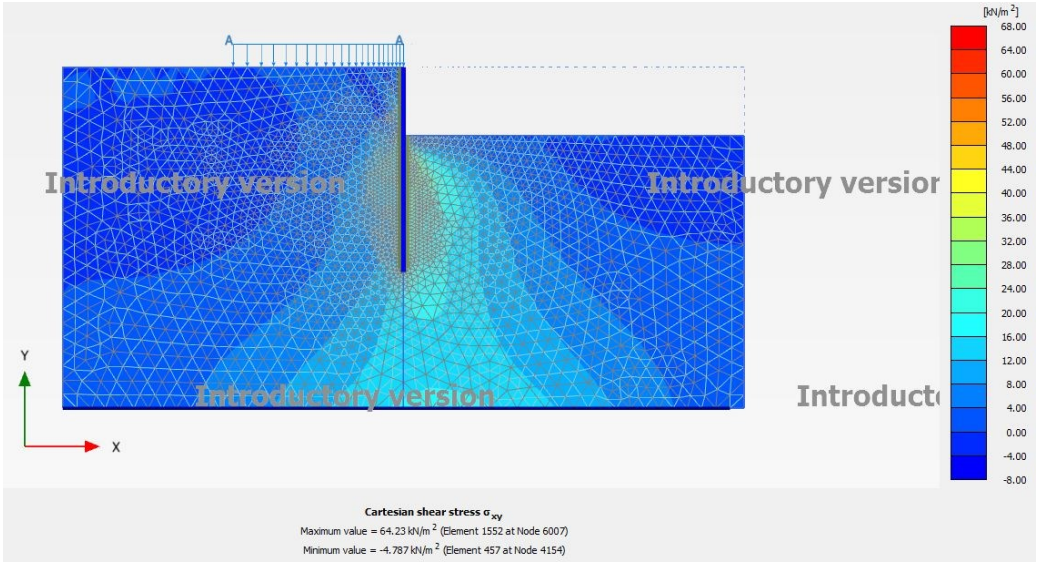

Figure 237: Total stress σ_{xy} for the case of a sheet pile of 12 m in sand using Plaxis

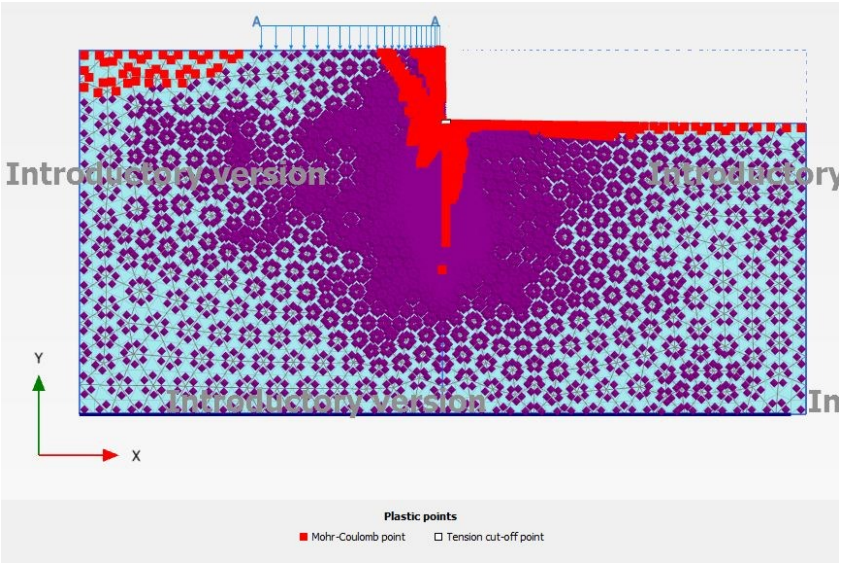

Figure 238: Plastic points for the case of a sheet pile of 9 m in sand using Plaxis

2.5.10 Plaxis No Interface – Sand – 2nd case (12 m) results

The only parameter that has been changed from previous chapter is the parameter Ri of the interface: it has been changed from Ri = 0.8 into Ri = 1 ("rigid"), this new condition simulates the lack of the interface between soil and structure. The other parameters are the same as chapter 2.5.9. The solutions with coarse and fine mesh are quite the same, whereas the model with fine mesh but with no interface differs from the previous solutions and provides lower displacement (Figure 241).

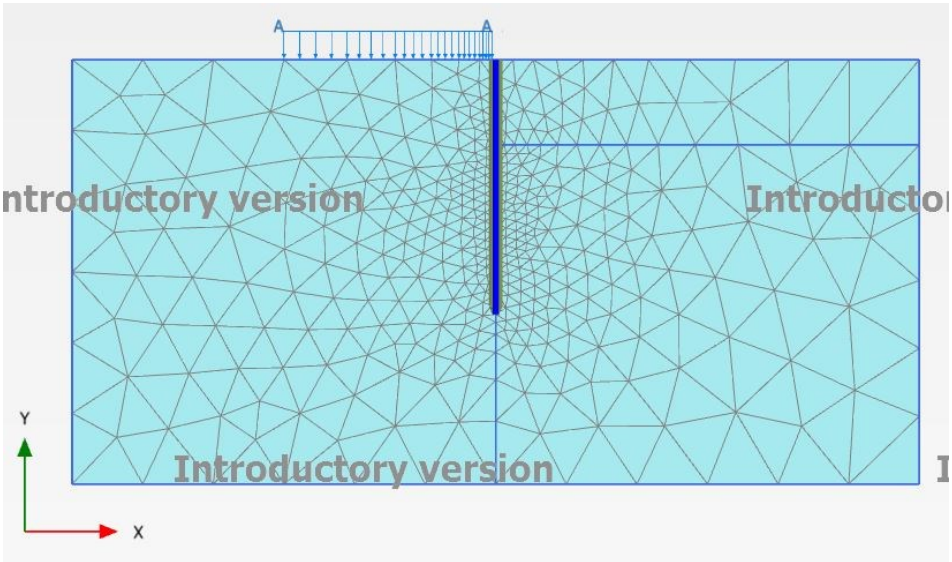

Figure 239: The mesh: "coarse" with tri-15 elements used at the beginning for the choice of the sheet pile's length

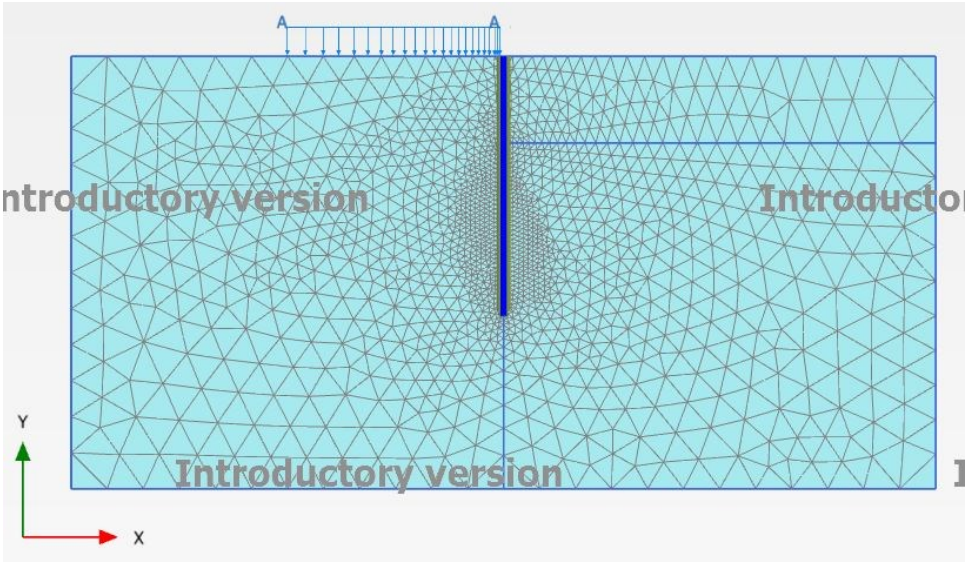

Figure 240: The mesh: "fine" with tri-6 elements with no interface (Ri=1)

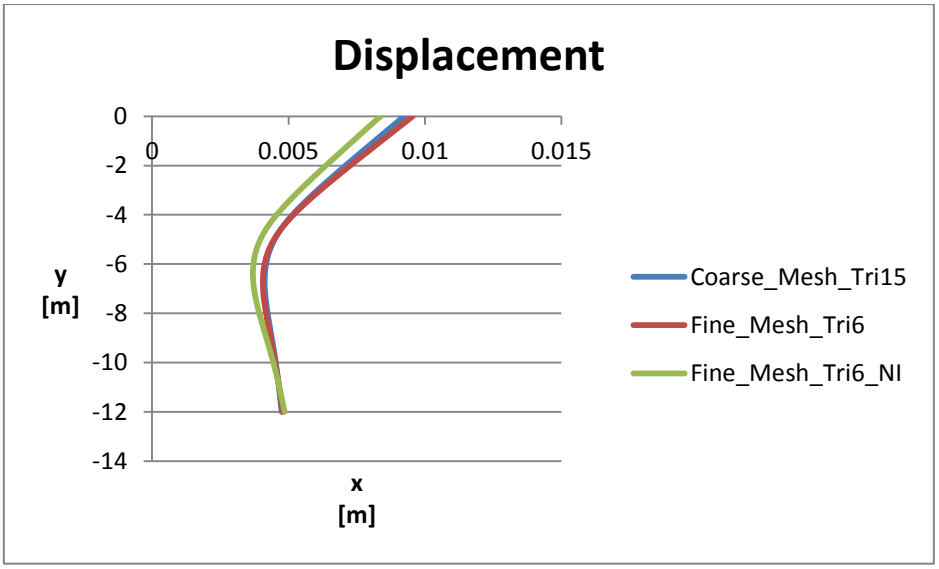

Figure 241: Displacement of a sheet pile of 12 m in sand using Plaxis with: coarse mesh and tri-15 elements, fine mesh and tri-6 elements, fine mesh and tri-6 elements with no interface

Table 19: Maximum and minimum values of the displacement in the sheet pile of 12 m in sand using Plaxis with: coarse mesh and tri-15 elements, fine mesh and tri-6 elements, fine mesh and tri-6 elements with no interface, absolute difference

DISPLACEMENT [m]					
MAXIMUM			MINIMUM		
COARSE	FINE	NI	COARSE	FINE	NI
0.00923	0.00955	0.00837	0.00413	0.00406	0.00370
ABS_DIFF	-3%	9%	ABS_DIFF	1%	10%

2.5.11 Sand – 2st case (12 m) comparison

As for the 1st case the values obtained with SheetPile2.0 and with the Classic Method can be considered useful to estimate the order of magnitude of the solution whereas

the FEM solutions can be chosen as more coherent with the real behavior of the soil-structure system. The difference between Plaxis and SheetPile2.0 decreases by 20% (Table 17, Table 20) by increasing the length of the sheet pile.

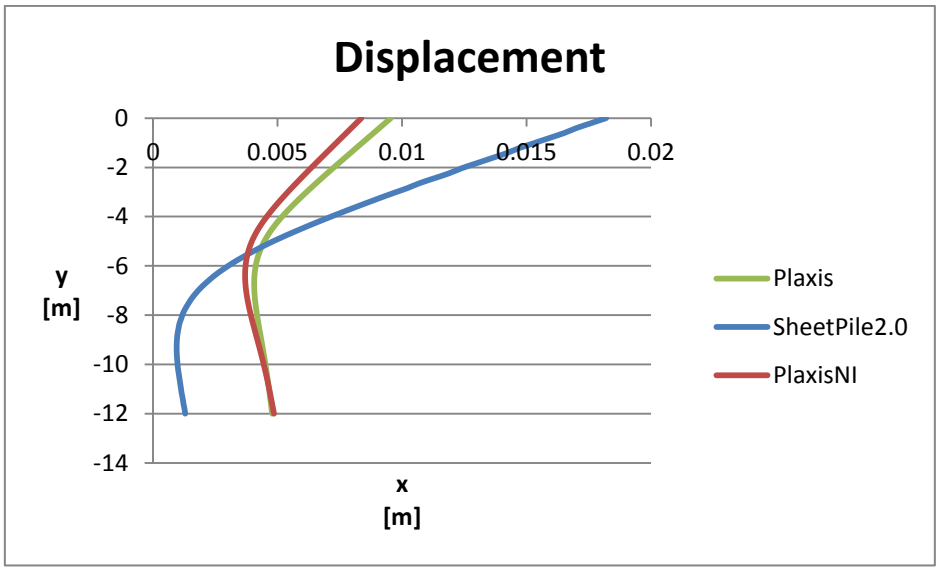

Figure 242: Displacement of a sheet pile of 12 m in sand using Plaxis, SheetPile2.0, Plaxis with no interface

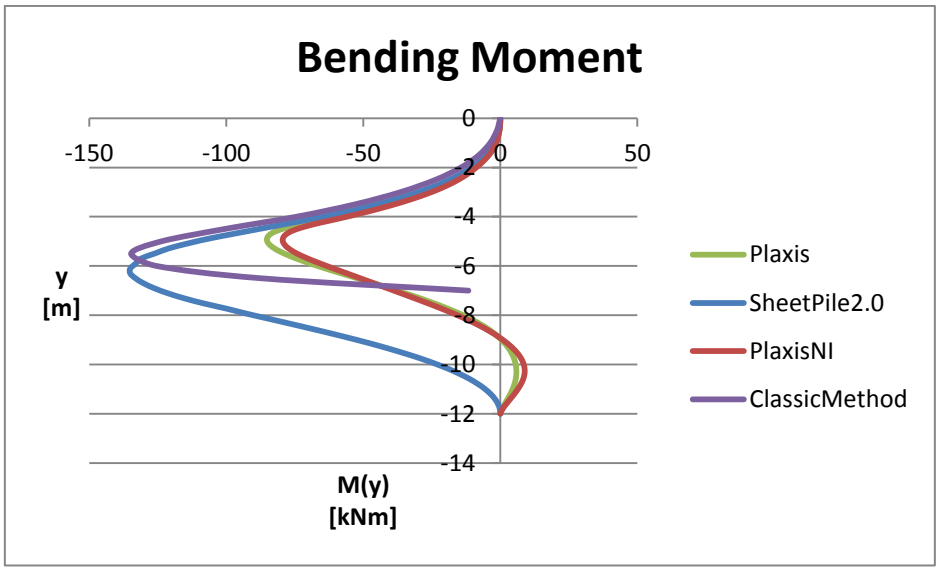

Figure 243: Bending moment of a sheet pile of 9 m in sand using Plaxis, SheetPile2.0, Plaxis with no interface, the Classic Method

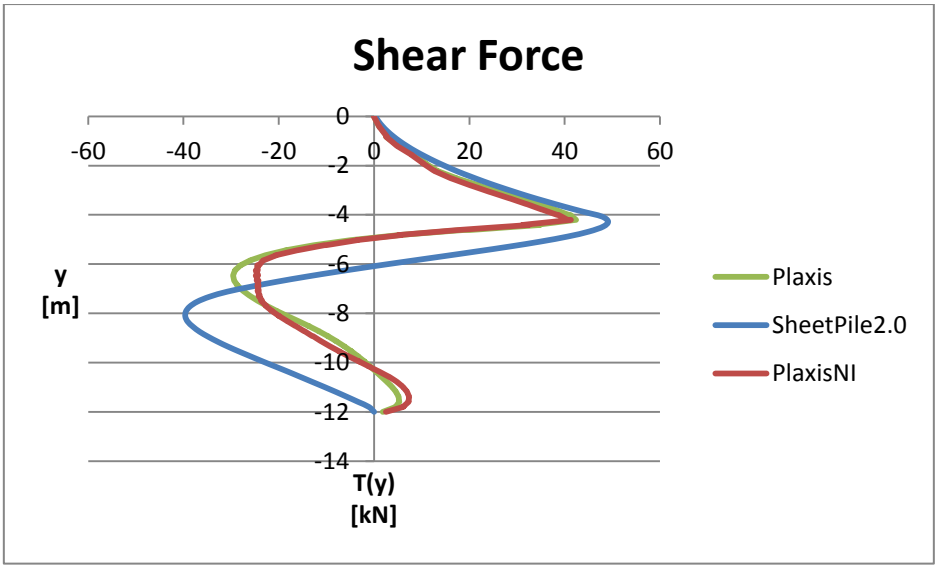

Figure 244: Shear force of a sheet pile of 9 m in sand using Plaxis, SheetPile2.0, Plaxis with no interface

Table 20: Maximum and minimum values of the displacement, bending moment, shear force in the sheet pile of 9 m in sand using Plaxis, SheetPile2.0, Plaxis with no interface and the Classic method, absolute difference

DISPLACEMENT [m]							
MAXIMUM				MINIMUM			
Plaxis	SP2.0	PlaxisNI	CM	Plaxis	SP2.0	PlaxisNI	CM
0.009552	0.018183	0.008368	-	0.00406	0.000946	0.003696	-
ABS_DIFF	-90%	12%	-	ABS_DIFF	77%	9%	-
BENDING MOMENT [kNm]							
MAXIMUM				MINIMUM			
Plaxis	SP2.0	PlaxisNI	CM	Plaxis	SP2.0	PlaxisNI	CM
5.851003	0	8.898036	0	-85.1901	-134.674	-79.4205	-134.696
ABS_DIFF	-	-52%	-	ABS_DIFF	-58%	7%	-58%
SHEAR FORCE [kN]							
MAXIMUM				MINIMUM			
Plaxis	SP2.0	PlaxisNI	CM	Plaxis	SP2.0	PlaxisNI	CM
42.37765	49.13711	41.29931	-	-29.5903	-39.6012	-24.8323	-
ABS_DIFF	-16%	3%	-	ABS_DIFF	-34%	16%	-

2.6 Overview of the results – Clay

2.6.1 Introduction: searching for the length to compare

As for the sheet pile embedded in the granular soil, also for the case of cohesive soil it is necessary to find the suitable length that could be compared in each solution. The "Classic Method" gives a solution already with 8.5 m, but as said before, because of its simplicity, this method is just considered a comparison solution. The minimum

value for Sheetpile2.0 is 10 m, but the displacement is 33.4 cm. The minimum value for Plaxis is 8.5 m, but the displacement is 37.870 cm (peak value). Plaxis provides an acceptable solution (6.811 cm) with a 12 m length sheet pile (by an increment of 1 m length the displacement decreases by 2%), but a stable solution is reached with 14 m (06.572 cm). Using a 15 m length sheet pile the performance worsens. As for the solution in the sandy soil two different "comparison lengths" for the sheet pile has been chosen: the first one is close to instability (10 m), the second one widely ensures the equilibrium (14 m). The other solution (for both 10 m and 14 m) has been made by using Plaxis but in this case the mesh has been set "fine" (around 600 elements and I_e = 2 m) keeping a 6-nodes triangle element, the value of R_i has been changed from R_i = 0.8 into R_i = 1 ("rigid"): this situation simulates the lack of the interface (only soil and plate).

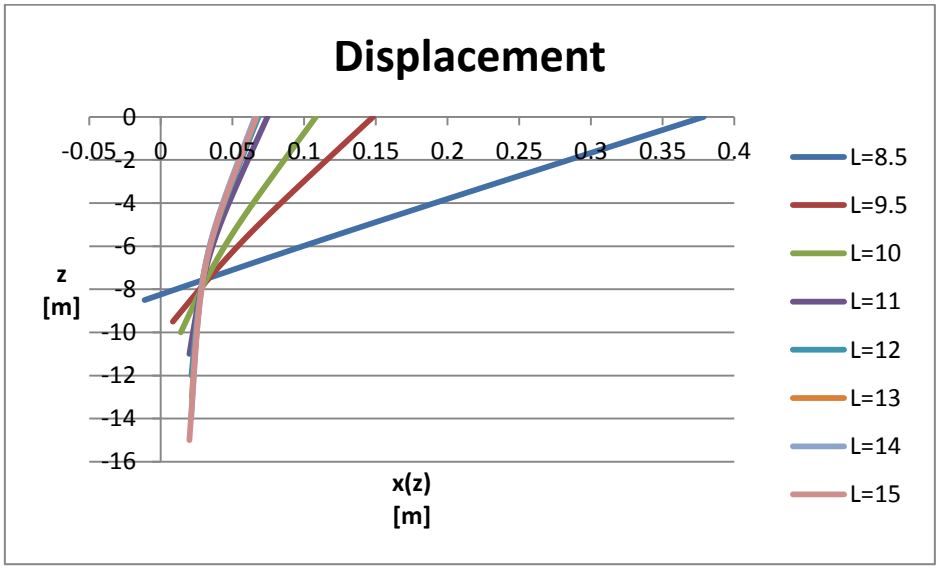

Figure 245: Horizontal displacement of the sheet pile varying its length

Table 21: Maximum and minimum values of the displacement of the sheet pile varying its length, absolute and relative difference of displacement between sheet piles with different lengths

DISPLACEMENT [m]							
MAXIMUM							
L = 8.5	L = 9.5	L = 10	L = 11	L = 12	L = 13	L = 14	L = 15
0.37870	0.14802	0.10823	0.07439	0.06811	0.06670	0.06572	0.06675
ABS_DIFF	61%	71%	80%	82%	82%	83%	82%
REL_DIFF	61%	27%	31%	8%	2%	1%	-2%
MINIMUM							
L = 8.5	L = 9.5	L = 10	L = 11	L = 12	L = 13	L = 14	L = 15
-0.01131	0.00840	0.01394	0.01995	0.02136	0.02164	0.02120	0.01995
ABS_DIFF	174%	223%	276%	289%	291%	287%	276%
REL_DIFF	174%	-66%	-43%	-7%	-1%	2%	6%

2.6.2 Classic Method – Clay - 1st case (10 m) results

Table 22: Parameters required in the Classic Method

CLAY						SP
H	γ	ϕ	c	q	dex	L
[m]	[kN/m^3]	[°]	[kPa]	[kN/m]	[m]	[m]
20	20	25	0	10	4	10

Where H is thickness of the layer, γ the self-weight of sand, φ the angle of friction of sand, c the cohesion of sand, q is the load, dex the excavation, L the final length that is required for equilibrium. The results are exposed in the following graphics. As the minimum required length to have equilibrium is 8.5 m, the trend of the bending moment is taken into account only within this length and not for the remaining part of the sheet pile (Figure 248).

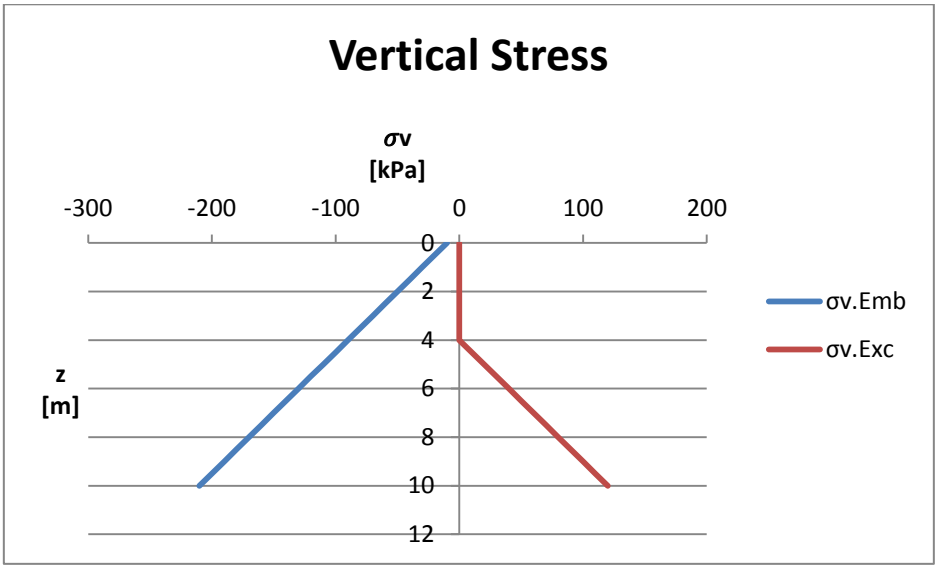

Figure 246: Vertical stress along a sheet pile of 10 m in clay using the Classic Method

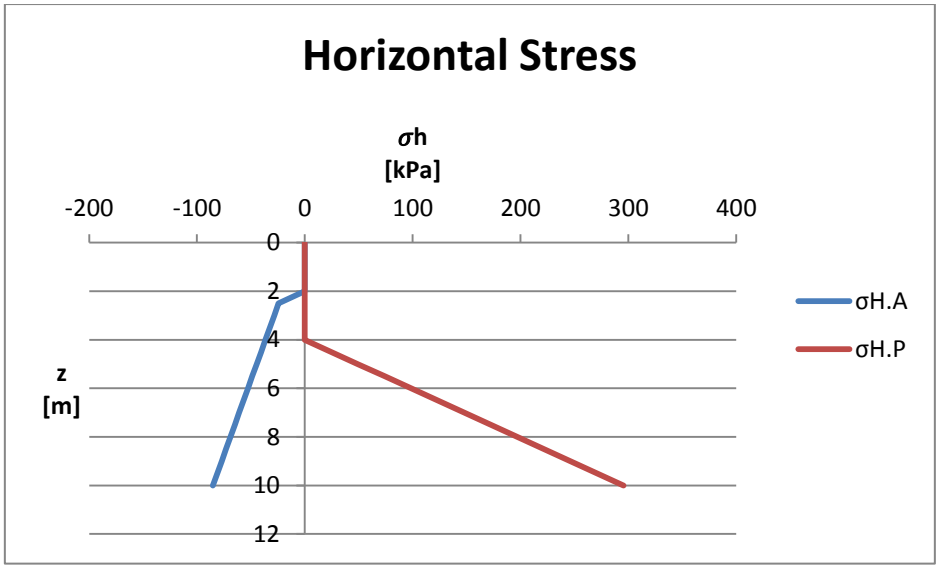

Figure 247: Horizontal stress along a sheet pile of 10 m in clay using the Classic Method

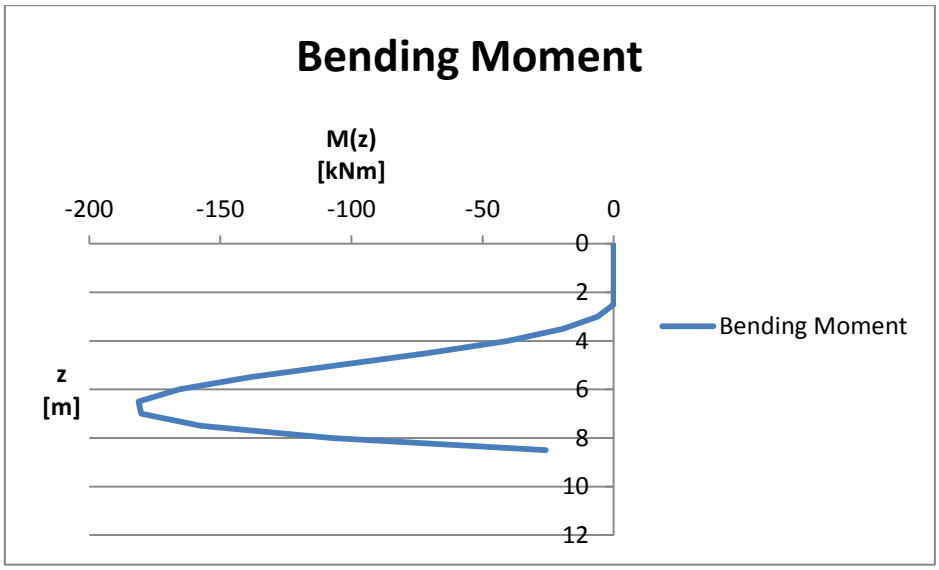

Figure 248: Bending moment of a sheet pile of 10 m in clay using the Classic Method

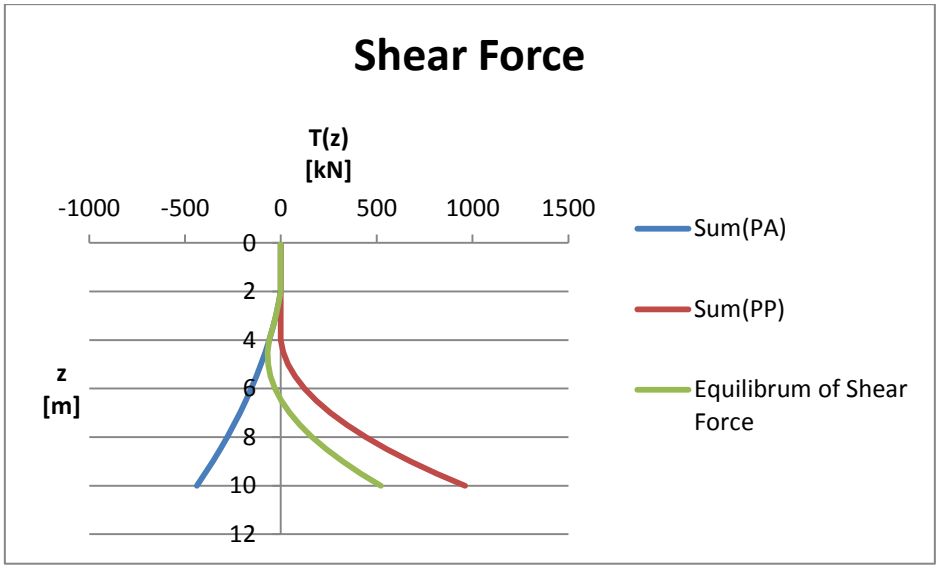

Figure 249: Shear force of a sheet pile of 10 m in clay using the Classic Method

2.6.3 SheetPile2.0 – Clay - 1st case (10 m) results

Table 23: Parameters required in SheetPile2.0

CLAY							SHEET PILE		
H	γ	ϕ	c	q	dex	dwl	t	Ep	L
[m]	[kN/m^3]	[°]	[kPa]	[kN/m]	[m]	[m]	[m]	[kPa]	[m]
20	20	25	0	10	4	0	0.5	20x10^6	10

Where H is thickness of the layer, γ the self-weight of sand, φ the angle of friction of sand, c the cohesion of sand, q is the load, dex the excavation, dwl the depth of the groundwater level, t , Ep and L are the thickness, the elastic modulus and the length of the sheet pile respectively. The results are exposed in the following graphics.

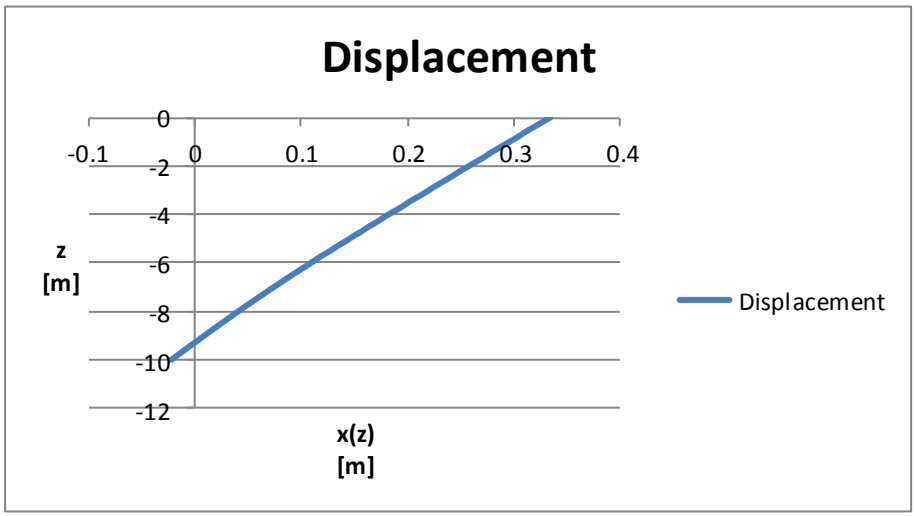

Figure 250: Displacement of a sheet pile of 10 m in clay using SheetPile2.0

Table 24: Maximum and minimum values of the displacement in the sheet pile of 10 m in clay using SheetPile2.0

DISPLACEMENT [m]	
MAXIMUM	MINIMUM
SP2.0-10m	SP2.0-10m
0.33400	-0.02200

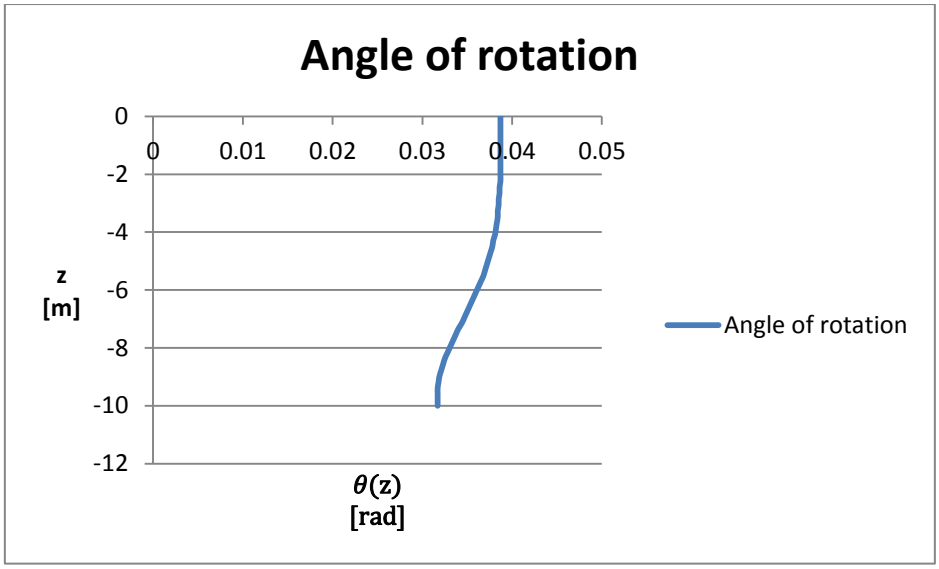

Figure 251: Angle of rotation of a sheet pile of 10 m in clay using SheetPile2.0

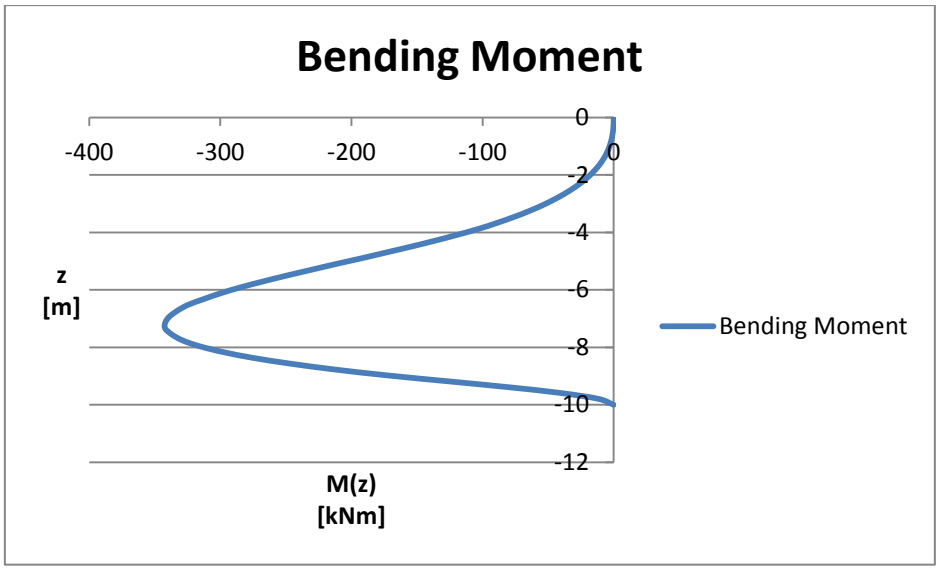

Figure 252: Bending moment of a sheet pile of 10 m in clay using SheetPile2.0

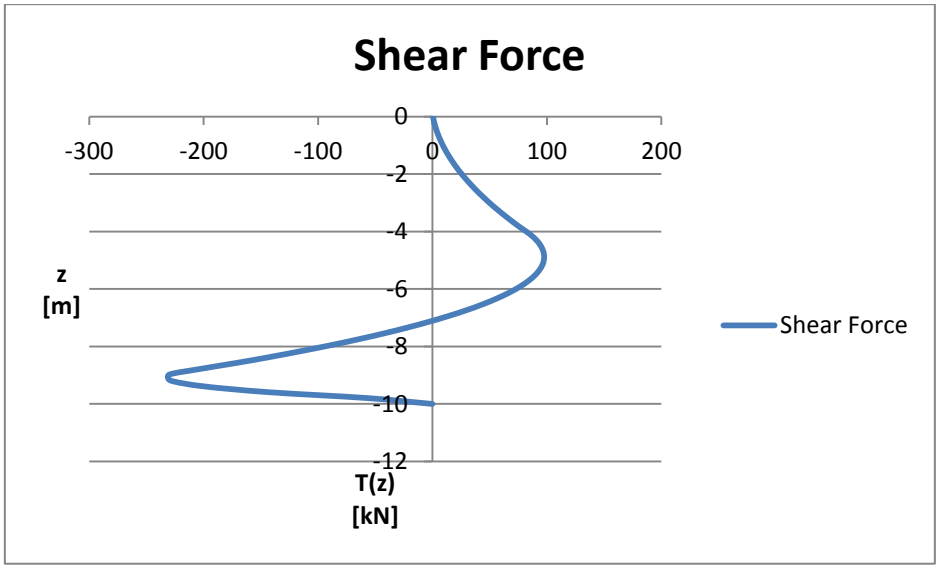

Figure 253: Shear force of a sheet pile of 10 m in clay using SheetPile2.0

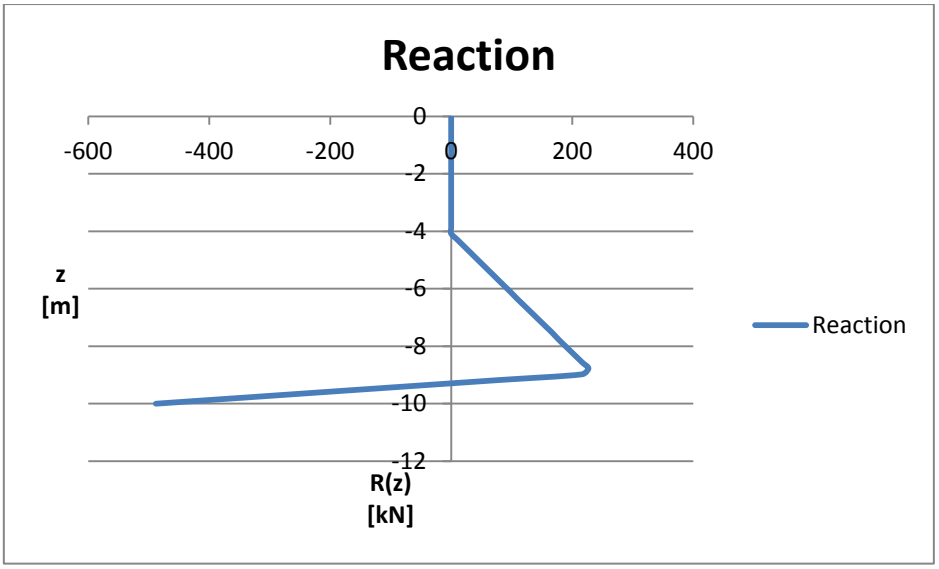

Figure 254: Reaction of a sheet pile of 10 m in clay using SheetPile2.0

2.6.4 Plaxis – Clay - 1st case (10 m) results

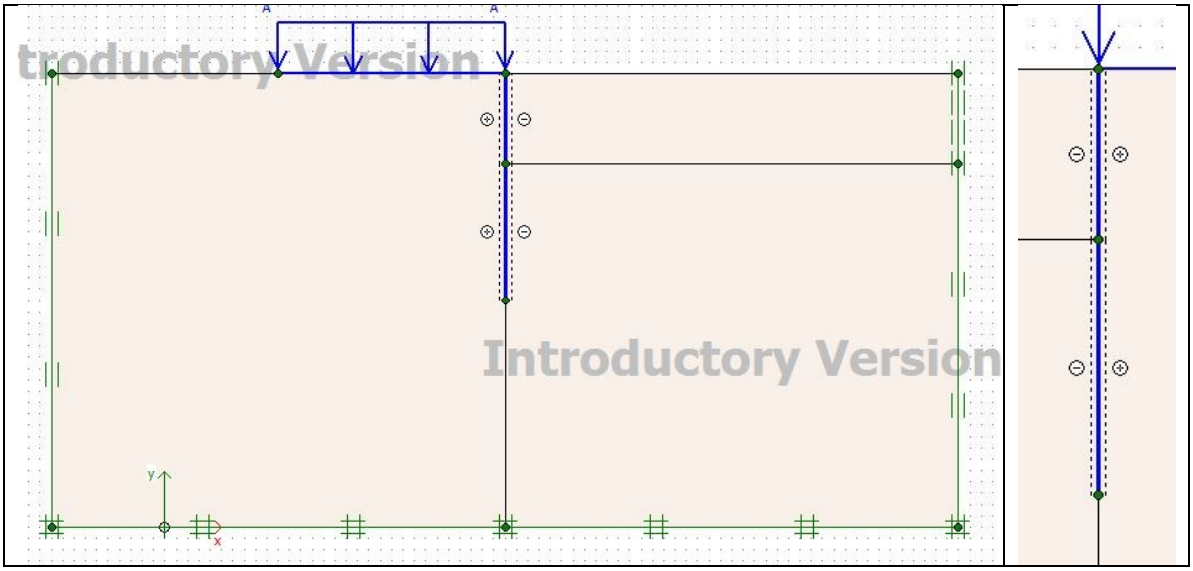

Figure 255: Model for the case of a sheet pile of 10 m in clay using Plaxis, particular of the interface

The generated mesh (Figure 256) is a fine element distribution.

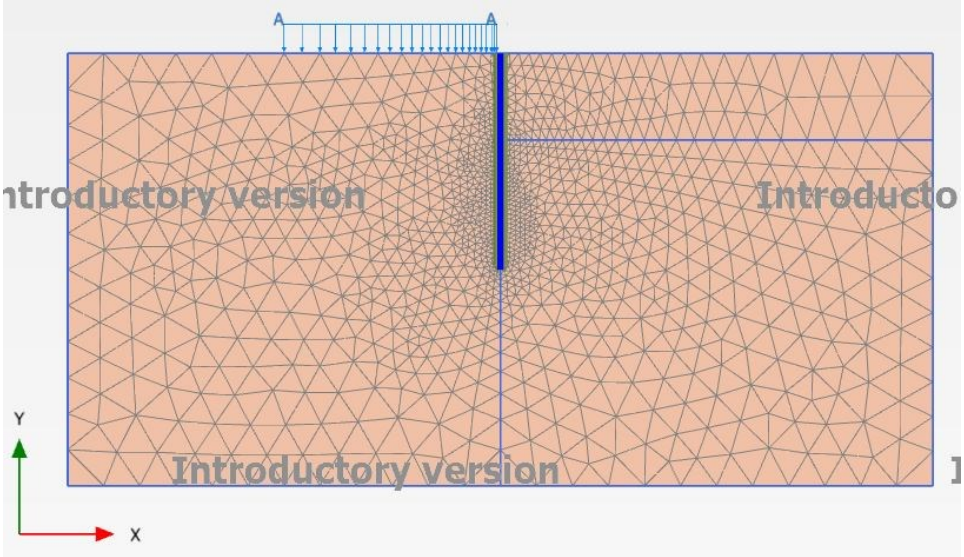

Figure 256: The mesh: "fine" with tri-6 elements

These are the main characteristics of the model. The results are illustrated in the following screenshots.

Table 25: Parameters required in Plaxis

CLAY								
H	γ	ϕ	c	ν	ψ	Es	q	dex
[m]	[kN/m^3]	[°]	[kPa]	[-]	[°]	[kPa]	[kN/m]	[m]
20	20	25	0	0.3	0	8x10^3	10	4

SHEET PILE					IF
L	w	EA	EJ	ν	Ri
[m]	[kN/m/m]	[kN/m]	[kNm^2]	[-]	[-]
10	12.5	10x10^6	208333.3	0.3	0.8

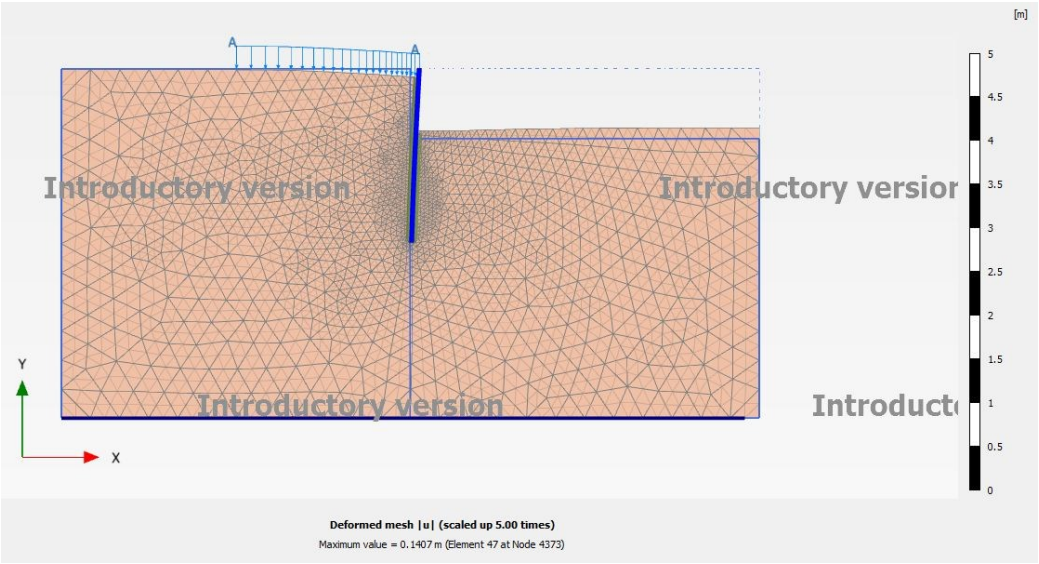

Figure 257: Deformed mesh for the case of a sheet pile of 10 m in clay using Plaxis

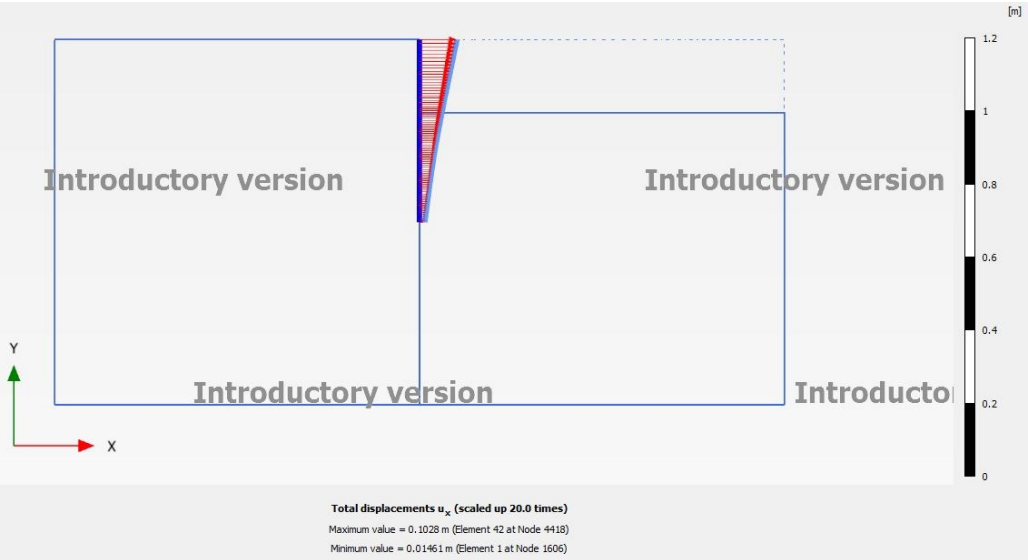

Figure 258: Displacement u_x of a sheet pile of 10 m in clay using Plaxis

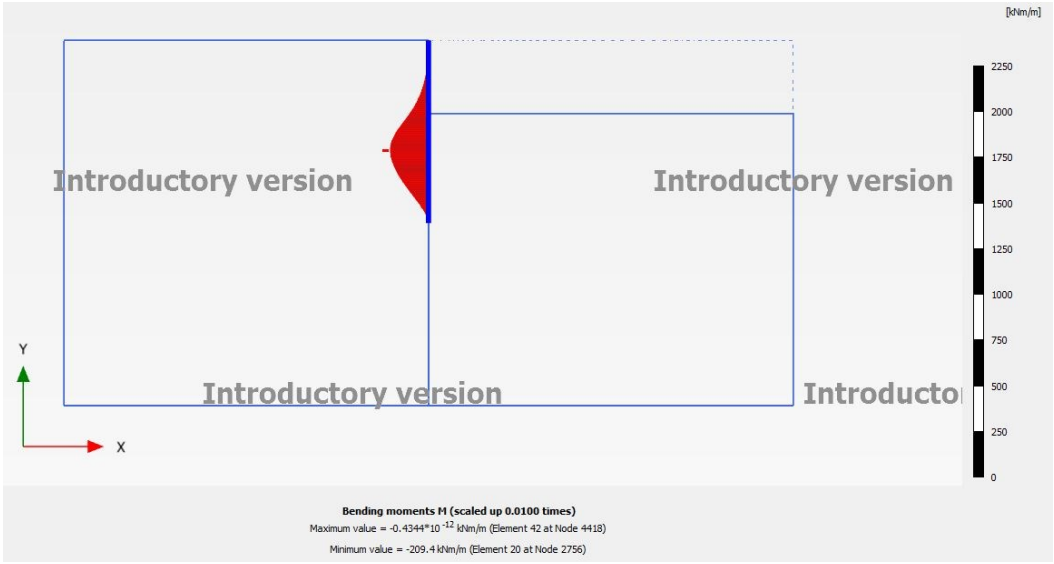

Figure 259: Bending moment of a sheet pile of 10 m in clay using Plaxis

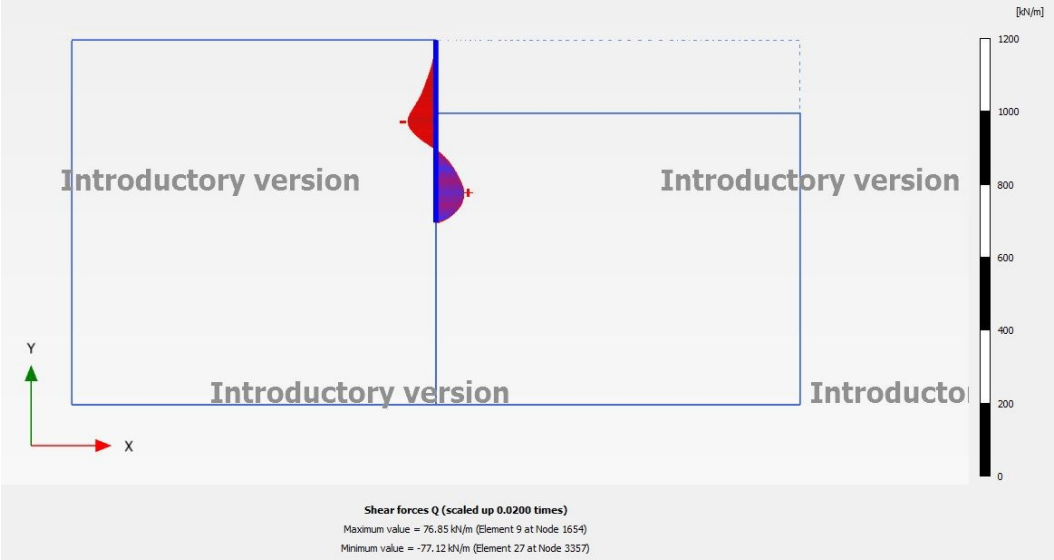

Figure 260: Shear force of a sheet pile of 10 m in clay using Plaxis

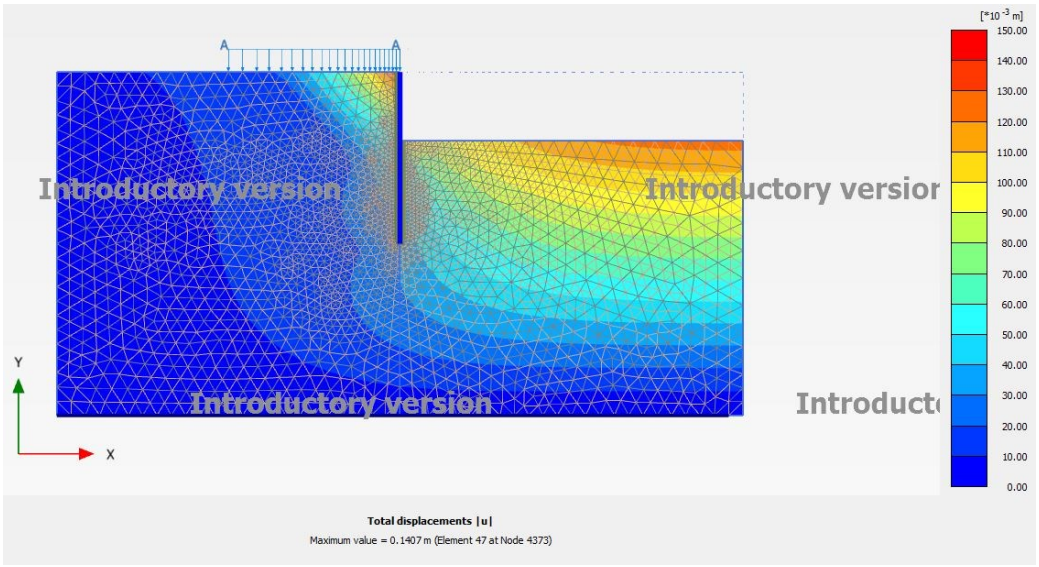

Figure 261: Total displacement u for the case of a sheet pile of 10 m in clay using Plaxis

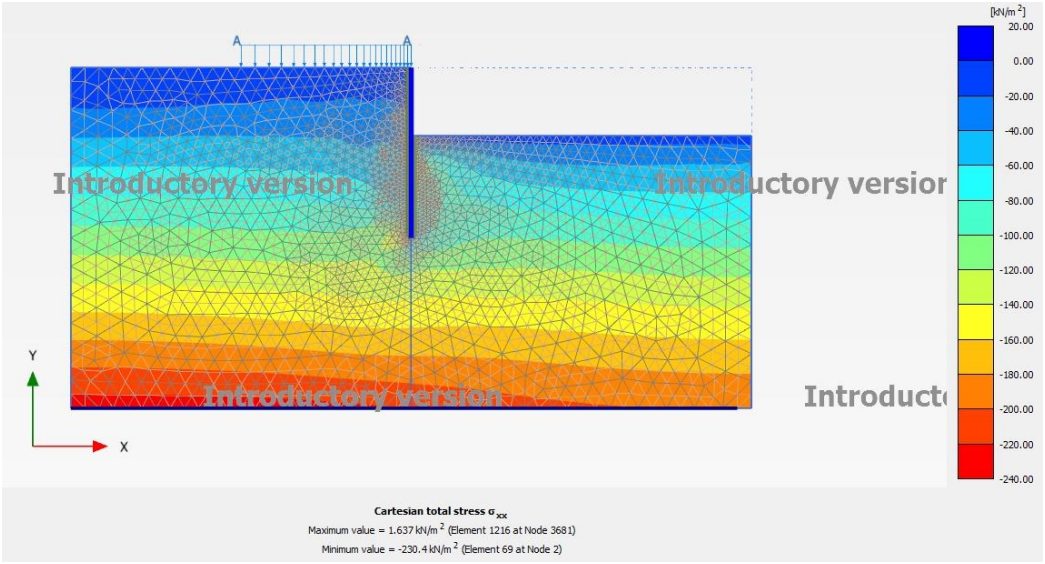

Figure 262: Total stress σ_{xx} for the case of a sheet pile of 10 m in clay using Plaxis

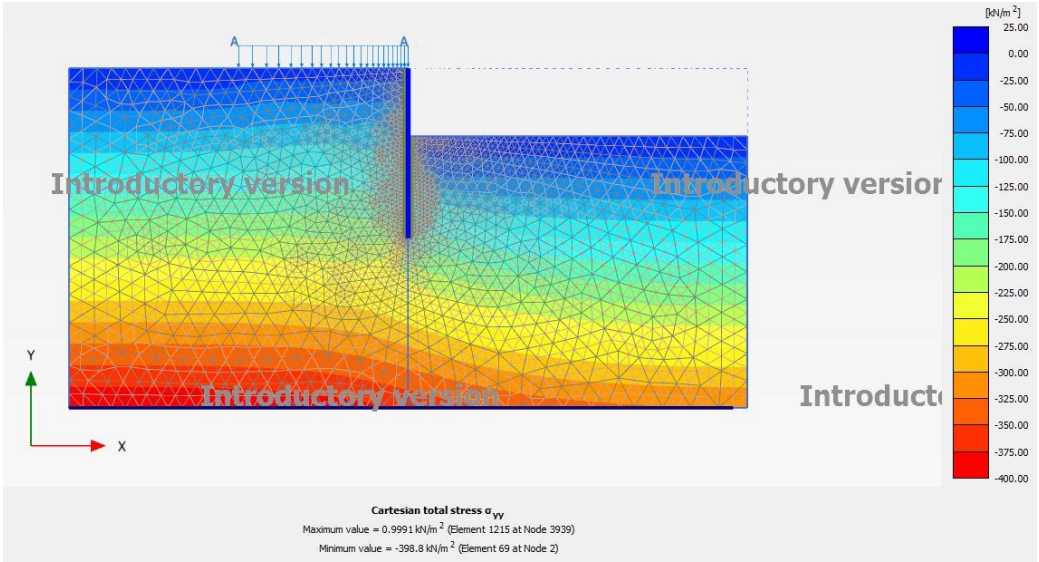

Figure 263: Total stress σ_{yy} for the case of a sheet pile of 10 m in clay using Plaxis

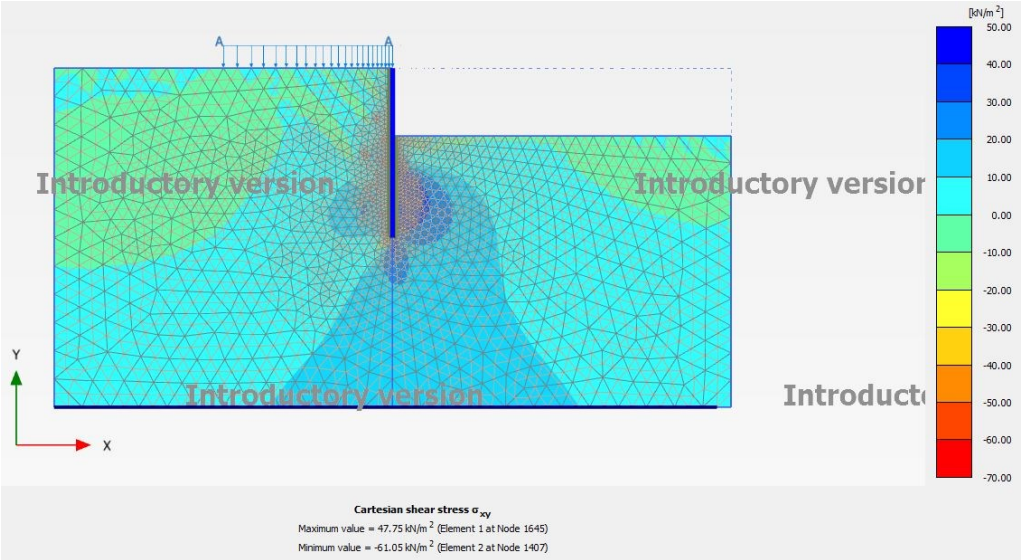

Figure 264: Total stress σ_{xy} for the case of a sheet pile of 10 m in clay using Plaxis

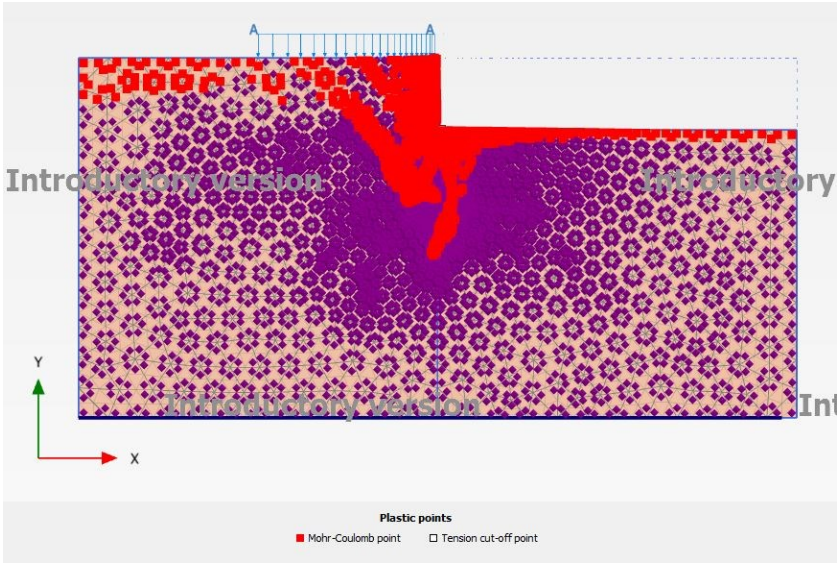

Figure 265: Plastic points for the case of a sheet pile of 10 m in clay using Plaxis

2.6.5 Plaxis No Interface – Clay - 1st case (10 m) results

The only parameter that has been changed from previous chapter is the parameter Ri of the interface: it has been changed from Ri = 0.8 into Ri = 1 ("rigid"), this new condition simulates the lack of the interface between soil and structure. The other parameters are the same as chapter 2.6.4. The solutions with coarse and fine mesh are quite the same, whereas the model with fine mesh but with no interface differs from the previous solutions and provides lower displacement (Figure 241).

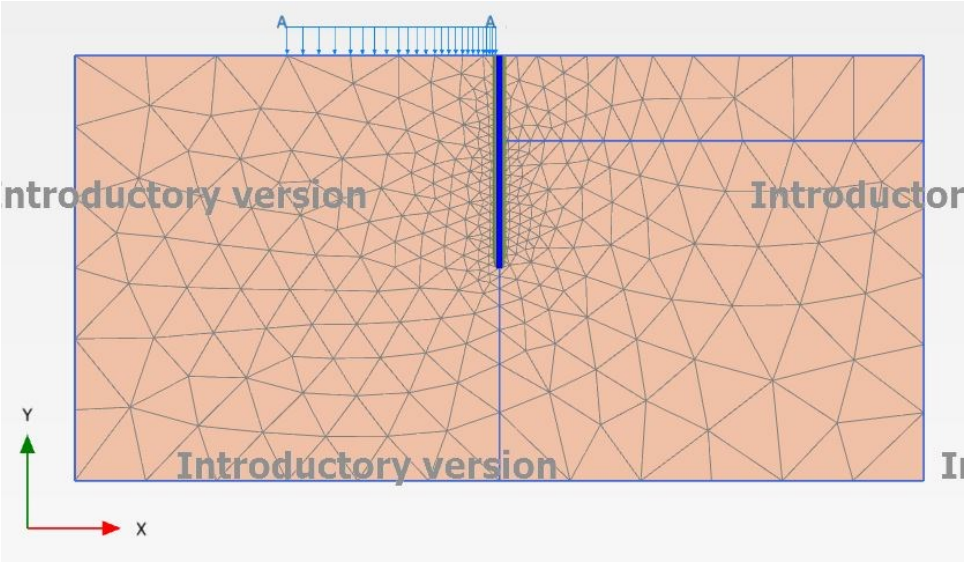

Figure 266: The mesh: "coarse" with tri-15 elements used at the beginning for the choice of the sheet pile's length

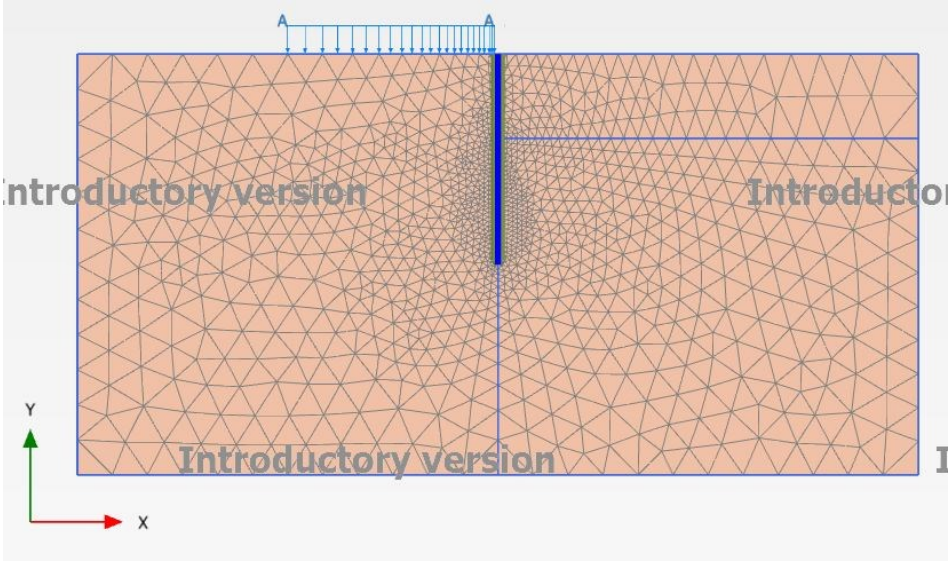

Figure 267: The mesh: "fine" with tri-6 elements with no interface (Ri=1)

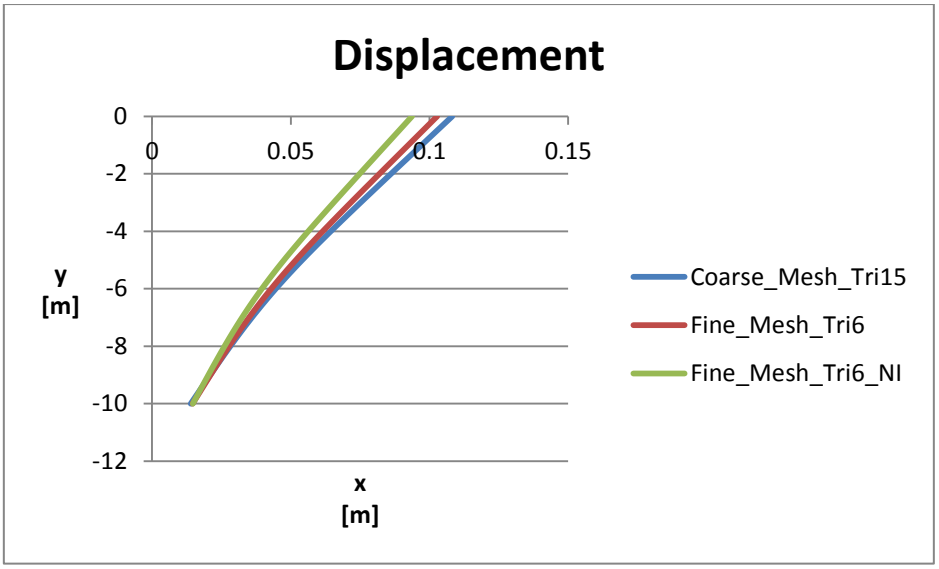

Figure 268: Displacement of a sheet pile of 10 m in clay using Plaxis with: coarse mesh and tri-15 elements, fine mesh and tri-6 elements, fine mesh and tri-6 elements with no interface

Table 26: Maximum and minimum values of the displacement in the sheet pile of 10 m in clay using Plaxis with: coarse mesh and tri-15 elements, fine mesh and tri-6 elements, fine mesh and tri-6 elements with no interface, absolute difference

DISPLACEMENT [m]					
MAXIMUM			MINIMUM		
COARSE	FINE	NI	COARSE	FINE	NI
0.10823	0.10278	0.09372	0.01394	0.01461	0.01468
ABS_DIFF	5%	13%	ABS_DIFF	-5%	-5%

2.6.6 Clay– 1st case (10 m) comparison

As for the solution with sand, the values obtained with SheetPile2.0 and with the Classic Method (as the minimum required length to have equilibrium is 8.5 m, the trend of the bending moment is taken into account only within this length and not for the remaining part of the sheet pile, Figure 270) can be considered adequate for a first approach to the problem whereas the FEM solutions can be chosen as more coherent with the real behavior of the soil-structure system. The latter behaves rigidly with small (Plaxis) or with almost no (SheetPile2.0) curvature (Figure 269) because the sheet pile is short.

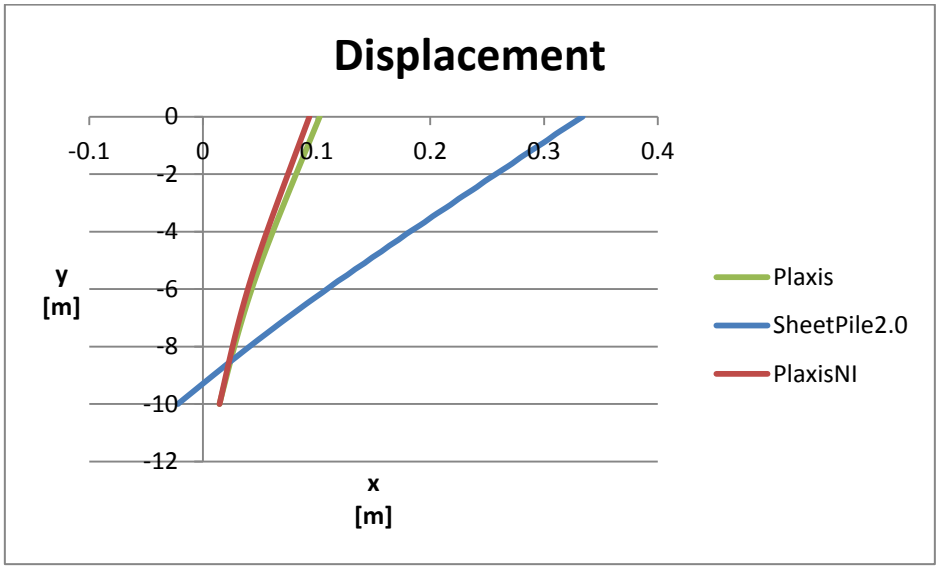

Figure 269: Displacement of a sheet pile of 10 m in clay using Plaxis, SheetPile2.0, Plaxis with no interface

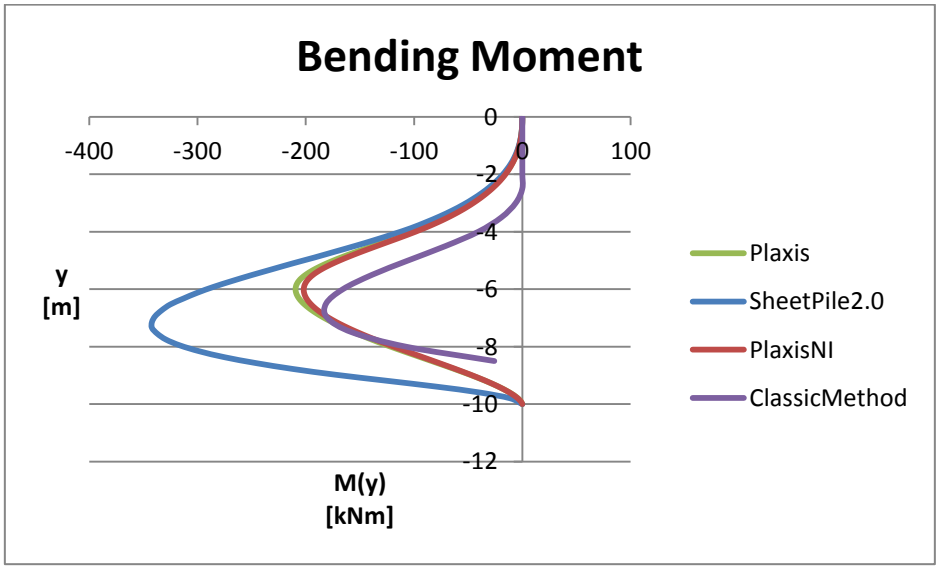

Figure 270: Bending moment of a sheet pile of 10 m in clay using Plaxis, SheetPile2.0, Plaxis with no interface, the Classic Method

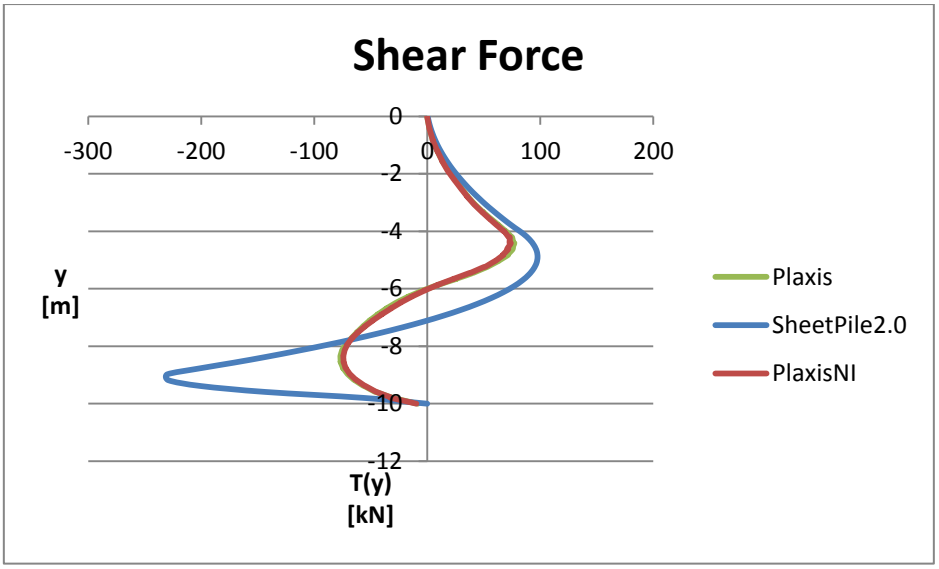

Figure 271: Shear force of a sheet pile of 10 m in clay using Plaxis, SheetPile2.0, Plaxis with no interface

Table 27: Maximum and minimum values of the displacement, bending moment, shear force in the sheet pile of 10 m in clay using Plaxis, SheetPile2.0, Plaxis with no interface and the Classic method, absolute difference

DISPLACEMENT [m]							
MAXIMUM				MINIMUM			
Plaxis	SP2.0	PlaxisNI	CM	Plaxis	SP2.0	PlaxisNI	CM
0.10278	0.02696	0.09372	-	0.01461	-0.00036	0.01468	-
ABS_DIFF	74%	9%	-	ABS_DIFF	102%	-1%	-
BENDING MOMENT [kNm]							
MAXIMUM				MINIMUM			
Plaxis	SP2.0	PlaxisNI	CM	Plaxis	SP2.0	PlaxisNI	CM
-4.3E-13	0	1.72E-13	0	-209.388	-164.7	-201.806	-181.198
ABS_DIFF	100%	140%	100%	ABS_DIFF	21%	4%	13%
SHEAR FORCE [kN]							
MAXIMUM				MINIMUM			
Plaxis	SP2.0	PlaxisNI	CM	Plaxis	SP2.0	PlaxisNI	CM
77.11684	59.63999	73.98901	-	-76.8479	-66.3923	-74.2937	-
ABS_DIFF	23%	4%	-	ABS_DIFF	14%	3%	-

2.6.7 Classic Method – Clay - 2st case (14 m) results

The only parameter that has been changed from the 1st case is the length of the sheet pile "L", from L = 10 m into L = 14 m. The other parameters are the same as chapter 2.6.2. The results are exposed in the following graphics. As the minimum required length to have equilibrium is 8.5 m, the trend of the bending moment is taken into

account only within this length and not for the remaining part of the sheet pile (Figure 274).

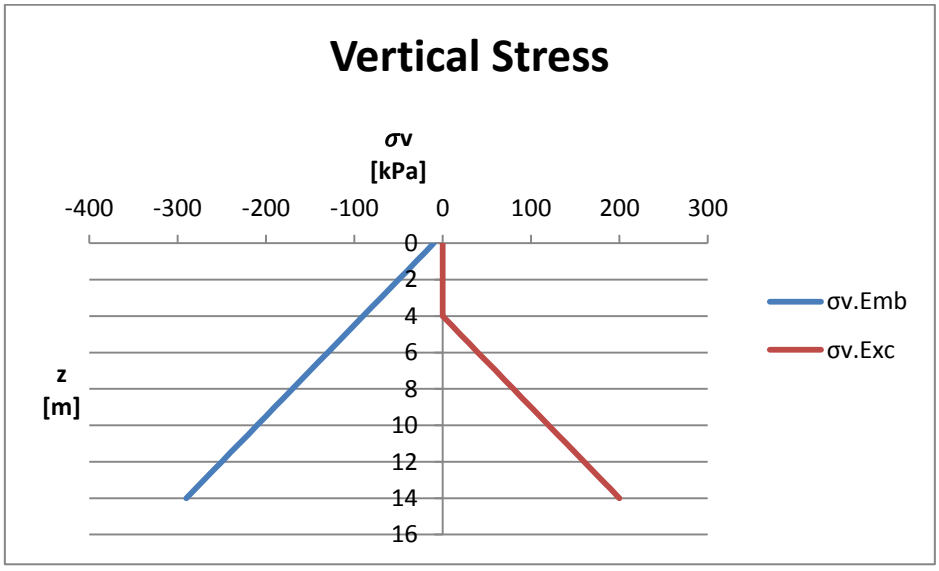

Figure 272: Vertical stress along a sheet pile of 14 m in clay using the Classic Method

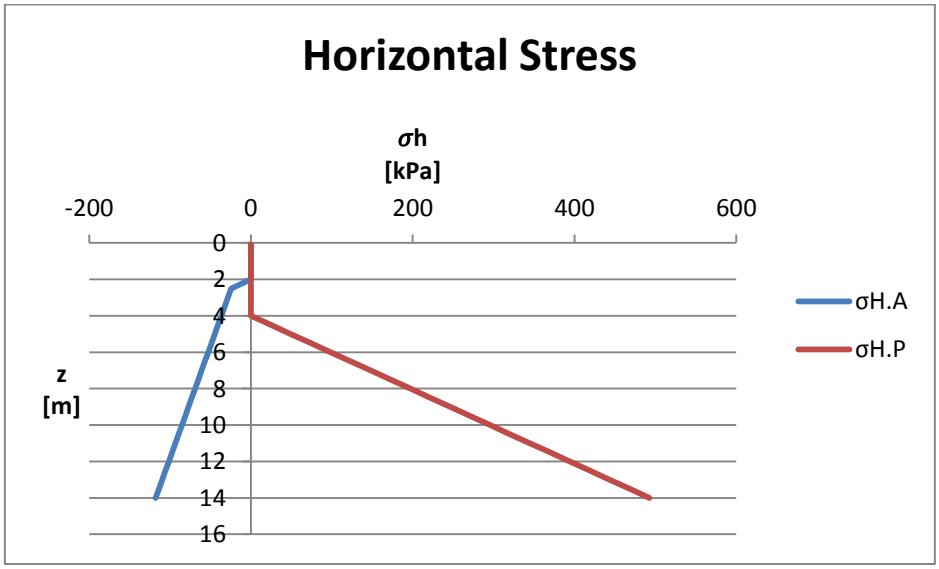

Figure 273: Horizontal stress along a sheet pile of 14 m in clay using the Classic Method

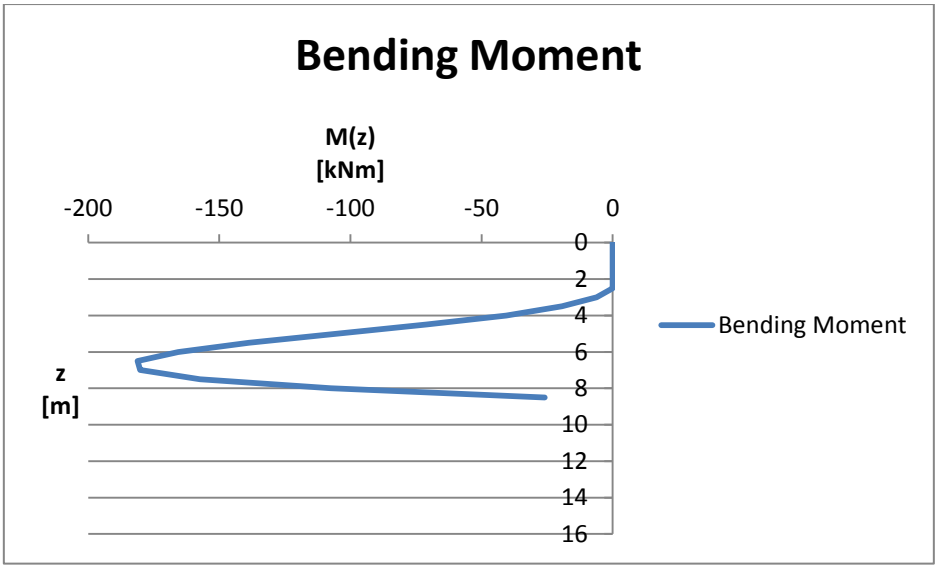

Figure 274: Bending moment of a sheet pile of 14 m in clay using the Classic Method

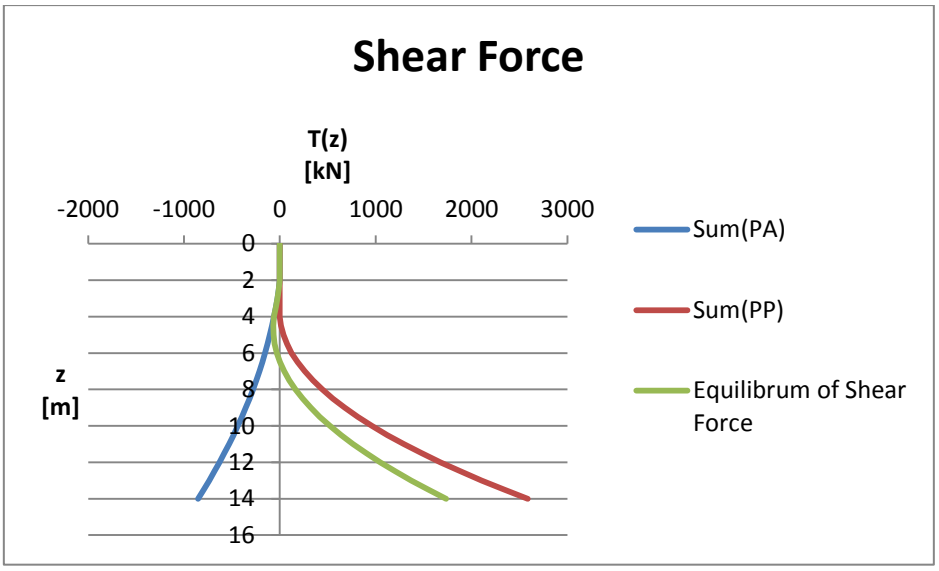

Figure 275: Shear force of a sheet pile of 14 m in clay using the Classic Method

2.6.8 SheetPile2.0 – Clay - 2st case (14 m) results

The only parameter that has been changed from the 1st case is the length of the sheet pile "L", from L = 10 m into L = 14 m. The other parameters are the same as chapter 2.6.3. The results are exposed in the following graphics.

Table 28: Maximum and minimum values of the displacement in the sheet pile 10 m and in the sheet pile of 14 m in clay using SheetPile2.0, absolute difference

DISPLACEMENT [m]			
MAXIMUM		MINIMUM	
SP2.0-10m	SP2.0-14m	SP2.0-10m	SP2.0-14m
0.33400	0.05780	-0.02200	0.00302
ABS_DIFF	83%	ABS_DIFF	114%

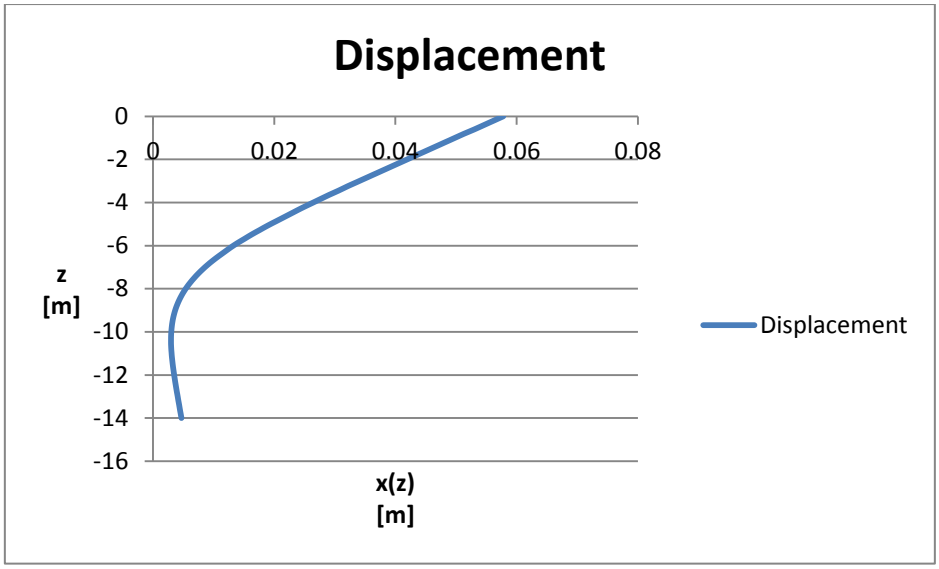

Figure 276: Displacement of a sheet pile of 14 m in clay using SheetPile2.0

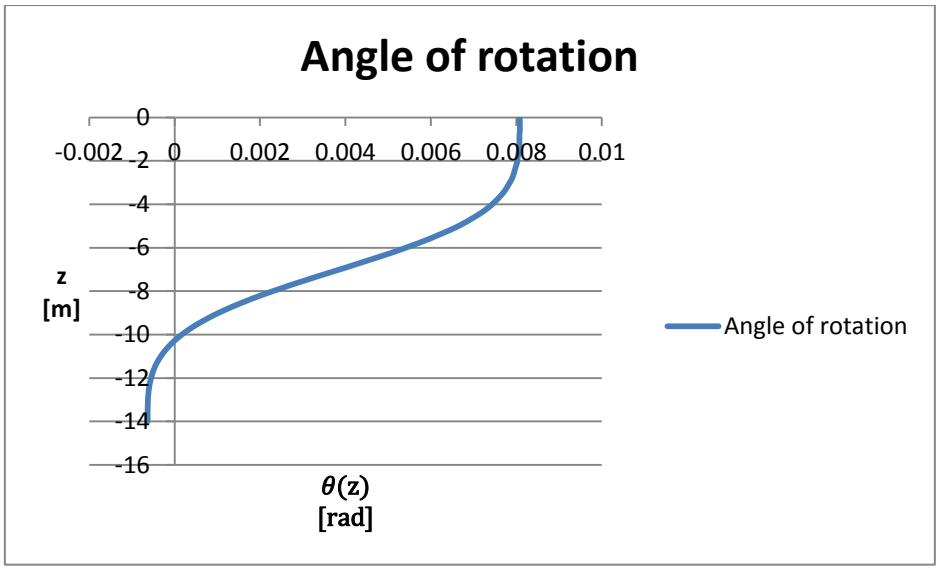

Figure 277: Angle of rotation of a sheet pile of 14 m in clay using SheetPile2.0

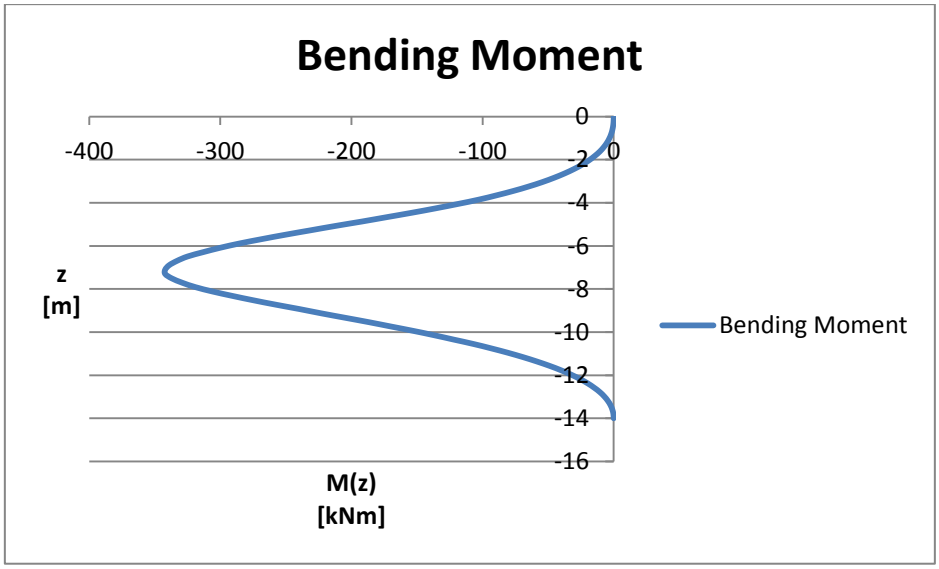

Figure 278: Bending moment of a sheet pile of 14 m in clay using SheetPile2.0

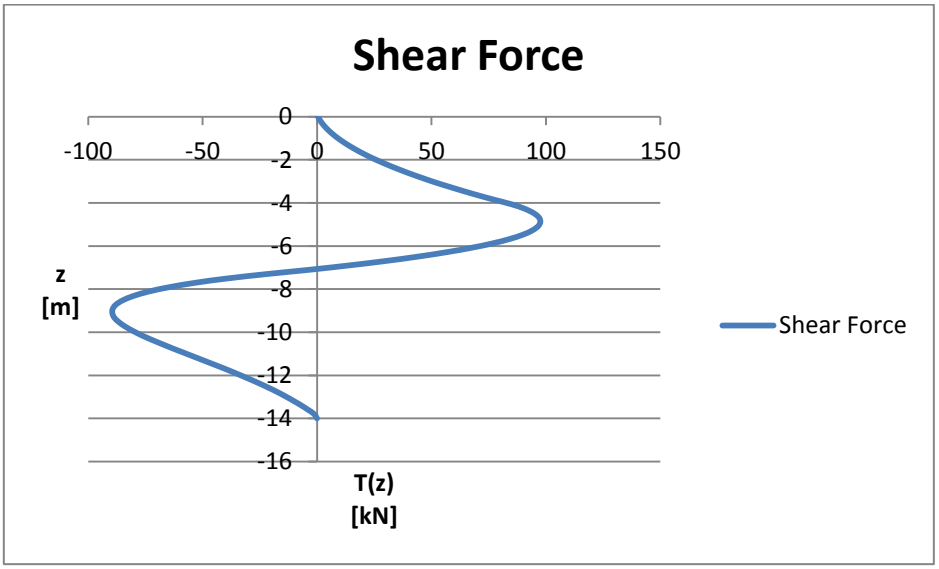

Figure 279: Shear force of a sheet pile of 14 m in clay using SheetPile2.0

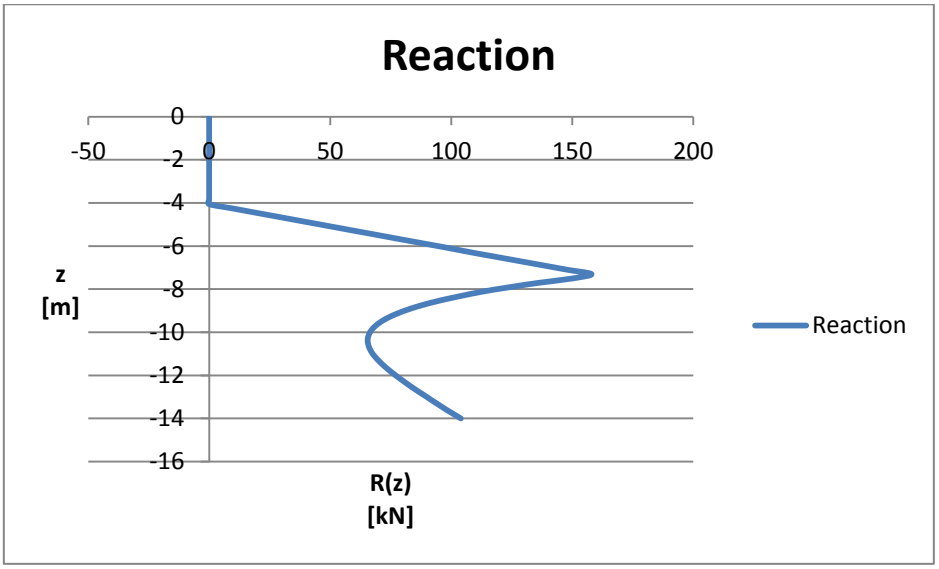

Figure 280: Reaction of a sheet pile of 14 m in clay using SheetPile2.0

2.6.9 Plaxis – Clay - 2st case (14 m) results

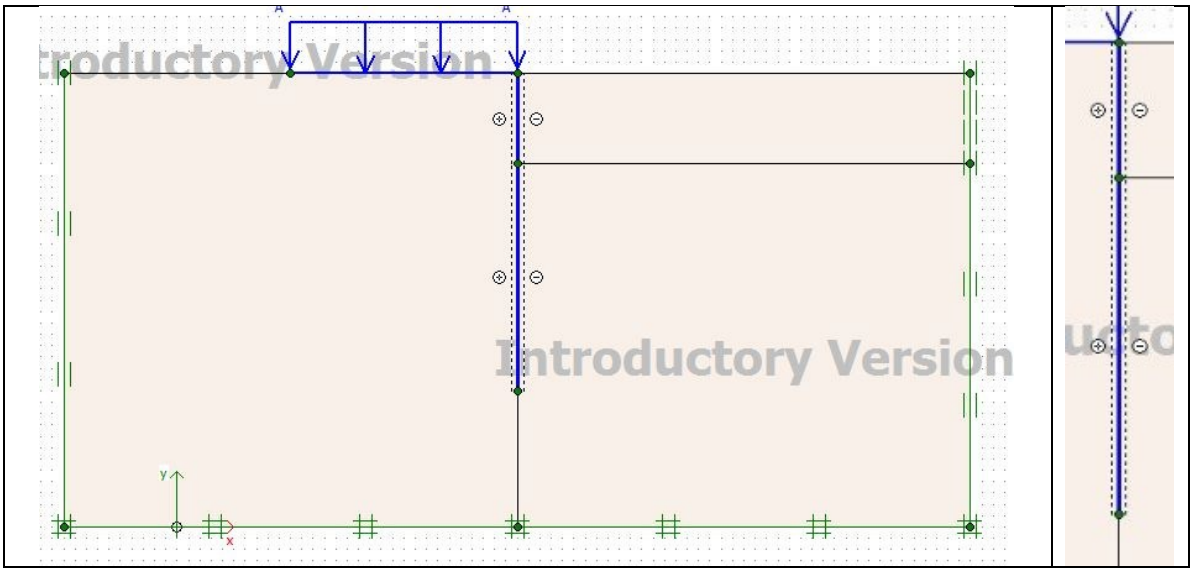

Figure 281: Model for the case of a sheet pile of 14 m in clay using Plaxis, particular of the interface

The only parameter that has been changed from the 1st case is the length of the sheet pile "L", from L = 10 m into L = 14 m. The other parameters are the same as chapter 2.6.4. The generated mesh (Figure 282) is a fine element distribution. The results are illustrated in the following screenshots.

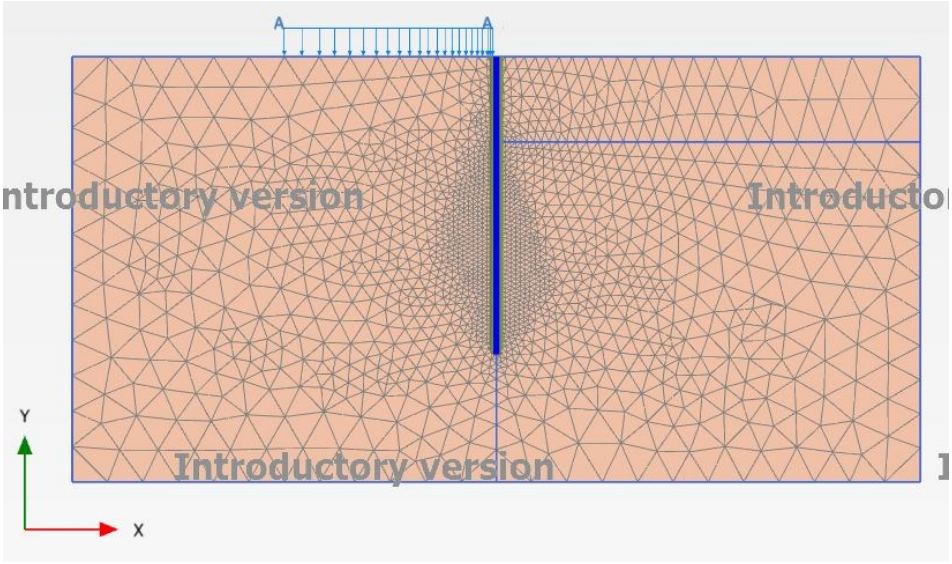

Figure 282: The mesh: "fine" with tri-6 elements

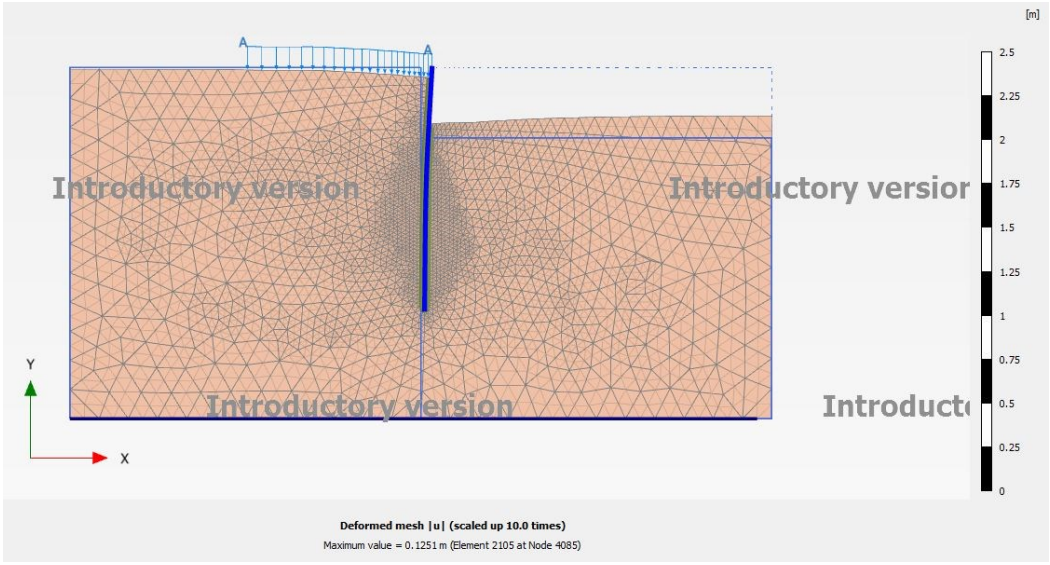

Figure 283: Deformed mesh for the case of a sheet pile of 14 m in clay using Plaxis

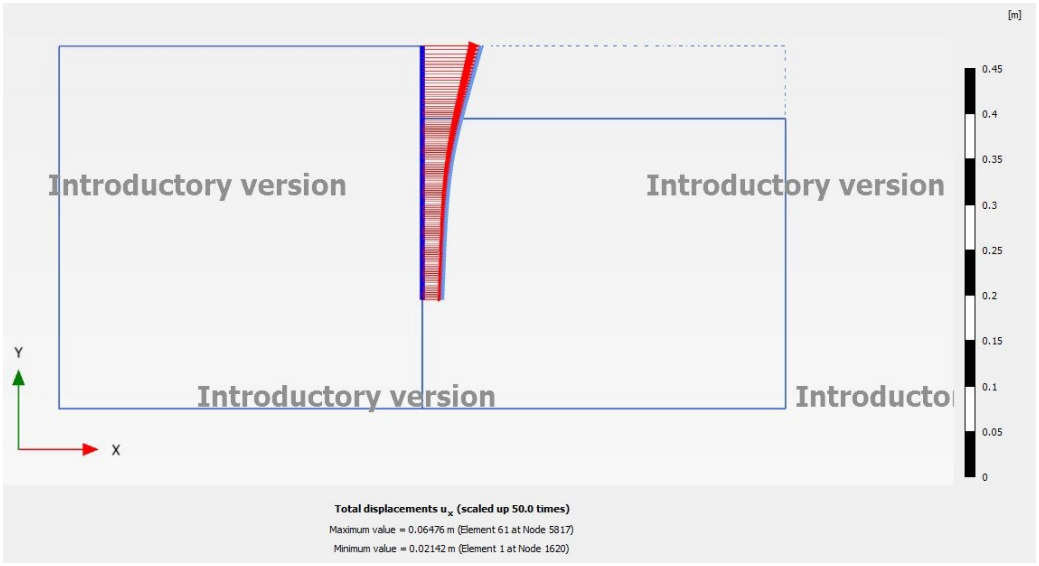

Figure 284: Displacement u_x of a sheet pile of 14 m in clay using Plaxis

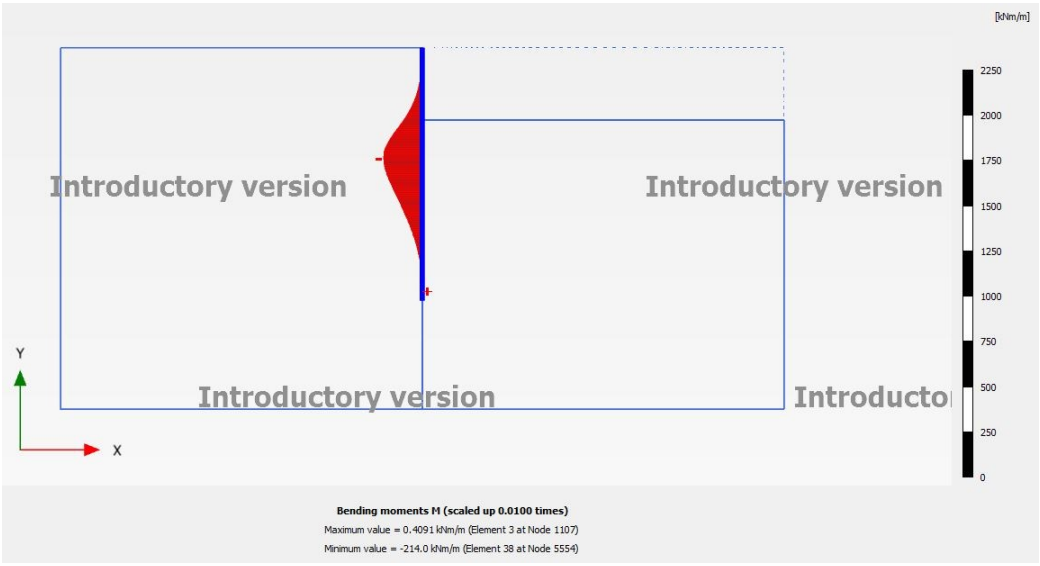

Figure 285: Bending moment of a sheet pile of 14 m in clay using Plaxis

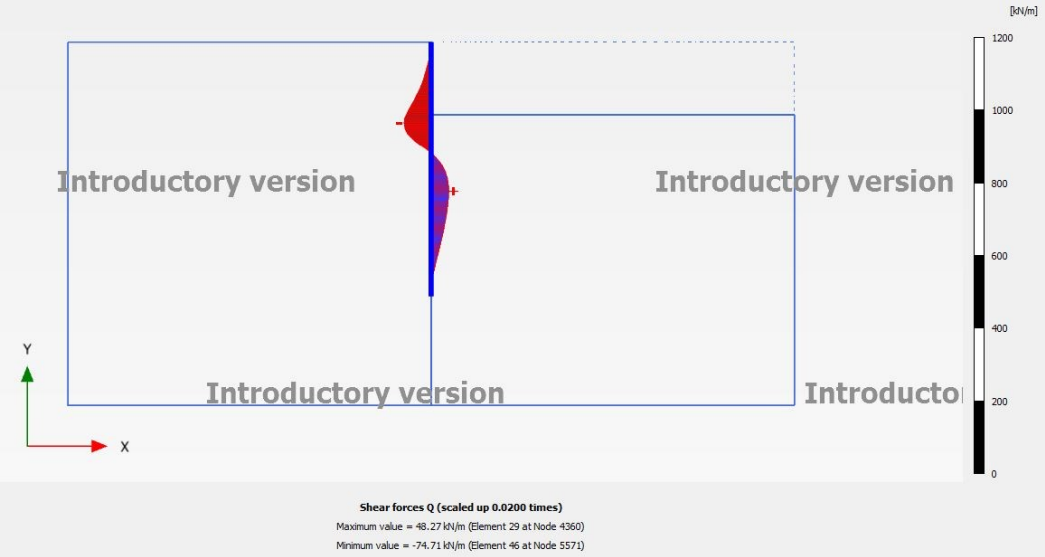

Figure 286: Shear force of a sheet pile of 14 m in clay using Plaxis

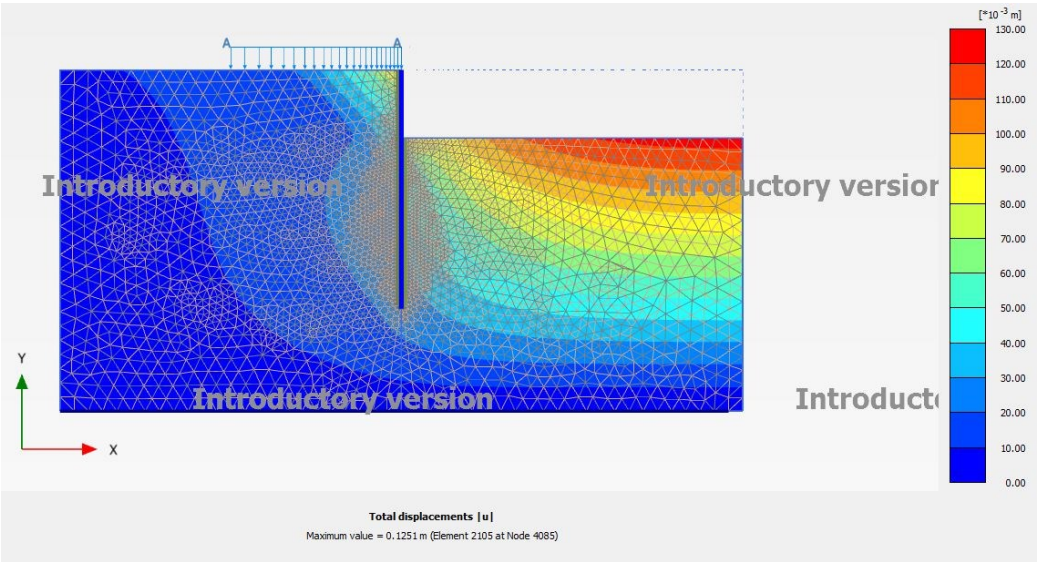

Figure 287: Total displacement u for the case of a sheet pile of 14 m in clay using Plaxis

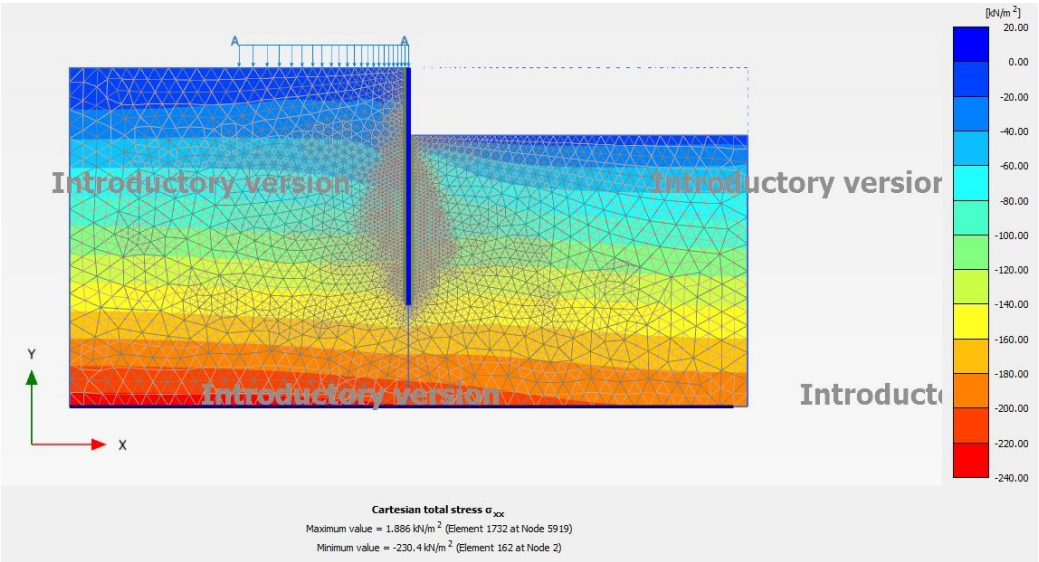

Figure 288: Total stress σ_{xx} for the case of a sheet pile of 14 m in clay using Plaxis

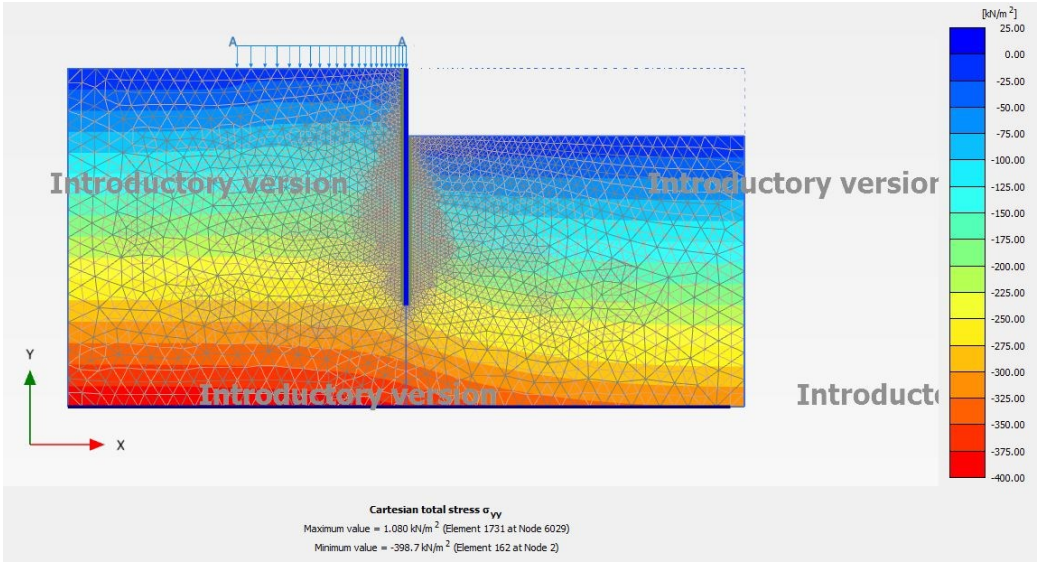

Figure 289: Total stress σ_{yy} for the case of a sheet pile of 14 m in clay using Plaxis

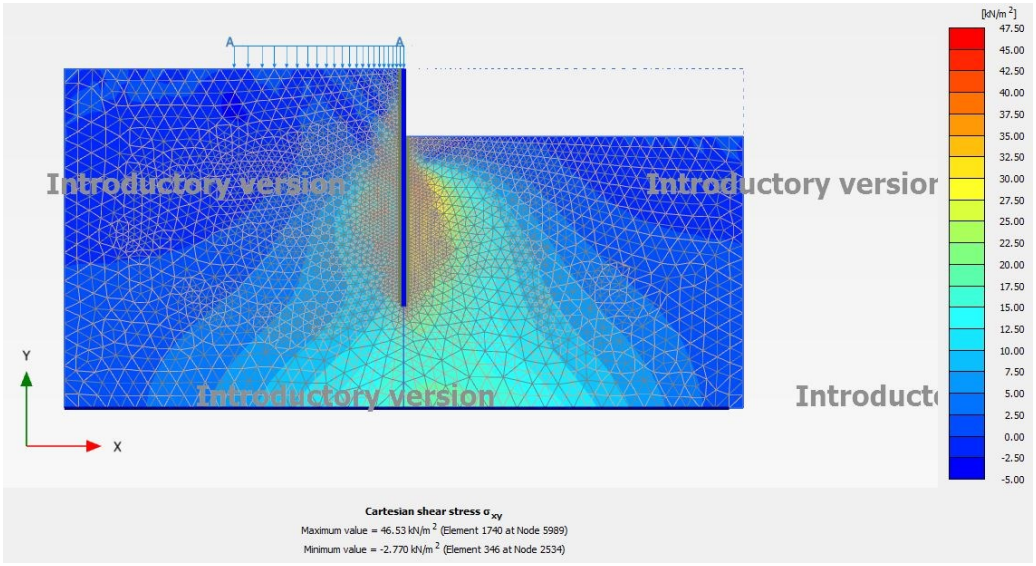

Figure 290: Total stress σ_{xy} for the case of a sheet pile of 14 m in clay using Plaxis

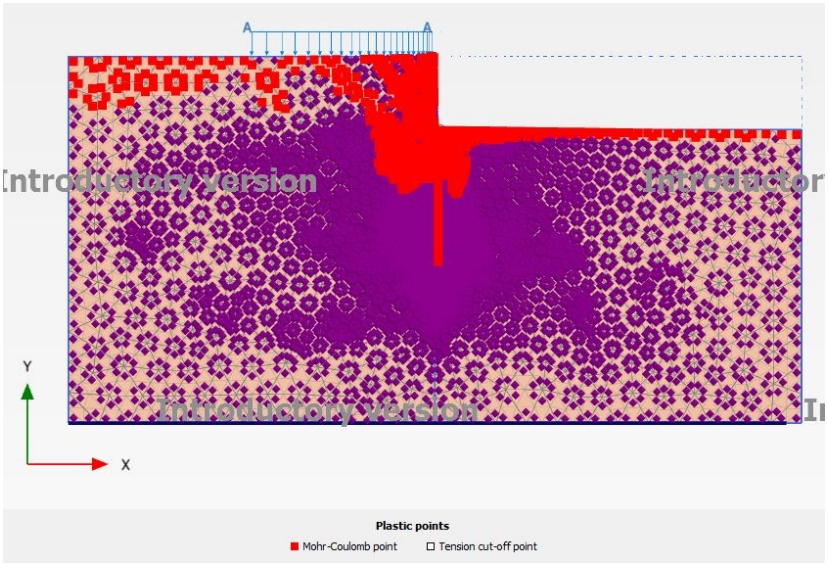

Figure 291: Plastic points for the case of a sheet pile of 14 m in clay using Plaxis

2.6.10 Plaxis No Interface – Clay - 2st case (14 m) results

The only parameter that has been changed from previous chapter is the parameter Ri of the interface: it has been changed from Ri = 0.8 into Ri = 1 ("rigid"), this new condition simulates the lack of the interface between soil and structure. The other parameters are the same as chapter 2.6.9. As for the previous cases the solutions with coarse and fine mesh are quite the same, whereas the model with fine mesh but with no interface differs from the previous solutions and provides lower displacement (Figure 294).

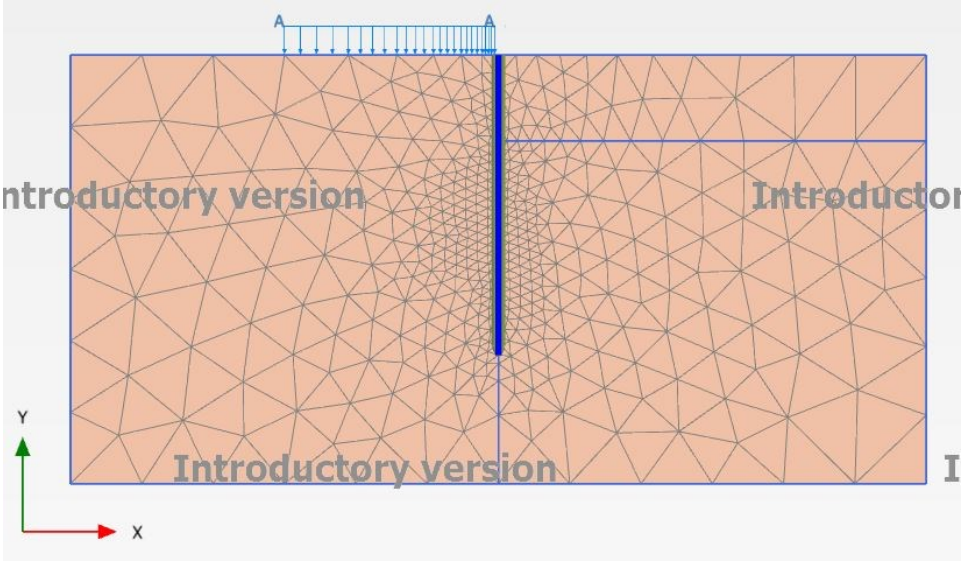

Figure 292: The mesh: "coarse" with tri-15 elements used at the beginning for the choice of the sheet pile's length

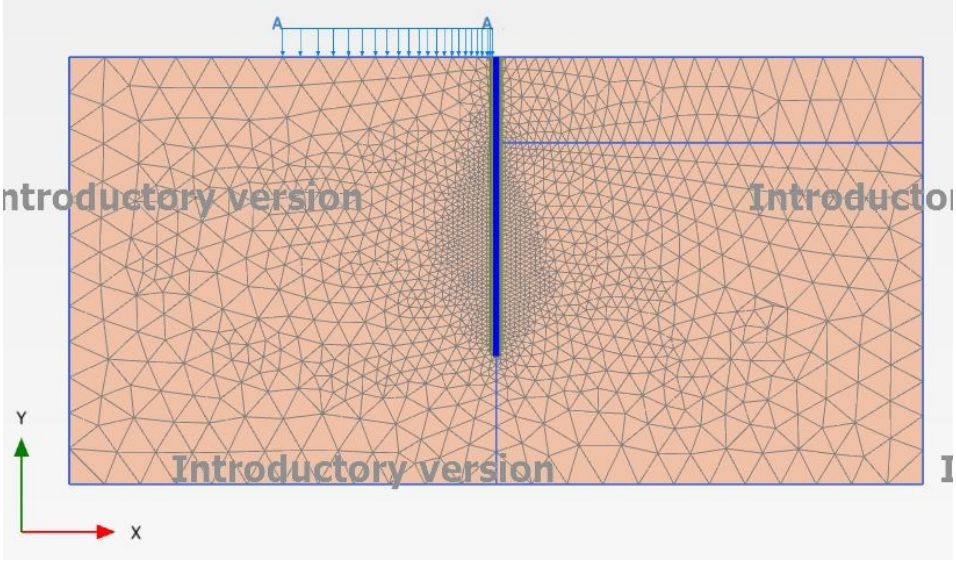

Figure 293: The mesh: "fine" with tri-6 elements with no interface (Ri=1)

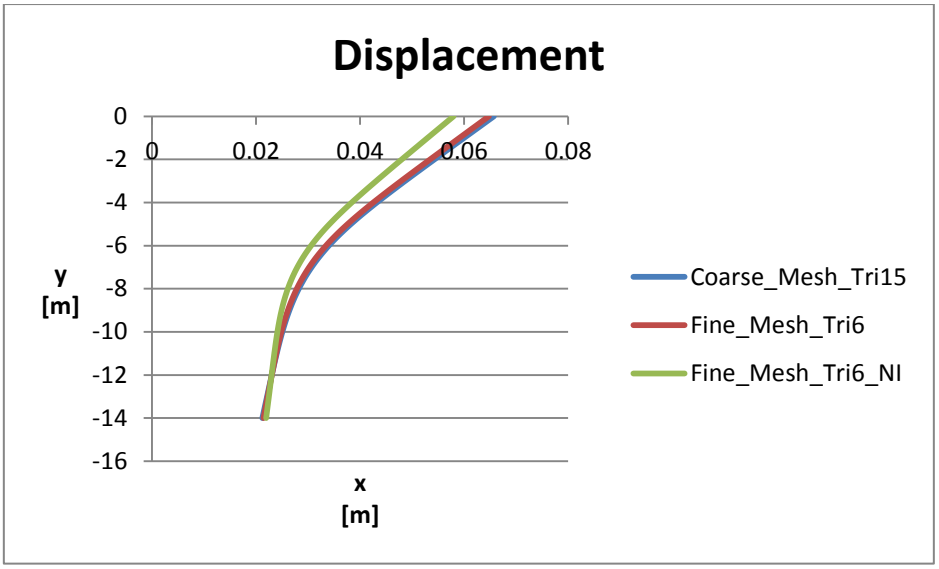

Figure 294: Displacement of a sheet pile of 14 m in clay using Plaxis with: coarse mesh and tri-15 elements, fine mesh and tri-6 elements, fine mesh and tri-6 elements with no interface

Table 29: Maximum and minimum values of the displacement in the sheet pile of 14 m in clay using Plaxis with: coarse mesh and tri-15 elements, fine mesh and tri-6 elements, fine mesh and tri-6 elements with no interface, absolute difference

DISPLACEMENT [m]					
MAXIMUM			MINIMUM		
COARSE	FINE	NI	COARSE	FINE	NI
0.06572	0.06476	0.05797	0.02120	0.02142	0.02193
ABS_DIFF	1%	12%	ABS_DIFF	-1%	-3%

2.6.11 Clay– 2st case (14 m) comparison

The comparison replies the evaluations exposed in the previous cases and can be assumed as a general description of the phenomenon: the solutions achieved with SheetPile2.0 and with the Classic Method (as the minimum required length to have equilibrium is 8.5 m, the trend of the bending moment is taken into account only within this length and not for the remaining part of the sheet pile, Figure 296) are more conservative than the ones obtained with Plaxis which; the latter better simulate the real behavior of the sheet pile and of the soil. By increasing the length of the sheet pile, the difference between Plaxis and SheetPile2.0 decreases by 60% (Table 27, Table 30): much more than the case of the sheet pile in sand. For this length of the sheet pile (14 m), the maximum displacement obtained with Plaxis differs only by 11% from the one of SheetPile2.0.

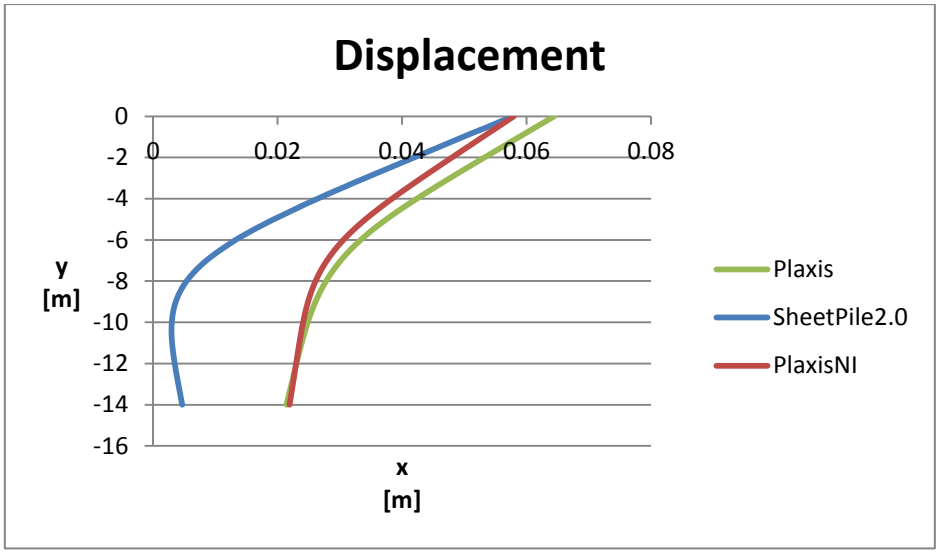

Figure 295: Displacement of a sheet pile of 14 m in clay using Plaxis, SheetPile2.0, Plaxis with no interface

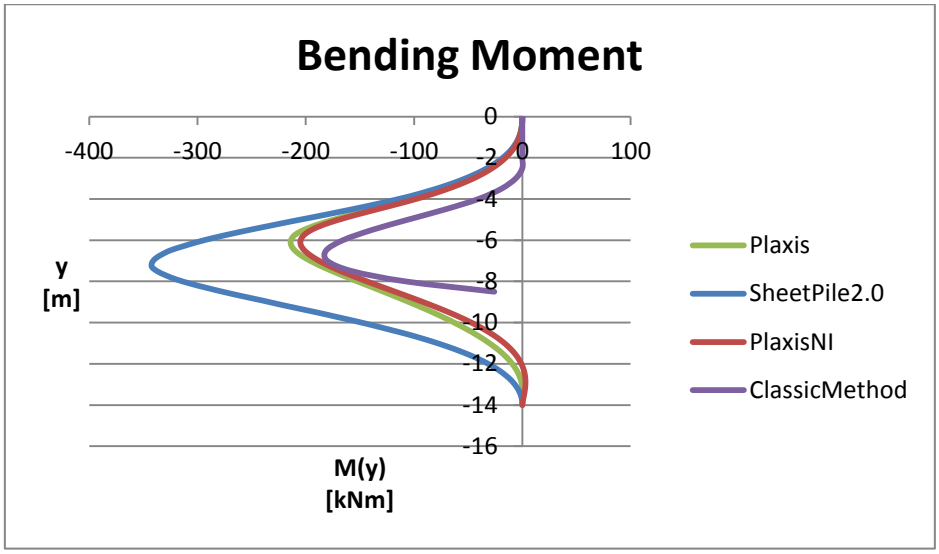

Figure 296: Bending moment of a sheet pile of 14 m in clay using Plaxis, SheetPile2.0, Plaxis with no interface, the Classic Method

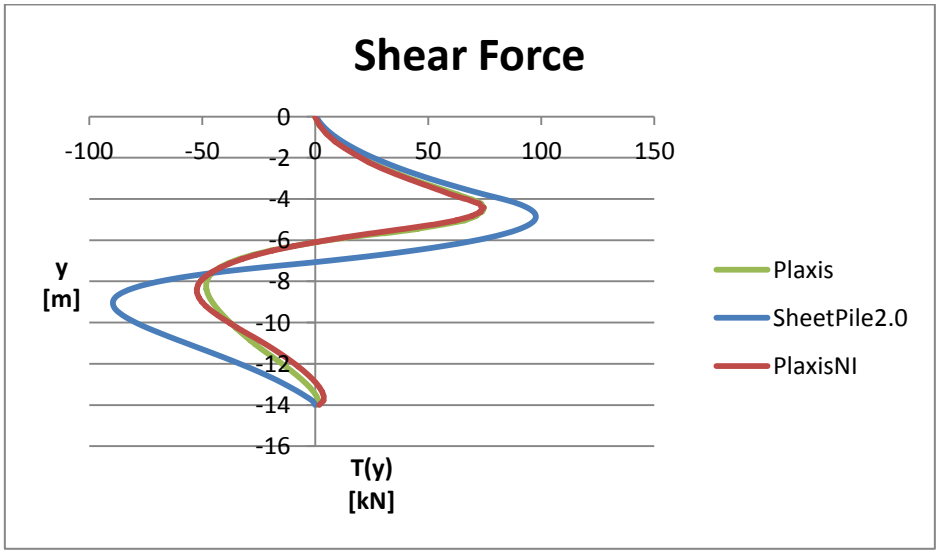

Figure 297: Shear force of a sheet pile of 14 m in clay using Plaxis, SheetPile2.0, Plaxis with no interface

Table 30: Maximum and minimum values of the displacement, bending moment, shear force in the sheet pile of 14 m in clay using Plaxis, SheetPile2.0, Plaxis with no interface and the Classic method, absolute difference

DISPLACEMENT [m]							
MAXIMUM				MINIMUM			
Plaxis	SP2.0	PlaxisNI	CM	Plaxis	SP2.0	PlaxisNI	CM
0.06476	0.05780	0.05797	-	0.02142	0.00296	0.02193	-
ABS_DIFF	11%	10%	-	ABS_DIFF	86%	-2%	-
BENDING MOMENT [kNm]							
MAXIMUM				MINIMUM			
Plaxis	SP2.0	PlaxisNI	CM	Plaxis	SP2.0	PlaxisNI	CM
0.409128	0	2.901867	0	-213.999	-342.322	-204.991	-181.198
ABS_DIFF	100%	-609%	100%	ABS_DIFF	-60%	4%	15%
SHEAR FORCE [kN]							
MAXIMUM				MINIMUM			
Plaxis	SP2.0	PlaxisNI	CM	Plaxis	SP2.0	PlaxisNI	CM
74.70678	97.58181	74.56294	-	-48.2688	-89.446	-52.4327	-
ABS_DIFF	-31%	0%	-	ABS_DIFF	-85%	-9%	-

3 Conclusions

In this report, regarding the horizontal structures, the analytical methods of Winkler and Pasternak have been exposed, pointing out the equations that describe the theories (chapters 1.1.1, 1.1.2, 1.2.1, 1.2.2). The formulae have been implemented in a spreadsheet and applied to soil with absolutely generic characteristics; then the results were graphically shown (chapters 1.1.3, 0, 1.2.2). Applications of Pasternak's theory have been highlighted (chapter 1.2). The numerical solution obtained with FEM program GeoStudio has been illustrated and compared to the analytical solutions (chapter 0). Description of the constitutive material models has been made; results obtained by elastic and elastic-plastic analysis applied to the previous issue using the FEM program Midas GTS have been exposed (chapter 1.3). In the following graphics and table a comparison between all these approaches is shown, highlighting the topic values (Figure 298, Figure 299, Figure 300, Table 31).

One can see that the Winkler's approach is the most conservative, and is matched by the solution of Pasternak adopting S = 1 kN (the membrane doesn't work), see Figure 298.

The solution of Pasternak adopting S calculated by the formula suggested in chapter 1.2.1 m provides lower displacement than the one of Winkler, and is closer to the solution by FEM.

Results by FEM programs GeoStudio (elastic) and Midas (elastic and elastic-plastic) match, with no differences between elastic and elastic-plastic due to the limited value of load applied to the foundations.

FEM programs give the most accurate solution to the problem considering the theoretical feedback that is compulsory in their implementation, but the simplified theories of Winkler and Pasternak can be successfully used in order to obtain an approximate solution to the problem and general information regarding the order of magnitude of the results.

The implementation of the analytical methods of Winkler and Pasternak is efficient because one obtains an immediate evaluation of the parameters changing the input data.

The solution with the spreadsheet is versatile because one can analyze different load conditions modifying the border conditions of the equation that describes the problem.

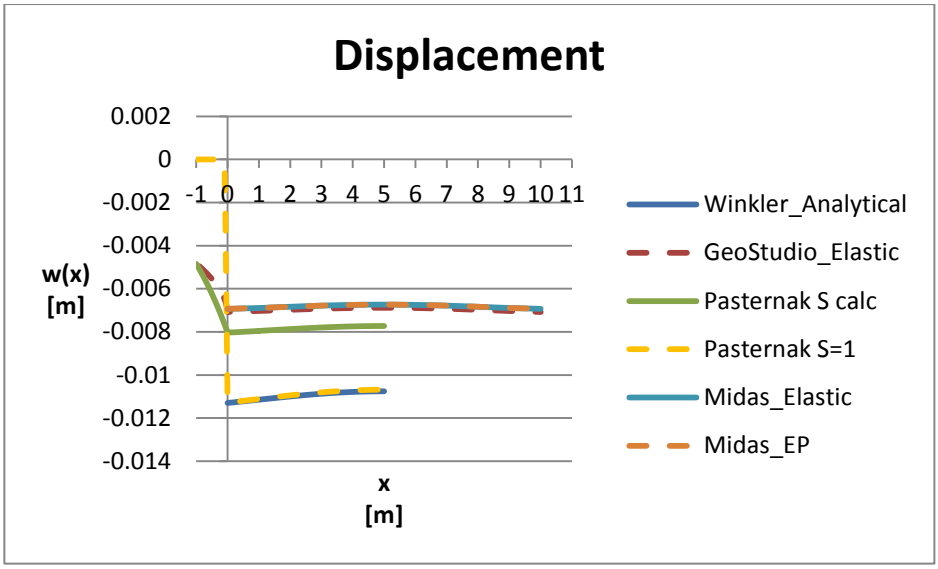

Figure 298: Displacement obtained by varying the approach to the issue

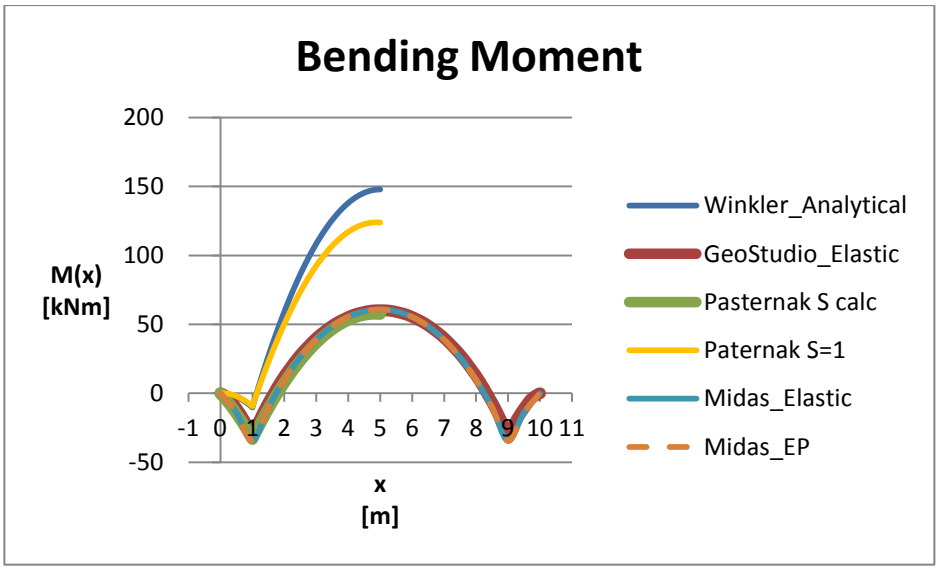

Figure 299: Bending moment obtained by varying the approach to the issue

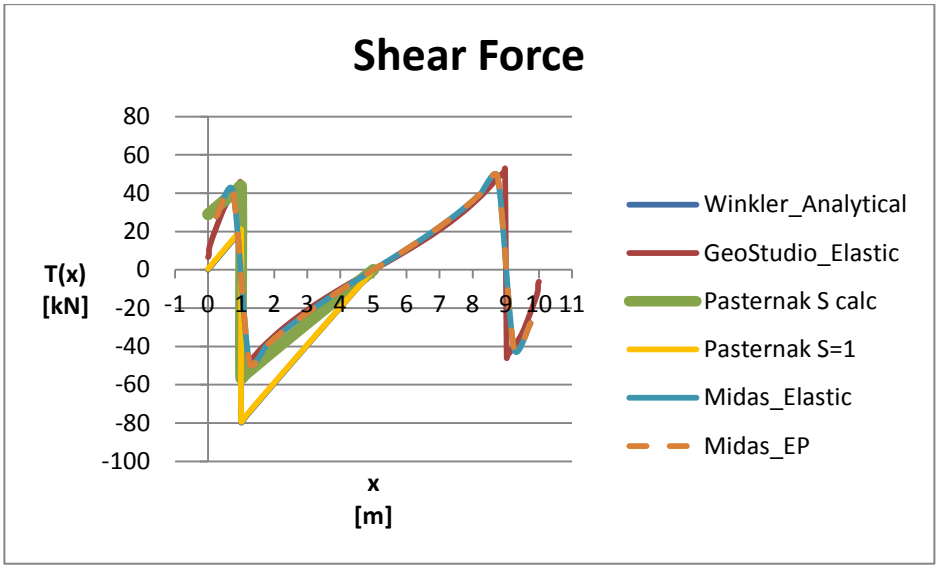

Figure 300: Shear force obtained by varying the approach to the issue

Table 31: Maximum and minimum values of the displacement, bending moment, shear force of the loaded beam varying the calculation approach (Winkle implemented in a spreadsheet, GeoStudio, Pasternak implemented in a spreadsheet with S calculated by the formula suggested in the chapter 1.2.1, Pasternak implemented in a spreadsheet with S=1 kN, Midas linear elastic, Midas elastic-plastic), absolute difference

DISPLACEMENT [m]					
MAXIMUM					
Winkler	GeoStudio_LE	Pasternak S calc	Pasternak S=1	Midas_LE	Midas_EP
-0.01076	-0.00688	-0.00773	-0.01069	-0.00674	-0.00674
ABS_DIFF	36%	28%	1%	37%	37%
MINIMUM					
Winkler	GeoStudio_LE	Pasternak S calc	Pasternak S=1	Midas_LE	Midas_EP
-0.01130	-0.00708	-0.00804	-0.01129	-0.00693	-0.00693
ABS_DIFF	37%	29%	0%	39%	39%
BENDING MOMENT [kNm]					
MAXIMUM					
Winkler	GeoStudio_LE	Pasternak S calc	Pasternak S=1	Midas_LE	Midas_EP
147.80820	60.20951	57.65565	123.92126	60.73399	60.73399
ABS_DIFF	59%	61%	16%	59%	59%
MINIMUM					
Winkler	GeoStudio_LE	Pasternak S calc	Pasternak S=1	Midas_LE	Midas_EP
-10.25935	-30.86267	-33.11338	-9.38980	-34.47295	-34.47295
ABS_DIFF	-201%	-223%	8%	-236%	-236%
SHEAR FORCE [kN]					
MAXIMUM					
Winkler	GeoStudio_LE	Pasternak S calc	Pasternak S=1	Midas_LE	Midas_EP
20.47270	52.81734	43.59109	20.91220	48.61631	48.61631
ABS_DIFF	-158%	-113%	-2%	-137%	-137%
MINIMUM					
Winkler	GeoStudio_LE	Pasternak S calc	Pasternak S=1	Midas_LE	Midas_EP
-79.52730	-52.81648	-56.40891	-79.08780	-48.61631	-48.61631
ABS_DIFF	34%	29%	1%	39%	39%

Regarding the vertical structures, the simplified limit equilibrium method has been exposed (chapter 2.2) and application of it on sheet pile embedded in either sandy or clay soil has been implemented (chapters 2.5, 2.6). The theory of the dependent pressure method has been illustrated (chapter 2.3) and the calculation with the relative program has been made, considering the same set of conditions (sand or clay, length of the sheet pile) used in the previous approach (chapters 2.5, 2.6). The FEM programs Plaxis and GeoStudio have been described (chapter 2.4), and the obtained results on the set of conditions previously enounced have been shown (chapters 2.5, 2.6). Comparison between all these approaches has been made, preliminarily varying the length of the sheet pile (using Plaxis) and afterwards choosing the comparison lengths: firstly, an embedment that widely ensures the equilibrium, secondly, a solution close to instability (chapters 2.5, 2.6). In the following graphics the topic results are summarized.

In Figure 301 one can see the behavior of the sheet pile varying the embedment length from an instable condition to a stable one, for sandy and clay soil.

In Figure 302 one can see the case of a sheet pile of 9 m embedded in sand studied by the support of the Classic Method, SheetPile2.0, GeoStudio and Plaxis. The FEM programs ensure the most accurate results, but SheetPile2.0 and the Classic Method (which can only estimate the bending moment along the sheet pile) could give an approximate evaluation of the solution which can be useful for preliminary studies on the issue.

In Figure 303 the behavior of a sheet pile of 10 m (close to instability) and that of a 14 m one (stable situation), both embedded in clay and with varying mesh coarseness, element types and both first considering then ignoring the interface element, is shown (using Plaxis). The accuracy of the solution changes according to the choice of the element and the coarseness, but not significantly: of course it depends on the precision required by the analysis. The lack of the interface element changes the solution providing lower displacement to the sheet pile, whereas the use of the interface element provides conservative results.

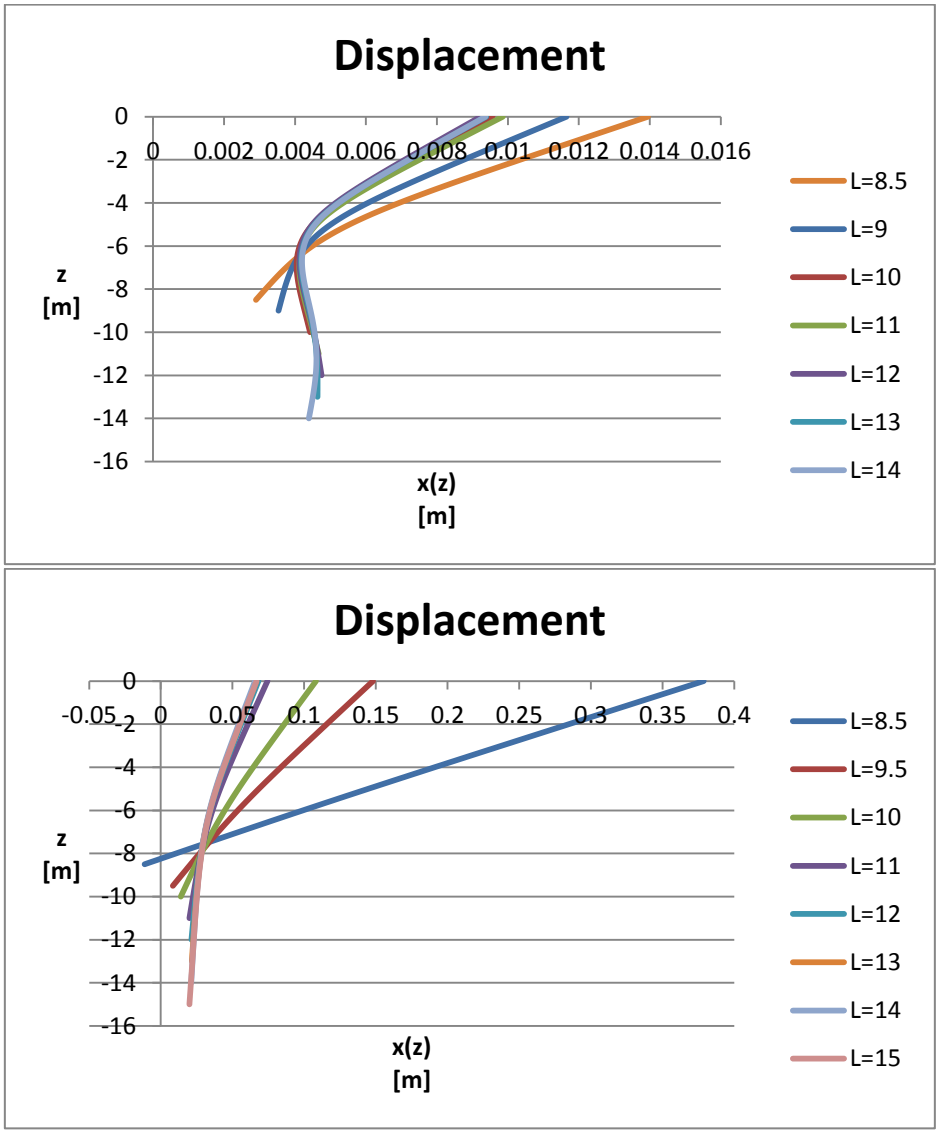

Figure 301: Searching for the length to compare by using Plaxis, sandy soil and clay soil

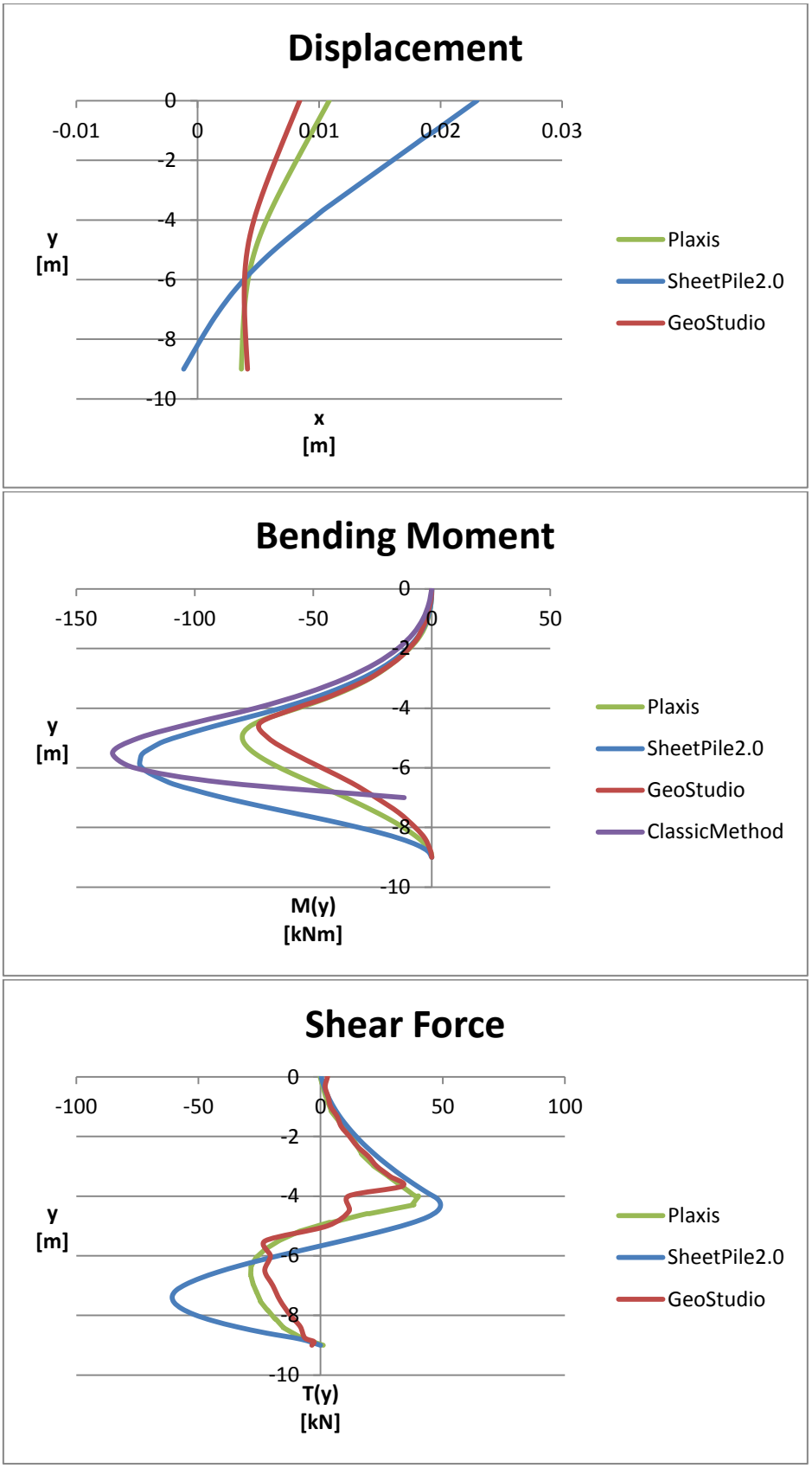

Figure 302: Displacement, bending moment, shear force of a sheet pile of 9 m in sand varying the calculation approach (Plaxis, SheetPile2.0, GeoStudio, Classic Method)

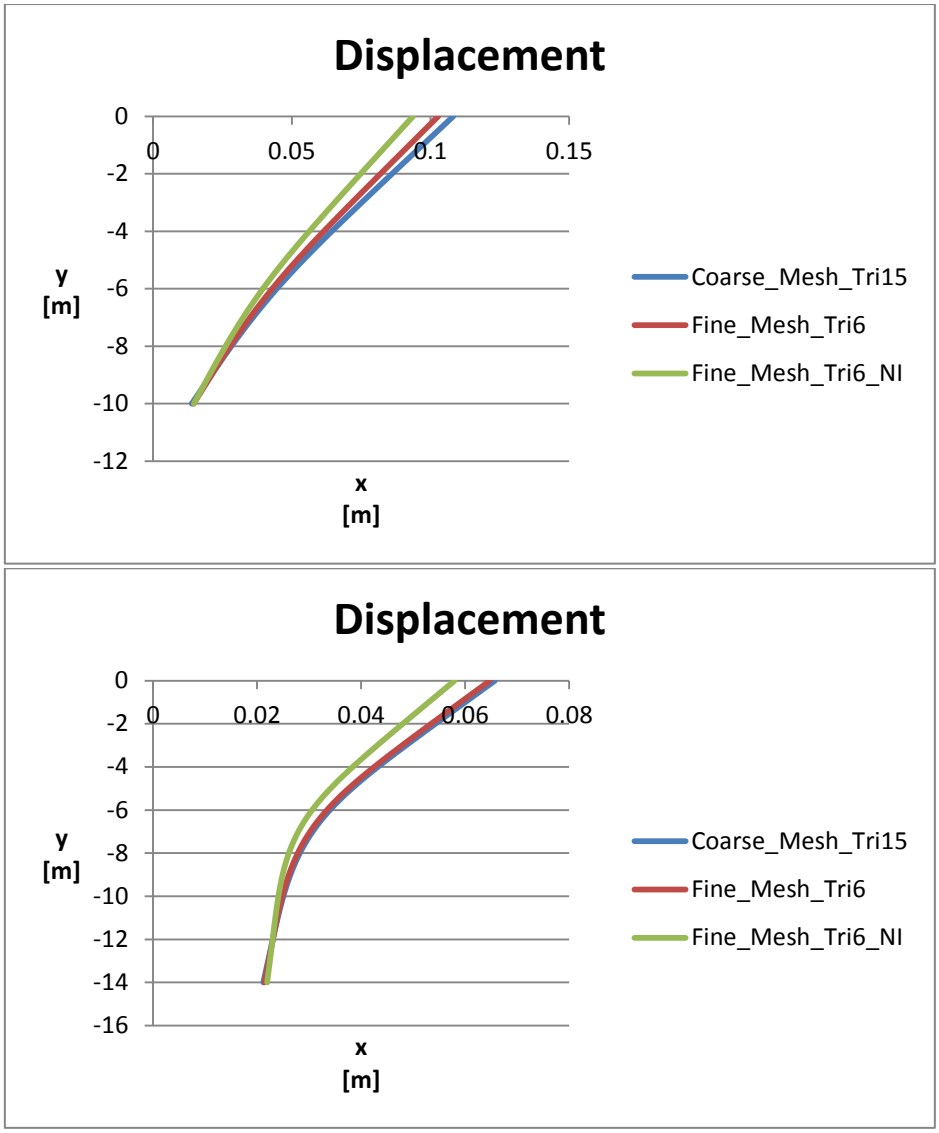

Figure 303: Displacement of a sheet pile of 10 m and of 14 m in clay using Plaxis varying the mesh coarseness, the element type and considering or not the interface element

Some further applications or studies can be suggested and summarized as follows:

- Analyses of the response of the foundation studied in chapter 1.3, modelized with "plate elements" instead of the "beam element", either with an elastic or elastic-plastic constitutive model: in this way the focus would be on the behavior of the foundations, simulating more accurately the trend of compression and tensile stress within the concrete
- Validation of the Pasternak 3D model illustrated in the chapter 1.2.2.3 (Figure 304) by comparison with real data from loaded membrane applied on gravel columns
- To verify if a further improvement of SheetPile2.0 program is achievable in order to gain more accuracy in terms of displacement and stress parameters

- Further studies on the "interface element", characteristic which highly influences both the response of the sheet pile in excavation and under load, and the soil-structure interaction considered in other application fields.

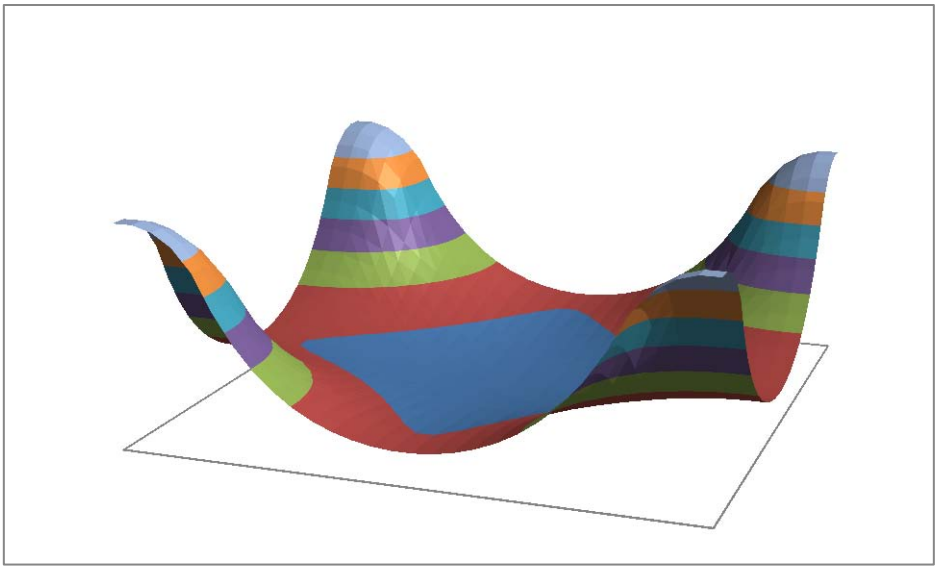

Figure 304: Behavior of a loaded membrane applied on gravel columns

4 References

1. **Scott, Ronald F.** *Foundation Analysis.* Englewood Cliffs, NJ 07632 : N. M. Newmark and W. J. Hall, 1981.

2. **Verruijt, Arnold.** *Computational Geomechanics.* Dordrecht/Boston/London : Kluwer Academic Publishers, 1995.

3. *Interazione terreno-fondazione, appunti delle lezioni.* **Cortellazzo, Giampaolo.** Padova, Italy : s.n., 2011-2012.

4. *Miglioramento dei terreni ed opere in terra.* **Cola, Simonetta.** Padova, Italy : s.n., 2011-2012.

5. **GEO_SLOPE International Ltd.** *Stress-Deformation Modeling with SIGMA/W 2007.* 3rd. Calgary, Alberta : GEO_SLOPE Internationa Ltd., 2008.

6. *Beam on the Pasternak soil (based on two parameter), illustration of the issues of the soil-structure interaction.* **Lefik, M.** Lodz, Poland : s.n.

7. *Lecture notes.* **Lefik, Marek.** Lodz, Poland : s.n., 2013.

8. **Midas I.T. Co.** *Analysis Reference.* Este : CSPFea s.c.

9. **Midas GTS.** *Constitutive Model.* Este : CSPFea s.c., 2013.

10. **Brinkgreve, R.B.J., et al., et al.** *Plaxis 2D Material Models Manual 2010.* Delft : Plaxis bv, 2011.

11. **Midas GTS.** *Analysis Case.* Este : CSPFea s.c., 2013.

12. —. *Finite Element Formulation.* Este : CSPFea s.c., 2013.

13. —. *Numerical Analysis.* Este : CSPFea s.c., 2013.

14. **ArcelorMittal.** *Piling Handbook.* 8th. Esch-sur-Alzette, Solihull : ArcelorMittal Commercial RPS, 2008.

15. *Design of diaphragm walls according to EN 1997-1:2004 Eurocode 7.* **A. Sieminska-Lewandowska, M. Mitew-Czajewska.** Warsaw, Poland, Warsaw University of Technology : s.n., 2004-2007.

16. *Artificial neural network as a multidimensional nomogram for engineering design of an optimal diaphragm wall.* **Marek Lefik, Marcin Krascinski.** Gdansk, Poland : s.n., 2010.

17. *Numerical Analysis of a diaphragm wall.* **Mitew-Czajewska, M.** Warsaw, Poland, Warsaw University of Technology : Taylor & Francis Group, London, 2006, Geotechnical Aspects of Underground Constructions in Soft Ground-Bakker et al.

18. *Design of deep excavations according to Eurocode 7.* **Anna Siemisnka-Lewandowska, Monika Mitew-Czajewska.** Grenoble, France : s.n., 2007.

19. **Brinkgreve, R.B.J., et al., et al.** *Plaxis 2D Reference Manual 2010.* Delft : Plaxis bv, 2010.

20. —. *Plaxis 2D Tutorial Manual 2010.* Delft : Plaxis bv, 2011.